2022-06-09

Autoignition Temperatures of Pure Compounds: Data Evaluation, Experimental Determination, and Improved Prediction

Mark Edward Redd
Brigham Young University

Autoignition Temperatures of Pure Compounds:

Data Evaluation, Experimental Determination,

and Improved Prediction

Mark Edward Redd

A dissertation submitted to the faculty of
Brigham Young University
in partial fulfillment of the requirements for the degree of

Doctor of Philosophy

W. Vincent Wilding, Chair
Thomas A. Knotts, IV
David O. Lignell
Larry L. Baxter

Department of Chemical Engineering

Brigham Young University

ABSTRACT

Autoignition Temperatures of Pure Compounds:
Data Evaluation, Experimental Determination,
and Improved Prediction

Mark Edward Redd
Department of Chemical Engineering, BYU
Doctor of Philosophy

The Design Institute for Physical Properties (DIPPR) maintains the DIPPR 801 database for the American Institute of Chemical Engineers. Autoignition temperature (AIT) is one of the properties included in the database and is the focus of this work including improvement of the overall state of AIT in the database.

Phenomena related to AIT as well as the relevant literature are reviewed. Likewise, the database is presented to respond to significant misuse of the DIPPR 801 database in the literature. The database is evaluated, respecting AIT, as a whole to show where improvement is needed.

An experimental study of minimum autoignition temperatures reveals unexpected behavior of pure *n*-alkanes not predicted by current current phenomenological understanding of autoignition processes. Measurements show an increase at C16 and a dramatic and previously unexplained step increase between C25 and C26. Experimental modifications are presented to compensate the effect of altitude. Measured values for several *n*-alkanes are reported and compared to the literature. Other ignition experiments and decomposition measurements using differential scanning calorimetry are also reported and examined to elucidate the unexpected trends. Explanations for these trends are proposed. Finally, the implications of this for trends in other chemical families are discussed.

A comprehensive examination of AIT family trends reveals variation from the *n*-alkane family trend. Measured AIT values are presented and discussed. Evaluated AIT values are recommended for several single-group chemical families. Phenomenological explanations for observed differences are proposed and discussed along with the broader implications for these trends.

Methods for predicting autoignition temperatures (AIT) have been historically inaccurate and are rarely based on the underlying physical phenomena leading to observed AIT. An improved method for predicting AIT based on the method by the late Dr. William H. Seaton is presented and discussed. The method of Seaton is described in detail. An evaluated data set is used to regress new parameters for the Seaton method parameters. Improvements to Seaton's model and underlying principles are presented and discussed. Finally, an improved AIT prediction method is presented and recommended.

Keywords: autoignition, autoignition temperature, DIPPR, flammability, ignition

ACKNOWLEDGMENTS

I gratefully acknowledge the generous support of the sponsors of the DIPPR 801 Project for funding this research. Special thanks are given to Shane Wood for consulting on the design of the ARIA, to Gabriel Alejandro Valdivia Berroeta and Dr. Stacey Smith for performing X-ray crystallography measurements and Dr. Jef Rowley for consulting on the project, providing his expertise on flammability limits, and giving us the idea to use DSC to measure decomposition temperatures. Thanks is also given to McKay Rytting for his initial measurements for the DIPPR 801 Project. Thanks to Sustainable Energy Solutions, Inc. for allowing use of their facilities and time to seal and pressure test the apparatus. Also, a special thanks goes to Alex Mansfield and Dr. James Archibald for their technical support on the project.

I prominently acknowledge the foundational scientific work and software development of the late Dr. William H. Seaton. His contributions stand out as a central focus of this work, and the advancements made here would be impossible without him.

I thank my graduate committee for their support and enthusiasm for this project and their willingness to offer counsel and ideas to make this project progress. Their help has ensured the results of this work are they best they can be.

This project would not be possible without the work of several undergraduate researchers at Brigham Young University including: Colin Anderson, Koen Bailey, Adam Bates, Joseph Black, Trevor Black, Derek Burnham, Caidin Cheney, Brad Crowther, Sarah Daines, Cassandra Guffy, Ethan Gustafson, Jared Hammon, Elizabeth Hart, Mark McDonald, Nathan McDonald, Keturah McQuade, Troy Ogilvie, Johnny Pershing, Nicole Quist, Jared Schaumann, Jacob Schmidt, Allie Shuman, Makenzie Smith, Brandon Timmerman, Sara Tingey, and Alexa Urrea.

CONTENTS

LIST OF TABLES

LIST OF FIGURES

NOMENCLATURE

A	Constant group parameter in the Seaton, Seaton-Redd and Seaton-Redd2 methods
AAD	Average Absolute Deviation
$AIChE$	The American Institute of Chemical Engineers
AIT	Autoignition Temperature
AIT_{est}	Estimated or predicted AIT
AIT_{exp}	Experimental AIT
$AITMP$	William H. Seaton's software for predicting AIT via his method
ANN	Artificial Neural Networks
ARD	Average Relative Deviation
$ARIA$	Automated robotic injector arm
$Bias$	Average Bias
$C\#$	Carbon number. The # sign a specific carbon number
C_p^{IG}	Ideal-Gas Heat Capacity
C_p^l	Liquid Heat Capacity
C_O	Oxygen-atom group parameter in the Seaton, Seaton-Redd and Seaton-Redd2 methods
d	Equivalence-ratio parameter in the Seaton-Redd2 method
DCT	Decomposition Temperature
$DIPPR$	The Design Institute for Physical Properties
DSC	Differential Scanning Calorimetry
E	Reactivity group parameter in the Seaton, Seaton-Redd and Seaton-Redd2 methods
$ETSI$	Electrotopological-State Indices
g	Log base 10 of the equivalence-ratio parameter in the Seaton-Redd2 method
GC	Group Contribution
$max(D)$	Maximum Deviation
ML	Machine Learning
MLR	Multi-linear Regression
NLR	Non-Linear Regression
p	Other-probability group parameter in the Seaton, Seaton-Redd and Seaton-Redd2 methods
PN	Polynomial Regression
$QSPR$	Quantitative Structure-Property Relationships
R^2	Correlation coefficient for experimental and estimated values
SVM	Support Vector Machines
VP	Vapor pressure
$\bar{y}$	Mean value of quantity y
$z_{95\%}$	Inverse normal distribution at a probability of 0.95 (has a value of $\tilde{1}.645$)
ΔH_{vap}	Heat of Vaporization
σ_{sample}	Standard deviation of the sample mean

CHAPTER 1. INTRODUCTION

Fire and explosion hazards are of particular interest when designing safe industrial processes. As a part of this, engineering designs must prevent catastrophic fires and explosions. These events most often trigger from a spark, flame or some other ignition event. However, an ignition source is not necessary in sufficiently high temperature conditions where a compound can autoignite. An autoignition event occurs when flammable compounds reach a sufficiently high temperature to ignite spontaneously in the presence of oxygen without a spark or other ignition source. This is the same phenomenon that occurs in engine knock for gasoline engines or normal operation of diesel engines. The difference is that the pressures are much higher in internal combustion engines. Knowing the minimum temperature at which autoignition occurs, the autoignition temperature (AIT), affects regulatory policy and can prevent loss of life and property [1–3].

Despite its importance, the phenomena and factors that influence autoignition events are poorly understood. Few experimental data have been published in journals over the last 30 years and attempts at predicting AIT in that same time frame are generally focused on empirical correlation and machine learning with little emphasis on understanding phenomena. AIT data in the literature can be significantly disparate based on the method of measurement and, more importantly, a laboratory-measured AIT will likely differ significantly from the temperature at which autoignition occurs under industrial conditions [4]. Much of this disparity arises from the fact that AIT is a non-fundamental property and thus must be defined per a set of conditions. The non-fundamental nature also makes autoignition inherently complex to understand and predict.

This dissertation presents work that treats many of these issues through critically evaluating experimental data and other sources of AIT values, measuring AIT using standard methodology, establishing general chemical family trends for AIT, and predicting AIT using methods based on first principles. Thermophysical data and their usage in the literature are reviewed focusing on data from the American Institute of Chemical Engineers' DIPPR 801 Database. A detailed study

of AIT for the normal-alkane chemical family reveals relevant phenomena and establishes limiting behavior for other chemical families. A critical evaluation of AIT values from 611 sources is used to recommend the best AIT values and build a data set used to regress parameters for a prediction method. The prediction method is also presented along with the first-principles theory on which it is based. Finally, a comprehensive examination of AIT trends for several chemical families shows the influence of common functional groups on the baseline behavior established for the normal alkanes.

CHAPTER 2. A COMPREHENSIVE REVIEW OF AIT IN THE LITERATURE

2.1 Autoignition Phenomena

2.1.1 Definitions

ASTM defines autoignition as "the ignition of a material commonly in air as the result of heat liberation due to an exothermic oxidation reaction in the absence of an external ignition source such as a spark or flame" [5]. This definition applies generally to autoignition events observed in any context. However, the scope of autoignition in this work is limited to autoignition in the context of safety and industrial environments.

The autoignition temperature (AIT) of a substance is defined by the ASTM as "the minimum temperature at which autoignition occurs under the specified conditions of test" [5]. This definition highlights the non-fundamental nature of AIT, that is, the measured value depends on the conditions of the experiment. AIT changes significantly depending on many conditions and therefore, AIT must be defined within the context of a set of conditions. This includes a definition as to what constitutes an autoignition event. Generally, an autoignition event is defined by the presence of a visible flame as per ASTM methods D2155 and E659 [5, 6]. Because of this, any reported AIT should specify the methodology of test. Methodologies for AIT measurement will be compared and discussed later.

2.1.2 General Phenomena

The phenomena of that control autoignition are closely tied to general mechanisms of ignition and combustion. These mechanisms are highly complex even for the simplest organic compounds such as methane [7]. Despite this, the following narrative illustrates the conventional model for an autoignition event.

Consider oxygen in an isolated container. The container is heated and allowed to come to thermal equilibrium, so the entire container is at a high, uniform temperature. A fuel at room temperature is then introduced into the container. The fuel evaporates, lowering the temperature somewhat, and mixes with the oxygen. At a sufficiently high temperature, spontaneous combustion occurs, increasing the temperature of the container. The higher temperature increases the combustion rate and increases the temperature further. This feedback loop continues until a thermal runaway occurs, leading to a visible flame.

Generally, there are three things that can affect the outcome of this scenario. First, the changes in enthalpy and entropy affect spontaneity of combustion and the amount of energy released in reactions. Second, the properties of the fuel and air in the system control heat and mass transfer. Third, the reaction mechanisms affect combustion rates and heat generation as well. Given these factors, it follows that AIT varies significantly per conditions.

However, many of these conditions can be set to compare the AIT of various compounds in a consistent way. In this comparison, kinetic mechanisms are of particular importance as they change significantly between different compounds. General mechanisms are discussed by Glassman and Yetter, namely chain branching ignition and thermal spontaneous ignition [8]. Both ways of considering autoignition are important and both sets of underlying phenomena influence observed AIT.

2.2 Autoignition in Industry

Many reactions and chemical processes are optimized at temperatures exceeding the AITs of their respective components. This makes it common for a process to be designed at temperatures well above the AIT values of its chemical components. While circumstances may necessitate exceeding a compound's AIT, heating compounds above their respective AIT should be considered in design and minimized where possible. Furthermore, measures should be taken to prevent fires in case of any leakage for such a process.

2.2.1 Regulations

The obvious importance of fire safety has led to government regulations to protect lives and prevent disasters that affect the public. The Occupational Safety and Health Administration (OSHA) classifies autoignition with other sources of ignition and specifies regulations surrounding flammable compounds [3]. These regulations include specifying requirements regarding handling and storage, general fire prevention, conditions of heating, ventilation, transport and explosion suppression.

It is a central part of engineering to consider pertinent laws and regulations when designing and implementing processes. Compliance with these laws depends on a conventional definition for AIT and knowing the pertinent AIT values as accurately as possible. Aside from laws and regulations, the more pressing concern is to prevent accidental fires or explosions. Regulations are intended, in part, to prevent such disasters. However, accidents still occur. The following is a discussion of some accidents that have occurred in connection with autoignition events.

2.2.2 Accidents

The CSB has investigated and reported on several industrial accidents involving flammable compounds at temperatures above their respective AITs. Two incidents are given as examples. Accidents generally happen due to a number of factors. However, compounds at temperatures above their AITs contributed to the consequences of these accidents.

First, a Tesoro oil refinery in Washington state experienced a devastating accident in 2010 [1]. During startup of a heat exchanger bank, one of the heat exchangers catastrophically ruptured releasing hydrogen gas and naphtha at temperatures exceeding $500^{o}F$. The flammable compounds reportedly autoignited upon contact with the air causing an explosion and fire that claimed the lives of 7 workers. The CSB called it the “largest fatal incident” at a refinery in the U.S. since 2005.

Another incident occurred at a Chevron refinery in California in 2012 [2]. A pipe carrying light gas oil out of the refinery began releasing the mixture and forming a vapor cloud around the area. In the details of the report, it was found that leaking fluid became hot enough to autoignite inside the piping insulation. This caused a small fire that in and of itself was of lesser consequence but slowed the process of handling the leak. A vapor cloud formed and ignited affecting thousands

of people in surrounding areas. In the weeks following the accident 15,000 people sought medical treatment in connection with this incident. The CSB found a report released to Chevron dated years prior to the accident that detailed the dangers of hot process fluid above its AIT that may lead to large fires. In addition, there was incorrect information given to the Chevron fire department that the flowing compound was below its AIT and even below its flash point when in fact the opposite was true. Ultimately, the CSB recommended that further protocols be instituted to work with compounds near their AIT.

Overall, autoignition is just one of many factors that lead to accidents like those explained here. Having reliable AIT values is one critical piece of information for safe process design not only to comply with regulations but also to prevent disasters in the chemical industry. A central goal of this work is to present improved understanding of autoignition to help prevent disasters like the ones above.

2.3 AIT Measurement

This section describes the history and some of the rationale for standard AIT measurement methods developed in the 20th century. As AIT is a non-fundamental property, many different methodologies for measuring AIT have been attempted. Reputable sources using different methods have reported measured AIT values that vary by more than 100K for the same material [9]. Babrauskas lists several factors that influence the measured AIT of a given compound including ambient pressure, oxygen and fuel concentrations, combustion vessel properties (i.e., size, shape, material of construction etc.), the method of heating, and the presence of turbulent flow [4].

To arrive at a useful value for AIT, methodologies have been prescribed to control for as many variables as possible while still approximating conditions that would commonly occur in an industrial environment. Both Setchkin and Babrauskas give histories and explanations of various methodologies for measuring AIT that have been employed throughout the 20th century [4, 10]. Many of these methods have likewise produced significantly different AIT values for the same compound. The standard methods that most often appear in the literature include the methods developed by ASTM International (D286, D2155 and E659), the German Institute for Standardization (DIN 51794) and the International Electrotechnical Commission (IEC 60079-4 and ISO/IEC 80079-20-1) [5, 6, 11].

2.3.1 History

AIT measurement methods were not standardized until 1930 when the United States Bureau of Mines developed the original standard AIT measurement method called D286 [4]. This method introduced samples of flammable compounds into a glass 200 mL flask submerged in liquid solder heated by a gas burner. This original AIT measurement method still influences modern methods of measurement [4].

Flammability phenomena, including autoignition, have been of special interest to the U. S. Bureau of Mines to prevent accidents as evidenced by the work of Zabetakis et. al. and their I-8 apparatus [12–14]. The I-8 apparatus used the same flask as the D286 method but heated it electrically and did not submerge the flask in solder [12]. These improvements on the D286 method were used to codify the ASTM D2155 method which replaced the ASTM D286 method in 1966 [6]. The work done by Zabetakis et. al. was so foundational that it is commonly referenced in modern publications.

There are also many data reported from sources with unconventional methodologies. These include the metal enclosures designed by Moore and later modified by Sortman et al. and Frank et al. [15,16], the larger flask and heating methods used by Setchkin and later by Affens et al. [10,17], the pressurized steel reaction vessel used by Furno et al. [18], and the quartz bulb used by Jones et al. [19]. Some of these methods' features were later used to derive standardized methods.

However, the foundational work for current AIT measurement was conducted by Setchkin [10] who used a 1-liter bulb flask that was uniformly heated to perform his experiments. His measurement apparatus bears only minor differences to the current E659 method [20]. However, the D2155 method became the preferred method for measuring AIT until, after a round-robin study, the E659 method was adopted for measuring AIT in 1978 [5]. The D2155 method is still used to measure AIT for aircraft hydraulic fluids [6].

The common features of all of the mentioned AIT measurement methodologies give insight into the general practice for measuring AIT. First, a sample of the material to be tested is introduced into an enclosed and heated environment with oxygen present (usually as an air mixture). The system is then allowed to sit undisturbed at some set of conditions for some amount of time to see if an autoignition event will occur. The temperature is then adjusted, and the process repeated

until a minimum temperature is found at which autoignition occurs. This minimum temperature is considered the AIT for that method.

In the literature, it is common to prefer the lowest AIT value or the set of conditions that tend to produce the lowest AIT value. For example, the AIT values reported by Frank et al. are consistently higher than those of Zabetakis et al. and Setchkin for the same compound [10, 12, 16]. The values and methods from Zabetakis et al. and Setchkin are favored over Frank's because, in producing lower AIT values, their methods represent a more conservative definition of AIT. Given this, it may seem reasonable to choose a set of conditions that will lead to the lowest measured AIT possible and could represent a theoretical limit for any set of conditions. However, such conditions do not reflect those commonly seen or even possible under real circumstances in industry. Since AIT is applied to such settings, standard AIT methodologies attempt to balance minimizing the measured AIT with mimicking real-world conditions.

2.3.2 ASTM E659

The currently accepted method for measuring AIT in the United States, ASTM E659, approaches this task by controlling for several variables. It uses a 500-cc borosilicate-glass bulb flask, covered in aluminum foil and suspended in a temperature-controlled oven or furnace. (See Figure 2.1.) Four K-type thermocouples are placed on various points around the flask to ensure temperature uniformity. This method controls for factors that affect the measured AIT including wall material, vessel shape and size, radiation effects, and uniform heating. Fuel-to-air ratios are set in the method with standard sample sizes that generally skew fuel-rich compared the amount of air in the flask at the AIT. Samples are measured at room temperature and introduced into the flask at a set temperature. The ambient pressure is defined at 1 atm. Most ot these conditions minimize the measured AIT, according to Babrauskas [4].

All the standardized methods for measuring AIT are largely similar. The ASTM D2155 method differs mainly in that it uses a 200 cc Erlenmeyer flask in place of the bulb flask. The results of these methods can be compared to literature as the E659 and D2155 methods are nearly identical to the methods of Setchkin and Zabetakis et al. respectively [10, 12]. These sources show that the E659 and D2155 methods produce results with an absolute error less than 1.2%, for the liquid compounds in the *n*-alkane family. Likewise, the DIN 51794 method differs from E659

in minor ways (e.g., the DIN measures temperature in a different spot on the bulb, uses fewer temperature probes etc.) such that Nabert considers them to be equally valid [21].

Unless otherwise noted, AIT experiments in this work conform to the ASTM E659 method. Experiments have been carried out that reproduced AIT values consistent with those in the literature that use the same methodology. This is done to ensure consistency and clarity in the experimental results as well as conform to applicable regulations and laws.

2.4 AIT Prediction

2.4.1 Early Observations

The earliest known correlation of any molecular descriptor to AIT was published by Zabetakis et al., who observed that AIT correlated with what they called the "average carbon chain length" for several members of the alkane family [12]. The shape of the curve they observed is similar to curves found in many chemical families. This behavior was later correlated to carbon number by Shimy for select hydrocarbons and alcohols [22]. The Shimy correlations could be extrapolated to predict AIT. These early attempts at understanding AIT trends and predicting AIT suffered from a narrow applicability and often failed to fit observed behavior. A later attempt by Shebeko also failed to capture AIT behavior and can be shown to more closely resemble the behavior of flash points [23]. All of the early attempts at predicting AIT are based on correlation to basic molecular descriptors such as carbon number and fail to address the phenomena and structural contributions that give rise to autoignition events.

2.4.2 Modern AIT Prediction Methods

More than 30 methods for predicting AIT have been produced since 1991. These approaches include a method for modeling compounds and a model for prediction. The literature contains only two approaches to the former: group contribution (GC) and quantitative structure-property relationship (QSPR) descriptors. Group contribution methods may include the use of first or second-order functional groups such as those used by Joback et al. [24] and Benson and Buss [25], respectively. QSPR descriptors may take many forms and are calculated a number of

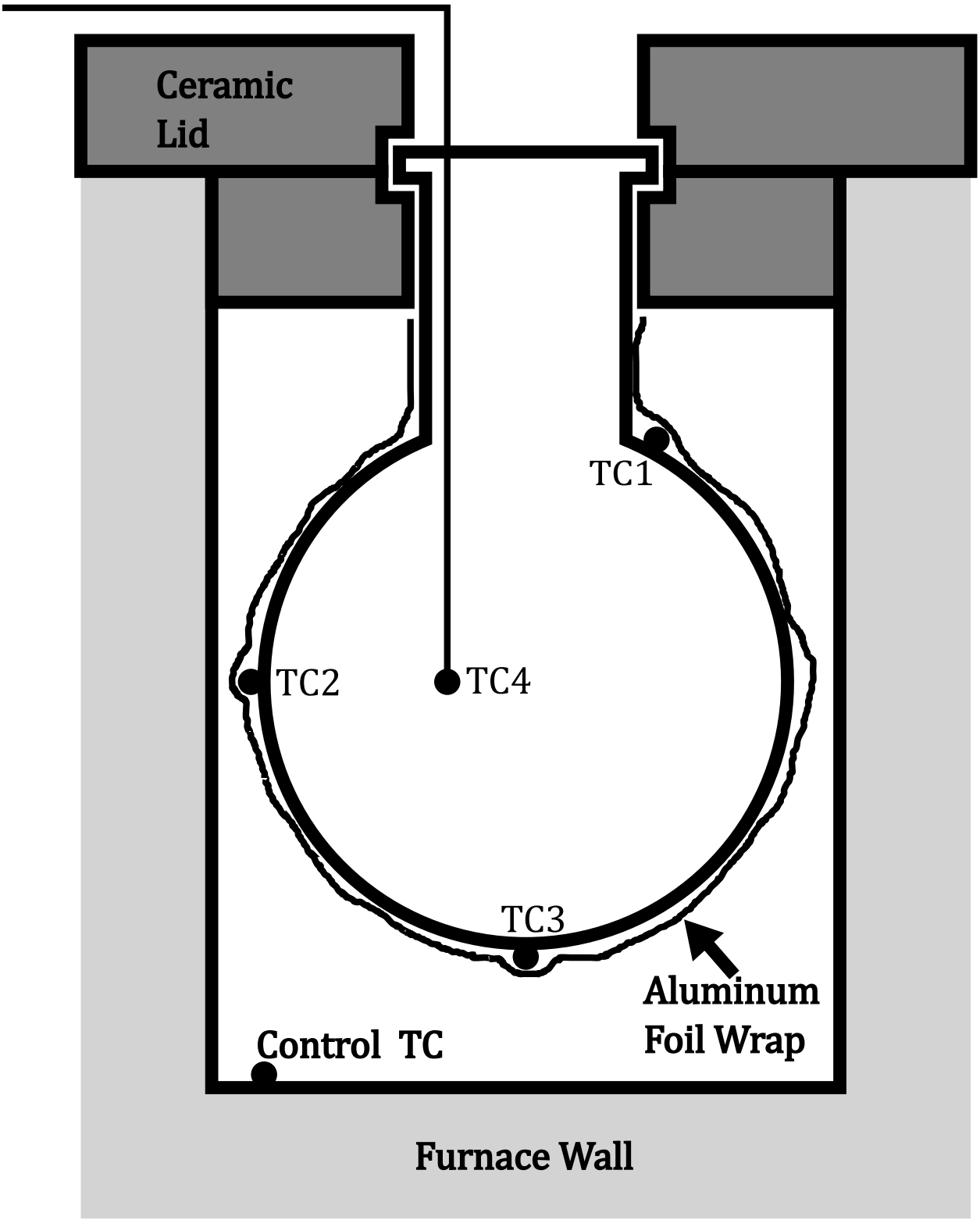

Figure 2.1: Diagram of the ASTM E659 apparatus, reproduced based on [5]. Four thermocouples (TC) are placed around the flask. The flask is covered in aluminum foil to aid temperature uniformity and control for radiation effects. TC4 is suspended in the approximate center of the flask.

ways. For the scope of this work, descriptors such as electrotopological-state indices (ETSI) are considered to be a subset of QSPR descriptors.

Prediction models in the literature take one of the following general forms: multi-linear regression (MLR), polynomial regression (PN), non-linear regression (NLR), artificial neural networks (ANN), and support-vector machines (SVM). Both ANN and SVM techniques fall into the category of machine learning (ML) prediction models. All literature methods from 1991 onward are summarized in Table 2.1 including the type of method used and relevant statistics for comparison. "N Inputs" refers to the number of descriptors used in the case of QSPR and the number of functional groups available in the case of GC. "N Data" refers to the number of data used in both the training, validation, and testing of the method. The other statistics found in the table (R^2, AAD, Bias) apply to the testing set only. R^2 refers to the "correlation coefficient" and AAD refers to the "average absolute deviation". Certain statistical figures are omitted in Table 2.1 in cases where they were either not reported in the literature, could not be calculated, and/or were ambiguously presented.

Table 2.1: AIT Prediction Methods Published Since 1991. "N Inputs" refers to the number of available groups for GC methods and number of descriptors for QSPR methods.

Primary Author	Year	Method Type	N Inputs	N Data	R^2	AAD (K)	Bias (K)	Reference
Egolf	1992	QSPR-MLR	22	58	0.98	12	0.04	[26]
Suzuki	1992	QSPR-MLR	5	50	0.89	33	0.70	[27]
Pintar	1996	GC-NLR	22	968	0.99	59	-10.20	[28]
Tetteh	1996	QSPR-MLR	6	233	0.81	90	4.20	[29]
Tetteh	1996	QSPR-ANN	6	233	0.84	30	1.20	[29]
Mitchell	1997	QSPR-MLR	35	327	-	-	-	[30]

Table 2.1: Continued

Primary Author	Year	Method Type	N Inputs	N Data	R^2	AAD (K)	Bias (K)	Reference
Mitchell	1997	QSPR-ANN	-	327	-	-	-	[30]
Kim	2002	QSPR-MLR	9	200	0.91	23	4.98	[31]
Albahri	2003	GC-PN	58	490	0.79	58	-	[32]
Albahri	2003	GC-ANN	58	490	0.98	17	3.08	[32]
Pan	2008	QSPR-MLR	16	118	0.81	32	8.33	[33]
Pan	2008	QSPR-ANN	16	118	0.91	22	5.24	[33]
Pan	2008	QSPR-MLR	6	50	0.80	43	4.79	[34]
Pan	2008	QSPR-ANN	6	50	0.97	16	4.17	[34]
Pan	2008	QSPR-SVM	6	50	0.98	13	-3.25	[34]
Pan	2008	QSPR-MLR	6	142	0.92	34	-9.90	[34]
Pan	2008	QSPR-ANN	6	142	0.95	28	-7.79	[34]
Pan	2008	QSPR-SVM	6	142	0.95	24	-4.69	[34]
Chen	2009	GC-PN	45	490	0.54	70	4.36	[35]
Pan	2009	QSPR-MLR	9	446	0.86	33	-	[36]

Table 2.1: Continued

Primary Author	Year	Method Type	N Inputs	N Data	R^2	AAD (K)	Bias (K)	Reference
Pan	2009	QSPR-SVM	9	446	0.87	29	-	[36]
Pan	2010	QSPR-MLR	5	153	0.90	28	-	[37]
Gharagheizi	2011	GC-ANN	146	1025	0.99	-	-	[38]
Lazzus	2011	GC-ANN	42	343	0.99	11	-1.14	[39]
Bagheri	2012	QSPR-MLR	3	48	0.93	-	-	[40]
Bagheri	2012	QSPR-ANN	3	48	0.95	-	-	[40]
Tsai	2012	QSPR-MLR	4	820	0.81	36	-	[41]
Keshavarz	2013	QSPR-MLR	4	274	0.86	-	-	[42]
Borhani	2016	QSPR-MLR	3	813	0.80	36	4.08	[43]
Borhani	2016	QSPR-ANN	3	813	0.80	41	3.71	[43]
Frutiger	2016	GC-NLR	176	513	0.76	-	-	[44]
Keshavarz	2018	QSPR-MLR	5	111	0.91	36	-	[45]
Dashti	2020	QSPR-NLR	9	446	0.88	-	-	[46]
Baskin	2020	QSPR-SVM	-	875	0.77	36.6	-	[47]

The relative advantages of GC versus QSPR inform their use in AIT prediction. QSPR tends to be more the flexible method of molecular modeling as it can capture complex behavior that is not always apparent from observing molecular structure alone. Given this, it is not surprising that QSPR constitutes the majority of methods in the literature. Molecular modeling with GC benefits from its relative simplicity; no calculation nor empirical knowledge of the compound is needed, only structural information.

An important feature of the molecular model used in prediction is the potential insight that can be gained from the process. Though it is not always the primary aim, the process of modeling may present patterns that reveal phenomenological insights into the property to be predicted. For example, Suzuki et al. showed molecular surface area and the connectivity of a hydrocarbon were strongly correlated with the observed AIT [27]. This observation concurs with the experimental observations of Zabetakis et al. [12] and suggests that the length and size of a molecule are connected with the observed AIT. Such insights are valuable, even though they do not comprehensively explain the complexity of the autoignition process.

The use of machine learning has become more prominent in the literature over the last 3 decades. Various machine learning approaches have been attempted and these generally outperform other conventional methods. These methods are used, in part, to attempt to deal with the complexity of the autoignition process without needing a comprehensive understanding of the underlying phenomena. This is both a strength and a weakness of the approach. Specifically, machine learning methods yield no fundamental insight into the problem and are prone to overfitting the data without regard to the significance of their fit. Furthermore, it is rare for these models to be published in a closed form such that they may be easily replicated and used outside the scope defined in their respective publications. For these reasons, machine learning is poorly suited to predict and understand AIT and associated phenomena.

Outside of the methods that use machine learning, most prediction techniques are linear combinations of parameters and inputs. Only three of the methods in Table 2.1 employ a non-linear approach to modeling autoignition. Pintar and Frutiger et al. both present models that use linear combinations of parameters that are then correlated to AIT using non-linear equations [28, 44]. Pintar's method uses a logarithmic model to correlate to the AIT behavior of many families as shown by Zabetakis [12]. Frutiger et al. uses a general group contribution correlation model orig-

inally presented by Hukkerikar et al. to regress the groups against AIT [48]. Dashti et al. present a non-linear QSPR model that includes a linear combination of 13 terms with many of the terms being non-linear combinations of the descriptor values and model parameters [46]. They arrived at the final model using evolutionary algorithms that included different ways of combining parameters as part of the set of decision variables. All these non-linear methods improve on their linear counterparts but still fail to model autoignition from a first-principles basis which captures the complexity of the process.

2.4.3 Data Quality

Another issue in the literature stems from the lack of availability of high-quality AIT data. The AIT, as previously stated, is a non-fundamental property and depends entirely on the circumstances of the autoignition event. Measured AIT values may be dramatically influenced by factors such as test vessel size, shape, and material of construction; turbulent air flow; fuel-to-air ratio; and surface catalytic effects [4]. Given this, any AIT prediction method should define the AIT value that the method returns and use data in the regression that has been measured using methodology consistent with this definition (e.g. a method that predicts the AIT value that would be observed from ASTM E659 methodology). If inconsistent data are used, the inconsistency should be considered when assigning uncertainty to the predicted values. The literature shows no instance of data being scrutinized in this way. Nor has there been any attempt to evaluate the data for quality. This makes the prediction method's definition of AIT and the uncertainty of the predicted values ambiguous.

Where possible, data should be reported with sources or at least with a specification of the method used to obtain the AIT values. For example, Pan and later Dashti appear to use data from various SDS's and university repositories [33,34,36,46]. These sources lack necessary information about methodology and uncertainty of data. While the values may be reliable there is no way to verify them. Therefore, prediction methods based on such data produce ambiguous results. Noting the methodology corresponding to each AIT value is the least that should be done to ensure a minimum level of consistency such as has been done by Nabert et al. [21].

Data must be evaluated not only for methodological consistency, but also must be vetted to ensure it is experimental. Of the 21 publications referenced in Table 2.1, at least 11 sourced

their regression data from AIChE's DIPPR 801 Database using database snapshots from various years [26,28,32,35,37,38,40,41,43–45]. In these cases, the recommended AIT values are generally used without reference to their source. Many recommended values in the DIPPR 801 Database are predicted and therefore are unsuitable for capturing experimental behavior. The use of these values may invalidate an entire model as was explained by Bloxham et al. [49]. At least two publications since 1991 have used significant amounts of predicted values in their model training and therefore their results are questionable [38, 45].

The issues raised in this section significantly decrease confidence in the reliability of many existing prediction methods, and little has been done to prevent or remedy the situation. Also recall that no published method has modeled autoignition using a first-principles approach. Both of these factors have contributed to high uncertainty and limited utility in existing AIT prediction. This work aims to remedy both of these issues.

CHAPTER 3. THE DIPPR 801 DATABASE AND AIT

3.1 Introduction

In 1978, the American Institute of Chemical Engineers (AIChE) launched the Design Institute for Physical Properties (DIPPR). Since 1998, DIPPR Project 801 has been hosted by Brigham Young University in Provo, Utah. The project centers around maintaining and expanding the DIPPR 801 Database, which contains thermophysical property data for pure compounds of interest in industry. This database is characterized by two hallmarks: accuracy and completeness. Accuracy is ensured by a careful process for the evaluation and recommendation of the best information. "Complete" means that, where possible, every compound in the database contains recommended values for all properties. Because of the high quality of the database, it is often used to do fundamental research. Unfortunately, many have used it without properly understanding the database which has led to dubious scientific claims. Also, prior to this work the state of AIT in the database was not up to the high standards the database is known for.

This chapter responds to both of these issues. A brief overview of the DIPPR 801 database along with recommendations for best practices for using the database provides background for the scope and aims of this work as part of the DIPPR 801 project. A report on the state of AIT in database follows to show where improvement could be made. Finally, objectives to improve on the database accomplished in this work are listed.

The following definitions are used throughout this work in the context of the DIPPR 801 Project:

- Data: information based on an experimental result
- Value: a database entry that can include experimental and/or predicted information
- Accepted Value: a value recommended by DIPPR in the 801 Database because it has been found to be the most reliable and consistent information available

- Predicted Value: a database entry that was produced from any kind of prediction or estimation method; used interchangeably with estimated value

3.2 Explanation of DIPPR Evaluation Processes

The goal of the DIPPR 801 database is to provide the most accurate and complete thermophysical property data for the 32 constant and 15 temperature-dependent properties in the database for pure compounds of industrial importance. This focus on industrial needs means it is not the largest database in terms of number of compounds, nor are all possible thermophysical properties found in the database. Rather, both the compounds and associated properties in the database are carefully curated so that users can be confident that needed values are both available and accurate.

The quality of the database depends on a well-developed evaluation process. This process is intended to involve evaluations of data by several individuals. This human element in the process allows careful alterations to achieve a result that is complete, consistent with literature, and self-consistent. The evaluation process is iterative as correlation models, methods, and best data sources are updated until a "Gold Standard" chemical profile is built that represents the best information related to the physical properties. Such thorough evaluation is needed because sponsors and other database users employ DIPPR recommended values for process design, simulation, and research purposes. The following are the unique elements of the evaluation process with a brief explanation of how they contribute to the quality and utility of the database.

- **Industrial Sponsorship:** More than forty companies and institutions sponsor the DIPPR 801 Project to aid in the design and operation of their chemical processes. Sponsors of the project have the most up-to-date access to the database as well as have a role in directing the project as well as ensuring the high quality of the database. Sponsorships fund original research tailored to the needs of the sponsor and the database including experimental measurement, development of new estimation methods, and molecular modeling. The results of such research are evaluated by DIPPR personnel, published in peer-reviewed literature, and added to the database.

- **Accepted Values:** When adding a compound to the database, all relevant data are analyzed and evaluated by project staff. The evaluation process produces values and correlations

considered to be the "best" for each property, meaning they meet the standards of property consistency, family trends, and other chemical information. These "best" values appear in the database with the "Acceptance" field marked "Accepted". Other available data can be found in the database with different acceptance values and express the results of DIPPR's expert review process. An "Accepted" value may be predicted and may not be the value with the lowest author-reported uncertainty but always represents the recommended value by the evaluation.

- **Uncertainty in the 801 Database:** DIPPR assigns uncertainty levels to constant values as a percentage of the given value. These uncertainty designations are assigned by DIPPR based on data type, availability, and agreement of data sources, acquisition method, and original reported uncertainty. For predicted values, uncertainty is assigned based on general knowledge about the prediction method given the chemical family and property. The uncertainties of input properties used in prediction methods are also considered. For the sake of simplicity and to be conservative with uncertainty, DIPPR assigns nine quantized uncertainty levels to any property value. Due to the quantized nature of DIPPR uncertainty levels and other information considered in property evaluation, the reported DIPPR uncertainty is commonly different from author estimates.

- **Inter-Property Consistency:** The analysis method DIPPR uses allows for a more holistic picture of a chemical's properties than can be found in other data sources. Many properties are dependent on other properties through thermodynamic or structural relationships. These interdependencies are illustrated in Figure 3.1 and Tables 3.1 and 3.2. Analyzing these properties independently can lead to inaccuracies, so DIPPR evaluators ensure that properties are consistent with known relationships. These relationships provide quality checks for the various properties and allow DIPPR personnel to quickly identify potential problems with database values.

- **Completeness:** To support sponsors' needs, DIPPR requires chemical profiles to have a complete set of values and correlations for all thermophysical properties available in the 801 Database, to the maximum extent possible. DIPPR uses all the available data and existing

prediction techniques to give recommendations for all the properties in the database. Specifically, DIPPR uses the most accurate estimation methods possible when reliable experimental data are unavailable. This ensures each compound has a complete set of recommendations for every constant property and temperature-dependent correlation. Thus, the 801 Database provides to users the highest likelihood of finding the value they need and avoiding frustrating blanks when looking for property values and correlations. The only exceptions are cases in which physical properties are not applicable to a particular compound (e.g., flammability properties do not apply to water) or when no data nor reliable prediction method exists for a particular property (e.g., many compounds do not have an experimental solid thermal conductivity or available prediction method).

- **Dynamic Nature of the Database:** Often, new data are found and entered into the database after a compound has already been added and been given a complete chemical profile. When this occurs, the new data are included as "Unevaluated" until they can be analyzed. When needed compounds may be reviewed and the corresponding data evaluated and updated. These reviews may reassign Accepted values to reflect better information. In this way, the 801 database is a dynamic and perpetually improving database. A particular snapshot of the database will reflect the best recommendations available at that time, but any property value may later be supplanted by better values as they are found and evaluated. These policies help to ensure the database remains the "Gold Standard" even as new data or prediction methods become available.

Table 3.1: Available Pure-Component Constant Physical Properties Studied and Recommended in the DIPPR 801 Database (Abbreviations used by DIPPR are given in parentheses)

Constant Properties	Constant Properties (cont.)
Molecular Weight (MW)	Std. Absolute Entropy (SSTD)
Critical Temperature (TC)	Heat of Fusion at Melting Point (HFUS)
Critical Pressure (PC)	Std. Net Heat of Combustion (HCOM)
Critical Volume (VC)	Flash Point (FP)

Table 3.1: Continued

Constant Properties	Constant Properties (cont.)
Critical Compressibility Factor (ZC)	Lower Flammability Limit Composition and Temperature (FLVL/FLTL)
Acentric Factor (ACEN)	Upper Flammability Limit Composition and Temperature (FLVU/FLTU)
Normal Boiling Point (NBP)	Autoignition Temperature (AIT)
Melting Point (MP)	Radius of Gyration (RG)
Triple Point Temperature (TPT)	Solubility Parameter (SOLP)
Triple Point Pressure (TPP)	Dipole Moment (DM)
Liquid Molar Volume (LVOL)	Van Der Waals Volume (VDWV)
Ideal Gas Enthalpy of Formation (HFOR)	Van Der Waals Area (VDWA)
Ideal Gas Gibbs Energy of Formation (GFOR)	Refractive Index (RI)
Ideal Gas Absolute Entropy (ENT)	Heat of Sublimation (HSUB)
Std Heat of Formation (HSTD)	Parachor (PAR)
Std Gibbs Energy of Formation (GSTD)	Dielectric Constant (DC)

Table 3.2: Available Pure-Component Temperature-Dependent Physical Properties Studied and Recommended in the DIPPR 801 Database (Abbreviations used by DIPPR are given in parentheses)

Temperature-Dependent Properties	Temperature-Dependent Properties (cont.)
Solid Density (SDN)	Thermal Conductivity of Liquid (LTC)
Liquid Density (LDN)	Thermal Conductivity of Solid (STC)
Heat Capacity of Ideal Gas (ICP)	Thermal Conductivity of Vapor (VTC)
Heat Capacity of Liquid (LCP)	Vapor Pressure of Liquid (VP)

Table 3.2: Continued

Temperature-Dependent Properties	Temperature-Dependent Properties (cont.)
Heat Capacity of Solid (SCP)	Vapor Pressure of Solid or Sublimation Pressure (SVP)
Heat of Vaporization (HVP)	Viscosity of Liquid (LVS)
Second Virial Coefficient (SVR)	Viscosity of Vapor (VVS)
Surface Tension (ST)	

3.3 Common Mistakes in Publications

As the "Gold Standard" in chemical property data, the DIPPR 801 Database is referenced in many publications. While many researchers use the database correctly, mistakes are common in the literature. These errors often involve a fundamental misunderstanding of the property values in the database. By pointing out common mistakes, we hope to avoid such problems in the future. The following lists the most common and egregious mistakes made:

- **Insufficient Citations:** In a recent article, data were used from DIPPR, DETHERM, and additional works [51]. While the authors have carefully noted the number of data collected and the version of the DIPPR 801 Database used, they neglected to cite the primary sources, which would allow researchers to better analyze and review their work by allowing scrutiny of the primary data. This is a frequent mistake in the literature as removing the references to the literature makes the value reference ambiguous. This is a particular problem with AIT where many data have been cited without referencing the original source nor the methodology. This obfuscates the data and can make tracing them back to their source impossible. These problems can be avoided by referencing the original sources where possible.

- **Interpreting Recommended Values as Experimental:** In a 2018 article, Keshavarz et al. published a quantitative-structure-property-relationship (QSPR) for the prediction of autoignition temperatures (AIT) [45]. In it, they claim to use experimental data for 54 compounds to relate molecular descriptors to AIT. However, upon closer inspection, 19 AIT values they attribute to the DIPPR database are predicted rather than experimental values.

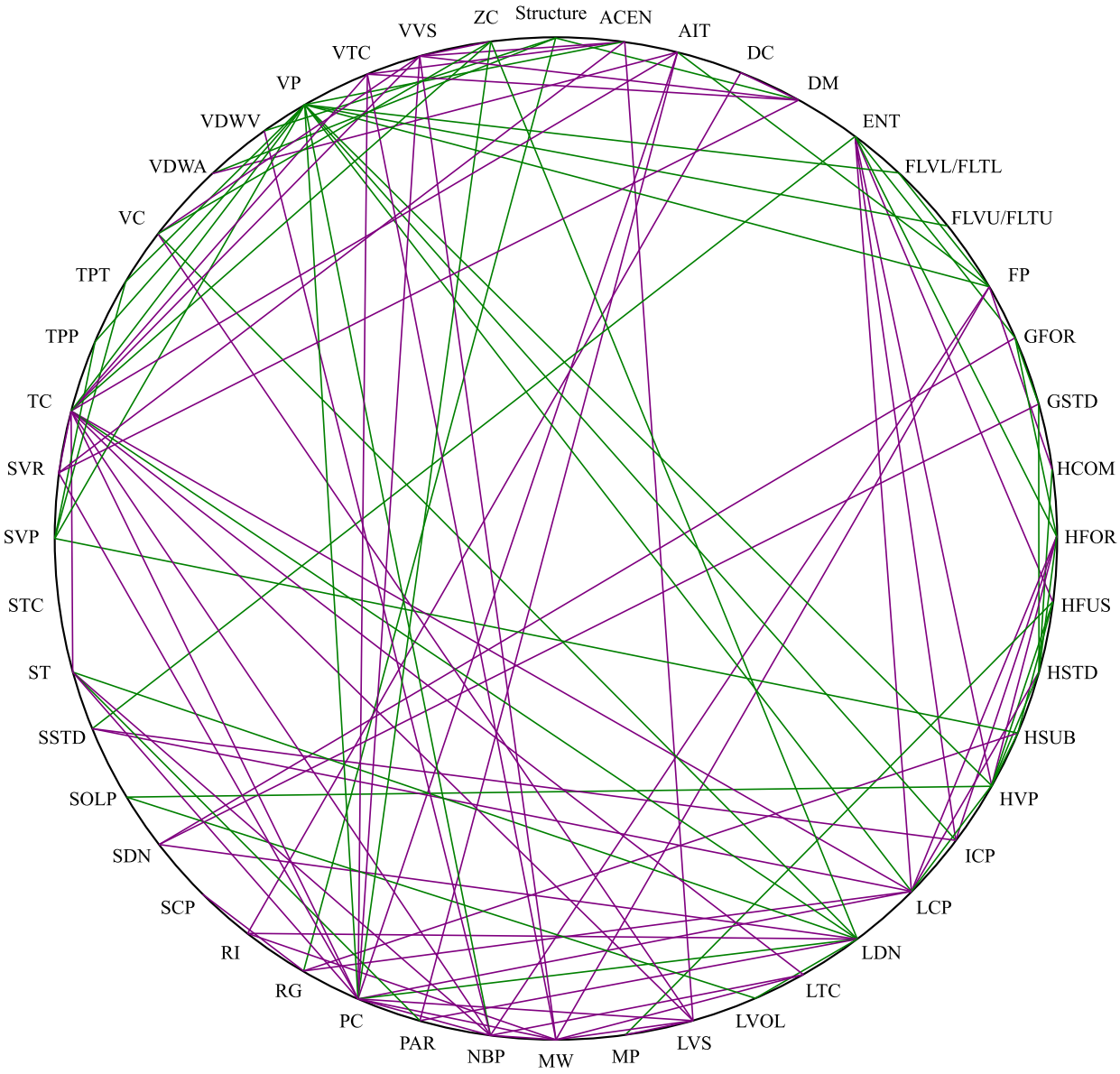

Figure 3.1: Interconnected properties used by the DIPPR database. Green lines show thermodynamic or rigorous relations and purple lines show predictive equation relationships. Abbreviation meanings are shown in Tables 3.1 and 3.2 in the Appendix. (This figure has been recreated based on Figure 1 from Rowley et. al. [50]).

The authors incorrectly selected "Accepted" values without examining whether the values were experimental or predicted. This neglect calls into question the entire prediction method because the regression is based on predicted values. Researchers can easily avoid this situation. DIPPR includes information for every recommended value to identify its origin and whether it is an experimental or predicted value. Researchers should screen the data they use for new prediction methods to avoid using non-experimental values.

3.4 How to Correctly Report DIPPR Values

Correctly using and citing DIPPR values can make data collection and processing easier, as well as increase the legitimacy of published findings. So far, common mistakes in the literature have been discussed and DIPPR processes have been explained. With this information, a discussion of best practices for authors and reviewers is appropriate. Following these suggested best practices will ensure the database is interpreted correctly and is used appropriately.

- **Understand Data Type:** Before using values collected from DIPPR, make sure the Data Type selected is appropriate for your application. For process design, the Accepted DIPPR value is generally the best choice and is the central use case for the database. For creating prediction methods, parameterizing group contribution methods, or other scientific work, use only experimental values, which are clearly marked as such in the database. If Accepted values are used for creating new estimation methods without reference to Data Type, there is a risk of only replicating the effectiveness of past methods rather than building new ones. This sort of error can introduce unforeseen uncertainty or even invalidate an estimation method.

- **Reference Original Source:** When using values or correlations from the DIPPR 801 database, cite DIPPR appropriately [52]. Additionally, reference the primary source including the original author or method used. The 801 database includes the source of each value where applicable. Using the primary source will ensure the property values are understood and reviewed in their original context. This also prevents the loss of important methodological information that is necessary for evaluating AIT values specifically.

- **Check Uncertainty:** As discussed previously, to simplify the database and allow for staff insight into data reliability, DIPPR uncertainty designations are quantized. This is often

not representative of the exact uncertainty that may be obtained from the original source of the value or correlation. When considering uncertainty, the recommended uncertainty in the database will be set according to the evaluation of the corresponding property value and thus may be safely used for design. However, if the property value is cited from the original source, the uncertainty should be reported according to the original source as that uncertainty will commonly differ from the reported uncertainty in the database.

3.5 State of AIT Values in the DIPPR 801 Database

A central goal of this project is to improve the amount and quality of data in the DIPPR 801 Database. A general evaluation of the DIPPR database for AIT shows both strengths and deficiencies in the database. This evaluation was accomplished near the beginning of the project. The goals of this evaluation were to ascertain the relative amounts of predicted and experimental data for AIT and identify compounds lacking data or needing improved AIT values.

The database shows the majority of compounds having accepted AIT values that are either predicted or not reported. There are various reasons why a compound may have no value reported such as the compound not being flammable as is the case with water. However, with regard to the predicted values, AIT prediction methods are known to commonly produce values that deviate from experimental values by more than 100 K.

This is a significant opportunity for improvement. Experiments and an improved prediction method, which are integral parts of this work, are intended to help solve both of these problems. In addition, an improved understanding of AIT phenomena and trends enables us to more reliably evaluate and predict AIT for the compounds with no value or high uncertainty. All of these will lead to a more complete and reliable database.

A summary of the evaluation results is in Table 3.3 and Table 3.4 below. There are 2386 compounds in the database with an 'Accepted' marker for AIT. This means that at some point these data were approved as the best available values for AIT for each compound. Table 3.3 lists the number of compounds with a particular data type. For predicted values, the method is also listed. For instances marked "No Value Reported", possible reasons are listed for the lack of data as well as the number of candidate compounds for which experiments could be performed. For reference, the data types listed in the table include:

- "Experimental" - Data that were produced experimentally using a variety of methods. For example, large portions of these data result from the older ASTM D2155 method.

- "Predicted" - AIT values were estimated using methods listed in the table and ordered by number of compounds predicted using the specified method. Many methods listed, such as "From Family Plots" and "Comparison to Similar Compounds" are internal methods used by DIPPR historically and may have unknown methodologies.

- "Not Specified, Smoothed or Unknown" - Many of the "Not Specified" or "Unknown" data are potentially suspect could be candidates for experimentation or improved prediction. However, they represent a small minority of compounds with accepted values.

- "No Value Reported" - These compounds were included in the database without AIT values assigned to them. The reasons for this vary but generally fit into three categories. First, the properties of the compound are unsuitable for the definition of an AIT (e.g., the compound is nonflammable, ignites spontaneously in air, is a flammable solid, decomposes, etc.) Second, the compound has properties that make it unsafe to measure AIT using conventional methods. Third, no reliable experimental data nor suitable prediction method could be found for the compound.

Table 3.3: General State of Accepted AIT Data in the DIPPR Database by Data Type *(Counts are the number of compounds that fit each criterion unless otherwise noted.)*

Criterion	Count
Total Number of compounds with an accepted value	2386
Experimental	**611**
Number of unique experimental sources	135
Predicted	**894**
Pintar Method	357
Seaton Method	310
From Family Plots	112
Comparison to Similar Compounds	62

Table 3.3: Continued

Criterion	Count
Other	24
Unspecified	11
Shebeko Method	10
Suzuki Method	8
Not Specified, Smoothed or Unknown	**54**
No Value Reported	**827**
Candidates for Measurement or Prediction	563
Nonflammable or Otherwise Inappropriate	205
Explosive	26
Spontaneously Ignites in Air	19
Flammable Solid	7
Other	7

The group of compounds classified as "Candidates for Measurement or Prediction" in Table 3.3 are compounds where no reliable experimental data nor suitable prediction method could be found for the compound. These compounds are an obvious area in which this work may significantly improve the database, whether by direct experimentation or by improved prediction.

A bar graph of the information in Table 3.3 is shown in Figure 3.2.

Table 3.4 shows the AIT database organized by common chemical families. From the family data, we see that many of the more common families have, on average, larger amounts of experimental values relative to predicted values or otherwise. Many of the compounds that lack any reported value fall under the more exotic compounds in the "Other" category. Many of these compounds without values likely fall into the categories in Table 3.3 under "No Value Reported" that make the compound inappropriate to have a meaningful AIT value.

The common families considered fall into the same categories as Table 3.3. The "Other" category contains the largest number of compounds in part because it represents all compounds

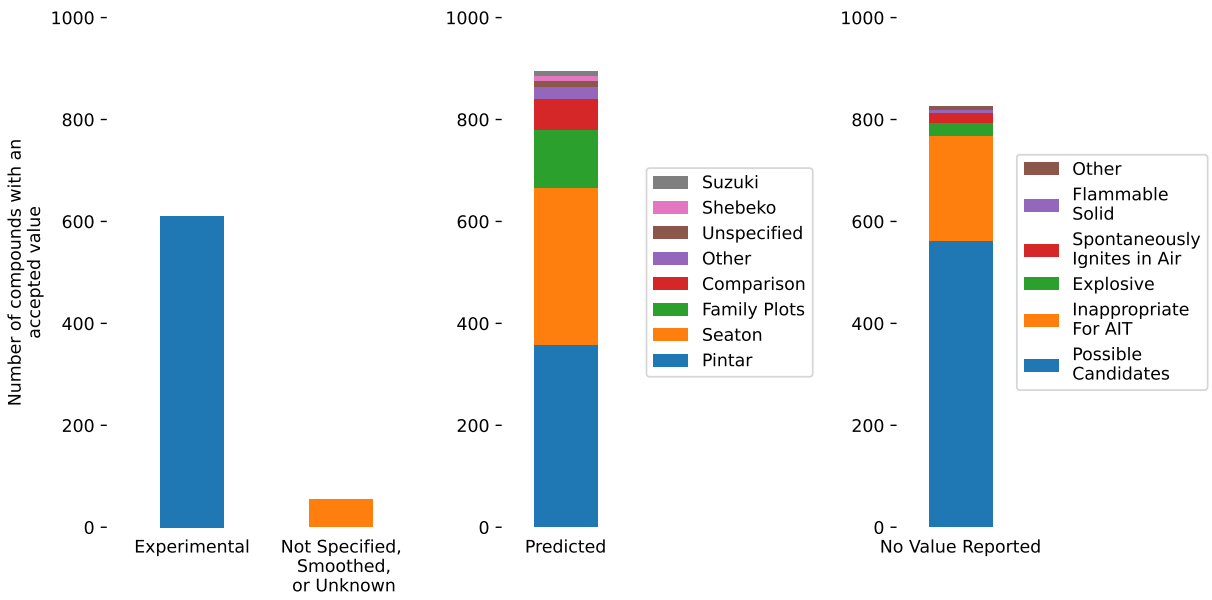

Figure 3.2: Counts of compound AIT values in the DIPPR 801 database separated by data type.

that have multiple functional groups or otherwise could not be categorized under this relatively narrow scope of families.

Table 3.4: General State of Accepted AIT Data in the DIPPR Database by Chemical Family. Values are the number of compounds that fit each criterion unless otherwise noted. “Hydrocarbons” includes alkanes, alkenes and aromatic hydrocarbons. “Substituted” indicates that one or more hydrogens have been substituted by a halogen or some other electronegative element.

Family	**Experimental**	**Predicted**	**Not Specified**	**No value**
Hydrocarbons	148	202	4	97
Alcohols	55	87	8	33
Ketones	20	26	1	5
Ethers	29	28	2	13
Esters	34	66	7	23
Amines	74	66	1	52
Acids	25	55	2	43
Substituted	56	93	5	139

Table 3.4: Continued

Family	Experimental	Predicted	Not Specified	No value
Other	176	272	23	414

Overall, the state of DIPPR's AIT data is incomplete with plenty of room for improvement. This evaluation informed choices about experimental candidates and data evaluation.

3.6 Objectives

We have briefly discussed DIPPR evaluations and processes, common mistakes in using DIPPR resources, and best practices in using DIPPR in scientific work. The usage recommendations herein will (if followed) ensure the correct use of DIPPR values, leading to more meaningful and transparent publications for engineers and scientists everywhere.

We have also shown that there is significant room for improvement regarding AIT in the database. A central goal of this work is to improve the state of AIT in the DIPPR 801 Database. To that end, the following objectives are accomplished in this work:

- A comprehensive examination of AIT values in the normal-alkane chemical family to establish limiting behavior for all chemical families and explain general family trends
- Selection and measurement of AIT for compounds from various chemical families that will establish family trends based on the examination of the normal alkanes
- A careful evaluation of AIT data in the literature to recommend the best values for inclusion in the 801 Database
- The derivation and implementation of an improved AIT estimation method using the measured data and evaluated data from the literature

These objectives and how they were accomplished are detailed in the following chapters and serve to expand the current understanding of phenomena that influence measured AIT, provide insight into autoignition mechanisms, and increase the quality and completeness of AIT values in the DIPPR 801 Database.

CHAPTER 4. A STUDY OF UNEXPECTED AUTOIGNITION TEMPERATURE TRENDS FOR PURE *N*-ALKANES

4.1 Introduction

This chapter characterizes AIT trends for the *n*-alkane family. This is important because the *n*-alkane family serves as the limiting behavior for many families as they increase in size. The trends in the *n*-alkane family are examined to propose similar trends for all organic chemical families.

Prior to this work, experimental AIT values for the *n*-alkane family were not available above C20 (*n*-eicosane). Trends from the literature show that AIT decreases as chain length increases until about C7 (*n*-heptane) where the AIT trend flattens at about 475 K. It was assumed this flat trend would continue indefinitely as chain length increases. However, AIT measurements in this work show the flat-trend assumption to be incorrect. The trends observed in this work challenge previous assumptions made about autoignition and the factors that influence it. These trends include a gradual rise in AIT between C16 (*n*-hexadecane) and C25 (*n*-pentacosane), and a large, discontinuous jump between C25 and C26 (*n*-hexacosane). The trend then increases gradually with carbon number.

The remainder of this document is structured as follows. First, an explanation of the apparatus and methods used to measure AIT, decomposition temperatures (DCT), melting points, and compound purities. Then, a historical view of AIT is presented to lay the foundation for understanding the previously held belief of the flat trend of AIT. Results are then presented and the trends are then examined in the context of measured values from this work and available in the literature.

4.2 Experimental Development and Methodology

AIT methodology in this work adheres to ASTM E659 [5]. However, certain details that affect AIT remain ambiguous or unspecified in the E659 method. Not controlling for these can lead to significant variance in results. Therefore, additional steps or specifications, still consistent with ASTM E659, were used where the method did not specify steps to control for these factors and details. These changes are intended to reduce or eliminate human error and subjective observation. Specific methodology used in this work is detailed in standard operating procedures. The most significant specifications are detailed below and the rest are presented in the Appendix B.

Uncertainties for experimental AIT values in this work are assigned per the ASTM Method, which specifies 2% uncertainty on a Celsius scale for values from the same laboratory and 5% uncertainty for values from different laboratories. As explained in Appendix B, AIT values are found via bracketing the minimum temperature at which autoignition occurs to within $\approx 3\ K$, that is, there is one experiment at a temperature where autoignition occurs and another experiment at a temperature that is about 3 K lower where it does not ignite. The lower temperature experiment is repeated at least three times with a minimum of 4 non-ignition experiments below the lowest temperature at which an ignition event was observed. When this criterion is met, the higher temperature where ignition occurred is considered to be the AIT value for the given sample size. This is done to ensure that the minimum temperature at which autoignition occurs has, in fact, been found. Near the AIT, autoignition events appear to become probablisitc with increasing temperature increasing the probablity of ignition. With 4 non-ignition events at temperatures slightly below the lowest ignition temperature, this methodology produces a reported AIT that has 50% or lower probablity of ignition at a confidence level above 93.7%. This brings the uncertainty of the AIT value to well within the uncertainties associated with temperature measurement, sample size, and other factors. Thus, the uncertainty given by the ASTM method will generally apply to these values.

4.2.1 Apparatus at Altitude

Furno et al. and later Brandes et al. demonstrated the effect of pressure on measured AIT [18,53]. Their results show AIT decreases with an increase in ambient pressure. Initial experiments were performed in Provo, Utah, United States which sits at an elevation of about 1400 meters (4600

feet) above sea level. This elevation corresponds to an atmospheric pressure averaging about 0.85 atm. This pressure difference from the standard 1 atm is sufficient to affect the AIT such that a result at altitude would be consistently higher than one measured at sea level. Therefore, a new apparatus was designed and constructed to measure AIT at 1 atm independent of ambient pressure, ensuring compliance with ASTM E659.

The original equipment available for this project were out of date and needed updating. Therefore, the data acquisition software, temperature measurement instrumentation and wiring, and standard operating procedure were redesigned and built new. Custom software to interface with the operator was written in Python. The new electrical components were designed using Arduino microcontrollers and compatible components. Overall, the finished redesign of the data acquisitions and sensors came at a fraction of the original projected cost. The only component from the original setup was the AIT oven.

The apparatus to pressurize the oven went through several iterations. Initially, the intent was to construct a reinforced wooden vessel as the gage pressures needed would be relatively low (≈ 3 *psig*). After consulting with various faculty in the Mechanical Engineering Department, we were recommended to purchase and modify a pressure cooker used in small brewery applications.

The vessel is a 30-gallon, 316 stainless-steel pressure cooker rated to 15 *psig*. In collaboration with the Precision Machining Laboratory on campus, we designed modifications that would allow extra NPT-threaded ports in the wall of the vessel. These ports would be populated with threaded hermetic feedthroughs to allow power and signal wiring into the pressurized environment. Also included are inlets and outlets for pressurized air to flow through the vessel, and a sight glass for flame-viewing convenience. Upon completion, the vessel was hydrostatically tested to 10 *psig* using facilities graciously provided by Sustainable Energy Solutions Inc. in Orem, UT.

Figure 4.1 is a simple diagram of the experimental setup. An E659-compliant furnace is placed in a pressure vessel with a removable lid for loading samples. Breathing-quality air, regulated to about 0.2 atm (3 psig), is fed into the pressure vessel from a gas cylinder. The absolute pressure in the vessel is kept precisely at 1.00 atm to within 0.007 atm ($\approx 5torr$). The mass flowrate through the vessel is controlled with a rotameter to a ≈ 25 *SCFH* (AIR at STP). The exhaust is ejected from the vessel through the lid before being discharged into a nearby fume hood.

Previous to using the apparatus, an operator would introduce flammable samples into the furnace by hand using a syringe or weigh boat and funnel. Due to the enclosed nature of the pressure vessel, this is impossible to do by hand and requires a way to remotely inject compounds into the furnace. To accomplish this, a remote injection device called the Automated Robotic Injector Arm (ARIA) was designed and constructed. This device is shown in Figure 4.2. The ARIA is constructed from 3D printer parts and can effectively introduce solids or liquids into the furnace. Advantageously, this solution removes potential human error from the AIT measurement process by ensuring that compounds are introduced into the flask in a consistent manner.

In addition, a GoPro® camera is mounted on the side of the furnace to record visible flames. This is an optional addition which helps ensure the quality of our data and allows us to collect video evidence of our experiments. The camera is controlled remotely and is set to capture at 720p at 100 fps. This addition ensures that short visible ignitions are not missed due to human error. The footage may also be timestamped to allow for increased accuracy in measuring the time between introduction of sample and ignition, which is called the lag time.

4.2.2 Apparatus Safety

Ensuring safety was central to the design of the apparatus. The main hazards considered were overpressure, electrical, and fumes from flames inside the oven.

The vessel was pressurized by an air cylinder. The hazard of overpressure was primarily controlled for by two stages of regulation (one to regulate cylinder pressure to about 40 *psig* then a second, high-precision regulator to regulate from 40 *psig* down to about 3 *psig*). Also, a pressure relief valve was installed between the two regulators and designed to relieve pressure before the inlet pressure to the lower-pressure regulator exceeded its design (≈ 250 *psig*).

In addition, a makeshift rupture disk was constructed from thin aluminum foil. This foil was tested and found to consistently rupture at or below 10 *psig*. This "rupture disk" is installed on an outlet of the vessel and allows emergency pressure relief in case of overpressure. Finally, a flow restrictor was installed on the outlet of the regulator, to ensure that a choked flow event could not happen inside the vessel due to high flow rates from a catastrophic failure in the pressure regulators. Pressure spikes from ignition events were also considered but found to be negligible.

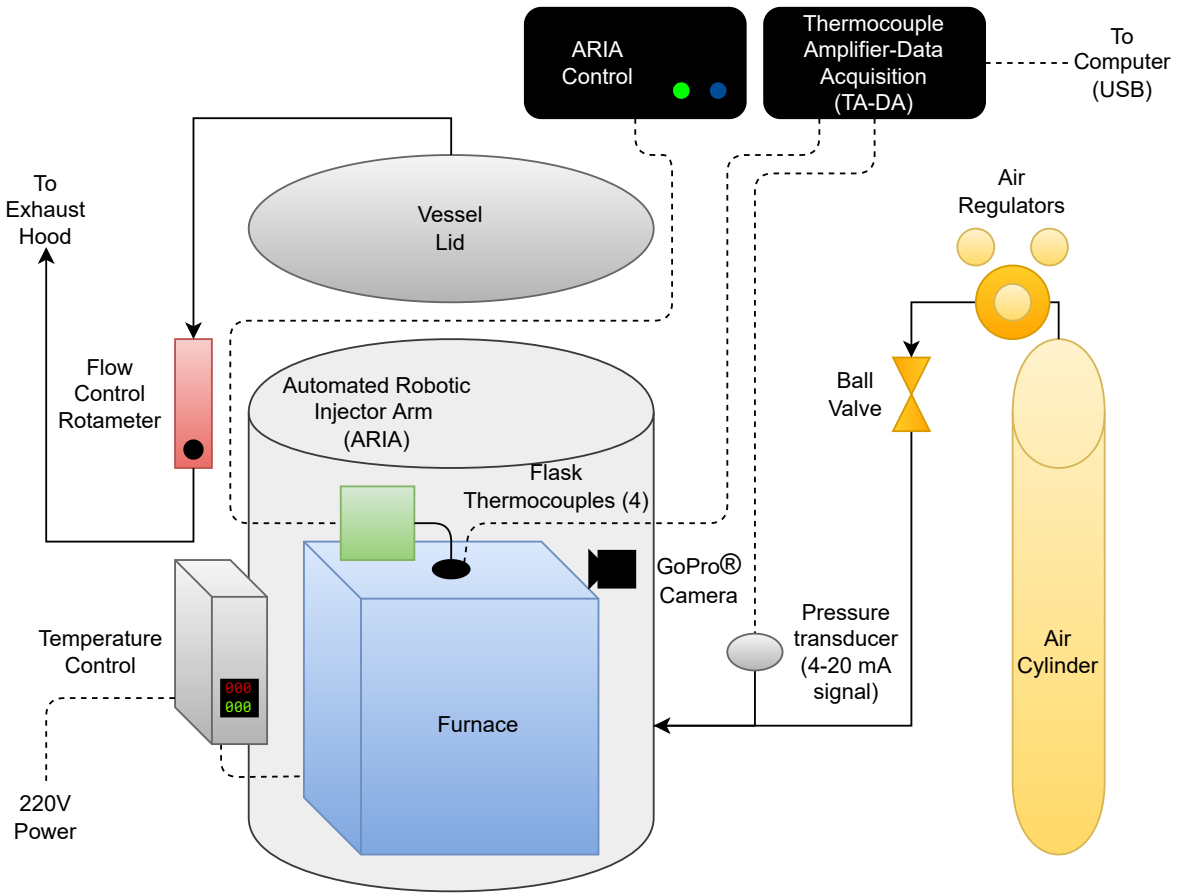

Figure 4.1: Diagram of the AIT Experimental Setup.

Electrical equipment was grounded on the vessel in every case and the grounds were combined to minimize risk of electrical shock. Best practices were employed for insulation to ensure the same. Where possible, wires were solid with no connections. Where connections were needed, wires were crimped into Molex plugs with unidirectional connections. This was done on every level of the process to ensure that wires could not be incorrectly connected. Molex connectors were also designed to be unique to ensure that no incorrect connection was possible.

Finally, the apparatus was too large to fit inside a standard ventilation hood. To ventilate experiments, a ventilation snorkel was plumbed to the apparatus. Smoke tests showed that fumes were effectively removed by the system but required a pair of operators to ensure that minimal fumes escaped when the lid was being opened or closed.

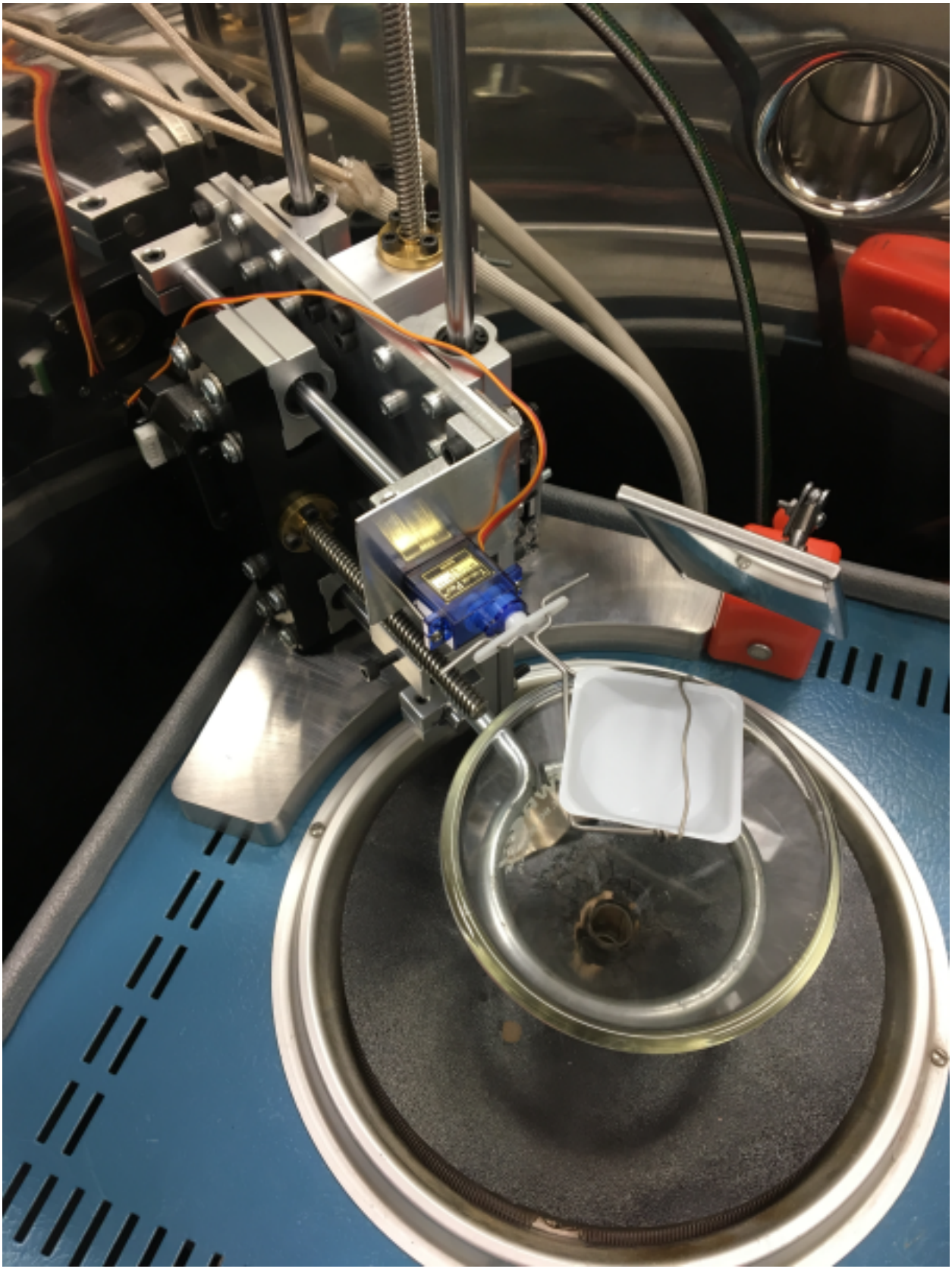

Figure 4.2: The ARIA mounted inside the pressure vessel.

4.2.3 DSC Methodology

Differential scanning calorimetry (DSC) measurements were used in this work to characterize the melting points and temperatures of decomposition for certain compounds. Decomposition temperatures were measured using a TA Instruments® Q2000 modulated differential scanning calorimeter (MDSC). TA Instruments' Tzero aluminum pans were filled with sample and sealed hermetically with Tzero aluminum lids and were tested in conjunction with an identical empty pan for reference. The samples were weighed with a Sartorius® MSE125P microbalance. This balance has a stated reproducibility of 0.015 mg.

The modulated differential scanning calorimeter (MDSC) was calibrated both for temperature and heat flow. First, the MDSC baseline was calibrated using sapphire disks and the temperatures were calibrated using ASTM method E967-08. For this method, the melting points of indium, adamantane, water, tin, and lead were measured which allowed temperature calibration across the range 210 K to 600 K using a cubic spline. The experimental uncertainty in the temperature from this procedure is estimated to be ± 0.5 K.

Daily heat flow calibrations were performed using indium according to ASTM method E968-02 [54]. The purge gas used was nitrogen to reduce the risk of oxidation. Decomposition temperatures were measured according to ASTM method E537-20 at a heating rate of 20 K/min, and then a method identical to the ASTM method but with a higher heating rate of 50 K/min [55]. This was done to more closely approximate the heat rate a compound would experience during an AIT experiment following ASTM E659. ASTM method E537-20 gives a mean repeatability of the decomposition temperature to be 0.52 K. Melting points were measured according to ASTM method E793 [56]. Method E793 has a reproducibility of under 2.8%.

4.2.4 Purity Measurements

Purity data reported in this work were measured by gas chromatography with an Agilent GC-FID instrument (Agilent Technologies 7890A GC System). The column used was a Restek® Rtx-1 (Crossbond 100% dimethyl polysiloxane) with dimensions $30m \times 0.53mm \times 0.25\mu m$. Heating programs were kept isothermal, and temperature was varied until good separation was ob-

served. A ramp rate was then introduced and varied until sharp and resolved peaks were observed. The results were then integrated to produce the percentages reported.

4.2.5 Flash Point Measurements

To confirm no change in flash point behavior with increasing carbon number, flash points for C16 and C26 were measured using ASTM method D3828 [57]. The measurements were made with an ERDCO Rapid Test RT-1 apparatus designed to be compliant with the ASTM method. Barometric pressure was noted and the flash point corrected to 1.0 atm using vapor pressure correlations from the DIPPR 801 database. The reported values are the pressure-corrected values obtained from experiments.

4.3 Recommended Literature AIT Values

Various experimental AIT values exist in the literature for the *n*-alkanes smaller than C20 (*n*-eicosane). Figure 4.3 plots these AIT values versus carbon number. The variance of the AIT values in literature can be attributed to differences in methodology. Despite the variance, the trend is consistent. The AIT of methane is highest and the trend decreases quickly until C7. Then the trend remains relatively constant with respect to chain length. Many other chemical families exhibit similar trends.

To reach a definitive trend, each source from Figure 4.3 was evaluated for consistency with the ASTM E659 method [5]. From this evaluation, a single value for each *n*-alkane was selected as the recommended AIT value shown in Figure 4.4. No experimental data consistent with ASTM E659 exist for C11, C13, C15, C17, C18. Recommended values for these compounds were predicted from linear interpolations between adjacent experimental values.

Before this work, there were no published experimental data for compounds above C20. Based on the family trend from C7 to C19, AIT was thought to asymptotically approach a constant value, the minimum value measured from the smaller compounds.

The trend in the range of carbon numbers up to C20 has been well studied. Gödde et al. proposed that the sharp decrease in AIT for carbon numbers up to C5 was due to the increased sites for the oxidation reaction to take place increased the likelihood of radical formation and

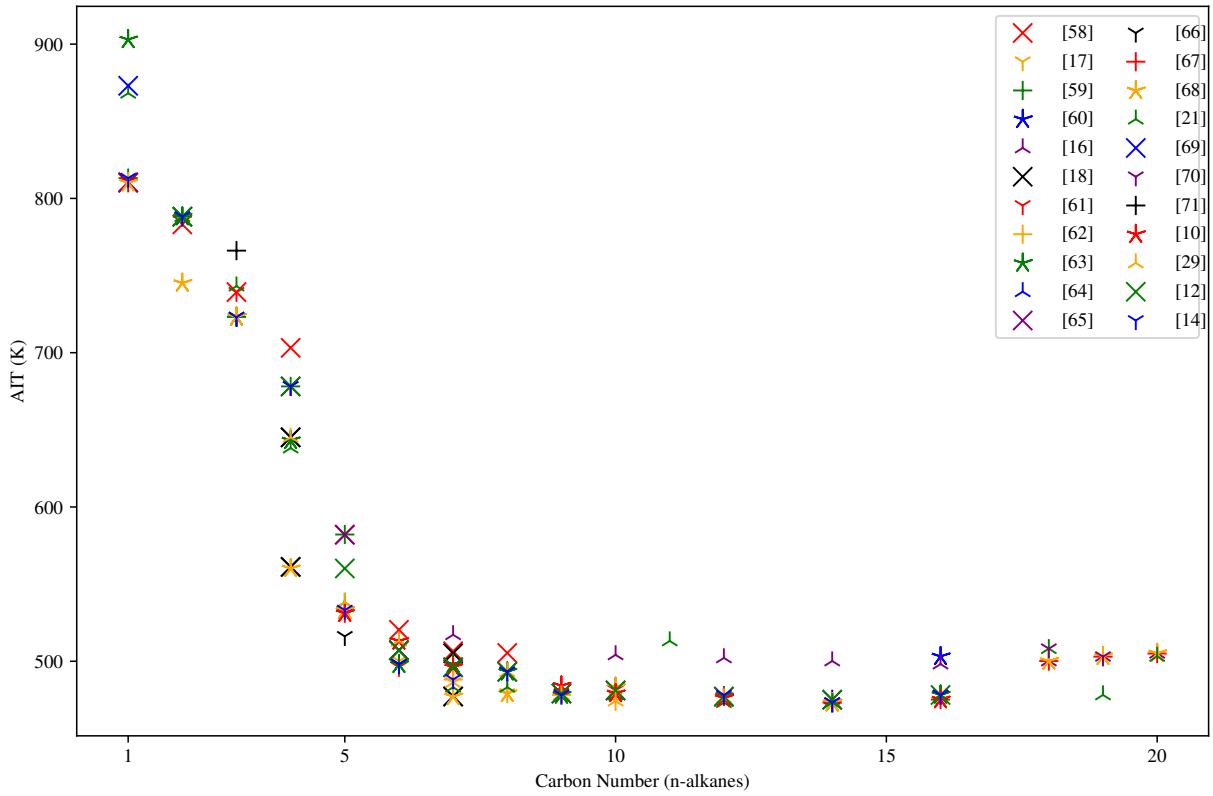

Figure 4.3: Experimental AIT from several sources

subsequent ignition [72]. This explanation does not seem to account for the flattening of the trend around carbon number 7 where the trend does not change significantly up to carbon number 19.

4.4 Results and Discussion

4.4.1 Experiments at Altitude ($\approx 0.85\ atm$)

Figure 4.5 shows the results of AIT experiments done by multiple researchers over several years for the n-alkanes using ASTM E659 but operating at ambient pressure at an altitude of ˜1400 meters above sea level (˜0.85 atm). These are compared to the recommended values from Figure 4.3 and the expected long-chain length trend described previously. A complete table of AIT data is given in Table A.5 in the appendix. Compounds of known AIT were measured to validate experimental methods. The new values below C16 agree with the literature but the values for C20-

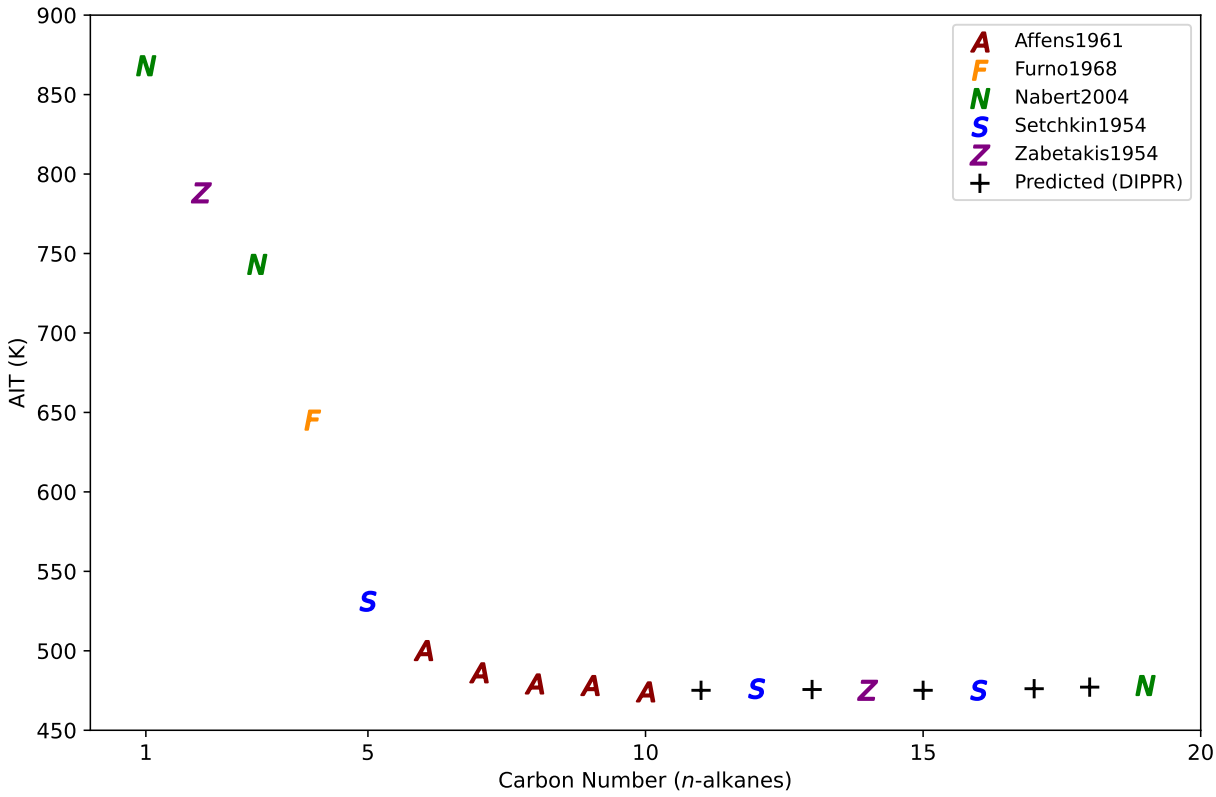

Figure 4.4: Recommended values for the *n*-alkanes for carbon numbers 1-20 and a predicted trend for *n*-alkanes with carbon number > 20. Values were chosen based on the source methodology and its similarity to ASTM E659. Predicted values are linear interpolations between experimental values and the Predicted Trend indicates the expected trend for *n*-alkanes from before this work. The sources are as follows: Affens1961 [17], Furno1968 [18], Nabert2004 [21], Setchkin1954 [10], and Zabetakis1954 [12].

C25 were higher than the expected asymptotic behavior and revealed a large discontinuity between C25 and C26. This discontinuity had not been reported in the literature prior to this work.

These unexpected trends invited further study and were initially hypothesized as due to the higher altitude. Notice the effect of altitude for smaller compounds with literature values including C6 (*n*-hexane), C7 (*n*-heptane), C10 (*n*-decane), and C16 (*n*-hexadecane). The AIT values that were measured at the lower ambient pressure for these species were, on average, 13 K higher than the literature values. This is expected, as the oxidation reaction for autoignition depends on a high collision rate between the fuel and oxygen, and the lower pressure would invariably decrease the collision rate, all other factors being equal. Furthermore, the ambient pressure per ASTM

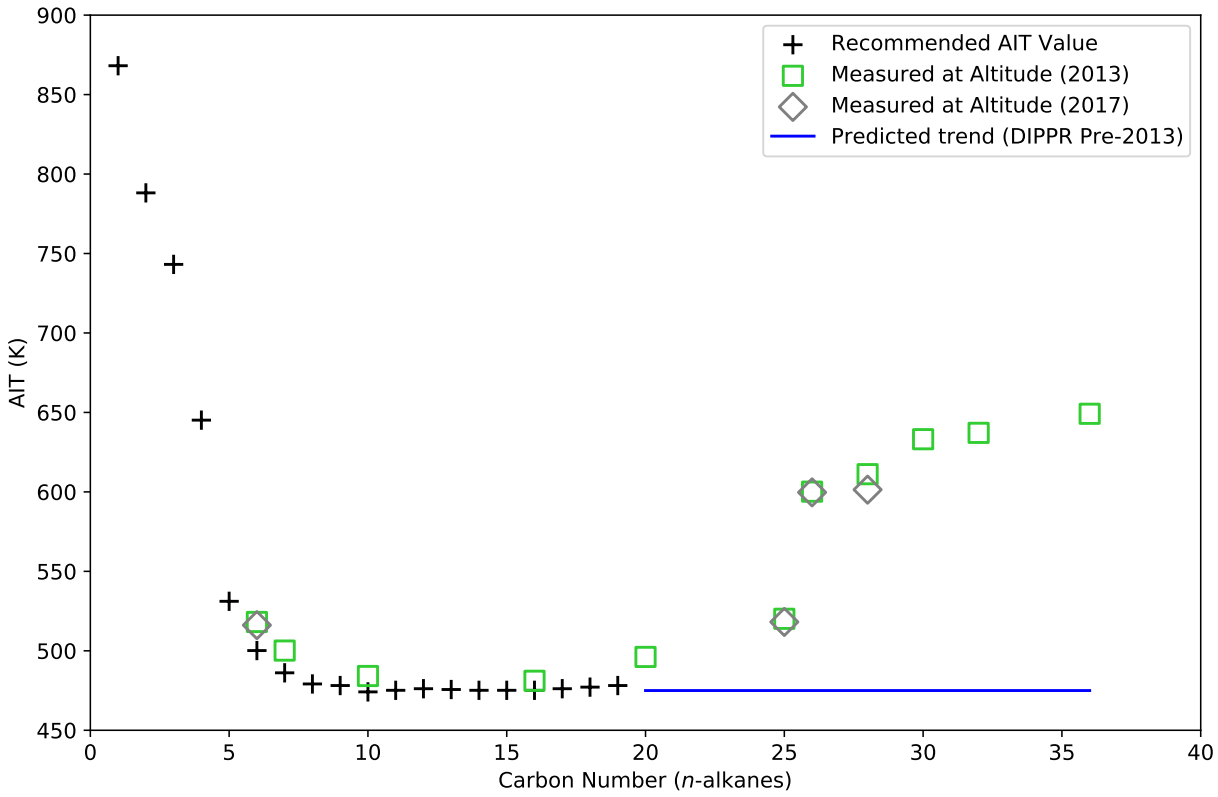

Figure 4.5: Initial AIT experimental results measured at altitude (˜ 0.85 atm ambient pressure) compared with recommended AIT values and predicted trends.

is specified at 1 atm. Therefore, a new apparatus was designed and built to control for pressure effects, maintain a pressure of 1 atm, and thus conform to the ASTM standard.

4.4.2 Experiments at 1 atm

Experiments were conducted for seven *n*-alkanes using the new 1-atm apparatus, including C7 (*n*-heptane), C16 (*n*-hexadecane), C22 (*n*-docosane), C24 (*n*-tetracosane), C25 (*n*-pentacosane), C26 (*n*-hexacosane), and C30 (*n*-triacontane). Samples from several manufacturers were compared for C25, C26, and C30. Table 5.1 gives the results of these AIT experiments along with the corresponding lag times and purities. Purities are reported as the lower value of either the value measured as part of this work or the value reported by the manufacturer. A complete set of purity data are given in Table A.2 in the appendix.

Table 4.1: Experimental AIT values measured at 1 atm with corresponding lag times. Purity values are reported by the manufacturer except where noted.

Cas No.	Compound	C#	Manufacturer	Purity	AIT (K)	Lag Time (sec)
142-82-5	*n*-heptane	7	J. T. Baker	99.4%	493	61
544-76-3	*n*-hexadecane	16	Sigma-Aldrich	99.1%	474	145
629-97-0	*n*-docosane	22	Alfa Aesar	99.9%	498	36
646-31-1	*n*-tetracosane	24	BeanTown Chemical	99.65%[1]	508	210
629-99-2	*n*-pentacosane	25	BeanTown Chemical	99.3%	505	124
629-99-2	*n*-pentacosane	25	Sigma-Aldrich	98.51%[1]	602	2
630-01-3	*n*-hexacosane	26	Alfa Aesar	99.59%	586	3
630-01-3	*n*-hexacosane	26	Sigma-Aldrich	99.6%	581	2
638-68-6	*n*-triacontane	30	BeanTown Chemical	98.48%[1]	607	2
638-68-6	*n*-triacontane	30	Sigma-Aldrich	98.1%	611	3

Figure 4.6 shows the results of the experiments done at altitude along with the 1 atm values just discussed. The values at 1 atm (triangles) are consistently lower than those at altitude showing that AIT depends significantly on pressure. From the validation study of C7 and C16, the values

[1] Measured using GC-FID as part of this work

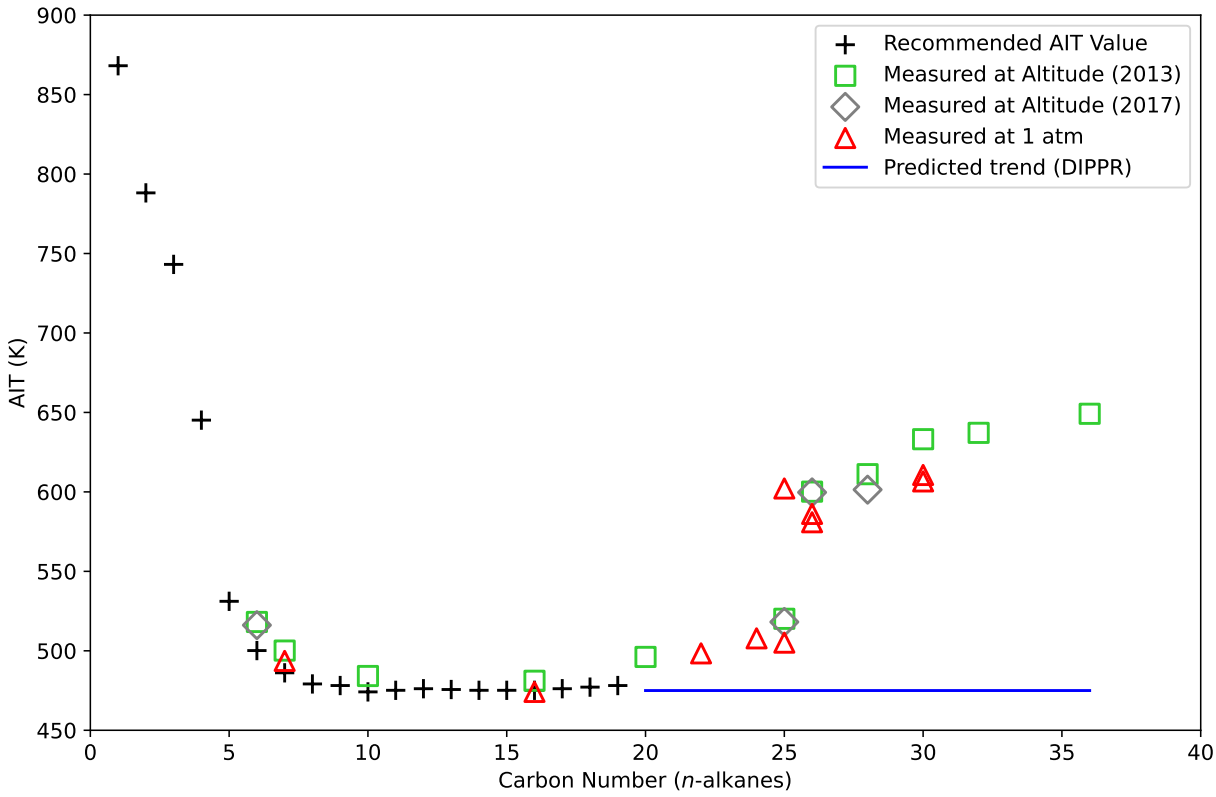

Figure 4.6: Experimental AIT results measured at altitude (˜ 0.85 atm ambient pressure) and 1 atm compared with recommended AIT values and predicted trends.

reported here are expected to accurately reproduce those that would be found with ASTM E659 at sea level.

In the 1 atm experiments, the previously observed deviations in the long-chain AIT trends persisted. First, the AIT rises for C16-C24 and C26-C36. Second is the discontinuity between C25 and C26. The difference between these AITs at 1 atm is ˜75 K, much larger than the changes observed by changing carbon number below or above this feature.

The data in Figure 4.6 show another unexpected feature. Experiments were done for C25 from different suppliers. For one supplier, the AIT value was ˜510 K, which is similar to the values found at both pressures. However, the C25 from another supplier produced an AIT value ˜97 K higher. This discrepancy is discussed in detail later.

4.4.3 Flash Point and AIT

Comparing flash point to AIT explains part of the unexpected trends. Figure 4.7 is a plot of both AIT and flash point versus carbon number. At C15, the flash point is approximately 100 K below the AIT and gradually increases with carbon number. The AIT and flash point trends then begin to approach each other. At C25 they differ by only ˜20 K. The AIT and flash point trend for C26 and higher roughly parallel each other. The flash point trend crosses the predicted AIT trend between C23 and C27.

Flash points values for C20 and higher are predicted by the method of Leslie and Geniesse [73]. As the discontinuity in the AIT trend was unexpected, confirmation was needed to ensure a similar discontinuity in flash point does not occur. To confirm this, the flash points for C16 and C26 were measured using ASTM method D3828 [57]. The value for C16 closely matches the literature values and the value for C26 is within 4% of the prediction [74]. This confirms that flash point exhibits no qualitative deviations from expected trends.

Flash points and AITs are both used to describe the flammability of a fuel, but on different levels. The flash point for a given compound is the minimum temperature at which flame will occur if an ignition source is present. The autoignition temperature is the minimum temperature at which flame will occur without an ignition source. Therefore, if the temperature is high enough to cause a flame without an ignition source (AIT), then the same temperature would allow a flame with an ignition source (flash point). Thus, the flash point should never be higher than the observed AIT for a compound.

Visible flames, the object of study in flash point and AIT experiments, occur in the vapor phase. Therefore, compound volatility influences both AIT and flash point. However, volatility only becomes a significant factor in AIT as compounds increase in size. For *n*-alkanes smaller than C16, the compounds are sufficiently volatile to ensure plenty of fuel is in the vapor phase near the AIT. However, volatility decreases as carbon number increases. Once the volatility of a compound is low enough, there is insufficient fuel in the vapor phase to support a sustained flame. Thus, the temperature must be higher to have enough fuel in the vapor phase to allow for autoignition to occur.

Therefore, the AIT trend cannot remain flat as indicated by the predicted trend (solid line) in Figure 4.7. Even if the AIT were equivalent to the flash point, a rise in AIT must inevitably occur.

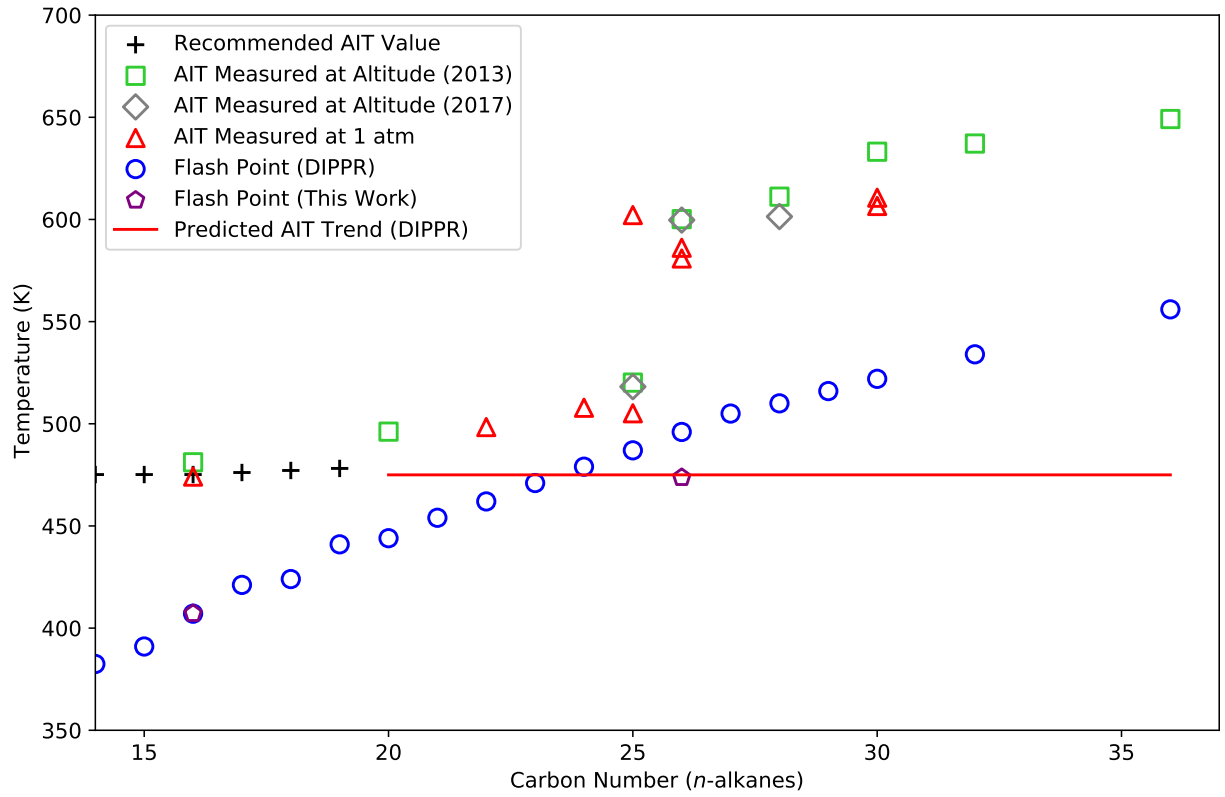

Figure 4.7: Experimental AIT results for selected compounds with carbon numbers 16 - 36 and recommended AIT values compared with recommended flash point values from [52] (Database name: DIPPR801_Sponsor_May2019) and measured according to ASTM method D3828 [57].

For compounds C16-C36, the gradual rise in AIT likely results from the decreasing volatilities of larger compounds. This relationship may be used to predict AIT trends for all compounds as volatility decreases with increasing size and molecular weight.

4.4.4 The Discontinuity Between C25 and C26

The most unexpected feature in the AIT data (see Figure 4.7) is the 75 K difference between C25 and C26. There is no obvious reason for a discontinuity to appear in AIT family trend. Using the 1-atm apparatus, C30, C26, and C25 were measured. All three samples were purchased from Sigma-Aldrich. The results from C30 and C26 are only ˜25 K lower than corresponding values obtained at ambient altitude pressure. This confirms that lower pressure does increase the AIT but is not the cause of the discontinuity. The C25 sample from Sigma-Aldrich returned an AIT value

more than 80 K higher than the value obtained at altitude. This made the C25 value fall more closely in line with the larger *n*-alkanes than the smaller ones. New samples of C25, C26, and C30 were sourced from Alfa Aesar and BeanTown Chemical to ensure the differences observed were not due to unknown source variables nor contamination. Upon re-measurement, C26 (Alfa Aesar) and C30 (BeanTown Chemical) produced similar values to the Sigma-Aldrich samples and the C25 sample (BeanTown Chemical) returned a value consistent with the smaller *n*-alkanes.

Purities and Multiple Solid Phases

Several experiments were done to investigate the discrepancy between the C25 AIT values from difference sources. Purity and crystallinity were examined. Either of these properties could explain observed discrepancies. Contamination can elevate a measured AIT significantly, and the crystalline structure can influence the melting point which confounds the AIT results.

As described in Section 4.2.4, the purity of the samples was measured using gas chromatography, and Table A.2 shows these experimental results as well as the purity values reported by the manufacturer. Purity values are omitted where values were not measured or the manufacturer certificates of analysis could not be obtained. Both the purities from GC-FID and the manufacturers show sufficiently high purity, eliminating contamination as the source of the discontinuity in AIT and the discrepancy between the C25 samples.

Once contamination was ruled out, crystal structure was investigated. The C25 samples that produced the higher and lower AIT values were sourced from Sigma-Aldrich and BeanTown Chemical, respectively. The two samples differed in their physical appearance. The sample from Sigma-Aldrich was composed of small waxy flakes that tended to clump into balls a few millimeters wide, and the BeanTown Chemical sample was made of larger shiny flakes that could be up to a couple of millimeters wide with no clumping. The samples were tested for different crystal polymorphs.

Melting points of each sample of the compound were measured using DSC using ASTM method E793, and the results are shown in Figure 4.8. Both samples were next examined using X-ray crystallography to determine if any differences in crystal structure could be found. Figure 4.9 shows the results of these experiments. The DSC and X-ray crystallography data for both samples

are virtually indistinguishable, eliminating differences in purity and crystalline phases as the cause of the discrepancy between the two C25 AIT values.

Observed Combustion Mechanisms

Competing mechanisms were next hypothesized to cause the discontinuity between C25 and C26, and the discrepancy between the C25 samples. Experiments with C26 (using the Alfa Aesar sample) were performed to observe differences inside the combustion environment. In the normal procedure, the phenomena that happen inside the chamber are not directly observed because the flask is inside an opaque furnace. Thus, the 500 mL bulb flask was removed from the furnace, mounted on a ring stand, and heated with a Bunsen burner. A thermocouple was placed inside the flask to measure the internal flask temperature. The flask was maintained at temperatures both above and below the measured AIT. Samples were introduced as before, and the results were filmed to observe compound behavior inside the flask environment. Because the flask is removed from the furnace with its precisely controlled temperature, only qualitative results are shown below. However, ASTM E659-compliant experiments were also performed with the normal apparatus and procedure to provide corresponding numerical results for the situation. The outcomes of the Bunsen-burner experiments are shown in Figures 4.10 and 4.12 with comparable temperature vs. time plots in Figures 4.11 and 4.13.

Figure 4.10 shows the results of an experiment where the internal temperature was below the AIT. The plot in Figure 4.11 shows the temperature and pressure measurements inside the vessel for an experiment at a similar temperature to Figure 4.10 but where the experiment is carried out in accordance with ASTM E659 methodology. Notice in Figure 4.10 that the sample melts, and, within 10 seconds, visible smoke or vapor is produced. Over time, the sample boils and the smoke/vapor continue to slowly swirl inside the flask. At lower temperatures, the temperature curve can produce significant heat as in Figure 4.11 but often is accompanied with fluctuations in temperature until the fuel completely diffuses out of the flask without igniting. This suggests the presence of both exothermic and endothermic processes.

In contrast, completely different behavior is found at flask temperatures above the AIT. In this case, ignition happens before any sample reaches the bottom of the flask. This type of event is shown in Figure 4.12. In the first frame of the figure, the falling flakes of sample are circled in

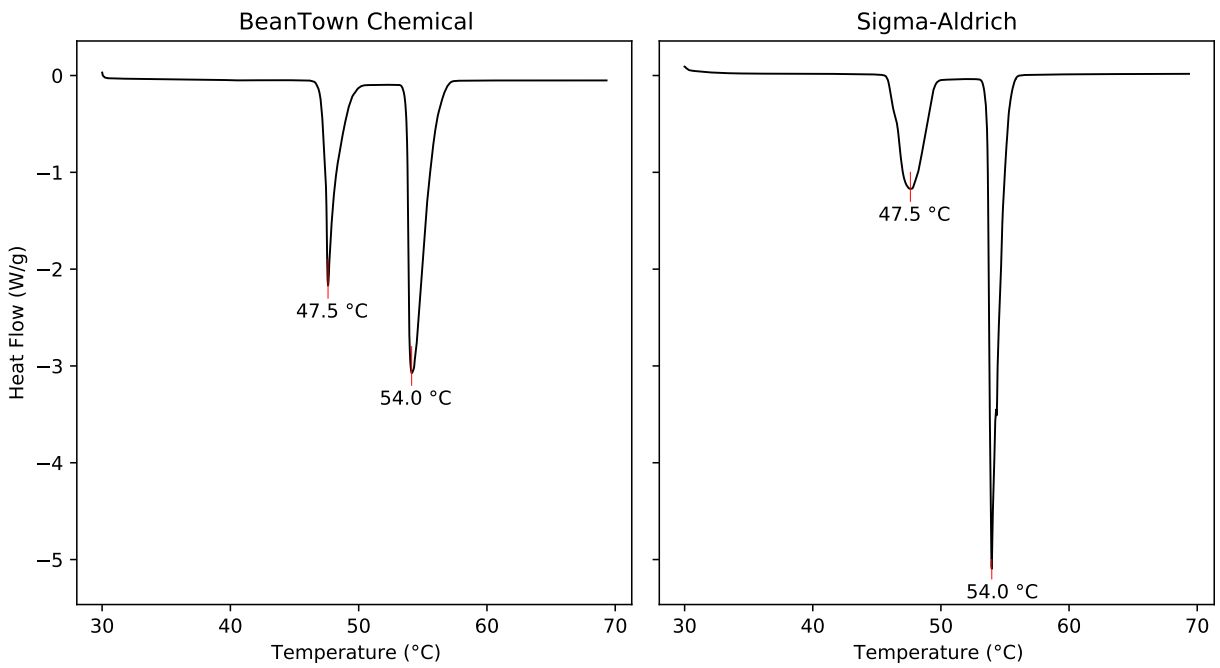

Figure 4.8: Melting point measurements for 2 samples of *n*-pentacosane (C25). Generated with differential scanning calorimeter (TA Instruments® Q2000). The plot on the left corresponds to the sample from BeanTown Chemical and the plot on the right corresponds to the sample from Sigma-Aldrich. The two peaks in each plot indicate a solid-solid phase transition (the left peak) before melting occurs (the right peak).

red. These flakes never reach the bottom of the flask before vaporizing. Ignition begins near the top of the bulb in the second frame less than a tenth of a second later leading to a yellow flame. As depicted in Figure 4.13, which is an ASTM E659-compliant experiment at a temperature above the AIT, autoignition occurs quickly upon sample introduction, rapidly increasing the temperature in the flask, with violent flames lasting a fraction of a second and an audible expulsion of gases.

Further insight is available by considering experiments with other *n*-alkanes. To demonstrate, Figure 4.14 shows the temperature curves for three compounds: C6, C25, and C26. In an experiment, the flask is set at a temperature and a sample of compound is introduced into the flask. This results in a small temperature drop as the compound melts and/or vaporizes. After some time, ignition occurs causing a temperature spike. At this moment, a visible flame appears and consumes the fuel. Once the flame disappears, the temperature returns to the set temperature. This general pattern is found for all compounds in the *n*-alkane family.

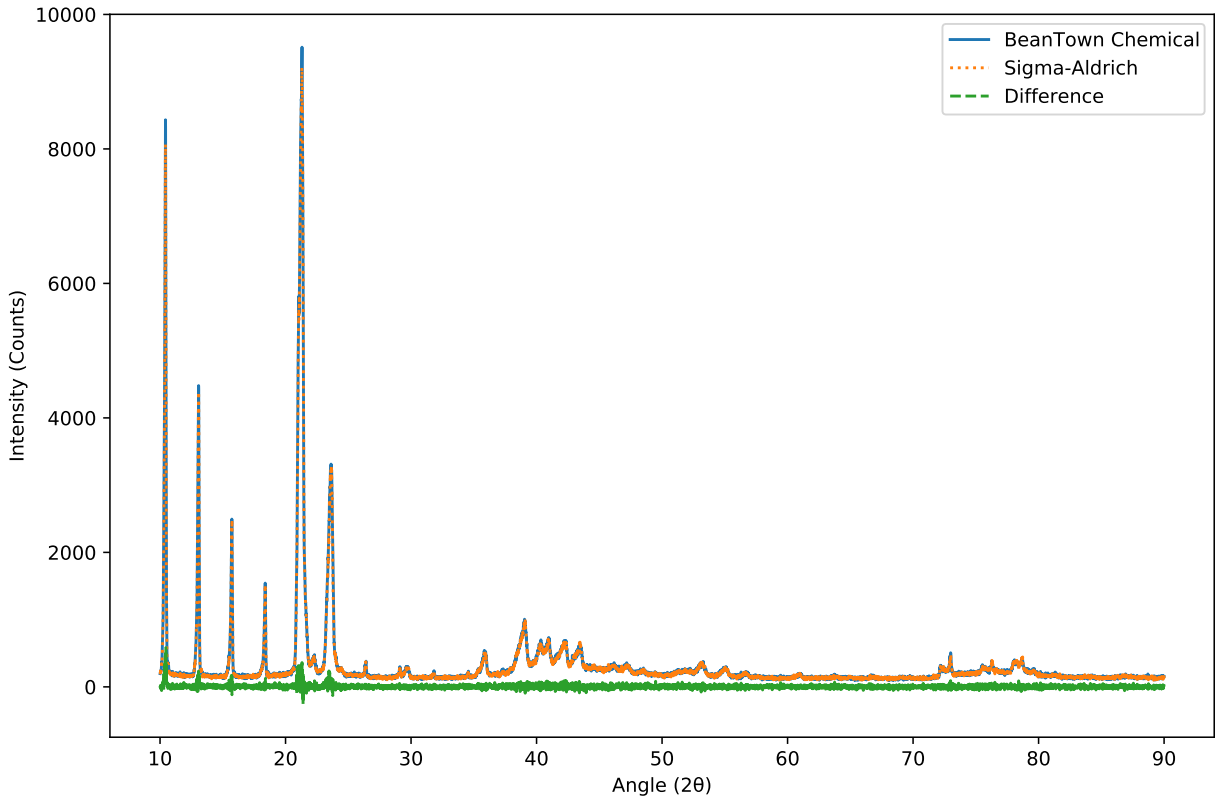

Figure 4.9: Plot of X-ray crystallography scans for two *n*-pentacosane samples from BeanTown Chemical and Sigma-Aldrich. The difference between the scans is indicates negligible differences between the two compounds' crystal structures.

For lower-carbon-number compounds like C6, we see a drop in temperature then a rise as slow combustion produces heat until the reaction runs away, producing a temperature spike and a visible flame. For C25 by contrast, the lag time is much greater. After the initial drop, the temperature fluctuates for some time before ignition occurs. Temperature vs. time plots for C22, C24, and C25 experiments commonly feature similar temperature fluctuations like those seen in Figures 4.11 and 4.14 (C25). Fluctuations in C22 experiments are noticeably more subtle than in the C24 and C25 experiments. Such fluctuations are not present in the C6, C7, and C16 plots, which are instead like the C6 plot in Figure 4.14.

In the case of C26 and larger compounds, the same fluctuations are observed at temperatures below their AIT values. This behavior persists down to the limit imposed by flash point as, at temperatures extrapolated from the trend from C20–C25, the fluctuations continue to occur for C26, similar to the C25 behavior but without the ignition event. C24 likewise has similar fluctua-

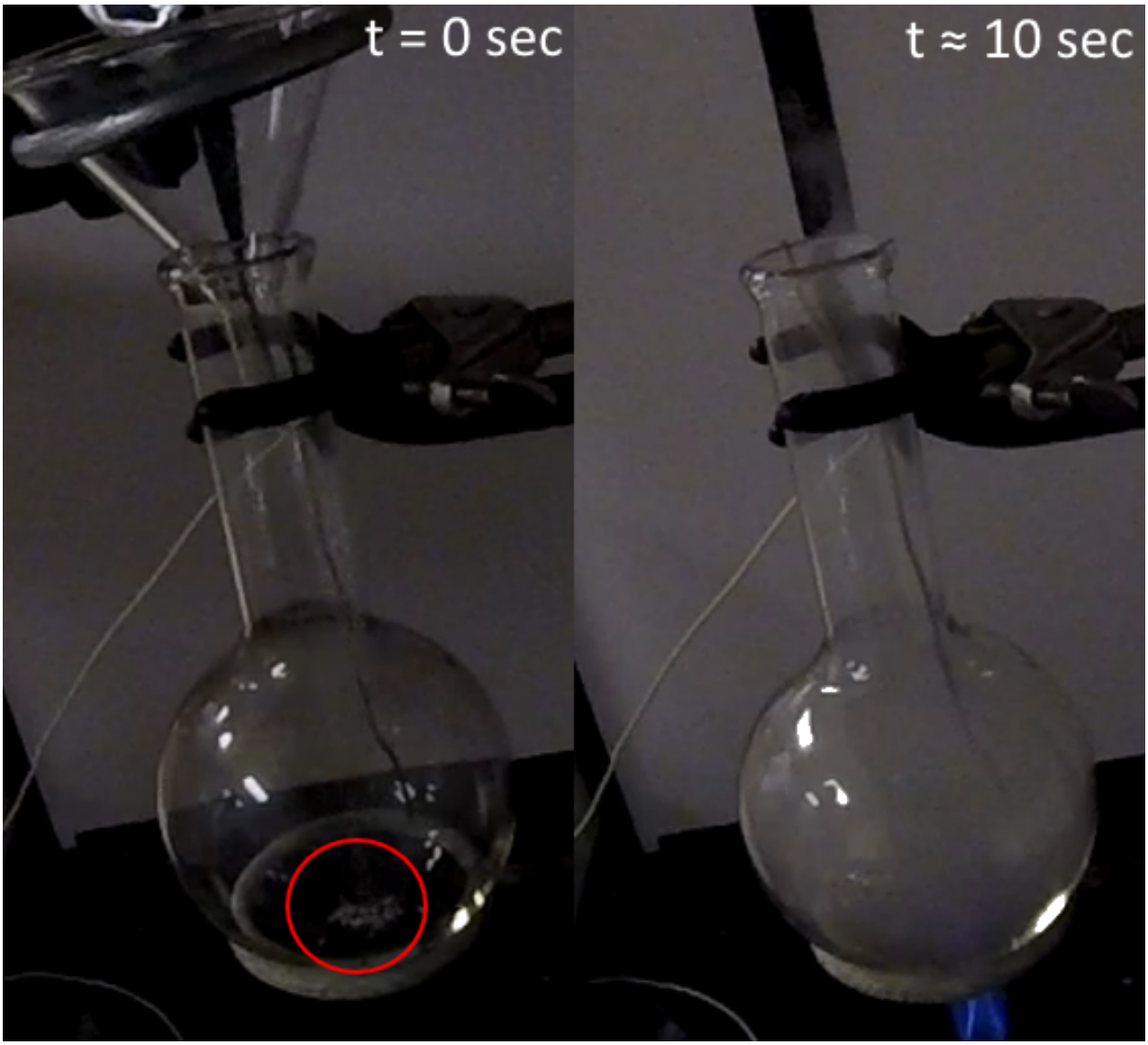

Figure 4.10: An autoignition experiment on *n*-hexacosane (C26) where the internal flask temperature is lower than the AIT. Upon introduction, the sample lands at the bottom of the flask and quickly forms a liquid puddle. This is highlighted by the red circle in the image on the left. After about 10 seconds a large cloud of visible smoke or vapor forms inside the flask. Heat is produced as some oxidation takes place.

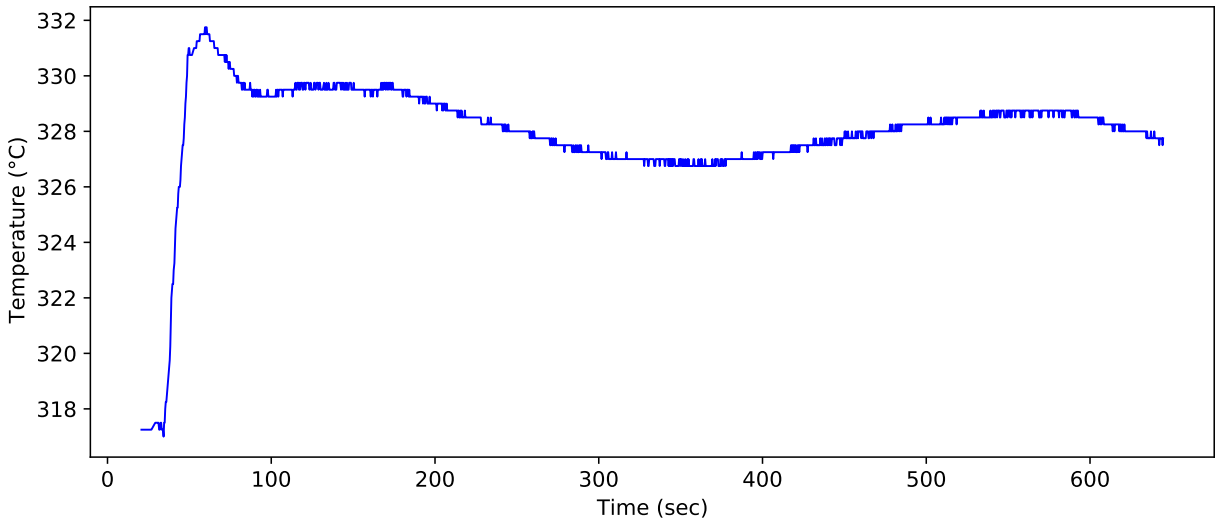

Figure 4.11: A plot of the internal flask temperature an experiment using ASTM E659 methodology for 150 mg of *n*-hexacosane (C26) at 317 °C, which is a temperature near its AIT. No ignition event was observed.

tions implying this is not limited to only two compounds. However, as temperature increases above the AIT, the temperature fluctuations become insignificant and the lag time shortens. At the higher temperatures, the behavior of the larger compounds is therefore much more like the behavior of C6 in Figure 4.14. The only difference is that they have much shorter lag times because they occur at higher temperatures.

Lag time data show a discontinuity similar to the AIT data. Figure 4.15 shows the AIT measured for several n-alkanes along with the corresponding lag time at the same temperature. The unfilled bars are the AIT for the compound and correspond to the left vertical axis, while the filled bars are the lag times as indicated by the right vertical axis. The variance in lag time is likely due to methodological factors and is insignificant compared to the abrupt change in lag time at C25. The C25 sample from BeanTown Chemical, with its lower AIT value, returned a lag time exceeding 100 seconds while the C25 sample from Sigma-Aldrich and both C26 samples have AIT values greater than 80 K higher and lag times under 4 seconds. Overall, lag times of compounds with higher AIT values (i.e. the AIT is greater than about 550K) are consistently an order of magnitude or more lower than the other compounds.

These observations are consistent with the lag time trends and correlations in literature. Zabetakis et al. noted that the lag time asymptotically approaches zero as temperature increases [12].

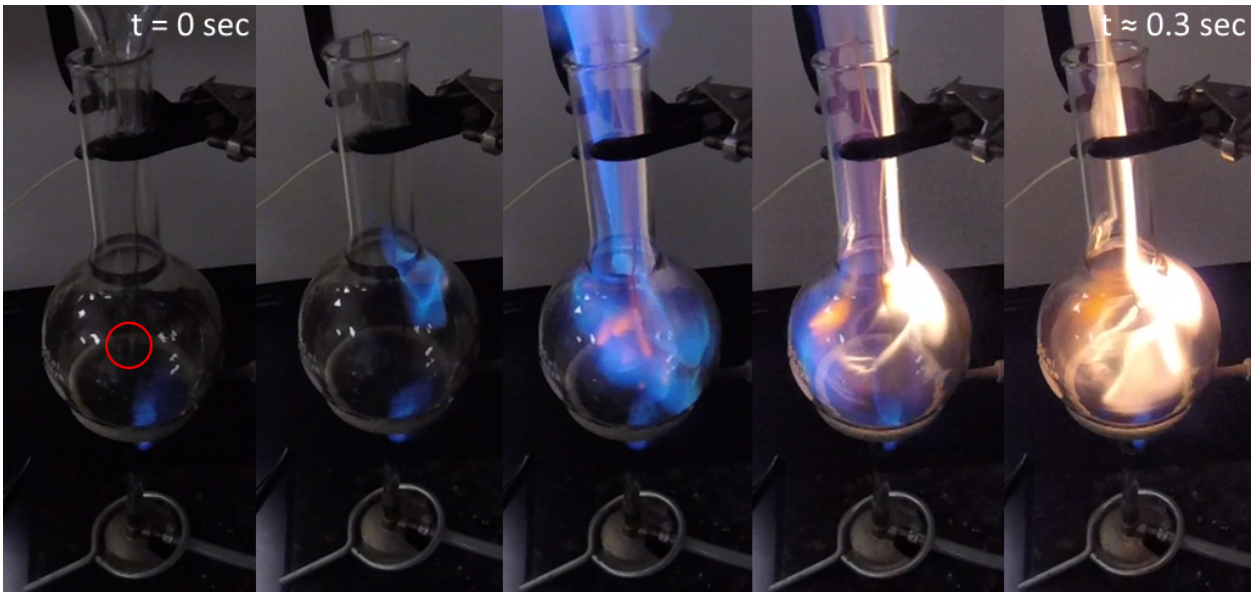

Figure 4.12: An autoignition experiment on *n*-hexacosane (C26) where the internal flask temperature is greater than the AIT. Upon introduction, the sample does not reach the bottom of the flask before vaporizing. A few flakes are still falling, as highlighted by the red circle in the image on the far left, but never reach the bottom of the flask. Within a couple of camera frames from the moment of introduction, an ignition event forms near the top of the flask (see the second image from the left) and quickly proceeds to a runaway combustion event within about 0.3 seconds from the moment of introduction.

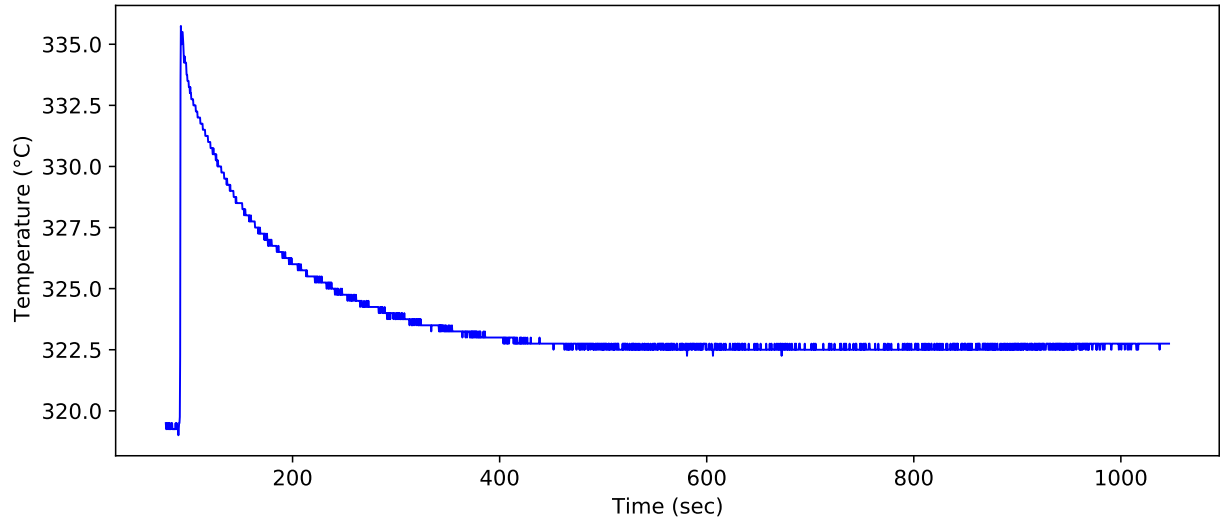

Figure 4.13: A plot of the internal flask temperature for an experiment using ASTM E659 methodology for 150 mg of *n*-hexacosane (C26) at 319 °C, which is a temperature near its AIT. A hot-flame ignition event was observed.

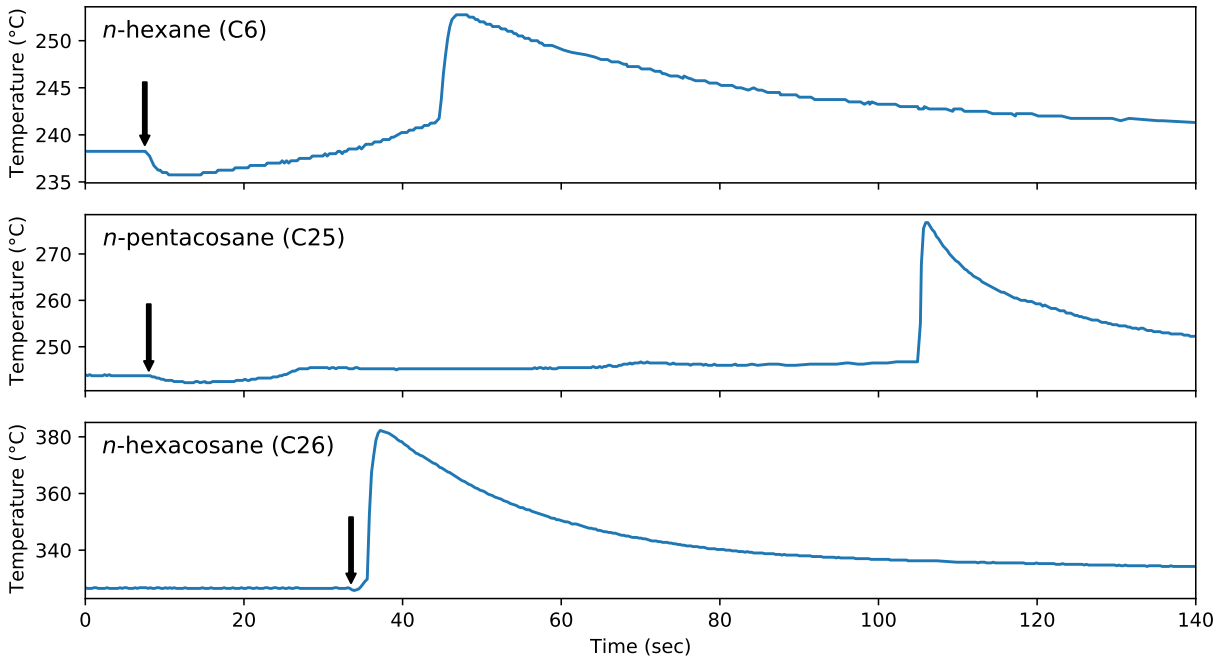

Figure 4.14: Temperature vs. time plots for 3 compounds. The arrows indicate the moment of introduction of the sample into the AIT flask. Ignition is indicated by a sharp temperature rise such as the spike at about 45 seconds for *n*-hexane.

This behavior is consistent with the trend seen in Figure 4.15. Since lag times are a manifestation of combustion kinetics, these results suggest that similar kinetic mechanisms control the combustion reactions for all of the compounds measured, including the combustion mechanisms of C25 and C26. Thus, the discontinuity between C25 and C26 does not result from disparate exothermic combustion mechanisms.

The results and patterns described above suggest that that exothermic combustion increasingly competes with an endothermic process as carbon number increases. The competition between these processes explains the temperature fluctuations and the patterns with increasing carbon number. A separate endothermic mechanism also explains the qualitative consistency seen in the lag time data, the endothermic mechanism being insignificant at the higher temperatures.

Changes to the ASTM E659 Method

To fully rule out the possibility that the discontinuity was not an artifact of the methodology, modifications were made to the E659 Method. These modifications included two sets of

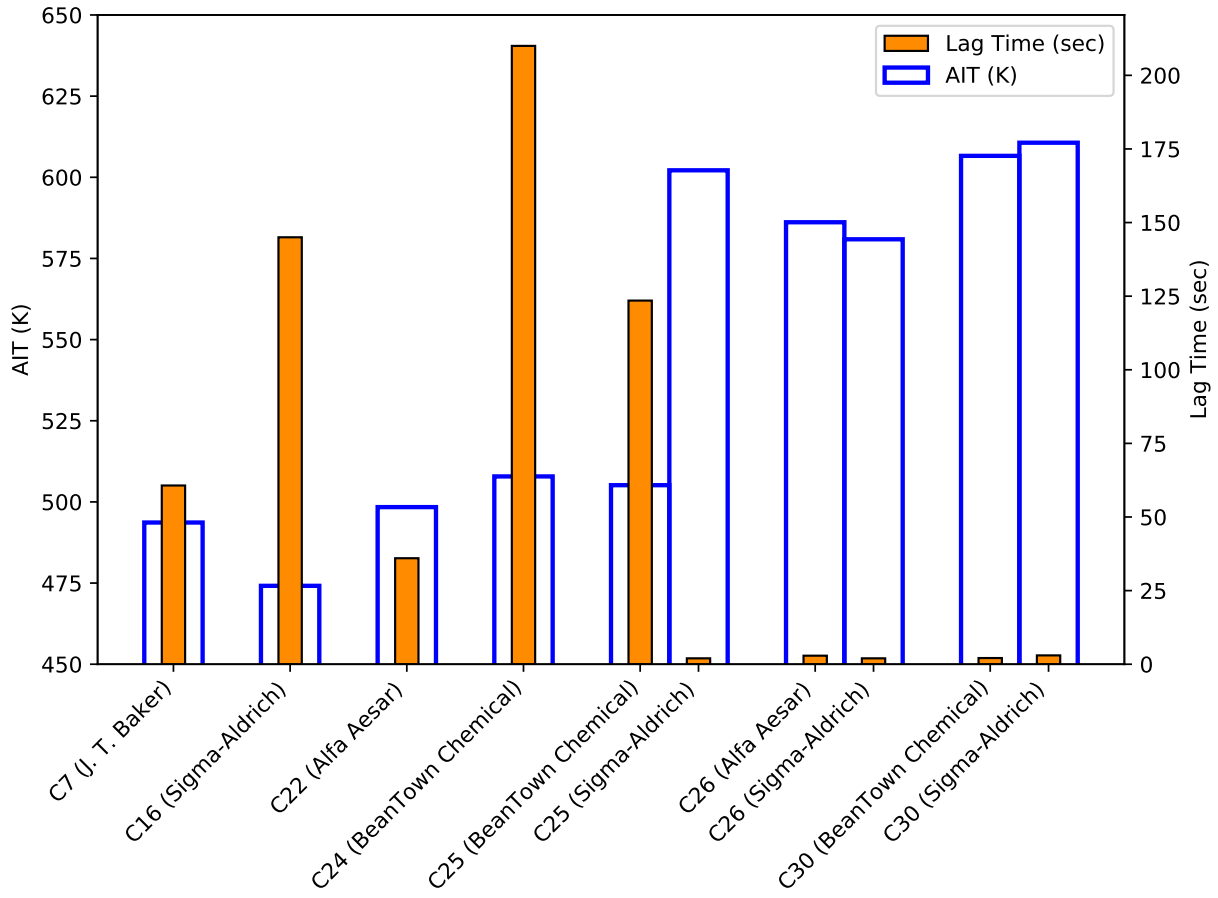

Figure 4.15: Measured AIT and lag times for all compounds measured in this work. Compounds are the normal alkanes with their carbon number given along with the manufacturer of the sample in parentheses Lag times for compounds with higher AIT values are all ≤ 3 seconds.

experiments, one where a larger 12 L flask and correspondingly larger AIT oven were used, and a second where hot air was continuously blown into the flask. Both sets of experiments were intended to account for the apparent lack of oxygen present in the combustion environment.

AIT experiments for *n*-hexacosane were modified by using a 12 L bulb flask and experiments were carried out at altitude ($\approx 0.85\ atm$). An oven originally designed to measure flammability limits was modified to accommodate the larger flask. Several, larger standard sample sizes were used and examined to find minimum AIT values using this new methodology. However, the methodology adhered to ASTM E659 methodology, in all other respects. The results of these experiments are shown in Figure 4.16.

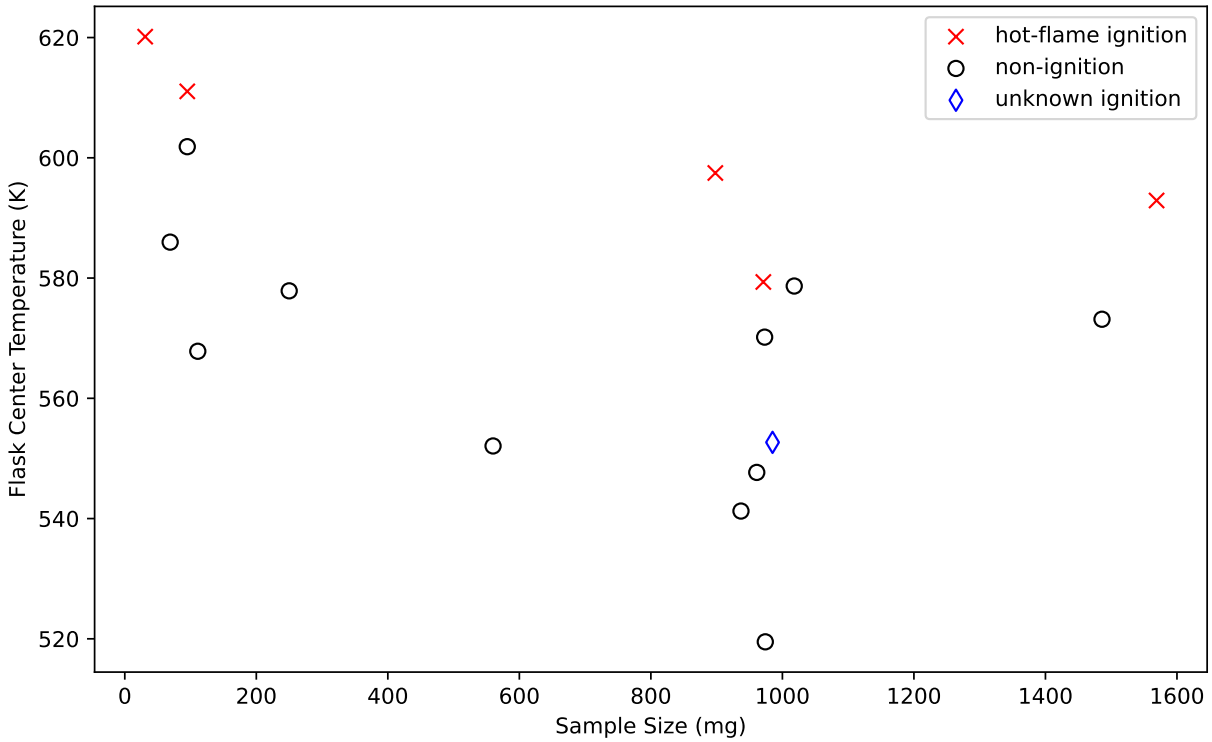

Figure 4.16: Experimental results for *n*-hexacosane using a 12 L bulb flask for AIT measurement.

The results showed no significant decrease in the measured AIT. In one case, a large temperature spike was observed but operators were unable to determine if a visible flame occurred or not. This corresponds to the "unknown ignition" in the scatter plot and may indicate a minimum ignition at a lower temperature. However, Coffee uses Beerbower's observations to predict the change in AIT from different based on Equation 4.1 [4, 59].

$$T_2 = 75 + (T_1 - 75)\left(\frac{12 - log_{10}(V_2)}{12 - log_{10}(V_1)}\right) \tag{4.1}$$

In this equation, T_1 is the AIT observed using a flask with volume V_1, and T_2 is the predicted AIT given the new volume V_2, with the temperatures in ^oC and the volumes in units of liters. Even if the difference in altitude is neglected, which would lower the AIT further, the value of the unknown ignition lies above the predicted AIT for the larger volume (~ 555 K). Because of this, we can confidently assume that the discontinuity is not due to a limitation based on the volume of the flask.

Similarly, hot air was injected into the flask to attempt to allow good mixing and constant fresh air to be introduced into the combustion environment. A modification to the apparatus was constructed and a demonstration of the modification is given in Figure 4.17.

This apparatus was tested using various flow rates. This modification proved to not affect the measured result significantly and, at higher flowrates, increased the measured AIT slightly. This is consistent with observations compiled by Babrauskas [4].

These experiments showed clearly that the discontinuity was no artifact of methodology and that there must be some fundamental phenomenological explanation for the discontinuity. Therefore, other possibilities were considered.

DSC Decomposition Measurements

The endothermic process leading to temperature fluctuations was hypothesized to relate to decomposition of the fuel before autoignition. To investigate this further, decomposition temperatures (DCT) were measured using DSC according to the ASTM E537-20 method. Additional ASTM E537-20 experiments were conducted with a modified heating rate of 50 K/min to better approximate the heating rates that would exist in the AIT oven. Table A.3 lists the results of the decomposition experiments with 95% confidence intervals. Figure 4.18 plots these DCT values and the lowest measured AIT values for each compound.

Notice that for C16 the DCT is significantly above the AIT and for C22 - C25 the DCT is lower than and/or within 7.0% of the AIT. These data show that significant decomposition occurs near the AITs for the *n*-alkanes approaching C25 and suggest that decomposition increasingly influences the measured AIT as carbon number increases. Also, DCT measurements confirm that decomposition for the *n*-alkanes is endothermic. Both observations support the conclusion that the temperature fluctuations are from endothermic decomposition competing in parallel with exothermic combustion.

In these experiments, the higher heating rate produced DCT values consistently higher than the lower heating rate. These differences are likely the result of the change in kinetics of reaction. The heating rate experienced by samples in the AIT oven are orders of magnitude higher than 50 K/min. Therefore, significant decomposition would likely occur at a higher temperature in the AIT oven than the data for 50 K/min show.

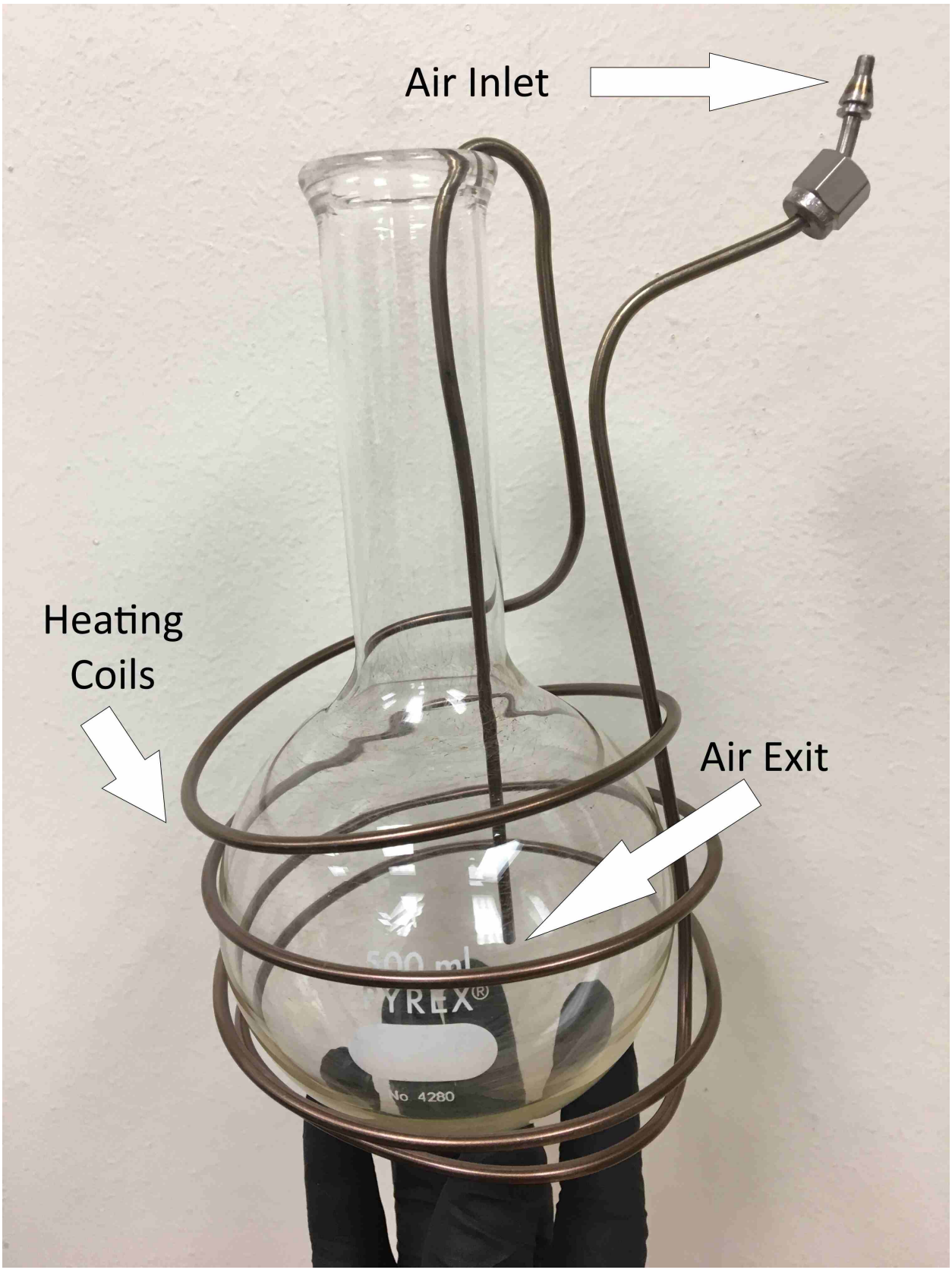

Figure 4.17: Demonstration of the modification to inject hot air into the apparatus. Air would be introduced via the air inlet and sent into the oven chamber to preheat the air (via the heating coils) before introducing the hot air into the flask at the air exit.

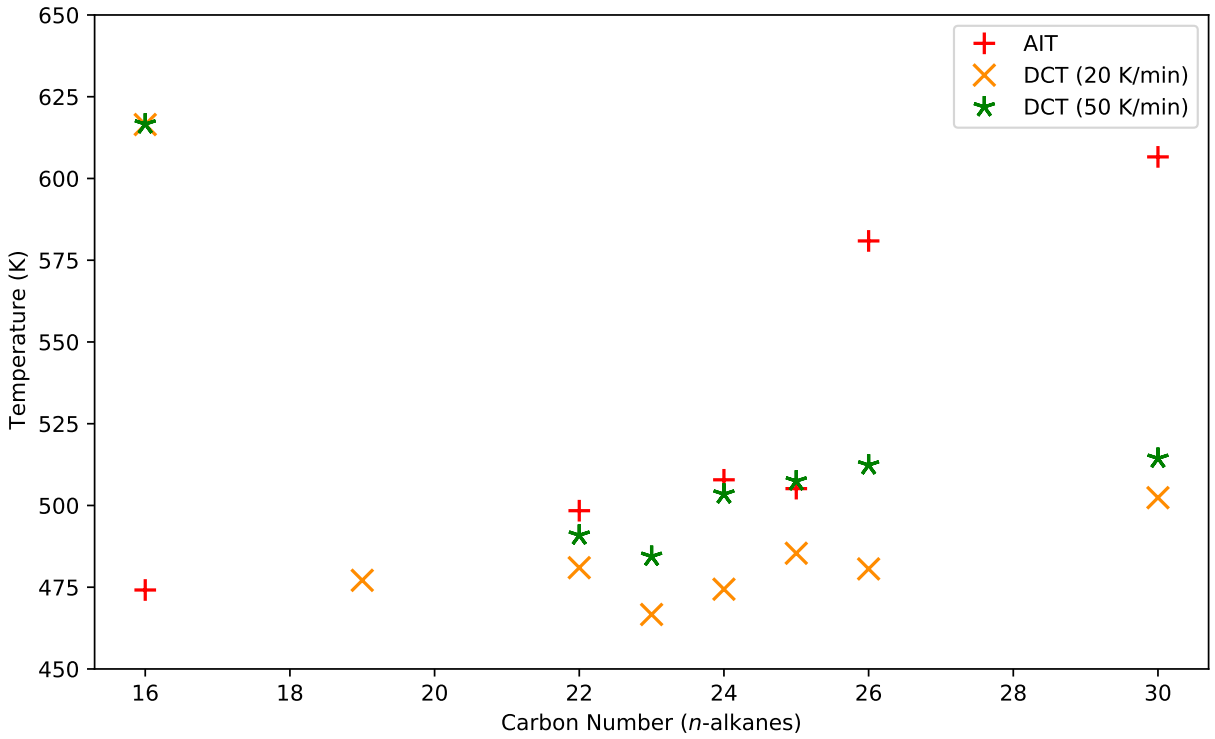

Figure 4.18: Measured autoignition temperatures (AIT) and decomposition temperatures (DCT) at 20 and 50 K/min heating rates for select *n*-alkanes.

Competing Mechanisms

All of the results presented in this section (Section 4.4.4) support the conclusion that the C25-C26 discontinuity is a result of two competing mechanisms and the shift in dominance between those mechanisms occurs between C25 and C26. One of the mechanisms is the exothermic "combustion" process that leads to autoignition by radical chain-branching. The other is the "decomposition" process which endothermically lowers the temperature and consumes fuel. The DCT may be thought of as a temperature at which significant decomposition occurs. Thus, the DCT values in Figure 4.18 show that decomposition begins to occur at a significant rate at temperatures near 510 K, with the prevalence of decomposition increasing with carbon number.

At carbon numbers below C20, the combustion process appears to dominate with little decomposition occurring near the AIT. Therefore, the decomposition process has little effect on AIT. As the carbon number approaches C25, the effects of decomposition begin to appear as temperature fluctuations as the endothermic decomposition lowers the temperature and combustion increases

the temperature. Despite this, the combustion process still dominates ensuring the AIT remains relatively low. But the lag time increases significantly as competition between the mechanisms delays the autoignition event.

For compounds larger than C25 below their measured AIT, decomposition prevents thermal runaway by consuming fuel and energy faster than combustion can produce energy, thus preventing autoignition. The temperature fluctuations seen in Figure 4.14 demonstrate this phenomenon. Some combustion occurs and produces heat and the temperature increases. The increase in temperature likewise increases the rate of decomposition, which then consumes generated heat and some fuel and the temperature drops. As the temperature drops, the decomposition rate slows and allows the combustion process to produce more heat. Thus, temperature fluctuations are observed. Therefore, the temperature must be elevated to allow the combustion process to dominate for the larger compounds. The higher temperature increases the combustion reaction rates to be greater than the decomposition reaction rates, allowing autoignition before decomposition can significantly affect the system.

At C25, the two mechanisms are competing so closely that small variables influence which mechanism dominates. Because of this, the discrepancy in AIT between the different C25 samples can be attributed to the fact that the sample from Sigma-Aldrich formed balls and, having less surface area, experienced a lower overall heating rate. As explained above, DCT values at the different heating rates show that significant decomposition occurs at higher temperatures with increasing heating rate. Therefore, a lower heating rate lowers the decomposition temperature and allows decomposition to prevent thermal runaway at a lower temperature. The BeanTown Chemical sample, by contrast, had more surface area leading to a higher heating rate, increasing the decomposition temperature, and allowing thermal runaway and autoignition at a lower temperature. C25 represents a tipping point where the dominant mechanism shifts from combustion processes to the decomposition process for C26 and larger molecules.

4.5 Conclusions and Recommendations

Measured AIT values for several *n*-alkanes are presented in this work. Based on these measurements, ASTM-E659-consistent values for AIT for the *n*-alkanes with carbon number up to 36 are recommended in Table A.4. Where experimental data lacks, AIT values are predicted

by considering the available data and using conservative estimation techniques. The experimental values include those measured in this work using a specialized apparatus to ensure consistency with ASTM E659 method at altitude. In measuring, previously unexpected AIT trends were observed and explained by observation of other chemical properties that relate to AIT.

The gradual rise of AIT for C16 - C25 is attributed to the lower volatility (or increase in flash point) of larger compounds. For larger compounds, insufficient amounts of fuel vaporize at ˜ 475 K (the minimum AIT for the *n*-alkanes) to support a visible flame. This supports the idea that AIT is always greater than flash point. This phenomenon is not specific to the *n*-alkane family and may be a lower bound for AIT prediction.

The C25-26 discontinuity in AIT is attributed to a shift in favorability between combustion and decomposition processes at temperatures near 510 K. For *n*-alkanes C26 and above, a higher temperature is needed to ensure autoignition takes place before significant decomposition occurs. The decomposition temperature may be used as a starting point to estimate the decomposition temperature of compounds subjected to a heating rate like that of an AIT apparatus. These conclusions are supported by external observation of AIT, DSC decomposition temperature measurements, and temperature-verses-time plots of AIT experiments. A more detailed study of the exact kinetic mechanisms of decomposition and combustion at temperatures near the AIT would give further insight into the mechanisms that control measured AIT values.

Figure 4.19 is a plot of the data in Table A.4 with annotations labeling the various AIT trends in the *n*-alkanes. The well-documented "Initial Drop" and "Flat Trend" trends indicate that, for small *n*-alkanes, the propensity to autoignite increases greatly as the chain length increases, leading to a large drop in AIT with increasing carbon number. This is discussed in more detail in Chapter 5. But, increasing chain length has diminishing returns on the propensity to autoignite as chain length reaches about C7, leading to the "Flat Trend". The "Flat Trend" continues until about C20. The influence of volatility ("Volatility Influence" on the plot) starts to be apparent by the small increase in AIT between C16 and C19, and the difference increases as the carbon number approaches 25. At C25, notice the shift between combustion and decomposition dominating the autoignition mechanism, noted by "Decomposition Effects" on the plot. The large discontinuous step change between C25 and C26 is the most unprecedented observation made in this work. The

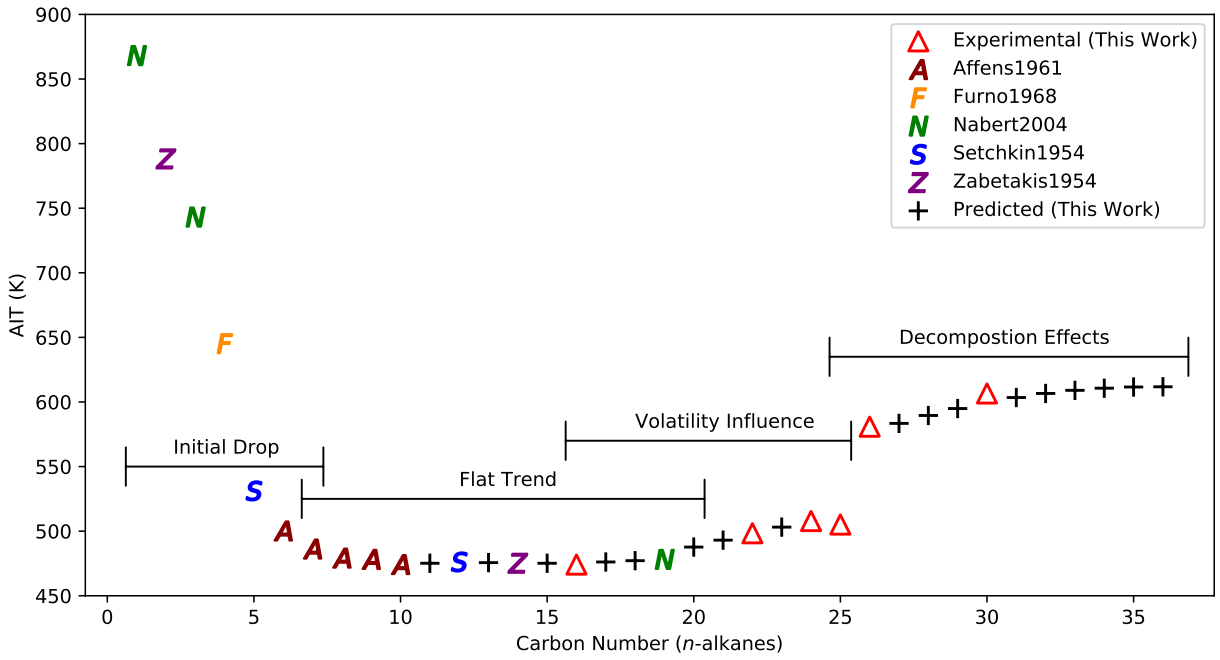

Figure 4.19: Plot of the recommended AIT values in Table A.4 with sources and data type. Also, annotations for the various trends in the *n*-alkane family. The sources for data from the literature are as follows: Affens1961 [17], Furno1968 [18], Nabert2004 [21], Setchkin1954 [10], and Zabetakis1954 [12].

AIT trend then continues gradually higher with increasing carbon number, roughly paralleling the flash point trend.

It is likely that other chemical families exhibit AIT trends like the *n*-alkanes presented here. There will likely be similar mechanism shifts for compounds that exhibit decomposition near the AIT. There will also likely be similar rises in AIT for compounds with low volatilities. Therefore, further study may be merited into other chemical families especially those like the *n*-alkanes (e.g., *n*-alcohols, 1-alkenes etc.) to ascertain the relationship of AIT to flash point and decomposition temperature more broadly. This work gives a fuller understanding of the phenomena and properties that influence AIT and the autoignition process generally and the insights here are recommended to professionals everywhere to promote safety and conscientious design of chemical processes.

CHAPTER 5. AUTOIGNITION TEMPERATURE TRENDS FOR VARIOUS CHEMICAL FAMILIES

With the trend for the normal alkanes firmly established, the next objective is to use the insight gained to inform other family trends. While there are many AIT data found in the literature and other sources such as safety data sheets (SDS), many of these data are of questionable quality or have ambiguous consistency with conventional methodologies, which can confuse any meaningful interpretation of the data.

In the literature, AIT as a property has been studied and better understood through the examination of chemical family trends. This is a useful way of organizing and studying AIT values because it can ensure consistency in and across different chemical families. It also informs phenomenological understanding factors that influence AIT, which aids estimation and prediction, and allows generalizations or limiting behavior to be observed that can increase confidence in extrapolation of the trends.

It is expected that family trends will smooth trends among chemical families. However, various common organic chemical families lack an established AIT trend for their most common members because the literature shows that many AIT data are disparate, and it is not always clear how these differences should be reconciled [47]. Various attempts to establish family trends have been published with varying degrees of success [12,72,75]. The main failure of these attempts lies in their disagreement with other literature data which can confuse the insight that would be gained from these trends.

This chapter attempts to address these issues and firmly establish trends for AIT for the most common chemical families while building on previous work. The disparate data are reconciled through careful evaluation [76]. Trends are established using the normal alkane family as a limiting case and the collective insight found in the literature. Where trends are ambiguous or data lacking, AIT values are measured and reported using the same methodology carefully derived from the ASTM E659 method discussed in a previous work [77] (also, see Chapter 4).

The structure of this chapter is as follows: a general review of the literature highlights the disparity of the data and gaps in previous attempts at establishing family trends. This is followed by a brief explanation of experimental methodology and results. Finally, family trends based on the best data possible and the attendant implications of the trends for understanding autoignition phenomena are presented and discussed. Also in this work, trends will be discussed in terms of their carbon number or length of the straight carbon chain. These will include notation to indicate this with the length of the chain prepended with "C" for carbon (e.g., *n*-heptane has a straight carbon chain length of 7 and would be denoted as C7).

5.1 AIT Family Trends in the Literature

The AIT trend for the *n*-alkanes has been explained comprehensively both by Gödde et al. and later by Redd et al. [75, 77]. As the limiting case for other chemical families, the *n*-alkanes provide a baseline behavior for AIT and allow isolation of the phenomenological factors that give rise to the observed trends without the interference of functional groups or branching that may affect the mechanisms of combustion and thus alter the trend, such as the partial oxidation introduced in the normal 1-alcohol family.

Gödde et al. uses kinetic mechanistic arguments to explain the initial drop in the *n*-alkanes up to *n*-pentane (C5), which are discussed later in this work. However, they fail to comment on why the trend flattens around *n*-heptane (C7), which is unexpected given their explanation for the initial drop. They also presumed that decreasing volatility led to the gradual rise in AIT for the larger *n*-alkanes. Redd et al. built on this by examining AIT for *n*-alkanes with carbon numbers greater than 20, in which study we confirmed the reason for the gradual rise by comparing AIT to flash points and found an unexpected step rise in AIT between C25 and C26. They showed that this step change was likely due to decomposition reactions competing with the combustion reactions and thus preventing thermal runaway without significantly increasing the temperature. This effect is expected to occur with any chemical species that contains a similarly long straight carbon chain. However, the expansion of these observations to other chemical families is beyond the scope of this work as the majority of chemical families lack AIT data for carbon numbers greater than C20.

The work of Gödde et al. is of particular interest to this work because they are the most recent and comprehensive example of studying and understanding AIT through establishing chemical

family trends. Their observations alone provide the basis for many of the family trends examined in this work. However, this work seeks to build on their work by treating some aspects of their analysis. First, explanation of the flattening of the trend around C7 in the *n*-alkanes is proposed. Secondly, disparate but reliable data from other sources suggest significant error in some of the trends proposed by Gödde et al. [21]. Experimental measurements performed in this work agree with the other sources and thus new trends are proposed.

Apart from the work of Gödde et al., the literature shows large gaps in experimental AIT values with few experimental data in the journal literature in the past 30 years. The compounds measured in this work were carefully chosen to help establish family trends so that the most value could be extracted from the fewest experimental measurements. Special care was taken to measure AIT for compounds with few functional groups (usually only one) to clearly ascertain the effect of adding a single functional group to a given member of a homologous series, which would be compared to the normal alkane family as the limiting case.

The work of Zabetakis et al. shows that a molecular descriptor they termed the "average carbon chain length" is correlated to the normal alkane trend for a wide variety of branched alkanes [12]. Despite being published nearly 70 years ago, there has been no attempt, insofar as the we are aware, to apply this simple descriptor to other chemical families and thus predict branched isomer behavior based on the normal series trend. If the descriptor correlates well to the normal series for other chemical families, it could be used to predict AIT for a wide variety of compounds when combined with the effect of a particular functional group.

The final gap in the literature arises from the fact that data are often presented without evaluation of their reliability nor consistency with established AIT measurement methodology. Nor are they commonly presented and evaluated based on consistent family trends. This makes the work of Gödde et al. a unique contribution to the subject of autoignition. Generally, disparate data are known to exist but little has been done to treat the issue [9, 47]. Previous work has treated this issue and will be used and expanded upon to evaluate and establish family trends in this work [76].

5.2 Results

Fourteen additional compounds were measured using the same methodology described in Chapter 4. The results of the measurements are given in Table 5.1. Purities are reported from

certificates of analysis provided by their respective manufacturers. Where multiple purities appear, the purities correspond to separate batches used from the same manufacturer. Lag times are also reported for the experiment corresponding to the measured AIT. Compounds to be measured were chosen in cases where available experimental data lacked, data were disparate but were similarly reliable, or had the potential to establish a trend their respective chemical family. Two or more compounds from a given family were measured to better establish a family trend where necessary.

Table 5.1: Experimental results of AIT measurements using methodology consistent with ASTM E659

CAS No.	Name	Purity	Measured AIT (K)	Lag time (s)
764-93-2	1-decyne	99.80%	499	65
291-64-5	cycloheptane	98.70%	510	203
292-64-8	cyclooctane	99.50%	517	286
6742-54-7	undecylbenzene	99.50%	491	95
821-55-6	2-nonanone	99.60%	504	
57-11-4	stearic acid	99.50%	510	245
123-99-9	azelaic acid	99.50%	659	4
106-33-2	ethyl laurate	99.70%	484	7
111-61-5	ethyl stearate	99%	509	20
111-82-0	methyl laurate	99.50%	486	111
112-61-8	methyl stearate	99.70%	498	40
57-13-6	urea	99.50%	> 800	-
140-10-3	*trans*-cinnamic acid	99.7%, 99.9%	721	8

The value for urea is given as greater than 800 K as, above that temperature, the electronics used in measurement began to fail at the higher temperatures and reliably measuring above that temperature became impossible. Other sources have reported higher AIT values for urea, but these may correspond the the AIT of ammonia, which is a decomposition product of urea [78].

5.3 Discussion

Each relevant chemical family is treated in the following subsections, and all AIT values presented are tabulated in the Appendix. For the purposes of this work, the foundation of discussion builds upon a comprehensive explanation of the trends seen in the normal alkanes. The larger normal alkanes (i.e. carbon number greater than 20) have been treated thoroughly in Chapter 4. However, the observations about the *n*-alkanes from previous works help explain the differences between the *n*-alkanes and the other families to be discussed. As there are few data for compounds above carbon number 20, the discussion will focus on species with carbon numbers under 20.

5.3.1 *n*-Alkanes

The AIT values for this family are based the work in Chapter 4. The reasons for the observed trends are proposed here, and the deviations from the baseline trend of the *n*-alkanes are the central focus of this work. The comprehensive explanation is given here starting with methane.

Methane combustion is modeled commonly using the GRI mechanism [7]. Using Cantera software (version 2.5.1) combined with the GRI mechanism allows for convenient modeling of a methane autoignition event [79]. Stoichiometric amounts of methane and air are present in a Cantera "IdealGasReactor" as a single-reactor network set to 1 atm pressure and some arbitrary temperature. The system is then advanced over 10 minutes. At sufficiently high initial temperatures, the temperature of the system will rapidly increase to temperatures exceeding 2000 K during the reaction time, indicating thermal runaway, while at lower temperatures the system will not significantly increase in temperature. By repeating this simulation at various initial temperatures, one may arrive at the limit where thermal runaway begins to occur for this system. This gives an AIT value of 736 K for methane, and the results of the limiting simulations are given in Figure 5.1. The code for these simulations was adapted from example code hosted on the Cantera website [79, 80].

These results suggest that the autoignition of methane is, in part, driven by these mechanisms. The value obtained in simulation is more than 100 K lower than the literature value of 868 reported by Nabert et al. [21]. However, this difference is expected given that this simulation assumes a vessel of non-finite volume with perfect mixing, no surface effects, and no heat nor

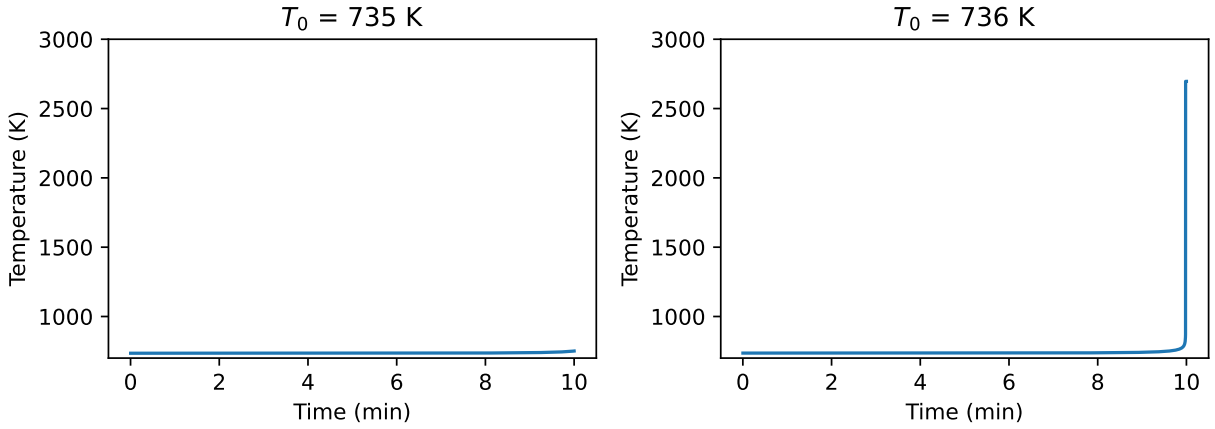

Figure 5.1: Temperature-time plots from combustion simulations of a stoichiometric mixture of methane and air at 1 atm absolute pressure and initial temperatures of 735 K and 736 K. Reactions and simulations were run using Cantera (Version 2.5.1) with the GRI Mechanism [7, 79, 80]. The low rise in system temperature over 10 minutes for the simulation with initial temperature T_0 at 735 K indicates no thermal runaway and thus no autoignition at this temperature. The rapid spike in temperature near the 10 minute mark for the simulation with the initial temperature at 736 K indicates thermal runaway and represents the limit at which autoignition occurs for methane in air per this model.

mass loss, all of which would contribute to a higher measured AIT value if considered. Thus, for consistency, the literature value is used to compare against other data.

From the literature value of methane, a relationship may be proposed to account for the differences in the subsequent members of the series. Redd et al. proposed that flash point correlated with AIT at higher carbon number. Also, Gödde discussed the energy of dissociation into radical species as related to autoignition temperatures. Finally, the kinetic theory of gases relates collision rate to temperature in a way that affects AIT. These properties combine to form the proposed relationship in Equation 5.1.

$$AIT - FP \propto \left(\frac{E_{dissociation}}{collision\ rate} \right)^2 \tag{5.1}$$

Where FP is the flashpoint for the compound corresponding to AIT, $E_{dissociation}$ is the energy of dissociation of an abstracted hydrogen and $collision\ rate$ is the collision rate of oxygen with the fuel. This relationship applied to the normal alkanes for carbon numbers 1-25 is shown in Figure 5.2. The values for carbon numbers 2-4 show agreement to within 3.4% of the literature

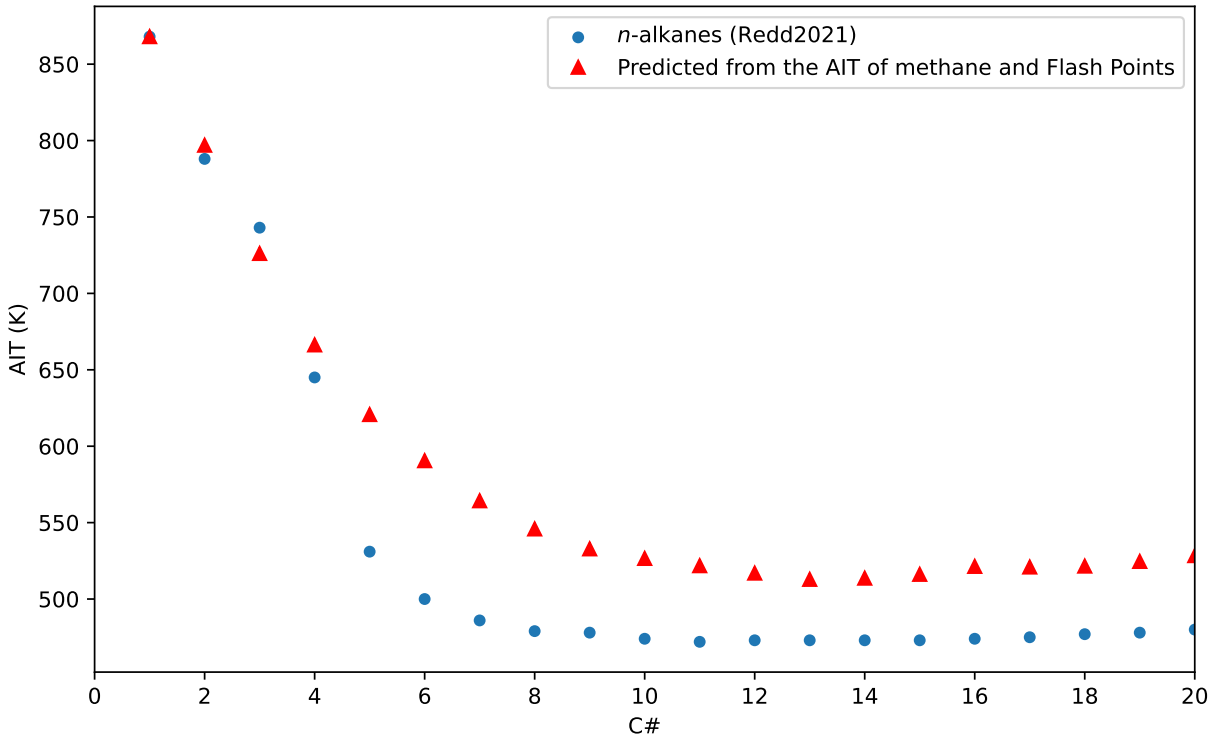

Figure 5.2: Comparison of the normal alkane AIT values from Redd et al. [77] to predictions based on the difference of AIT and flash point being proportional to the ratio of the energy of dissociation of the radical and the collision rate with oxygen squared (See Equation 5.1). The literature value of methane was used to produce the proportionality.

value. Carbon number 5 and larger shows differences greater than 100 K. This difference is explained by Gödde et al. as the *n*-pentane allows for peroxide isomerization of radicals that occur on the 2 and 4 carbon atoms. As this process is intramolecular it does not require collisions to occur and thus proceeds more rapidly. This contributes to a lower measured AIT and explains the large step change between *n*-butane and *n*-pentane and the larger compounds.

These results highlight the importance of the peroxide isomerization explained by Gödde et al. and suggest that similar effects will occur independent of chemical family. The data support this idea, as a comprehensive plot of AIT values for several simple chemical families that include straight carbon chains show convergence in the limit of high carbon number. This is shown in Figure 5.3.

From the plot, the shorter-chain members of the families show wide disparities in AIT exceeding 400 K but around carbon number 14, all trends flatten out and AIT values lie within

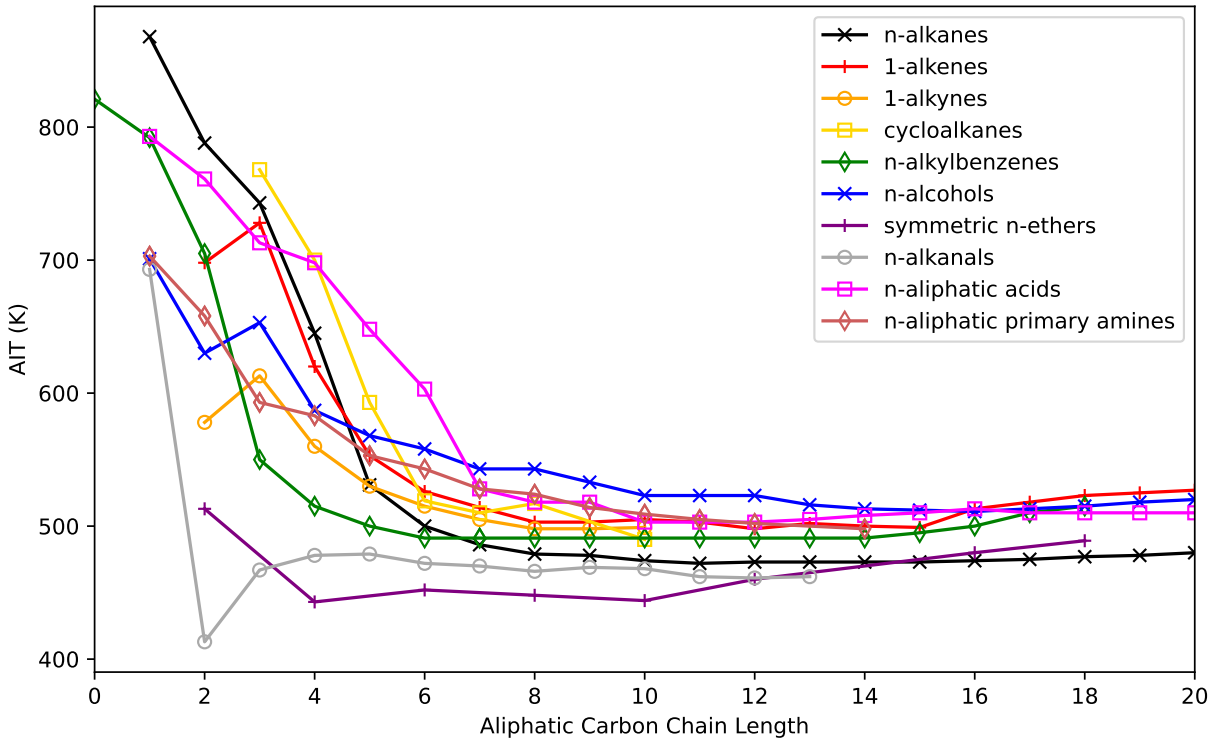

Figure 5.3: Plot of AIT values for some simple mono-functional-group chemical families. Experimental and predicted AIT values are included in this plot.

a range of about 50 K. This convergence of values suggests that the effect of the isomerization reaction predominantly controls the combustion mechanism in roughly the C7–C20 range of carbon chain lengths. Therefore, for any family, the AIT trend will converge to this range in the limit of sufficiently long chain lengths. The consistent offset form the *n*-alkane trend for the other families appears to be caused by a combination of volatility differences and the functional groups marginally affecting the trend independently from carbon chain length. This mechanism may also explain the observations of Zabetakis et al. surrounding branched alkanes as branching will likely inhibit the ability for isomerization to occur [12].

5.3.2 Alkenes and Alkynes

The trends for the 1-alkenes, 1-alkynes, and the *n*-alkanes are plotted in Figure 5.4.

In the alkyne family, experimental data exist only for carbon numbers 2, 3, 8, and 10. Due to the lack of data, the trend is fairly unclear at lower carbon numbers. To provide some clear trend,

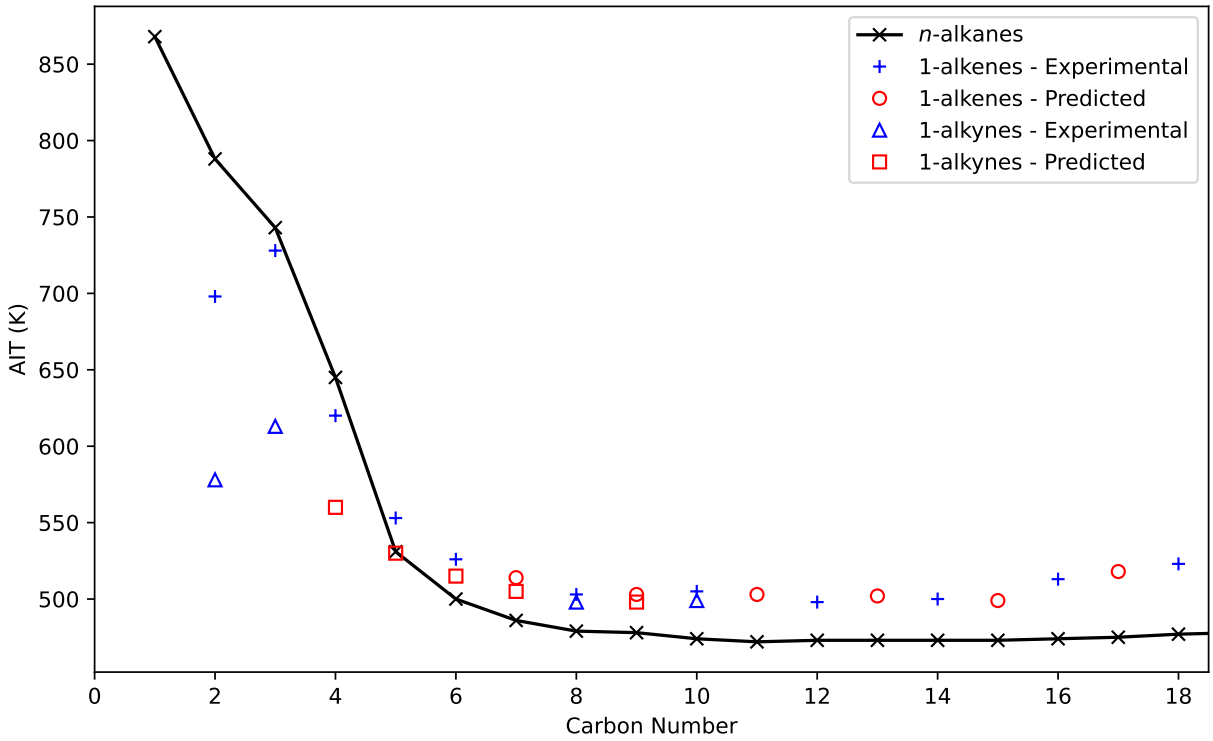

Figure 5.4: Comparison of evaluated AIT values for the *n*-alkane, 1-alkene, and 1-alkyne chemical families. All values presented are experimental except for the 1-alkynes, which has predicted values carbon numbers 4-7 and 9.

the missing carbon numbers were inferred from the available experimental data. However, it could be reasonably assumed that the AIT values will follow a trend similar to the alkenes, starting lower than the alkane of the same carbon number, and once it reaches carbon number 8, the AIT remains constant for at about 20 degrees higher than the AIT for an alkane of the same carbon number.

For carbon numbers 5 and larger, the AIT trends for 1-alkenes and 1-alkynes are consistently higher than that of an *n*-alkane of the same carbon number while the compounds for carbon number 4 and below are significantly lower than their respective *n*-alkane counterparts. The only exception to this is for propylene, which has an AIT value close to that of propane. This flat trend lying consistently above the *n*-alkane trend occurs similarly for various other chemical families with a single terminal functional group, as will be shown later. This suggests that the presence of a single instance of some functional groups marginally changes the mechanisms of combustion.

The lower AIT values for ethylene and acetylene compared to ethane seem to arise from the presence of double and triple bonds increasing the favorability autoignition. This favorability

is counterintuitive based on the energy of hydrogen abstraction which is about 10% higher for ethylene compared to ethane [75]. However, the key difference between the two compounds is the presence of pi-bonded carbons, which are accessible to oxygen attack. This likely fundamentally changes the mechanism of combustion as the initial hydrogen abstraction is no longer a required step in the mechanism. The accessibility of oxygen to the carbons is even greater for acetylene, which likely contributes to its even lower AIT value.

However, the isomerization that occurs in the *n*-alkanes also may occur as the chain length increases. Although the trends for higher carbon number 1-alkenes and 1-alkynes approach the *n*-alkane trend, they never fully converge, remaining about 20 - 30 K higher than the *n*-alkane trend. The isomerization that takes place for the *n*-alkanes is likely occurring in tandem with the mechanism of combustion for ethylene and acetylene. Thus, it is reasonable to expect a much less dramatic drop in AIT and a subsequently higher trend for these families compared to the normal alkanes.

While there are only experimental data for 1-alkenes up to C18, one may assume the 1-alkene and 1-alkyne trends will act in a similar way to the *n*-alkane trend in the limit of long carbon chain lengths. The expected trends include the gradual rise around C20 due to decreasing volatility and the discontinuity around C25 due to thermal decomposition effects.

5.3.3 Cycloalkanes

The cycloalkanes are plotted compared to the normal alkanes in Figure 5.5.

The cycloalkane trend appears to have nearly the same shape as the *n*-alkane trend but is consistently higher throughout the trend. This is likely due to the reduced number of degrees of freedom inherent to cyclic compounds. This reduced mobility seems to inhibit the isomerization mechanism for cyclopentane as, for C5 and smaller members of this family, the carbons are nearly on the same plane. However, the bond angles in cyclohexane may be close enough to those in *n*-pentane that isomerization may readily occur. Thus, the C6 and larger members of the family would exhibit the same mechanisms seen in the normal alkanes. This is evidenced by cyclohexane and cycloheptane having similar AIT values to *n*-pentane. Similar to the alkenes and alkynes, the cycloalkane trend flattens out at a marginally higher value than the *n*-alkanes.

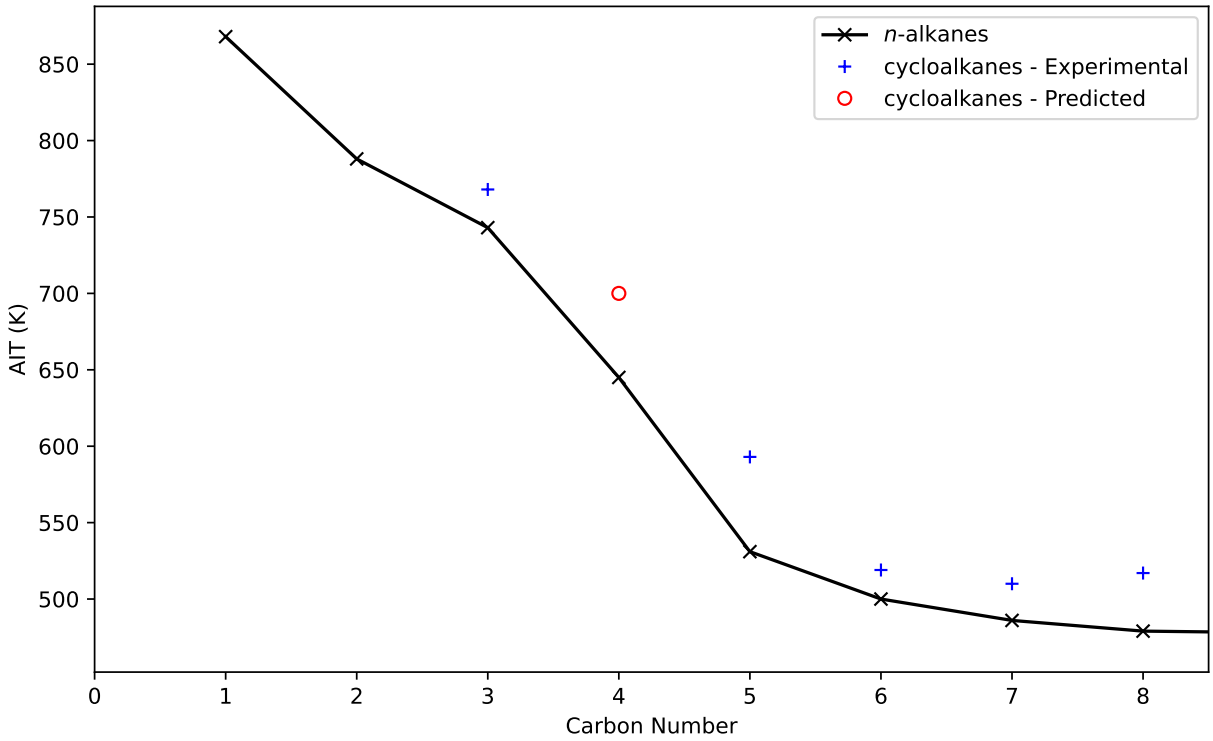

Figure 5.5: Cycloalkane AIT trend compared to the normal alkanes.

5.3.4 *n*-Alkylbenzenes

Only 5 members of the *n*-alkylbenzene family have measured AIT values obtainable from the literature: benzene, toluene, *n*-ethyl-, *n*-propyl-, and *n*-butylbenzene. The available data for this family show similar trends to the alkene and alkyne families on the basis of straight carbon chain length (i.e., benzene has a carbon number of 0, toluene 1, ethylbenzene 2 etc.). Previous to this work, the trend was extrapolated using the Seaton-Redd2 method, which predicted the trend for carbon chain length out to C18 (*n*-octadecylbenzene) [76]. However, the measured value for *n*-undecylbenzene (C11) shows that the Seaton-Redd2 method predicts AIT values more than 100K higher for the longer members of the series. The previous trend is compared to the improved trend and the *n*-alkane trend in Figure 5.6.

From the plot, the newly measured value for C11 highlights how strategic measurements can inform an entire family trend and increase the confidence in extrapolated values. The extrapolated values predicted in the improved family trend are inferred from the C11 value. These inferred values are meant to represent conservative estimates of AIT values, that is, the experimental AIT

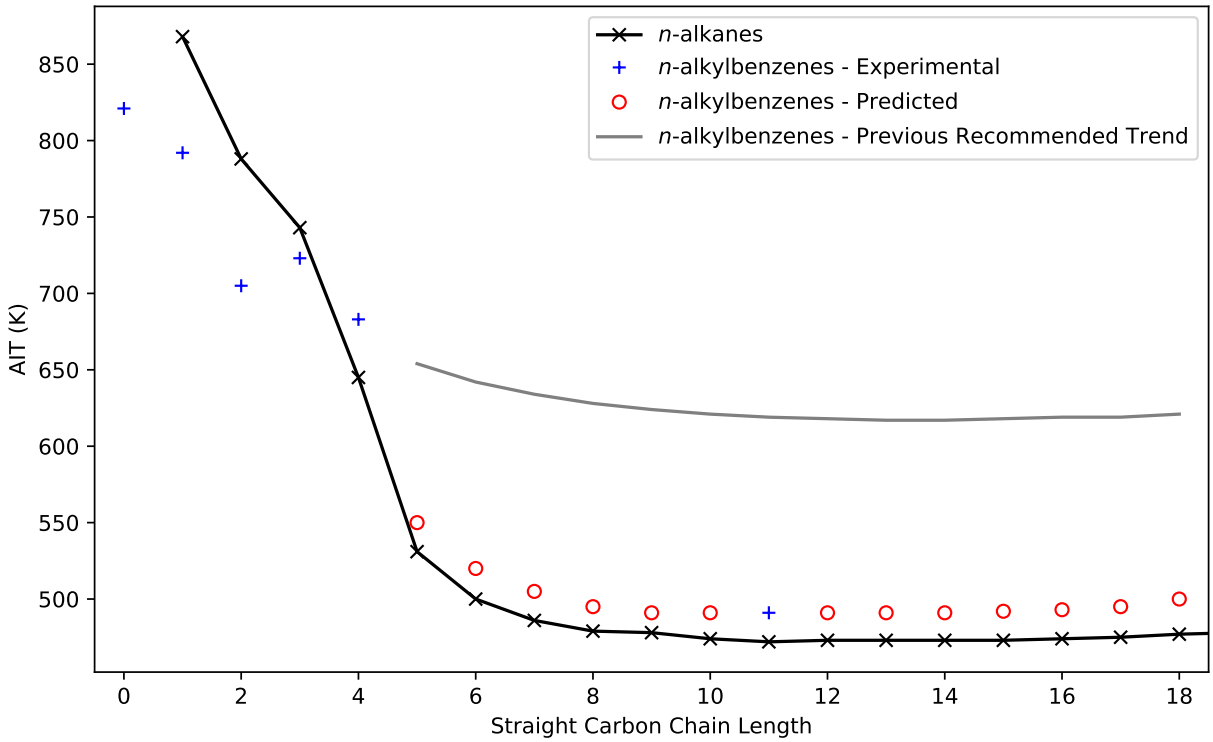

Figure 5.6: AIT trend of the *n*-alklybenzenes compared to the *n*-alkanes and a previously predicted trend based on the Seaton-Redd2 prediction method [76].

values for these species may lie at higher temperatures but, based on the data and trends for the other families, we have high confidence that they do not lie at significantly lower temperatures than presented in Figure 5.6. This confidence is justified by the similarity between the *n*-alkane *n*-alkylbenzene families, the sole structural difference being the addition of the aromatic ring. Similarities in AIT behavior, such as the isomerization mechanism affecting the measured AIT for chain lengths above that of C5, may therefore be reasonably assumed and appear to be borne out in the data. Also, the same trends likely apply in the limit of larger carbon numbers exceeding 20. Further experiments are needed to confirm or rebut this hypothesis.

5.3.5 *n*-Amines

The normal primary amines are plotted with the *n*-alkanes in Figure 5.7.

This chemical family is well defined and seems to exhibit some of the same characteristics found in other families. The trend starts lower than the *n*-alkanes but levels off at a higher AIT

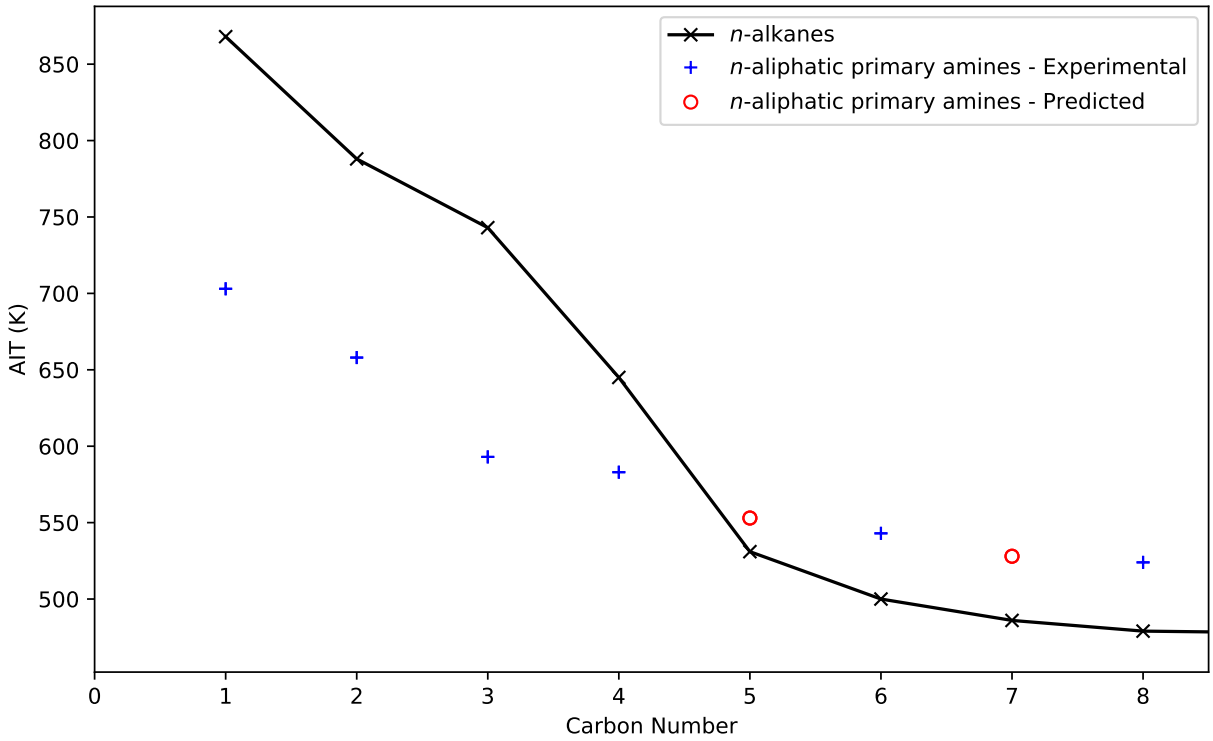

Figure 5.7: Comparison of the *n*-alkanes to the *n*-aliphatic primary amines.

value than the *n*-alkanes. This behavior is consistent with the alkenes and alkynes. The presence of the amine group increases the propensity to autoignite and continues to marginally affect the mechanism of reaction with longer carbon chain length. It is similarly expected that the longer amines will likewise exhibit similar trends to the alkenes and alkynes.

5.3.6 1-Alcohols and Glycols

The 1-alcohol trend is qualitatively similar to the alkene and alkyne trends in that the smaller members of the series are much lower than the *n*-alkanes and flatten out at marginally higher AIT value than the *n*-alkanes in the limit of high carbon number. The alcohol trend is plotted along with available data for the terminal *n*-glycols and the *n*-alkane trend in Figure 5.8.

The initial part of the 1-alcohol trend suggests that the presence of a single alcohol group increases the favorability of autoignition. However, multiple instances of an alcohol group appear to increase the AIT trend as can be seen from the terminal *n*-glycol data. The apparent insensitivity to the possibility of isomerization as the carbon chain length increases suggests that the presence of

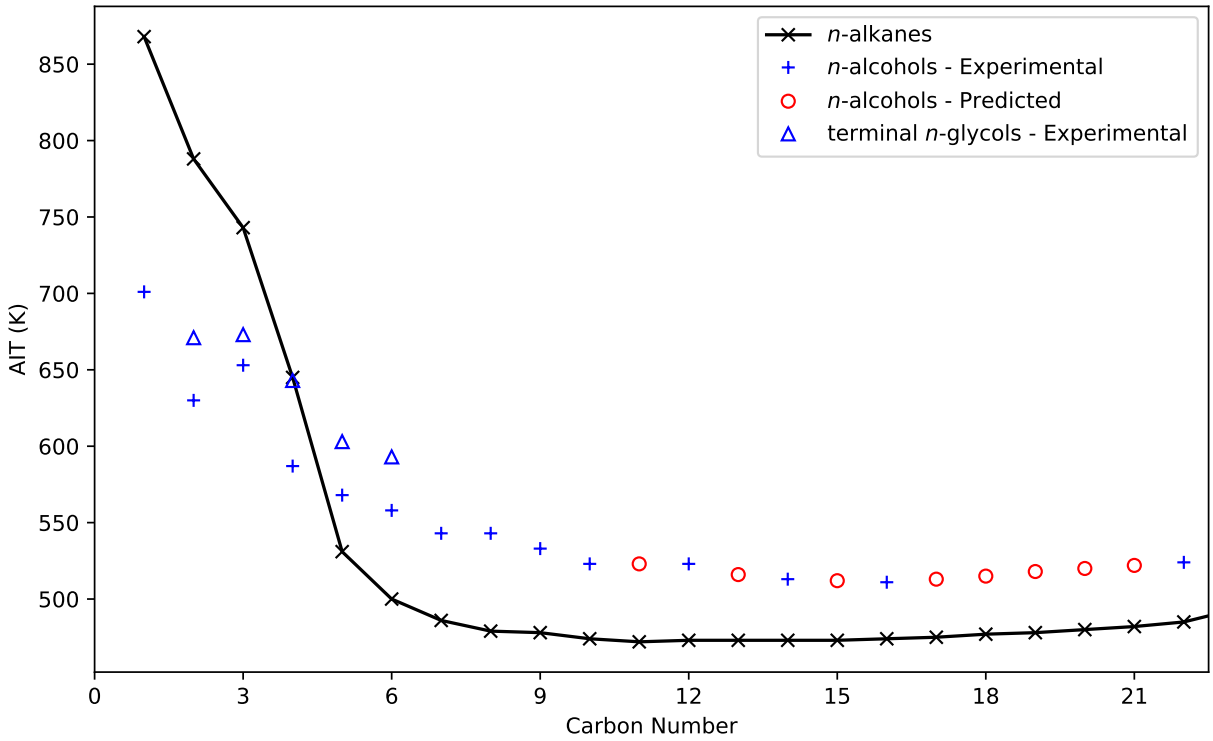

Figure 5.8: Comparison of AIT values from the *n*-alkane, 1-alcohol, and terminal *n*-glycol families.

the alcohol group changes the underlying mechanisms of combustion even in the limit of long carbon chain lengths. However, both the 1-alcohol and the terminal *n*-glycol trends appear to approach the *n*-alkane trend as carbon number increases, suggesting that the same *n*-alkane mechanisms are still present. The difference between the flat part of the trend for the 1-alcohols and the *n*-alkanes is significantly greater than the alkenes and alkynes and thus may be, in part, due to the difference in volatility of alcohols, which tend to have significantly lower vapor pressures than similar *n*-alkanes at the same temperature. This general feature holds for many of the chemical families presented in this work and indicates that the trends lying consistently above the *n*-alkane trend result from a combination of factors in addition to the change in mechanisms from the functional groups. As shown in Figure 5.2, the propensity to autoignite only increases with increasing size and carbon chain length and is counteracted by volatility decreases, which are represented via the flash point in that model.

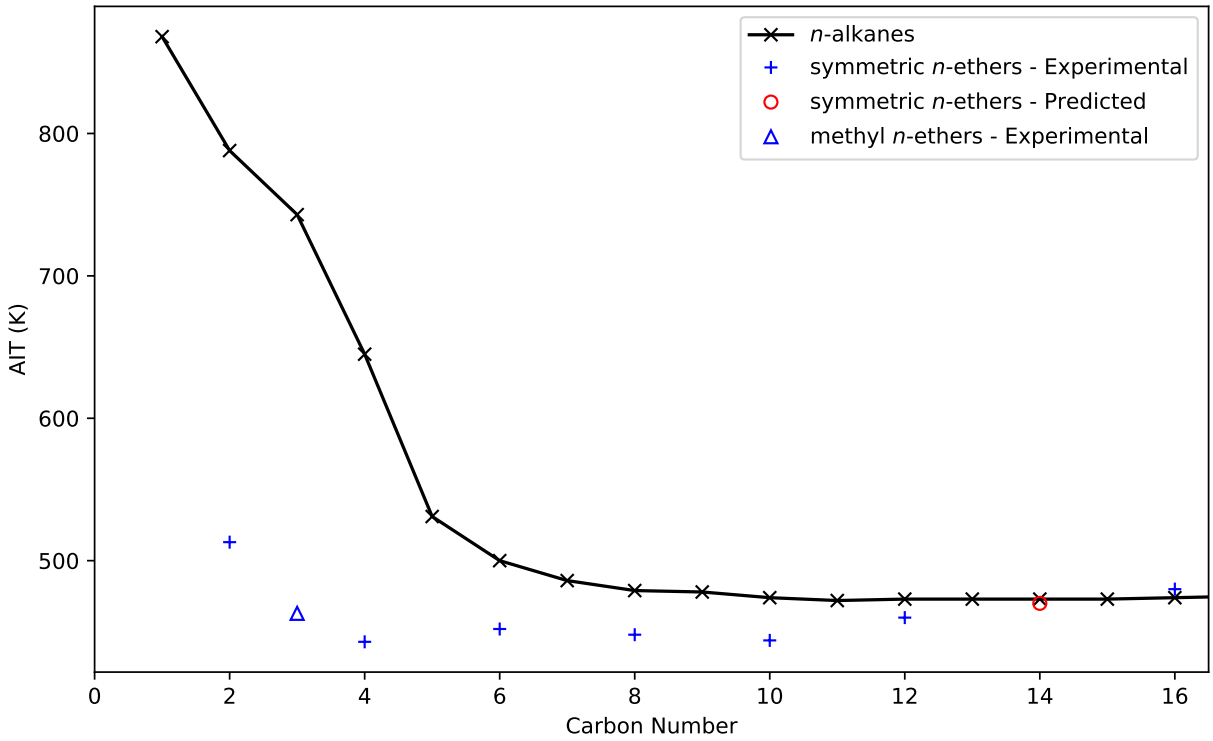

Figure 5.9: Comparison of AIT values from the *n*-alkane and *n*-ether chemical families.

5.3.7 *n*-Ethers

The trend for the normal ethers is unique in that all values appear to lie below the trend for the *n*-alkanes. This is a notable inversion of the trends seen thus far. There is only one reliable experimental point for an asymmetric ether, but the symmetric ethers have more data. The ether trend is plotted in Figure 5.9.

Similar to the alcohol family, the presence of the oxygen greatly lowers the AIT value compared to the corresponding *n*-alkane. The trend stays low but appears to approach the *n*-alkane behavior near carbon number 14 for the symmetric ethers. The value of the methyl ether data point suggests that the position of the ether in the carbon chain has little effect on the AIT value, but more data would be needed to show this with any confidence.

For the alcohols and ethers, the presence of the oxygen in the chain greatly changes the mechanism of combustion. This is apparent from the large difference in AIT for the smaller members of the families. It is possible that, partially combusted species such as these more easily form

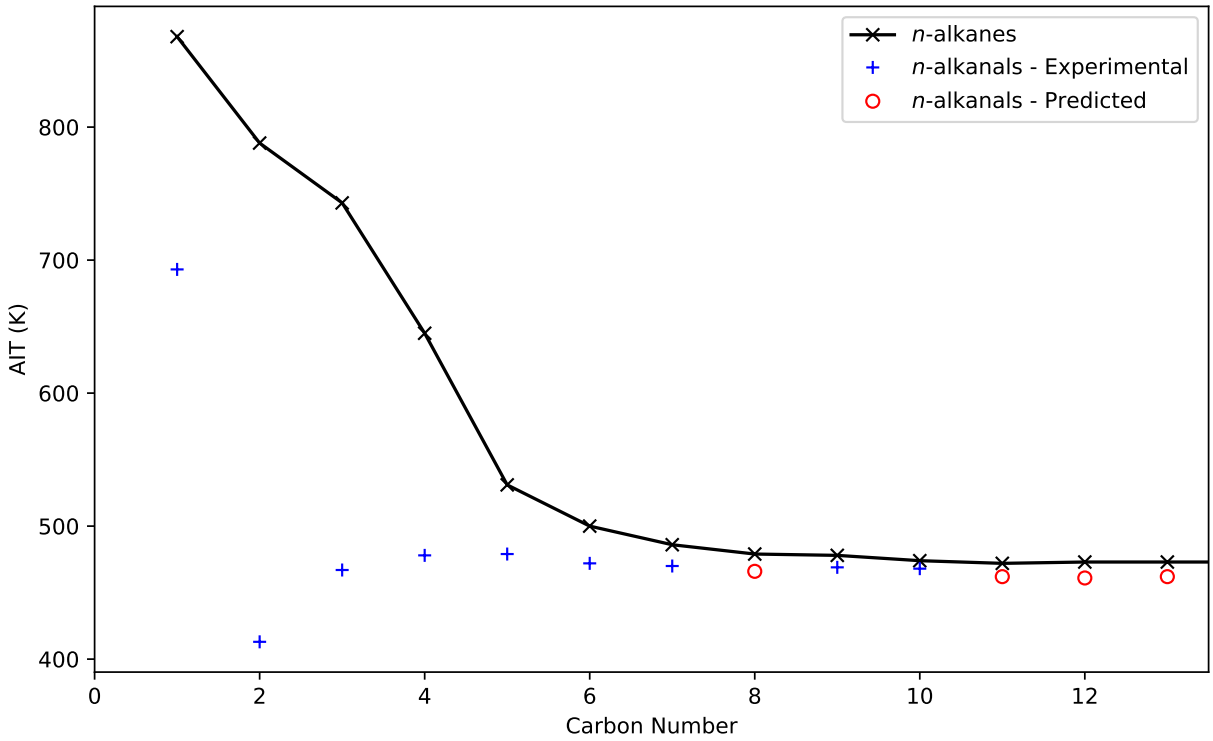

Figure 5.10: AIT trend comparison plot of the *n*-alkanes with the normal aldehydes.

peroxide radicals and thus facilitate combustion and subsequent thermal runaway, leading to lower AIT values.

5.3.8 *n*-Alkanals

At the larger carbon numbers (i.e. carbon number > 7) the normal aldehyde trend closely converges on the *n*-alkane trend. Again, this particularly close convergence to the *n*-alkane trend is a notable exception among the chemical family trends examined in this work that only appears with the *n*-alkanals and the ethers. However, the smaller family members' AIT values lie significantly lower than the corresponding *n*-alkane values. The normal aldehydes are compared to the *n*-alkanes in Figure 5.10.

The value for formaldehyde is significantly lower than methane. This is likely due to a number of factors intrinsic to the aldehyde's structure including pi-bonds with oxygen, allowing direct access for an oxygen attack. Likely, the partial oxidation of formaldehyde and the other *n*-alkanals also contributes to their respective combustion mechanisms and lower AIT values.

The normal alkanals show a surprisingly different trend from other families. Instead of starting high and monotonically decreasing with increasing carbon chain length, the trend is inverted for acetaldehyde and larger compounds, starting at a minimum and then gradually increasing until converging on the normal alkane trend at around C8.

This unique trend indicates a strong propensity to autoignite, which must be driven by the presence of the aldehyde group. However, the effect of the aldehyde group is diminished as carbon chain length increases. The shape of this trend may arise from the accessibility of the carbonyl group to oxygen attack as has been already discussed, but also may be affected by the relatively low energy of dissociation of the carbonyl hydrogen which is 11% lower for acetaldehyde compared to dissociation of a hydrogen from ethane [75]. These two factors provide a possible explanation for the initial trend and then, as with other families, the trend converges on the normal alkane trend with increasing carbon number. Notably, the trends for the ethers and alkanals converge more closely to the *n*-alkanes than the rest of the families considered. This difference may be due to the higher propensity to ignite not affecting the isomerization reactions, which would occur as carbon chain length increases.

5.3.9 Ketones

In literature, there are many disparate data for the AIT of the 2-alkanones larger than C7. Both Gödde et al. and Nabert et al. record significantly different values for C7, C8 and C9 in this family. These values appear in Table 5.2. To reconcile these disparities in the ketone family, 2-nonanone was measured as part of this work. The experimental value (504 K) is within 3% of the value found by Gödde et al. The agreement with their value confirms the family trend they presented. From the experimental work, it is unsurprising the AIT values were so disparate, as the value between sample sizes varied by more than 100 K, and the compound would commonly fail to ignite at temperatures well above the final AIT value. This unpredictable behavior made measuring 2-nonanone relatively difficult and may explain the disparity in the data.

Table 5.2: Experimental AIT data for select 2-alkanones from Gödde et al. and Nabert et al. [75, 81].

Name	C#	AIT (K)	Reference
2-heptanone	7	580	[75]
2-heptanone	7	578	[81]
2-octanone	8	572	[75]
2-octanone	8	693	[81]
2-nonanone	9	504	This Work
2-nonanone	9	516	[75]
2-nonanone	9	678	[81]

In the analysis by Gödde et al. they claim that non-terminal functional groups such as carbonyl groups in ketones block reaction possibilities and increase ignition temperature compared to n-alkanes of the same chain length. They also explain why the ignition temperatures of isomeric ketones differ from one another based on position of the carbonyl group: the ignition temperature is significantly influenced by the length of the longest alkyl group, because it determines the number of possible intramolecular reactions by the peroxide radicals. To explore this analysis, various alkanones are plotted against the longest straight carbon chain length possible in each compound in Figure 5.11. Plotting in this way reveals a clear trend similar to other chemical families that are similarly comparable to the *n*-alkanes. The data would seem to confirm the explanation proposed by Gödde et al. However, the 3-alkanone trend deviates significantly from the other ketone sub-family trends. This deviation suggests that while the longest carbon chain length certainly contributes, it is insufficient to explain the overall trend.

There are many valid ways that the carbon number or relevant carbon chain length could be described or calculated, such as the "average carbon chain length" descriptor proposed by Zabetakis et al. [12]. However, the lack of reliable data preclude any meaningful assertions about trends based on such descriptors. More consistent AIT data are needed to establish the full effect of the carbonyl group on AIT trends. However, one relevant conclusion can be made that the ke-

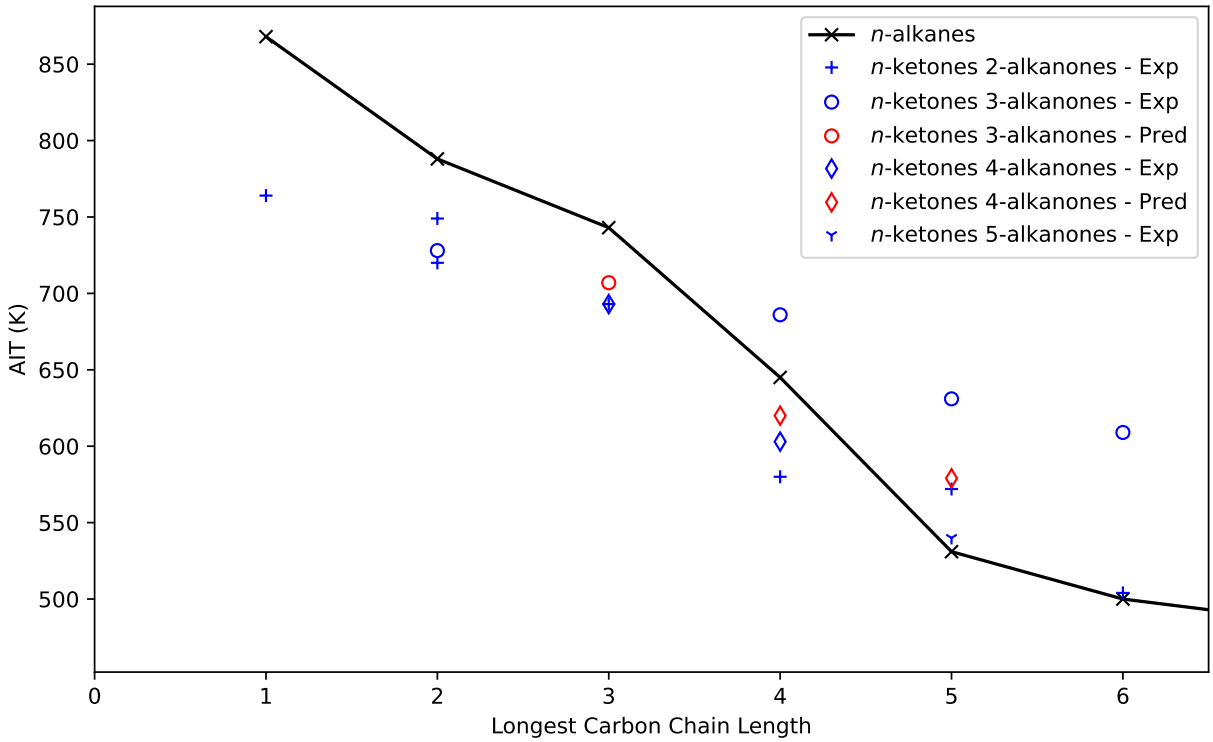

Figure 5.11: Comparison of various ketone AIT family trends to the *n*-alkane trend by the length of the longest carbon chain uninterrupted by the carbonyl group (e.g., acetone corresponds to 1 on the x axis).

tone trend is entirely unrelated to the normal aldehyde trend which suggests distinct mechanisms produce the observed trends of each family.

5.3.10 1-Acids and Diacids

The acid and diacid family trends are plotted in Figure 5.12.

The normal 1-acids are well established up to stearic acid (C18). The trend for this family appears to coincide more closely with the *n*-alkanes with a less dramatic difference between formic acid and methane compared to the differences discussed so far. Again, the trend flattens out near C7 at a marginally higher AIT value than the *n*-alkanes. The flat trend again may be influenced by the significantly lower volatility of the acids compared the alkanes. Otherwise, the trend appears to match closely to the *n*-alkanes with a larger drop between carbon numbers 6 and 7, which may suggest the same isomerization mechanisms are influencing the measured AIT values.

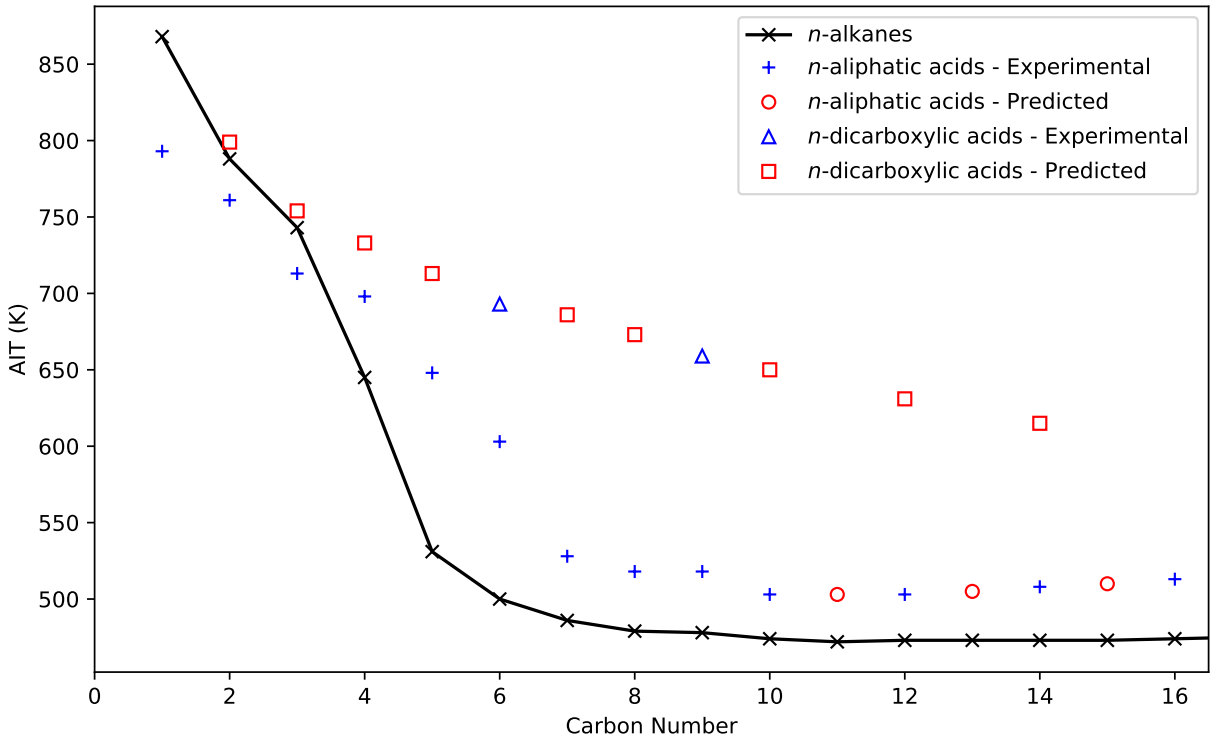

Figure 5.12: Comparison of the normal alkane AIT trend to that of the normal 1-carboxylic acids and the normal dicarboxylic acids.

The diacids are significantly higher in AIT value than the corresponding 1-acid. This may be due to a number of factors but is almost certainly influenced by the fact that diacids readily decompose at temperatures below their AIT value (e.g. oxalic acid decomposes at 439-453 K) [82]. The effect of decomposition and how it competes with combustion and thus increases the AIT value was proposed in Chapter 4. Decomposition in these cases is generally endothermic and consumes the fuel, competing with the parallel combustion reaction. This, in turn, prevents thermal runaway and ignition. Given this effect, it is not surprising that the diacids will have much higher AIT values. Previous to this work, reliable AIT data only existed for adipic acid (C6) and the measurement of azelaic acid in this work allowed a proposed trend to be adopted for this chemical family, as seen in the "predicted" trend for the *n*-dicarboxylic acids.

5.3.11 Esters

Normal esters, as a class of compounds, may be logically grouped into sets of well-defined homologous series in at least two ways. Specifically, the homologous series may be defined similar to the acids with the carbon chain attached to the oxygen as part of the functional group, or the series may be defined like an alcohol with the carbon chain attached to the carbonyl as part of the functional group. Defining esters using the former method produces families such as methyl esters, ethyl esters, propyl esters etc. and the latter produces families such as formates, acetates, propionates etc. Because of this, establishing an overall family trend can be ambiguous.

In this work, experiments were conducted to reconcile large disparities in data for the methyl, ethyl, and *n*-butyl esters. As a result, the focus of this section will be on those families defined using the "acid" definition. However, it is equally valid to consider esters using the "alcohol" definition and plots of trends are included in the appendix for the normal formates, acetates, propionates, and *n*-butyrates compared against the normal alkanes.

The methyl and ethyl esters are plotted against the *n*-alkanes in Figure 5.13. A value for *n*-butyl stearate is included as well. Carbon number is counted using the acid side of the molecule for consistency of comparison. For example, methyl and ethyl laurate have the same carbon number (C12) in this plot.

This family shows remarkable similarity in the flat part of the trend with the *n*-alkanes likely for the same reasons seen in other families previously discussed. Furthermore, the difference between the methyl and ethyl laurate is insignificant, per ASTM E659, and the differences are relatively small for the other corresponding pairs for which experimental data are available. This suggests that the mechanisms leading to autoignition for these esters are driven primarily by the acid part of the ester. Similar to other families, the gradual rise in AIT due to decreasing volatility appears to be present for this family as well.

Previous to the measurements made in this work. Many disparate AIT values existed in the literature and could be obtained through prediction. These data, along with the recommended values are given in Figure 5.14.

The disparate set of AIT values in this plot highlight a problem that exists in many chemical families. However, the 4 AIT values measured in this work allowed a family trend to be inferred and the higher AIT values for carbon chain lengths above 6 to be safely ignored. This highlights

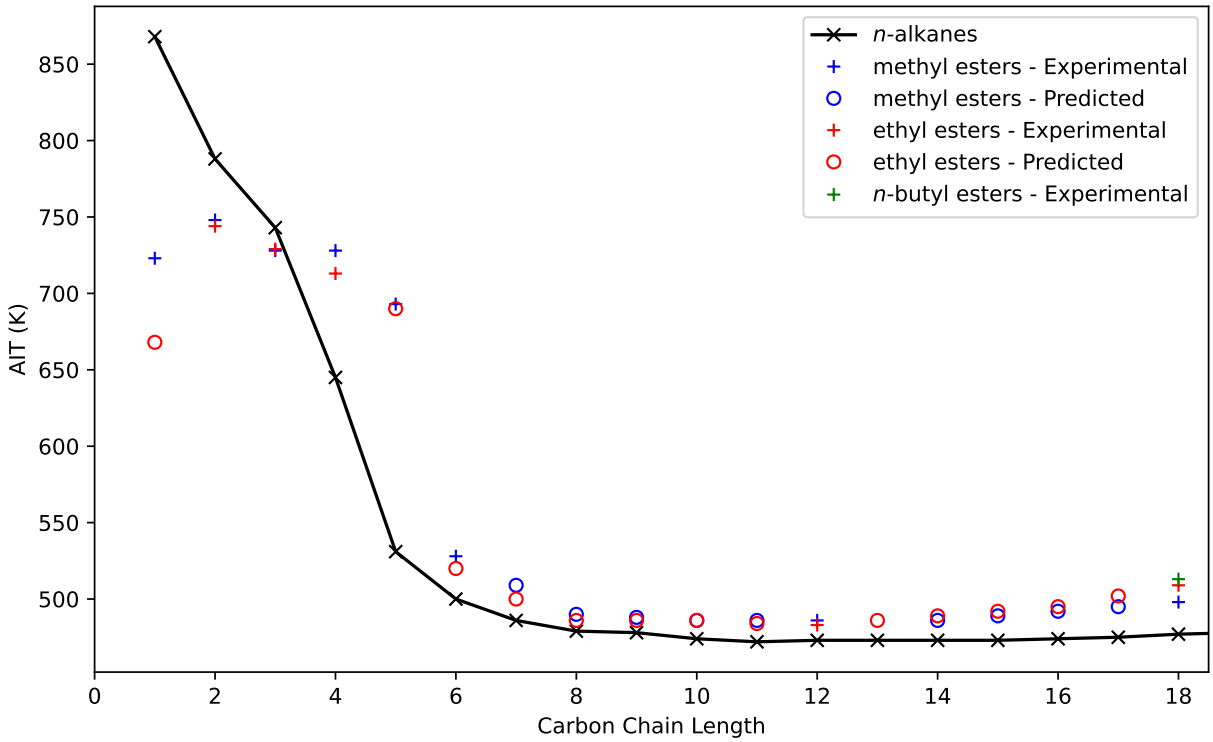

Figure 5.13: AIT trend comparison plot of the normal methyl, ethyl, and butyl esters. For the esters, "Carbon Chain Length" refers to the length of the carbon chain connected to (and including) the carbonyl group on the ester.

that, through strategic measurement of a few key compounds, the disparate values may be vetted, and a family trend may be inferred with high confidence.

5.3.12 Branched Species

A disadvantage to the approach using family trends to understand autoignition characteristics is that families must be well defined and be organized in a logically progressing series. The focus in this work has been on series that contain straight carbon chains. Thus, compounds with poorly defined families, multiple functional groups, branching, or inconsistent homology will require different methods of characterization by family. A similar study of family trends could be conducted given sufficient quantities of consistent and reliable AIT data. Unfortunately, data in the literature tend to be increasingly sparse for more exotic compounds.

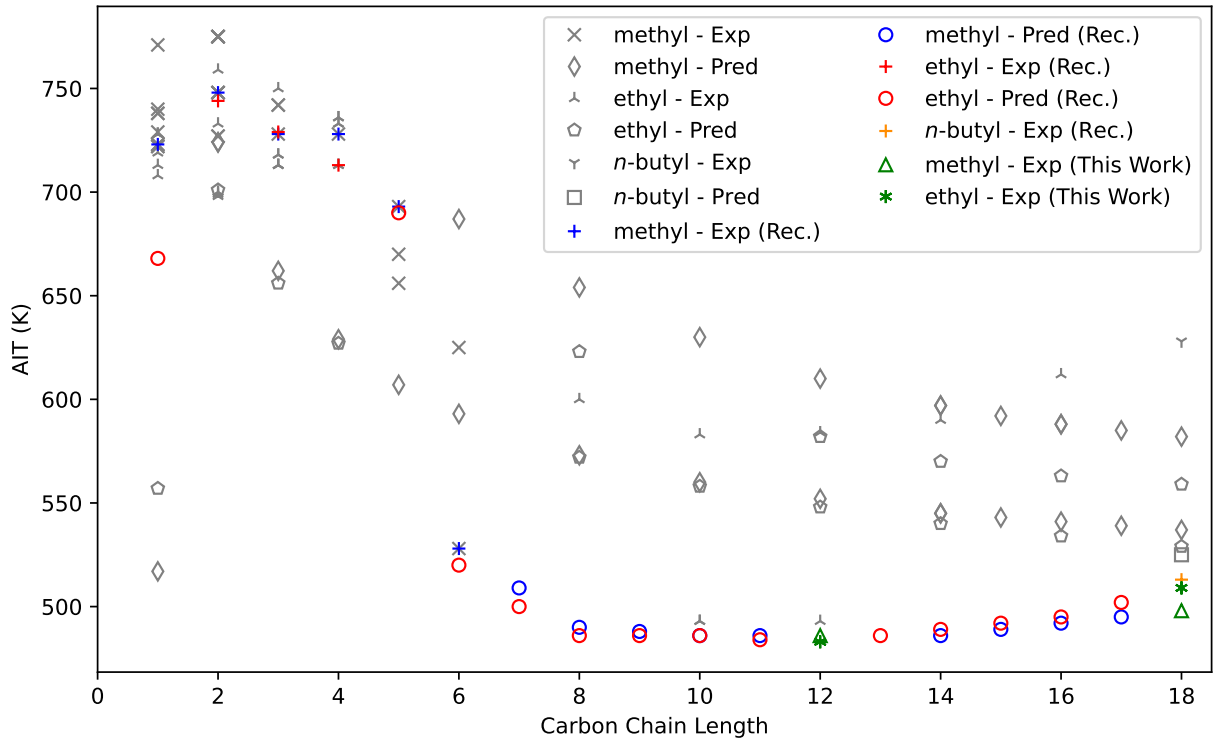

Figure 5.14: AIT values for selected ester families including the methyl, ethyl, and *n*-butyl esters. "Carbon Chain Length" refers to the length of the carbon chain connected to (and including) the carbonyl group on the ester. The legend specifies the specific ester family (i.e., "methyl", "ethyl", and "*n*-butyl"), and the type of data shown ("Exp" for experimental values, and "Pred" for predicted values). "Rec." indicates the recommended value for the family trend which is informed by careful evaluation of the available AIT values and is informed by the values measured in this work.

Zabetakis et al. correlated branched alkanes to the *n*-alkane trend using a descriptor called "average carbon chain length" that seems to show good agreement with the *n*-alkane trend [12]. This correlation showed that, if the normal trend was known, the "average carbon chain length" for a given branched species would lie on the *n*-alkane trend to well within 5% of the trend. Since this correlation worked well for the alkanes, it was tested in this work for the aldehyde family. This family was chosen because the functional group is, by definition, terminal, which clearly defines the longest carbon chain length. Secondly, the normal trend and data for the branched species are generally reliable enough to make meaningful observations. Carbon chain length was counted including only carbon atoms (e.g., formaldehyde would have a carbon chain length of 1), as opposed to considering the carbonyl oxygen as part of the chain. The results of this comparison are shown in Figure 5.15.

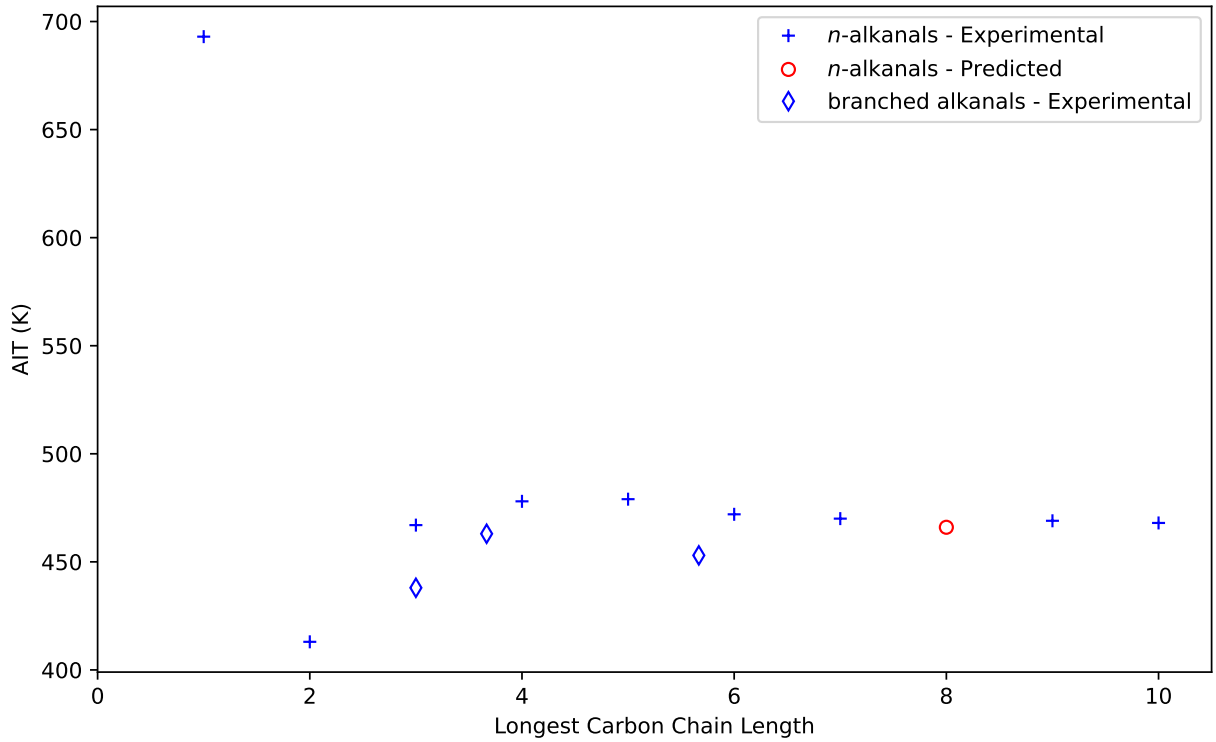

Figure 5.15: Comparison of the *n*-alkanes with the *n*-alkanals and three branched alkanals.

This plot shows qualitatively that there is some agreement between the branched and the normal trends based on average carbon chain length though the agreement is not nearly as close as it is for the normal alkanes. This suggests that this correlation may exist, and better agreement may be found by revising the method of counting carbons to account for those effects that make the family trend qualitatively match the *n*-alkanes, similar to how Zabetakis et al. calculated carbon number [12]. This also suggests that mechanisms of combustion are only marginally affected by branching and isomerization must also play a role in the mechanism for the non-alkane species. However, there are insufficient data at this time to propose anything beyond this.

To further flesh out these relationships, this process was repeated with the n-esters. Because the ester functional group is in the middle of the carbon chain, various possible conventions for counting carbon chain length are possible. Various methods were attempted and the R^2 values for each method per agreement with the normal series is listed in Table 5.3. Specifically, the R^2 values are based on deviation of AIT values between the four branched esters and interpolated values based on the normal ester trend. The four branched-ester AIT values were available for the

following species: ethyl trimethyl acetate, ethyl isovalerate, isopentyl isovalerate, and isopropyl palmitate. The values for each were chosen based on the most consistent data available. Without a well-defined family trend, the only criterion to choose the best value was consistency with standard methods.

Table 5.3: Carbon counting method performances per agreement with the normal series using R^2 values. Each method is briefly explained and the results are given for each corresponding method.

Method Explanation	R^2
Count every oxygen as a carbon without distinction between double and single bonds.	-0.412
Ignore oxygens completely.	0.111
Count each oxygen as a half carbon.	-0.718
Ignore the double bonded oxygen and treat the in-branch oxygen as a full carbon.	0.609
Ignore the double bonded oxygen and treat the in-branch oxygen as a half carbon.	0.246
Treat the branches on either side of the ester group as different branches, making the carbon on either side of the in-branch oxygen endpoints.	-0.849

These results show poor correlation to the normal trend based on any of the attempted methods for carbon counting. This is, in part, due to lack of reliable data, which would increase the confidence in the correlation and predictive relationship between normal and branched species. However, neglecting oxygen and counting the in-branch oxygen as a half a carbon seemed to work best in this case.

5.3.13 Polyfunctional Species

The focus of this work so far has been on normal, single-group families. However, there are many opportunities for future work by measuring and studying polyfunctional compounds and investigating the relationships and effects that functional groups have on each other. Included in this work are two examples of this: urea, and *trans*-cinnamic acid. These were chosen because there were no reliable AIT data on them in the literature and they are industrially relevant. However, they

also represent initial data for possible future work in the scope of AIT values for polyfunctional species.

The effect of the amine and carbonyl groups that constitute urea (the simplest carbamide compound) appears to have a dramatic impact that resists combustion at temperatures under 800 K. This agrees with some sources that suggest that urea is non-flammable. This suggests that similar results may be found with other carbamide–containing compounds.

The AIT value of *trans*-cinnamic acid was found to be 721 K. As a possible example, comparison with possible surrogate constituent parts such as acetic acid (AIT value: 761 K), propylene (AIT value: 728 K), and benzene (AIT value: 821 K) reveal possible interactions that may control the mechanisms of combustion for this species. There are many ways to interpret each case of a polyfunctional molecule and it is not clear which is correct and how this will impact the measured AIT value. However, the comparison of AIT values for this species may suggest that the lowest AIT value of a constituent part may control the AIT value of the whole, being the lowest barrier to reaction initiation. This is supported by the fact that the AIT values for propylene and *trans*-cinnamic acid are so close to one another, and is also supported, in principle, by the autoignition model of Seaton [76]. Overall, more data are needed to support and establish these relationships and flesh out the sparse amount of data on more exotic species.

5.4 Conclusion

In this chapter, AIT values for 12 compounds were measured and reported per ASTM E659 methodology using the apparatus and methods reported by Redd et al. [77]. Urea was also measured but no autoignition was observed at or below 800 K. The compounds measured were strategically chosen to inform the AIT trend for their respective chemical families and for their industrial relevance.

AIT values from various sources were considered and evaluated to establish family trends for 16 straight-carbon-chain homologous series that constitute a chemical family. Data were evaluated based on consistency with ASTM E659 methodology and internal family consistency. The established trends were compared to the normal alkane family trend, the limiting case for straight-carbon-chain homologous series, to propose phenomenological reasons for the differences in the

trends, based on mechanistic explanations found in the literature. Family trends inform internal consistency for AIT and should be considered when reconciling sets of disparate AIT values.

Strategic measurement of key species can inform a family trend for the purposes of interpolation. Understanding the general trends among various families increases confidence in extrapolation based on those trends. Branched species may be correlated to the normal homologues by considering carbon chain lengths, but more data are needed to support this hypothesis. The AIT values for polyfunctional species may be estimated based on constituent groups, however more data are needed to establish specific relationships. More experimental AIT data are needed generally to establish trends for families not discussed in this work.

The evaluations and recommendations in this work represent the highest quality AIT values and trends available and all of the AIT values presented in this work are included in the appendix along with relevant bibliographic information. Therefore, the trends presented in this work represent the most reliable and consistent AIT trends for a wide variety of compounds and will ensure the highest standards of safety for chemicals process design and operation, which will prevent loss of life and property due to accidental fires.

CHAPTER 6. AN IMPROVED AIT PREDICTION METHOD BASED ON FIRST PRINCIPLES

6.1 Introduction

Under real-world conditions, the temperature at which autoignition occurs may vary drastically from what is observed in a controlled laboratory environment. This may be due to several factors such as catalytic, radiation, and turbulence effects that are not present in the standard methods. Because of these factors, the measured AIT will likely differ significantly from the minimum temperature at which autoignition occurs outside the laboratory environment, and designs should account for this difference. Doing so should mitigate the associated fire risks of an accidental high-temperature release of flammable materials.

Despite the associated uncertainty, knowing the measured AIT for a flammable material is essential to fire prevention. As the experimental data in the literature are not exhaustive, many methods to predict AIT have been developed. The last 30 years have seen more than 30 different methods for predicting AIT. However, these methods tend to fall short in that they are either narrowly applicable, use low quality data to train and test their methods, or fail to capture the complexity of autoignition events and the underlying phenomena that influence AIT.

This chapter presents a method built on the pioneering work of by the late Dr. William H. Seaton that incorporates a first-principles approach to explain and predict AIT for compounds using group contribution (GC) methodology to model compounds. The original work of Dr. Seaton was proprietary and never openly published. Now, his heirs have graciously provided access to the foundational materials behind the method to open this work to the general scientific community. The new method improves on Seaton's method with an evaluated and more reliable regression data set, a more phenomenologically rigorous model of autoignition, and new groups, which better represent the available data and represent a much larger variety of compounds.

The chapter is structured as follows. First, Seaton's autoignition model and an explanation of the original method are presented. Improvements to the method are then outlined which include a new regression of the method using a larger and higher-quality data set and a new model that relaxes certain assumptions in the original method. Finally, the advantages of the new methods over the original Seaton Method are discussed.

6.2 The Seaton Method

The late Dr. William H. Seaton derived a new method based on first principles for predicting AIT circa 1991. His method was sold as licensed software until his death in 2003. Dr. Seaton's other contributions to flammability and other thermophysical properties are present in the literature [83–86]. The copyright, documentation, and source code for the software and the associated method have been released for the production of this work. The entire method will be presented in two parts, the theoretical basis and mechanics of the method, and the details of implementation. Both are explained below.

6.2.1 The Seaton Theory of Autoignition

The following is a summary of Seaton's autoignition model and a derivation of the Seaton method. It is based on Seaton's documentation and source code including "Theory of Autoignition Temperature Model of W. H. Seaton", an unpublished document written by William H. Seaton dated March 11, 2003 [87, 88].

In this document, Seaton defines autoignition as an event where oxygen attacks a single group on a molecule leading to a runaway reaction that results in a visible "hot-flame" ignition event. This excludes the so-called "cold-flame" ignition events and is consistent with the ASTM E659 method's definition of "hot-flames". Likewise, he defines the AIT as "[t]he lowest temperature at which [a hot-flame ignition] can occur in a mixture of optimum composition." Seaton assumes the optimum composition to be a stoichiometric ratio for all fuels. All autoignition events are assumed to have occurred in air (assumed to be 21% O_2 and 79% N_2 on a molar basis) at 1 atm absolute pressure.

Per Seaton's definition, a single oxygen attack on a single functional group is the initial step that leads to ignition. Therefore, each functional group (k) has a certain probability of leading to autoignition (p) which depends on temperature (T) that may be expressed as $p_k(T)$. As these probabilities are mutually exclusive, the probability that a pure compound will autoignite at a given temperature is the sum of the probabilities for each group k. Since the AIT is the temperature at which autoignition occurs it may be assumed that the AIT produces an overall probability of ignition approaching 1. Therefore, the AIT of a compound may be expressed in terms of the probability of ignition as follows:

$$1 = \sum_k p_k(AIT) \tag{6.1}$$

Seaton then derives a temperature-dependent probability for a single group ($p_k(T)$). First, Seaton assumes a probability associated with fuel-to-air ratio which is fixed at stoichiometric in this model. This returns: $p_{fuel-O_2} = A_i X_{fuel} X_{O_2}$ where A_i is a scaling constant and X_{fuel} and X_{O_2} are the stoichiometric fuel and oxygen mole fractions, respectively.

Second, Seaton expresses the probability of collision with an oxygen molecule as proportional to the square-root of the temperature, citing the kinetic theory of gases. This produces the following relationship: $p_{collision} = B_i T^{\frac{1}{2}}$ where B_i is a scaling constant and T is absolute temperature.

Third, Seaton considers the reactivity of each group using an Arrhenius expression to produce a probability of reaction with oxygen. This is expressed as: $p_{rxn} = C_i exp\left(\frac{-E_i}{RT}\right)$ where C_i is a scaling constant, E_i is the characteristic activation energy for a reaction with oxygen of group i with units of energy/mole, R is the ideal gas constant, and T is absolute temperature.

Finally, a characteristic probability of a group leading to ignition is considered for all other factors. This probability is assumed to be constant with respect to temperature. However, should multiple instances of the given group exist in the molecule the probability that one group should lead to ignition and not any of the others must be considered. This probability may be expressed as: $p_{other} = n_i p_i (1 - p_i)^{n_i - 1}$ where n is the number of instances of group i in the molecule, and p is the probability of one instance of group i leading to ignition.

All other model variables are assumed to be constant and therefore do not affect the probability of ignition. As all the probabilities must coincide to lead to ignition, these four probabilities are multiplied together to obtain the single-group probability (i.e. $p_k(T) = p_{fuel-O_2}\, p_{collision}\, p_{rxn}\, p_{other}$). Substituting this expression into Equation 6.1, combining the scaling constants and rearranging produces:

$$1.0 = X_{fuel}X_{O_2}\sum_k A_k AIT^{\frac{1}{2}} exp\left(\frac{-E_k}{AIT}\right) n_k p_k \left(1-p_k\right)^{n_k-1} \tag{6.2}$$

where A, E, and p are parameters that must be regressed for each group k.

To be useable, Equation 6.2 must be simplified, and the fuel-air term ($X_{fuel}X_{O_2}$) must be specified in a way that it can be calculated from structure. Under the assumption of stoichiometric ratio of fuel to air, this term may be expressed as follows:

$$X_{fuel}X_{O_2} = \frac{0.0882 n_O}{\left(n_O + 0.42\right)^2} \qquad n_O = \sum_k n_k C_{O(k)} \tag{6.3}$$

where n_O is the number of oxygen atoms needed to completely combust one molecule of fuel. Each functional group may be assigned a characteristic contribution (C_O) to n_O and each group's contribution summed together to calculate the fuel-air term. Substituting the fuel-air term and rearranging Equation 6.2 gives:

$$1.0 = \frac{0.0882 n_O}{\left(n_O + 0.42\right)^2}\sqrt{AIT}\sum_k A_k n_k p_k \left(1-p_k\right)^{n_k-1} exp\left(\frac{-E_k}{AIT}\right) \tag{6.4}$$

Equation 6.4 is implicit in AIT, so it must be numerically solved. Newton's method or a bisection method bound at reasonable temperature limits (e.g., between 300 and 2000 K) are suitable for this purpose.

6.2.2 Seaton's Implementation (AITMP™ 95C)

Seaton regressed his method against the best data available at the time. The sources of all the data he used in the regression are not clearly cited; however, his documentation seems to indicate that his original data set came from Bond's appendices [89]. In his appendices, Bond references several literature sources that represent a reasonable compendium of experimental AIT

values. Subsequent data were found from SDS's and possibly other unnamed sources. Seaton's documentation specifies that he performed evaluations on AIT values when more than one existed in the literature [88]. His focus was on promoting internal consistency of the data to ensure his method produced the best results possible.

Seaton used second-order groups with notation defined by Benson and Buss to model molecular structure [25]. The groups, along with his regressed parameters A, p, and E, are given in Table D.1 in the appendix. Also included in the table are C_O values that are used for the calculation of n_O.

Seaton's source code shows several other parameters that were regressed to deal with special cases. These are shown in Table D.2 in the appendix. Each special case replaces the original parameters if the case applies. These cases were implemented to both deal with anomalous behavior in the data for applicable compounds and to make corrections for compounds that had few data points for regression.

Seaton coded his implementation in Fortran IV and released it under the name AITMP™ of which the source code version 95C (hereafter denoted as AITMP™ 95C) was provided for this work. The software was compiled for MS-DOS on a 16-bit x86 architecture and included a command-line user interface for entering groups and pertinent information and then reporting the calculated AIT.

6.3 Improvements to the Seaton Method

The Seaton method represents a great leap forward in AIT prediction compared to the methods listed in Table 2.1. Its first-principles approach to modeling autoignition events sets it apart from any other existing method. However, the method has two major weaknesses. First, as the software was closed source, the insight that could be gained from Seaton's method was limited. Second, the amount of data available to Seaton was small compared to the data available today, and many of the original data were found to be from sources that used non-standard methodologies. This work aims to improve on the original Seaton method by widening the set of compounds that may be predicted by the Seaton method, improving the reliability of the data used in regression, and increasing the rigor of Seaton's autoignition model of by relaxing assumptions made in the original formalism.

6.3.1 Data Evaluation

Data for regression were taken from the latest version of the DIPPR 801 Database [52]. The following values were compiled from the database for each data point: A unique compound identifier, name, chemical family, sub-family, chemical formula, experimental AIT value, SMILES formula, molecular weight, and bibliographic information for the experimental AIT value. The initial data set consisted of 3690 AIT values for 908 unique compounds from 573 unique sources. All sources were evaluated for consistency with ASTM E659 and usability for regression. After evaluation, the data set was reduced to 948 values for 807 unique compounds from 187 unique sources. The evaluation process is explained here and the final data set may be found in the supplementary material.

AIT values were given a priority based on the source of each value and its reliability. The priority values and their corresponding meanings are shown in Table 6.1. The larger the priority values are considered to be more reliable in this work, with 1 and 0 being the least reliable. All values that were found to be unusable for regression (e.g., predicted values) were assigned a priority of 0 and were discarded from the set. The set was then automatically "pruned" using the following rules. For each unique compound:

1. Obtain all the AIT values for the compound.
2. Discard all AIT values with a priority value (PV) lower than the highest PV present if any PV of that set is 4 or 5; otherwise keep all the values.
3. Discard any duplicate values

Table 6.1: Priority Values and Corresponding Meanings Used in Data Selection

Priority number	Meaning
5	Primary; consistent with ASTM E659 or similar method
4	Cited; consistent with ASTM E659 or similar method
3	Primary; inconsistent method
2	Cited; inconsistent method

Table 6.1: Continued

Priority number	Meaning
1	Unknown method or source
0	Predicted, unusable for regression

These rules consider PVs 1-3 as having the same reliability because there are large sets of AIT values found in various books that do not cite the original source but include methodology that is inconsistent with standard methods. Given that it would be impossible to track down each original source for these large data sets they are assumed to be of relatively low quality and are discarded unless higher-priority AIT values cannot be found.

The pruned data set was then examined and more AIT values were discarded for various reasons. The most significant reasons for removal from this set are given here:

- Compounds could not be meaningfully represented with groups used for prediction (e.g., methane, formaldehyde, formic acid etc.).
- Duplicate AIT values were discovered.
- Values were outliers that disagreed significantly with other data or their family trends.
- Compounds decomposed or polymerized at temperatures below their AIT values.

AIT values were considered outliers if they deviated significantly from the trend of a homologous series (usually by 100 K or more). Also, outliers in family trends were discarded for many of the early members of a homologous series (i.e. compounds in series with a carbon number less than 4) as these have commonly been found to fall significantly out of line with the rest of the series. These smaller compounds usually have reliable experimental data and therefore are not a meaningful target for prediction nor do they inform prediction well. Given this, where these compounds deviated significantly from the family trend they were discarded.

Other outliers were examined, and literature searches revealed uncommon properties that explained their unusual AIT values such as their propensity to decompose or polymerize at temperatures below their AIT which makes the method of prediction meaningless for the pure compound.

This sort of prediction is outside the scope of this method as it is modeled and therefore, they were discarded as well. Overall, the number of outliers discarded for these reasons include 22 AIT values that were outliers in the family and 10 AIT values that decomposed or polymerized at temperatures below their AIT. Overall, this is a relatively small set of compounds and is not expected to significantly affect the results.

The final data set consists of the highest quality data possible, giving confidence in the quality of the regression and the reliability of the method. This final set was used to regress and test new parameters for the Seaton method.

6.3.2 Group Selection

The final data set was parsed to find the available groups that could be regressed. Based on the SMILES formulas for each compound, all first-order functional groups present in the data set were parsed and counted. Then, second-order atoms were added to groups that had sufficient representation in the data. Parsing was done using SMARTS formulas and the Python libraries written for RDKit [90]. The Python scripts used for this process are included in the supplementary material. The groups, along with a corresponding SMARTS formula and the number of instances found in the final data set, are given in Table D.3.

6.3.3 Regression Methodology

The number of parameters to be regressed was 201 parameters with 67 groups and 3 parameters per group, namely A, p, and E. The objective function for optimization was the sum of absolute error added to the absolute total bias (Equation 6.5),

$$Objective(Parameters) = \sum_i |AIT_{est(i)} - AIT_{exp(i)}| + |\sum_i AIT_{est(i)} - AIT_{exp(i)}| \tag{6.5}$$

where, $Parameters$ is a given parameter set, $AIT_{est(i)}$ is the estimated AIT value corresponding to each experimental AIT value ($AIT_{exp(i)}$) and i corresponds to each individual experimental AIT value. The parameters were bounded on intervals, creating a subspace in which to optimize.

In this subspace any combination of parameter values may be used. However, there are combinations of parameter values that produce a case where no solution exists to the Seaton Model. In such cases, the estimated AIT was set to a value ≤ 0 K, thereby punishing the objective function. These cases were caught by testing the model equation (e.g., Equation 6.4) at extreme limits to ensure the root of the equation was bracketed. This objective function was chosen based on trial and error with several options. Using an objective function based on sum of squared errors yielded undefined solutions for some compounds over several attempts at optimization. This result likely stems from a relatively large variance in the AIT data that would lead to errors being non-normally distributed, which is a key assumption of a sum-of-squared-errors objective. The sum of absolute errors was similarly tested and was able to find solutions for all compounds in the data set. However, the performance of the sum of absolute errors proved insufficient and included results with unacceptable biases. Therefore, the absolute value of the total bias was added to account for this. The final objective function produced the highest performance and solutions for all compounds in the data set.

As the objective function is highly non-linear and non-continuous, a gradient-based optimization is insufficient for this application. Therefore, the Leapfrogging Optimization algorithm was used for regression [91–93]. The method is a non-gradient, multiplayer, direct-search algorithm sufficient for this application. In Leapfrogging Optimization, optima are searched for on bounded intervals. Given this, domains and search intervals for optimization needed to be determined for A, p, and E. For A, the domain could be any real number ($[-\infty, \infty]$). The domain of p, which is modeled as a probability, lies between 0 and 1 ($[0.0, 1.0]$). As E represents an activation energy, its domain can only exist for positive values ($[0, \infty]$). Given that the intervals for optimization must be finite and closed, infinity was replaced with a value of 20000, an arbitrary value that is one order of magnitude larger than any of Seaton's parameters. The final intervals for optimization are listed in Table 6.2.

Table 6.2: Bounds of Optimization for regression of the Seaton Method

Parameter	Interval
A	$[-20000.0, 20000.0]$
p	$[0.0, 1.0]$

Table 6.2: Continued

Parameter	Interval
E	$[0.0, 20000.0]$

The regression process was executed on a server with an Intel® Xeon® Silver 4216 CPU @ 2.10GHz with 64 cores and 256 GB of RAM running Red Hat Enterprise Linux Server version 7.8. Python (3.6.8) with NumPy (1.19.2), SciPy (1.5.2), Pandas (1.1.3), and the Leapfrog Optimizer Package (1.0.1) were used for the optimizations [94–97]. Associated scripts and other pertinent data are included in the supplementary material.

With the objective function and parameter bounds defined, the process of regression proceeds as follows. Initially, all groups are given guess parameters $[1.0, 0.5, 10.0]$ for A, p, and E respectively. Parameters A, p, and E are regressed simultaneously for each group. Each group is regressed sequentially, in order of decreasing representation in the data set (see Table D.3). As each group is optimized, the parameters are updated so that each subsequent optimization includes parameters from all previously optimized groups. A regression of all the possible groups and updating of parameters constitutes a "trial". Trials are repeated until the objective function stops improving.

Data are selected for regression only if they can be represented by groups that are currently being optimized or were optimized in a previous trial. This avoids biasing the optimization with irrelevant data. Groups that have insufficient representation in the data are included with similar groups and these sets of groups are regressed as if they are one group (e.g., Si, SiH, SiH2, and SiH3 all have the same parameter values).

The following example illustrates this process. In Trial One, only "CH2-(C,C)" (the group with the highest representation) is regressed first. There are no compounds that can be represented with only this group so it is skipped. Next "CH3-(C)" (the next-highest-represented group) is regressed. The only compound that can be represented with only this group is ethane, so the parameters are fit to ethane. Next, "O-(C,C)" is regressed. There are still a limited number of compounds that can be represented using only "O-(C,C)" and "CH3-(C)" so "O-(C,C)" is regressed

against these. This continues until all groups have either been regressed or skipped, ending Trial One.

Trial Two begins and uses the parameters regressed from Trial One. "CH2-(C,C)" (the group with the highest representation) is regressed first. Now that "CH3-(C)" has been regressed, "CH2-(C,C)" may be regressed using all of the normal alkane data and data from other compounds with groups that were regressed in Trial One. "CH3-(C)" is then re-regressed using all the compounds with groups that were regressed in trial one and the newly regressed "CH2-(C,C)" parameters. This continues until all groups have either been regressed or skipped, ending Trial Two.

Each subsequent trial will include more and more of the final data set until all of the data are used and none of the groups are skipped. As each set of parameters are updated each group is re-regressed to fit to the new parameters. This process continues until the objective function for the entire data set stops improving significantly.

As the Leapfrogging algorithm is a stochastic optimization method, optima between attempts for each group in each trial may vary significantly. Therefore, in each trial, each group optimization is executed 20 times in parallel and the best results are kept. This makes the global optimum more likely to be found. Also, the best results are kept only if they improve over results from the previous trial. If the previous trial result is better than any from the current trial, all current solutions are discarded. All optimization trials were finally completed using this methodology. In every case, an optimum was found that improved on the initial guess values.

To determine transferability, parameters were first regressed using a 100% training set. This allowed examination of the dataset as a whole and allowed identification of outliers in the data. Next, parameters were regressed using an 80-20 training-testing split. The best results from each set of trials are reported in the supplementary material. For the trials with a testing set, each trial included a unique random split into training and testing sets, making the global optimum a moving target. This strategy protects against accidentally finding an ideal training and testing set that produces an artificially low optimum.

6.3.4 Changes to the Seaton Model

Once the original Seaton method was newly regressed with the new groups, the form of Equation 6.4 was modified to relax or change the assumptions of the model. Improvement was found by relaxing the assumption that the optimum fuel-to-air ratio was stoichiometric. This produced Equation 6.6,

$$1.0 = \sqrt{AIT}\sum_k A_k \frac{0.0882 d_k n_O}{(n_O + 0.42 d_k)^2} n_k p_k (1-p_k)^{n_k - 1} exp\left(\frac{-E_k}{AIT}\right) \tag{6.6}$$

where d_k is a parameter representing a theoretical optimal equivalence ratio and was given bounds $d_k \in [10^{-16}, 10^{16}]$. However, the random values used in Leapfrogging are distributed uniformly. In a uniform distribution the grand majority of the random values would fall in the range between 1 and 10^{16} which is the fuel-rich region of this range. So, to represent both the fuel-rich and lean parts of this range, Equation 6.6 had to be modified with the following substitution: $d_k = 10^{g_k}$ where $g_k \in [-16, 16]$. This substitution allows uniform scattering on the basis of fuel-to-air ratio instead of biasing towards fuel-rich equivalence ratios.

This modified model was regressed following the same procedure as described for the original model with the only change being the additional parameter per group. The original model and the model described here are the only models compared and discussed in this work. The three prediction methods presented here will be referred to as "AITMP™ 95C" for Seaton's original implementation, "Seaton-Redd" for the implementation with the new data set and groups using Seaton's original model (Equation 6.4), and "Seaton-Redd2" for the implementation with the new data set and groups using Equation 6.6.

6.4 Results and Discussion

In this work, AAD refers to average absolute deviation, is calculated as $AAD = \frac{1}{N}\sum_i^N |AIT_{est(i)} - AIT_{exp(i)}|$, and has units of Kelvin. ARD is the average relative deviation, is expressed as a percentage with no units, and is calculated as $ARD = \frac{1}{N}\sum_i^N \frac{|AIT_{est(i)} - AIT_{exp(i)}|}{AIT_{exp(i)}}\%$. The bias has units of Kelvin and is calculated as $Bias = \frac{1}{N}\sum_i^N AIT_{est(i)} - AIT_{exp(i)}$. $max(D)$ refers to the maximum deviation, has units of Kelvin and is calculated as $max(D) = maximum([|AIT_{est(1)} - AIT_{exp(1)}|, |AIT_{est(2)} - AIT_{exp(2)}|, ... |AIT_{est(N)} - AIT_{exp(N)}|])$. Finally, R^2 refers to the correlation coefficient and is calcu-

lated using Equation 6.7,

$$R^2 = 1 - \frac{\sum_i^N (AIT_{est(i)} - AIT_{exp(i)})^2}{\sum_j^N (AIT_{exp(j)} - \overline{AIT_{exp}})^2} \tag{6.7}$$

where $AIT_{exp(i)}$ and $AIT_{est(i)}$ are corresponding experimental and estimated AIT values, respectively, and $\overline{AIT_{exp}}$ is the mean value of all experimental AIT values in the given data set.

The progression and improvement over each trial for the Seaton-Redd and Seaton-Redd2 regressions for both trials with and without testing sets are demonstrated in Figure 6.1, which shows the AAD as a function of optimization trial number for each case. Predictably, the initial optimization trials yielded poor performance, but the situation quickly improved as more groups were represented. For the trials with no testing set, after the initial drop in average absolute deviation (AAD) the improvements were incremental and small. Trials were continued until the AAD for the entire set stopped improving. For each trial with a training-testing split, the data were split randomly into the training or testing set and all parameters were regressed anew in attempt to improve on the performance of the parameters regressed in the previous trial. For both models, the training set performance progression was relatively stable after the initial drop in AAD, but the testing-set performance varied significantly.

The trials with no testing set represent a larger data set that, if transferrable, would increase confidence in the method. Therefore, to determine the transferability of the parameters, statistical calculations were performed on the data from trials after the training set performance progression flattened out. The trials selected for these comparisons are enclosed in a black rectangle in Figure 6.1.

6.4.1 Transferability

Table 6.3 shows the statistical performance of Seaton-Redd and Seaton-Redd2 methods over all the trials inside the rectangles in Figure 6.1. For both methods, the training sets perform similarly on average. However, the Seaton-Redd2 method outperforms the Seaton-Redd method by nearly every statistical measure studied. This suggests the modified Seaton-Redd2 model is capturing more of the variance seen in the experimental data.

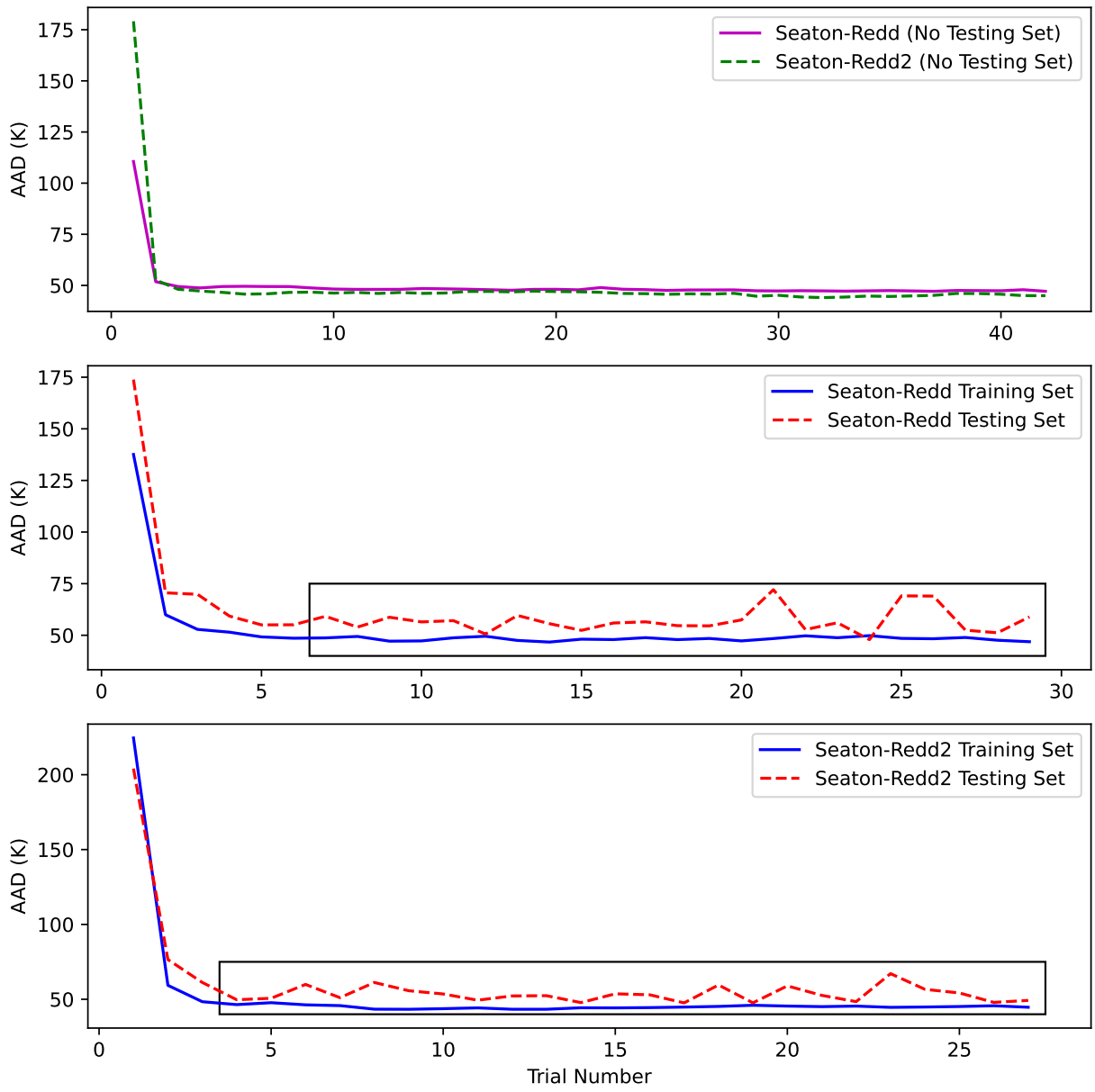

Figure 6.1: Average absolute deviation (AAD) progress over 4 independent sets of trials for 100% training set (first plot) and an 80-20 training-testing split (second and third plots) and for the Seaton-Redd and Seaton-Redd2 methods. For the training-testing trials, the data set was split randomly for each trial and regressed anew while attempting to improve on the parameters regressed in the previous trial. To measure transferability, statistical calculations were performed for the 80-20-split trials and included only information from the trials inside the boxes in the second and third plots.

Table 6.3: Comparison of average absolute deviations (AAD) and maximum deviations ($max(D)$) from the 80-20-split trials for the Seaton-Redd and Seaton-Redd2 methods. The given statistics include the mean ($\bar{y}$), sample standard deviation (σ_{sample}), and a "worst-case scenario" (y_{worst_case}) that is the sum of the mean and the single-point prediction interval at a 95% confidence level ($z_{95\%}\,\sigma_{sample}$). These statistics were taken from the results of trials plotted inside the rectangles on the second and third plots in Figure 6.1. Each trial used a randomized 80-20 training-testing split in the regression data. All statistical figures have units of Kelvin.

	Training Set		Testing Set	
	AAD	$max(D)$	AAD	$max(D)$
Seaton-Redd				
$\bar{y}$	48.29	261.82	57.05	406.61
σ_{sample}	0.91	46.90	5.95	223.08
$y_{worst\_case} = \bar{y} + z_{95\%}\,\sigma_{sample}$	49.78	338.96	66.83	773.54
Seaton-Redd2				
$\bar{y}$	44.89	242.75	53.34	338.62
σ_{sample}	1.11	33.91	5.08	177.20
$y_{worst\_case} = \bar{y} + z_{95\%}\,\sigma_{sample}$	46.71	298.53	61.70	630.09

The statistics in Table 6.3 represent a distribution of random possible training-testing splits. Therefore, any combination of a training-testing split is expected to perform within those bounds to the given confidence level. Given this and the larger training set, the trials with no testing set are expected to perform no worse than the trials with training-testing splits at the given confidence level for compounds outside the set. For comparison, the highest-performing trials with no testing set with their corresponding statistics are given in Table 6.4. Their corresponding parameters are given in the supplementary material for having the largest regression set, possibly making them more reliable than the parameters regressed with and 80-20 split.

Table 6.4: Best performances from trials with no testing set

	AAD (K)	*ARD* (%)	*Bias* (K)	$max(D)$ (K)	R^2
Seaton-Redd	47.14	7.64	0.49	281.87	0.71
Seaton-Redd2	44.05	7.18	0.7	190.35	0.75

6.4.2 Performance

The parameters from the 80-20-split trials that produced the best results are compared in Table 6.5. The parameter sets were chosen based on the overall performance and similarity of performance between the training and testing sets, indicating consistent performance across the widest range of compounds. These sets are recommended as having the highest verified performance, despite being trained with a smaller data set.

Table 6.5: Best performances from optimization trails with an 80-20 training-testing split. Best sets were chosen based on overall performance and similarity of the training and testing performance. Statistics were calculated based on deviation (D) from experimental values (i.e., $D_i = AIT_{est(i)} - AIT_{exp(i)}$). Therefore, it is expected that these parameters should never deviate greater than the "worst case" deviation at a 95% confidence level.

	Seaton-Redd		Seaton-Redd2	
	Training Set	Testing Set	Training Set	Testing Set
AAD (K)	47.60	51.20	44.66	49.25
ARD (%)	7.69	8.31	7.20	7.74
Bias (K)	0.27	3.84	0.09	-5.09
$max(D)$ (K)	251.54	229.74	223.69	233.46
R^2	0.71	0.68	0.74	0.69
$\sigma_{D,sample}$ (K)	61.93	64.99	58.02	67.79
$D_{worst\_case} = \lvert Bias \rvert + z_{95\%}\,\sigma_{D,sample}$ (K)	102.13	110.75	95.52	116.60

In the final analysis, four different parameter sets were considered for recommendation with the two differences being the use of different models or the presence or absence of a testing set. Two sets were regressed with no testing set but are expected to perform similarly to the statistical metrics in Table 6.3. The other two are verified with testing sets but use a smaller training set and therefore may be less reliable.

However, the Seaton-Redd2 method consistently predicts more accurately than Seaton-Redd by any metric. Because of this, Seaton-Redd2 is the recommended method in this work for the most accurate prediction. However, a part of this work is to verify that improvements have been made to the original method. Therefore, the best parameter sets from the trials with training-testing splits were compared to Seaton's original method to compare performance.

6.4.3 Comparison to Seaton's Original Method

The new methods have obvious advantages over the original Seaton method in their applicability to a larger set of compounds. However, a comparison to the original method shows that the performance of the original has been maintained. A smaller set of compounds that could be modeled by all of the methods was used for comparison, and included 561 AIT values from 490 unique compounds. Performance statistics of the original Seaton method (AITMP™ 95C) and the new methods (Seaton-Redd and Seaton-Redd2) for this data set are shown in Table 6.6.

Table 6.6: Statistical comparison of the original Seaton method (AITMP™ 95C), the new method regressed with the evaluated data set, new groups, and the original model (Seaton-Redd), and the new method regressed with the evaluated data set, new groups, and the modified model (Seaton-Redd2). This comparison uses a smaller set of 561 AIT values from 490 unique compounds that could be modeled by both the original Seaton method and the new methods.

	AITMP™ 95C	Seaton-Redd	Seaton-Redd2
AAD (K)	42.00	44.09	41.63
ARD (%)	6.88	7.34	6.90
Bias (K)	-0.16	1.21	-0.55
$max(D)$ (K)	298.76	188.05	233.46

Table 6.6: Continued

	AITMP™ 95C	Seaton-Redd	Seaton-Redd2
R^2	0.64	0.69	0.71

The performance in AAD between AITMP™ 95C and the new methods differs by less than 5%, but the improvements to the maximum deviation are significant. For the maximum deviation, the Seaton-Redd and Seaton-Redd2 methods improve on the original by 37% and 21% respectively. These lower values for max deviation suggest that the methods are more transferable and result in fewer egregious outliers than AITMP 95C. Overall, the Seaton-Redd2 method performs more consistently than AITMP™ 95C while increasing the functional groups available to the technique.

6.4.4 Limitations

The statistical figures shown in this work constitute the expected performance of the Seaton-Redd and Seaton-Redd2 methods for compounds outside of the evaluated data set. However, there are caveats in the methods that are noted here. Some of the groups could not be combined with other groups for regression and, because of their low representation in the data, are overfitted in the regressions. These include an oxygen connected to a carbon and a nitrogen (i.e. "O-(C,N)"), a double-bonded nitrogen (i.e. "=N"), and an iodine group (i.e. "I").These groups were included in the regression for completeness and should still provide some utility in prediction. However, predicted AIT values for compounds that include these groups should be considered as having higher uncertainties than other predicted values.

6.5 Conclusions and Recommendations

New non-linear, group-contribution methods for predicting AIT have been presented based on the work of the late Dr. William H. Seaton. These methods' main advantages lie in their modeling autoignition events from a first-principles basis and represent the most successful attempts in modeling the complexity of the autoignition process. Thus, these models serve to improve phenomenological understanding of autoignition events. The new methods presented are also unique

in that they are regressed using *evaluated* data whereas previous approaches used data of questionable quality. The evaluated data set is given in the supplementary material.

The Seaton-Redd2 method, which includes the model represented by Equations 6.6 and 6.3, and the corresponding parameter set regressed with the 80-20 split given in the supplementary material, is recommended over all other prediction approaches currently available for AIT. The Seaton-Redd2 method may be used to predict AIT for a large set of increasingly exotic compounds to within statistical figures described without the need for process of measurement, which can be costly and, for some compounds, dangerous. These improvements to efficiently predict AIT and the evaluated data set will allow the prevention of devastating fires and promote improved safety for industrial processes everywhere.

CHAPTER 7. SUMMARY AND RECOMMENDATIONS

7.1 Summary

In this work, the problems and limits of phenomenological understanding associated with AIT are detailed including some examples of their applications in regulations and chemical plant design. In particular the weaknesses in the literature were reviewed along with general misuse of thermophysical data in the literature and subsequently with the DIPPR 801 Database. These issues were treated in this work through the following findings.

First, a comprehensive study of AIT in the normal alkane chemical family revealed and explained two previously unexplained trends that appeared at carbon numbers greater than 20. The first is the gradual rise in AIT due to lower volatility of the increasingly larger compounds. This trend may be correlated to the flash point trend for the same compounds. The second was a discontinuity between C26 and C26 in the *n*-alkanes. This was found to be a tipping point for competing mechanisms that control the measured AIT. The first mechanism is the expected combustion process that produces heat and leads to thermal runaway. The second is decomposition that prevents thermal runaway though consuming heat and fuel. Thus, a higher temperature is needed to overcome the effect of decomposition.

As part of the normal alkane study, a new apparatus and experimental setup were designed and constructed to compensate for the high altitude where the experiments took place, which was found to bias measured AIT values to be artificially high. The new experimental setup also removed human error through an automated injection system and a camera to record ignition events.

Secondly, other chemical families were investigated and AIT values were measured for a total of 20 compounds including the *n*-alkanes. Multiple chemical families were evaluated and trends were recommended. These trends were then compared to the results of the *n*-alkanes to qualitatively show the effect of a given functional group on the limiting trend of the *n*-alkanes.

Third, a careful evaluation of experimental AIT values from 611 sources was conducted to find and recommend the best experimental values for use in the DIPPR 801 database and for the purposes of training an improved prediction method. This evaluation produced an AIT data set of 948 values for 807 unique compounds from 187 unique sources of data.

Fourth, this data set was used to train and test an improved method of prediction built on the work of the late William H. Seaton. Two models and 4 parameter sets are given in this work in Chapter 6 Appendices C and D. Results show the methods match or improve on the performance of the Seaton's original method while expanding applicability to many other compounds. The applicability of the new methods produced a 72% reduction of compounds in the DIPPR 801 Database that have no reported AIT value. The models also provide insight into the mechanisms of autoignition and are unique in their first-principles approach.

Finally, a final recommended set of AIT values is given for inclusion in the DIPPR 801 Database. This set is recommended based on evaluations from this work as well as all of the insight gained from every other part of this work. This represents a significant step forward in the quality and completeness of AIT data in the DIPPR 801 Database.

7.2 Recommendations

The recommendations for usage of DIPPR data in the literature explained in Chapter 3. The set of recommended AIT values for compounds referenced in this work is given in Table E.1. The recommended model and parameters for the Seaton-Redd2 method are given in Equations 6.3 and 6.6, and in Appendix D respectively.

It is recommended that all AIT values be evaluated by considering consistency with standard methods. AIT values obtained from inconsistent measurement methodologies should be considered as having higher uncertainties than those from standard methods including ASTM E659, ASTM D2155, and DIN 51794 specifically. Uncertainties from the accepted standard methods should continue to be assigned per method specifications. Care should be taken that future AIT measurements adhere to ASTM E659 methodology for consistency. AIT values from standard methods should not be considered as equivalent to the minimum temperature at which autoignition occurs under any circumstances. In industry, the measured AIT should be considered as having

higher uncertainty than reported in this work. Various sets of specific conditions may alter a compounds minimum temperature of autoignition significantly.

The AIT values of pure polyfunctional compounds are sparse in the literature and merit study to observe the interactions between various functional groups and the subsequent effect on the measured AIT value. AIT mixture measurement also represents a possible area of future study as relatively few mixtures have been measured in the literature. This represents a particularly important area of study as mixtures are ubiquitous in industrial applications. A detailed study of the kinetics of combustion and decomposition will shed further light on the interaction of these competing mechanisms as it relates to autoignition. The Seaton-Redd2 method should be investigated further and modified to better capture the complexity of the autoignition process. Finally, a more detailed study of the relationships between AIT and other flammability and thermophysical properties will further push general understanding of the autoignition process.

Bibliography

[1] CSB, 2014. Catastrophic rupture of heat exchanger (seven fatalities) Tech. Rep. 2010-08-I-WA, U.S Chemical Safety and Hazard Investigation Board, May. 1, 5

[2] CSB, 2015. Chevron richmond refinery pipe rupture and fire Tech. Rep. 2012-03-I-CA, U.S. Chemical Safety and Hazard Investigation Board, Jan. 1, 5

[3] OSHA, 2019. *Occupational Safety and Health Standards: Flammable liquids. - 1910.106.*, Vol. 6 of *29 CFR* Occupational Safety and Health Administration, June. 1, 5

[4] Babrauskas, V., 2003. *Ignition Handbook*. Fire Science Publishers, Issaquah, WA. 1, 6, 7, 8, 15, 54, 55

[5] ASTM, 2015. Astm e659-15 standard test method for autoignition temperature of chemicals. x, 3, 6, 7, 10, 31, 37

[6] ASTM, 2012. Astm d2155-12 standard test method for determination of fire resistance of aircraft hydraulic fluids by autoignition temperature. 3, 6, 7

[7] Smith, G. P., Golden, D. M., Frenklach, M., Moriarty, N. W., Eiteneer, B., Goldenberg, M., Bowman, C. T., Hanson, R. K., Song, S., Gardiner, W. C., Jr., Lissianski, V. V., and Qin, Z. Gri-mech 3.0. xi, 3, 65, 66

[8] Glassman, I., and Yetter, R. A., 2008. *Combustion*., fourth ed. Elsevier. 4

[9] Carhart, H. W., 1979. *Factors in UsingKerosine Jet Fuel of Reduced Flash Point, ASTM STP 688*. American Society for Testing and Materials, ch. Jet Fuel Safety and Flash Point, pp. 35–45. 6, 63

[10] Setchkin, N. P., 1954. "Self-ignition temperatures of combustible liquids." *Journal of Research of the National Bureau of Standards,* **53**(1), July, pp. 49–66. x, xi, 6, 7, 8, 38, 39, 60, 119, 120, 121, 122, 123, 125, 209, 213, 216, 218, 220, 221, 229

[11] DIN, 2003. Din 51794 testing of mineral oil hydrocarbons - determination of ignition temperature, Jan. 6

[12] Zabetakis, M. G., Furno, A. L., and Jones, G. W., 1954. "Minimum spontaneous ignition temperatures of combustibles in air." *Industrial and Engineering Chemistry,* **46**(10), Oct., pp. 2173–2178. x, xi, 7, 8, 9, 14, 38, 39, 50, 60, 61, 63, 68, 78, 83, 84, 118, 119, 120, 121, 122, 123, 125, 126, 209, 214, 218, 236

[13] Zabetakis, M. G., Scott, G. S., and Kennedy, R. E., 1962. Autoignition of lubricants at elevated pressures Tech. Rep. Report of Investigations 6112, Bureau of Mines, United States Department of the Interior. 7

[14] Zabetakis, M. G., 1965. Flammability characteristics of combustible gases and vapors Tech. Rep. Bulletin 627, Bureau of Mines, United States Department of the Interior. 7, 38, 118, 119, 120, 121, 122, 123, 215, 229, 232, 233

[15] Sortman, C. W., Beatty, H. A., and Heron, S. D., 1941. "Spontaneous ignition of hydrocarbons zones of nonignition." *Industrial and Engineering Chemistry,* **33**(3), Mar., pp. 357–360. 7

[16] Frank, C. E., and Blackham, A. U., 1952. "Spontaneous ignition of organic compounds." *Industrial and Engineering Chemistry,* **44**(4), Apr., pp. 862–867. 7, 8, 38, 121, 122, 123, 124

[17] Affens, W. A., Johnson, J., and Carhart, H. W., 1961. "Effect of chemical structure on spontaneous ignition of hydrocarbons." *Journal of Chemical and Engineering Data,* **6**(4), Oct., pp. 613–619. x, xi, 7, 38, 39, 60, 120, 121, 122, 125, 209, 210, 211, 213

[18] Furno, A. L., Imhof, A. C., and Kuchta, J. M., 1968. "Effect of pressure and oxidant concentration on auto-ignition temperatures of selected combustibles in various oxygen and dinitrogen tetroxide atmospheres." *J. Chem. Eng. Data,* **13**(2), Apr., pp. 243–249. x, xi, 7, 31, 38, 39, 60, 119, 120, 121, 125, 209

[19] Jones, G. W., Seaman, H., and Kennedy, R. E., 1933. "Explosive properties of dioxan-air mixtures." *Industrial & Engineering Chemistry,* **25**(11), pp. 1283–1286. 7, 228

[20] Babrauskas, V., 2008. "Ignition of gases, vapors, and liquids by hot surfaces." In *Proceedings of the 3rd International Symposium on Fire Investigation Science and Technology*, Fire Science & Technology Inc., National Association of Fire Investigators. 7

[21] Nabert, K., SchÃ¶n, G., and Redeker, T., 2004. *Sicherheitstechnische Kenngrößen brennbarer Gase und Dämpfe*. Deutscher Eichverlag. x, xi, 9, 15, 38, 39, 60, 63, 65, 118, 119, 120, 121, 122, 123, 124, 125, 126, 209, 210, 211, 212, 213, 214, 215, 216, 217, 218, 219, 220, 221, 222, 223, 224, 226, 229, 232, 233, 234

[22] Shimy, A. A., 1970. "Calculating flammability characteristics of hydrocarbons and alcohols." *Fire Technology,* **6**, pp. 135–139. 9

[23] Shebeko, Y. N., Korol'chenko, A. Y., Ivanov, A. V., and Alekhina, E. N., 1984. "Calculation of flash points and ignition temperatures of organic compounds." *The Soviet Chemical Industry,* **16**(11), pp. 1371–1375. 9

[24] Joback, K., and Reid, R. C., 1987. "Estimation of pure-component properties from group-contributions." *Chemical Engineering Communications,* **57**(1-6), pp. 233–243. 9

[25] Benson, S. W., and Buss, J. H., 1958. "Additivity rules for the estimation of molecular properties. thermodynamic properties." *The Journal of Chemical Physics,* **29**(3), Sept., pp. 546–572. 9, 92

[26] Egolf, L. M., and Jurs, P. C., 1992. "Estimation of autoignition temperatures of hydrocarbons, alcohols, and esters from molecular structure." *Industrial & Engineering Chemistry Research,* **31**(7), pp. 1798–1807. 11, 16

[27] Suzuki, T., Ohtaguchi, K., and Koide, K., 1992. "Correlation and prediction of autoignition temperatures of hydrocarbons using molecular properties." *Journal of Chemical Engineering Japan,* **25**, pp. 606–608. 11, 14

[28] Pintar, A. J., 1996. "Estimation of autoignition temperature." *Technical Support Document, DIPPR Project 912*, July. 11, 14, 16

[29] Tetteh, J., Metcalfe, E., and Howells, S. L., 1996. "Optimisation of radial basis and backpropagation neural networks for modelling auto-ignition temperature by quantitative-structure property relationships." *Chemom. Intell. Lab. Syst.,* **32**(2), pp. 177–191. 11, 38, 119, 120, 121, 122, 228, 232, 233

[30] Mitchell, B. E., and Jurs, P. C., 1997. "Prediction of autoignition temperatures of organic compounds from molecular structure." *Journal for Chemical Information and Computer scientists,* **37**, pp. 538–547. 11, 12

[31] Kim, Y., Lee, S., Kim, J., Kim, J., and Tai No, K., 2002. "Prediction of autoignition temperatures (aits) for hydrocarbons and compounds containing heteroatoms by the quantitative structureâ€"property relationship." *Journal of the Chemical Society. Perkin Transactions 2,* **2**(12), pp. 2087–2092 cited By 21. 12

[32] Albahri, T. A., and George, R. S., 2003. "Artificial neural network investigation of the structural group contribution method for predicting pure components auto ignition temperature." *Industrial & Engineering Chemistry Research,* **42**(22), pp. 5708–5714. 12, 16

[33] Pan, Y., Jiang, J., Wang, R., Cao, H., and Zhao, J., 2008. "Prediction of auto-ignition temperatures of hydrocarbons by neural network based on atom-type electrotopological-state indices." *Journal of Hazardous Materials,* **157**(2), pp. 510 – 517. 12, 15

[34] Pan, Y., Jiang, J., Wang, R., and Cao, H., 2008. "Advantages of support vector machine in qspr studies for predicting auto-ignition temperatures of organic compounds." *Chemometrics and Intelligent Laboratory Systems,* **92**(2), pp. 169 – 178. 12, 15

[35] Chen, C.-C., Liaw, H.-J., and Kuo, Y.-Y., 2009. "Prediction of autoignition temperatures of organic compounds by the structural group contribution approach." *Journal of Hazardous Materials,* **162**(2), pp. 746–762. 12, 16

[36] Pan, Y., Jiang, J., Wang, R., Cao, H., and Cui, Y., 2009. "Predicting the auto-ignition temperatures of organic compounds from molecular structure using support vector machine." *Journal of Hazardous Materials,* **164**(2), pp. 1242 – 1249. 12, 13, 15

[37] Pan, Y., Jiang, J., Ding, X., Wang, R., and Jiang, J., 2010. "Prediction of flammability characteristics of pure hydrocarbons from molecular structures." *AIChE Journal,* **56**(3), pp. 690–701. 13, 16

[38] Gharagheizi, F., Eslamimanesh, A., Mohammadi, A. H., and Richon, D., 2011. "Use of artificial neural network-group contribution methodto determine surface tension of pure compounds." *Journal of Chemical & Engineering Data,* **56**(5), May, pp. 2587–2601. 13, 16

[39] LazzÃºs, J. A., 2011. "Autoignition temperature prediction using an artificial neural network with particle swarm optimization." *International Journal of Thermophysics,* **32**(5), p. 957. 13

[40] Bagheri, M., Borhani, T. N. G., and Zahedi, G., 2012. "Estimation of flash point and autoignition temperature of organic sulfur chemicals." *Energy Conversion and Management,* **58**, pp. 185–196. 13, 16

[41] Tsai, F.-Y., Chen, C.-C., and Liaw, H.-J., 2012. "A model for predicting the auto-ignition temperature using quantitative structure property relationship approach." *Procedia Engineering,* **45**, pp. 512 – 517 2012 International Symposium on Safety Science and Technology. 13, 16

[42] Keshavarz, M. H., Gharagheizi, F., and Ghanbarzadeh, M., 2013. "A simple correlation for prediction of autoignition temperature of various classes of hydrocarbons." *Journal of the Iranian Chemical Society,* **10**(3), pp. 545–557. 13

[43] Borhani, T. N. G., Afzali, A., and Bagheri, M., 2016. "Qspr estimation of the auto-ignition temperature for pure hydrocarbons." *Process Safety and Environmental Protection,* **103**, pp. 115 – 125. 13, 16

[44] Frutiger, J., Marcarie, C., Abildskov, J., and Sin, G., 2016. "Group-contribution based property estimation and uncertainty analysis for flammability-related properties." *Journal of Hazardous Materials,* **318**, pp. 783 – 793. 13, 14, 16

[45] Keshavarz, M. H., Jafari, M., Esmaeilpour, K., and Samiee, M., 2018. "New and reliable model for prediction of autoignition temperature of organic compounds containing energetic groups." *Process Safety and Environmental Protection,* **113**, pp. 491 – 497. 13, 16, 22

[46] Dashti, A., Jokar, M., Amirkhani, F., and Mohammadi, A. H., 2020. "Quantitative structure property relationship schemes for estimation of autoignition temperatures of organic compounds." *Journal of Molecular Liquids,* **300**, p. 111797. 13, 15

[47] Baskin, I., Lozano, S., Durot, M., Marcou, G., Horvath, D., and Varnek, A. "Autoignition temperature: comprehensive data analysis and predictive models." pp. 597–613 PMID: 32646236. 13, 61, 63

[48] Hukkerikar, A. S., Sarup, B., Ten Kate, A., Abildskov, J., Sin, G., and Gani, R., 2012. "Group-contribution+ (gc+) based estimation of properties of pure components: Improved property estimation and uncertainty analysis." *Fluid Phase Equilibria,* **321**, pp. 25–43. 15

[49] Bloxham, J. C., Redd, M. E., Giles, N. F., Knotts, T. A., and Wilding, W. V., 2021. "Proper use of the dippr 801 database for creation of models, methods, and processes." *Journal of Chemical & Engineering Data,* **66**(1), pp. 3–10. 16

[50] Rowley, R. L., Wilding, W. V., Congote, A., and Giles, N. F., 2010. "The use of database influence factors to maintain currency in an evaluated chemical database." *International Journal of Thermophysics,* **31**(4), pp. 860–874. x, 23

[51] Tatar, A., Moghtadaei, G. M., Manafi, A., Cachadiña, I., and Mulero, A., 2020. "Determination of pure alcohols surface tension using artificial intelligence methods." *Chemometrics and Intelligent Laboratory Systems,* **201**, p. 104008. 22

[52] Wilding, W. V., Knotts, T. A., Giles, N. F., and Rowley, R. L., 2020. *DIPPR® Data Compilation of Pure Chemical Properties*. Design Institute for Physical Properties, AIChE, New York, NY. x, 24, 44, 93

[53] Brandes, E., Hirsch, W., and Stolz, T., 2005. "Autoignition temperatures for mixtures of flammable liquids with air at elevated pressures." In *Proceedings of the European Combustion Meeting*. 31

[54] ASTM, 2014. Astm e968-02 standard practice for heat flow calibration of differential scanning calorimeters. 36

[55] ASTM, 2020. Astm e537-20 standard test method for thermal stability of chemicals by differential scanning calorimetry. 36

[56] ASTM, 2018. Astm e793-06 standard test method for enthalpies of fusion and crystallization by differential scanning calorimetry. 36

[57] ASTM, 2016. Astm d3828 - 16a standard test methods for flash point by small scale closed cup tester. x, 37, 43, 44

[58] AFMFIC, 1940. "Properties of flammable liquids, gases, and solids." *Industrial & Engineering Chemistry,* **32**(6), pp. 880–884 The Associated Factory Mutual Fire Insurance Companies. 38, 118, 119, 120, 121, 228, 233

[59] Coffee, R., 1980. "Cool flames and autoignitions: Two oxidation processes." *Loss Prevention,* **13**, pp. 74–82. 38, 54, 118, 119, 120

[60] , 1982. Item 82030: Fire hazardous properties: Flash points, flammability limits, and autoignition temperatures Tech. rep., Engineering Science Data, London. 38, 123, 234

[61] Hilado, C. J., 1973. *Flammability Test Methods Handbook*. Technomic Publishing Co. 38, 118, 119, 120, 121, 122, 123

[62] INTERNATIONAL ELECTROTECHNICAL COMMISSION, 1970. *Publication 79-4A: Electrical Apparatus for Explosive Gas Atmospheres. Part 4. Method of Test for Ignition Temperature*., supplement 1 ed. Geneva. 38, 120, 121, 123

[63] Kuchta, J. M., 1985. Bull. no. 680: Investigation of fire and explosion accidents in the chemical, mining, and fuel-related industries - a manual resreport 680, U. S. Bureau of Mines, Washington D. C. 38, 118, 119, 120, 121, 122, 123, 212, 229, 232, 233

[64] Lewis, R., 1992. *Sax's Dangerous Properties of Industrial Materials, 8th Ed.*. Van Nostrand, New York. 38, 123

[65] Tryon, G., 1962. *Fire Protection Handbook, 12th ed.*., 12th ed. National Fire Protection Association, Boston, Massachusetts. 38, 118, 119, 120, 121, 122, 123

[66] , 1969. *Fire Protection Guide on Hazardous Materials 3rd Ed.*., 3rd ed. National Fire Protection Association, Boston, Massachusetts. 38, 119, 120, 122

[67] , 1991. *Fire Protection Guide to Hazardous Materials 10rd Ed.*., 10th ed. National Fire Protection Association, Boston, Massachusetts. 38, 122, 123, 124

[68] , 2002. *Fire Protection Guide to Hazardous Materials 13rd Ed.*., 13th ed. National Fire Protection Association, Boston, Massachusetts. 38, 118, 119, 120, 121, 122, 123, 124, 228, 232, 233

[69] Robinson, C., and Smith, D., 1984. "The auto-ignition temperature of methane." *Journal of Hazardous Materials,* **8**(3), pp. 199 – 203. 38, 118

[70] Sax, N., 1979. *Dangerous Properties of Industrial Materials, 5th ed.*. VanNostrand Reinhold Company, New York. 38, 123

[71] Scott, G. S., Jones, G. W., and Scott, F. E., 1948. "Determination of ignition temperatures of combustible liquids and gases." *Analytical Chemistry,* **20**(3), pp. 238–241. 38, 119

[72] Gödde, M., Brandes, E., and Cammenga, H. K. "Zündtemperaturen homologer reihen - teil 2: Untersuchungen zum einfluß funktioneller gruppen." pp. 437–441. 38, 61, 211, 212, 220, 221

[73] Leslie, E. H., and Geniesse, J. C., 1927. *International Critical Tables*., Vol. 2 McGraw-Hill. 43

[74] Luning Prak, D. J., 2016. "Density, viscosity, speed of sound, bulk modulus, surface tension, and flash point of binary mixtures of butylcyclohexane with toluene or n-hexadecane." *Journal of Chemical & Engineering Data,* **61**(10), pp. 3595–3606. 43

[75] Gödde, M., Brandes, E., and Cammenga, H. K. "Zündtemperaturen homologer reihen - teil 1: Untersuchungen bei normaldruck." pp. 79–92. vii, 61, 62, 70, 77, 78, 210, 218, 219, 220, 221, 225, 232, 234, 235

[76] Redd, M. E., Seaton, W. G., Giles, N. F., Thomas A. Knotts, I. V., and Wilding, W. V. "An improved method for predicting autoignition temperatures based on first principles." (Under Review). xii, 61, 63, 71, 72, 86

[77] Redd, M. E., Bloxham, J. C., Giles, N. F., Knotts, T. A., and Wilding, W. V. "A study of unexpected autoignition temperature trends for pure n-alkanes." p. 121710. xi, 61, 62, 67, 86

[78] Tischer, S., Börnhorst, M., Amsler, J., Schoch, G., and Deutschmann, O. "Thermodynamics and reaction mechanism of urea decomposition." pp. 16785–16797. 64

[79] Goodwin, D. G., Speth, R. L., Moffat, H. K., and Weber, B. W. Cantera: An object-oriented software toolkit for chemical kinetics, thermodynamics, and transport processes `https://www.cantera.org` Version 2.5.1. xi, 65, 66

[80] reactor1.py: Constant-pressure, adiabatic kinetics simulation. xi, 65, 66

[81] Nabert, K., Schön, G., and Redeker, T. *Sicherheitstechnische Kenngrößen brennbarer Gase und Dämpfe*. Deutscher Eichverlag. vii, 78, 213, 214, 222, 229, 234

[82] Kirk-Othmer *Encyclopedia of Chemical Technology, 3rd ed.*. Interscience. 80

[83] Seaton, W. H., 1979. "Viscosity of strongly associating gases." *Can. J. Chem. Eng.,* **57**, pp. 523–526. 89

[84] Seaton, W. H., 1980. "Thermal conductivity of acetic acid in the gas state." *Can. J. Chem. Eng.,* **58**, pp. 416–418. 89

[85] Harrison, B. K., and Seaton, W. H., 1988. "Solution to missing group problem for estimation of ideal gas heat capacities." *Ind. Eng. Res.,* **27**, pp. 1536–1540. 89

[86] Seaton, W. H., 1991. "Group contribution method for predicting the lower and the upper flammable limits of vapors in air." *J. Hazard. Mater.,* **27**, pp. 169–185. 89

[87] Seaton, W. H., 2003. Theory of autoignition temperature model of w. h. seaton Mar. 89

[88] Seadata, 1994. *AITMP User's Guide*., version 94a ed. Seadata. 89, 92

[89] Bond, J., 1991. *Sources of Ignition*. Butterworth-Heinemann Ltd pp. 22-25 and 69-127 (Appendix 1). 91

[90] Landrum, G., De Winter, H., Sforna, G., and Deric, 2020. Rdkit: Open-source cheminformatics, Sept. 95

[91] Rhinehart, R. R., Su, M., and Manimegalai-Sridhar, U., 2012. "Leapfrogging and synoptic leapfrogging: A new optimization approach." *Computers & Chemical Engineering,* **40**, pp. 67–81. 96

[92] Manimegalai-Sridhar, U., Govindarajan, A., and Russell Rhinehart, R., 2014. "Improved initialization of players in leapfrogging optimization." *Computers & Chemical Engineering,* **60**, pp. 426–429. 96

[93] Rhinehart, R. R., 2014. "Convergence criterion in optimization of stochastic processes." *Computers & Chemical Engineering,* **68**, pp. 1–6. 96

[94] Harris, C. R., Millman, K. J., van der Walt, S. J., Gommers, R., Virtanen, P., Cournapeau, D., Wieser, E., Taylor, J., Berg, S., Smith, N. J., Kern, R., Picus, M., Hoyer, S., van Kerkwijk, M. H., Brett, M., Haldane, A., del Río, J. F., Wiebe, M., Peterson, P., Gérard-Marchant, P., Sheppard, K., Reddy, T., Weckesser, W., Abbasi, H., Gohlke, C., and Oliphant, T. E., 2020. "Array programming with NumPy." *Nature,* **585**(7825), Sept., pp. 357–362. 97

[95] Jones, E., Oliphant, T., Peterson, P., et al., 2001–. SciPy: Open source scientific tools for Python. 97

[96] pandas development team, T., 2020. pandas-dev/pandas: Pandas, Oct. 97

[97] Redd, M. E. Leapfrog optimizer package. 97

[98] ASTM, 2009. Astm d2883-95 standard test method for reaction threshold temperature of liquid and solid materials. 131

[99] Chen, C.-C., and Hsieh, Y.-C. "Effect of experimental conditions on measuring autoignition temperatures of liquid chemicals." pp. 5925–5932. 216

[100] Chen, C.-C., Liaw, H.-J., Shu, C.-M., and Hsieh, Y.-C. "Autoignition temperature data for methanol, ethanol, propanol, 2-butanol, 1-butanol, and 2-methyl-2,4-pentanediol." pp. 5059–5064. 216

[101] Msds for n-aliphatic acids www.Fishersci.com. 221

[102] Tryon, G. *Fire Protection Handbook, 12th ed.*., 12th ed. National Fire Protection Association. 228, 232, 233, 234

[103] Weber, B. W., Bunnell, J. A., Kumar, K., and Sung, C.-J. "Experiments and modeling of the autoignition of methyl pentanoate at low to intermediate temperatures and elevated pressures in a rapid compression machine." pp. 479–486. 228

[104] HadjAli, K., Crochet, M., Vanhove, G., Ribaucour, M., and Minetti, R. "A study of the low temperature autoignition of methyl esters." pp. 239–246. 229

APPENDIX A. DATA REFERENCED IN CHAPTER 4

Table A.1: A summary of experimental AIT data referenced in this work.

CAS No.	compound	C#	AIT (K)	Reference
74-82-8	methane	1	810.15	[58]
74-82-8	methane	1	810.15	[61]
74-82-8	methane	1	810.15	[68]
74-82-8	methane	1	810.37	[58]
74-82-8	methane	1	810.4	[65]
74-82-8	methane	1	813.15	[59]
74-82-8	methane	1	813.15	[14]
74-82-8	methane	1	868.15	[21]
74-82-8	methane	1	873	[69]
74-82-8	methane	1	903	[63]
74-84-0	ethane	2	745.15	[68]
74-84-0	ethane	2	783.15	[58]
74-84-0	ethane	2	788.15	[59]
74-84-0	ethane	2	788.15	[61]
74-84-0	ethane	2	788.15	[63]
74-84-0	ethane	2	788.15	[21]
74-84-0	ethane	2	788.15	[65]
74-84-0	ethane	2	788.15	[12]
74-84-0	ethane	2	788.15	[12]
74-84-0	ethane	2	788.15	[14]
74-98-6	propane	3	723	[14]

Table A.1: Continued

CAS No.	compound	C#	AIT (K)	Reference
74-98-6	propane	3	723.15	[59]
74-98-6	propane	3	723.15	[63]
74-98-6	propane	3	723.15	[66]
74-98-6	propane	3	723.15	[68]
74-98-6	propane	3	739.15	[61]
74-98-6	propane	3	739.26	[58]
74-98-6	propane	3	743.15	[21]
74-98-6	propane	3	766.15	[71]
106-97-8	*n*-butane	4	560.15	[68]
106-97-8	*n*-butane	4	561.15	[18]
106-97-8	*n*-butane	4	561.15	[18]
106-97-8	*n*-butane	4	638.15	[21]
106-97-8	*n*-butane	4	643.15	[63]
106-97-8	*n*-butane	4	645.15	[18]
106-97-8	*n*-butane	4	645.15	[18]
106-97-8	*n*-butane	4	645.15	[29]
106-97-8	*n*-butane	4	678.15	[59]
106-97-8	*n*-butane	4	678.15	[61]
106-97-8	*n*-butane	4	678.15	[65]
106-97-8	*n*-butane	4	678.15	[12]
106-97-8	*n*-butane	4	678.15	[14]
106-97-8	*n*-butane	4	703.15	[58]
109-66-0	*n*-pentane	5	516.15	[66]
109-66-0	*n*-pentane	5	531.15	[61]
109-66-0	*n*-pentane	5	531.15	[10]
109-66-0	*n*-pentane	5	533.15	[63]
109-66-0	*n*-pentane	5	533.15	[68]

Table A.1: Continued

CAS No.	compound	C#	AIT (K)	Reference
109-66-0	*n*-pentane	5	533.15	[14]
109-66-0	*n*-pentane	5	538.15	[21]
109-66-0	*n*-pentane	5	538.15	[29]
109-66-0	*n*-pentane	5	560.15	[12]
109-66-0	*n*-pentane	5	582	[65]
109-66-0	*n*-pentane	5	582.04	[58]
109-66-0	*n*-pentane	5	582.15	[59]
110-54-3	*n*-hexane	6	496.15	[61]
110-54-3	*n*-hexane	6	498	[63]
110-54-3	*n*-hexane	6	498.15	[66]
110-54-3	*n*-hexane	6	498.15	[14]
110-54-3	*n*-hexane	6	500.15	[17]
110-54-3	*n*-hexane	6	507	[65]
110-54-3	*n*-hexane	6	507.15	[18]
110-54-3	*n*-hexane	6	507.15	[12]
110-54-3	*n*-hexane	6	513.15	[21]
110-54-3	*n*-hexane	6	513.15	[10]
110-54-3	*n*-hexane	6	513.15	[29]
110-54-3	*n*-hexane	6	520.37	[58]
142-82-5	*n*-heptane	7	477.15	[18]
142-82-5	*n*-heptane	7	477.15	[18]
142-82-5	*n*-heptane	7	477.15	[68]
142-82-5	*n*-heptane	7	483.15	[21]
142-82-5	*n*-heptane	7	486.15	[17]
142-82-5	*n*-heptane	7	486.15	[29]
142-82-5	*n*-heptane	7	488.15	[62]
142-82-5	*n*-heptane	7	488.15	[14]

Table A.1: Continued

CAS No.	compound	C#	AIT (K)	Reference
142-82-5	*n*-heptane	7	496	[65]
142-82-5	*n*-heptane	7	496.15	[61]
142-82-5	*n*-heptane	7	496.15	[10]
142-82-5	*n*-heptane	7	496.15	[12]
142-82-5	*n*-heptane	7	498.15	[63]
142-82-5	*n*-heptane	7	505.15	[18]
142-82-5	*n*-heptane	7	506.48	[58]
142-82-5	*n*-heptane	7	517.15	[16]
111-65-9	*n*-octane	8	479.15	[17]
111-65-9	*n*-octane	8	479.15	[68]
111-65-9	*n*-octane	8	483.15	[21]
111-65-9	*n*-octane	8	493.15	[61]
111-65-9	*n*-octane	8	493.15	[63]
111-65-9	*n*-octane	8	493.15	[65]
111-65-9	*n*-octane	8	493.15	[29]
111-65-9	*n*-octane	8	493.15	[12]
111-65-9	*n*-octane	8	493.15	[14]
111-65-9	*n*-octane	8	505.37	[58]
111-84-2	*n*-nonane	9	478.15	[17]
111-84-2	*n*-nonane	9	478.15	[62]
111-84-2	*n*-nonane	9	478.15	[63]
111-84-2	*n*-nonane	9	478.15	[21]
111-84-2	*n*-nonane	9	478.15	[29]
111-84-2	*n*-nonane	9	478.15	[14]
111-84-2	*n*-nonane	9	479	[65]
111-84-2	*n*-nonane	9	479.15	[61]
111-84-2	*n*-nonane	9	479.15	[12]

Table A.1: Continued

CAS No.	compound	C#	AIT (K)	Reference
111-84-2	*n*-nonane	9	484.15	[10]
124-18-5	*n*-decane	10	474.15	[17]
124-18-5	*n*-decane	10	474.15	[29]
124-18-5	*n*-decane	10	478.15	[21]
124-18-5	*n*-decane	10	479.15	[10]
124-18-5	*n*-decane	10	481	[65]
124-18-5	*n*-decane	10	481.15	[61]
124-18-5	*n*-decane	10	481.15	[12]
124-18-5	*n*-decane	10	483.15	[63]
124-18-5	*n*-decane	10	483.15	[68]
124-18-5	*n*-decane	10	504.15	[16]
1120-21-4	*n*-undecane	11	513.15	[21]
112-40-3	*n*-dodecane	12	473.15	[21]
112-40-3	*n*-dodecane	12	476.15	[68]
112-40-3	*n*-dodecane	12	476.15	[10]
112-40-3	*n*-dodecane	12	476.15	[29]
112-40-3	*n*-dodecane	12	477	[65]
112-40-3	*n*-dodecane	12	477.15	[61]
112-40-3	*n*-dodecane	12	477.15	[63]
112-40-3	*n*-dodecane	12	477.15	[12]
112-40-3	*n*-dodecane	12	478.15	[14]
112-40-3	*n*-dodecane	12	502.15	[16]
629-59-4	*n*-tetradecane	14	473.15	[61]
629-59-4	*n*-tetradecane	14	473.15	[63]
629-59-4	*n*-tetradecane	14	473.15	[21]
629-59-4	*n*-tetradecane	14	473.15	[66]
629-59-4	*n*-tetradecane	14	473.15	[67]

Table A.1: Continued

CAS No.	compound	C#	AIT (K)	Reference
629-59-4	*n*-tetradecane	14	473.15	[68]
629-59-4	*n*-tetradecane	14	473.15	[14]
629-59-4	*n*-tetradecane	14	474.15	[62]
629-59-4	*n*-tetradecane	14	475	[65]
629-59-4	*n*-tetradecane	14	475.15	[12]
629-59-4	*n*-tetradecane	14	475.372	[64]
629-59-4	*n*-tetradecane	14	500.15	[16]
544-76-3	*n*-hexadecane	16	475.15	[67]
544-76-3	*n*-hexadecane	16	475.15	[68]
544-76-3	*n*-hexadecane	16	475.15	[10]
544-76-3	*n*-hexadecane	16	478.15	[61]
544-76-3	*n*-hexadecane	16	478.15	[63]
544-76-3	*n*-hexadecane	16	478.15	[21]
544-76-3	*n*-hexadecane	16	478.15	[70]
544-76-3	*n*-hexadecane	16	478.15	[12]
544-76-3	*n*-hexadecane	16	478.15	[14]
544-76-3	*n*-hexadecane	16	498.15	[16]
544-76-3	*n*-hexadecane	16	503.15	[60]
593-45-3	*n*-octadecane	18	500.15	[16]
593-45-3	*n*-octadecane	18	500.15	[67]
593-45-3	*n*-octadecane	18	500.15	[68]
593-45-3	*n*-octadecane	18	508.15	[21]
593-45-3	*n*-octadecane	18	508.15	[70]
629-92-5	*n*-nonadecane	19	478.15	[21]
629-92-5	*n*-nonadecane	19	503	[67]
629-92-5	*n*-nonadecane	19	503	[70]
629-92-5	*n*-nonadecane	19	503.15	[16]

Table A.1: Continued

CAS No.	compound	C#	AIT (K)	Reference
629-92-5	*n*-nonadecane	19	503.15	[68]
112-95-8	*n*-eicosane	20	503.15	[21]
112-95-8	*n*-eicosane	20	505	[67]
112-95-8	*n*-eicosane	20	505.15	[16]
112-95-8	*n*-eicosane	20	505.15	[68]

Table A.2: Relevant purity and source information for samples used in AIT experiments at 1 atm. Reported purities came from certificates of analysis provided by the corresponding manufacturer. Other purities were measured using GC-FID.

Cas No.	Compound	Manufacturer	Reported Purity	GC-FID Purity
142-82-5	*n*-heptane	J. T. Baker	99.4%	-
544-76-3	*n*-hexadecane	Sigma-Aldrich	99.1%	-
629-97-0	*n*-docosane	Alfa Aesar	99.9%	-
646-31-1	*n*-tetracosane	BeanTown Chemical	-	99.65%
629-99-2	*n*-pentacosane	BeanTown Chemical	99.3%	99.35%
629-99-2	*n*-pentacosane	Sigma-Aldrich	98.80%	98.51%
630-01-3	*n*-hexacosane	Alfa Aesar	99.59%	99.68%
630-01-3	*n*-hexacosane	Sigma-Aldrich	99.6%	-
638-68-6	*n*-triacontane	BeanTown Chemical	98.56%	98.48%
638-68-6	*n*-triacontane	Sigma-Aldrich	98.1%	-

Table A.3: Decomposition temperature (DCT) data for select *n*-alkanes. Uncertainties are given as 95% confidence intervals.

Cas No.	Compound	C#	DCT (20 K/min)	DCT (50 K/min)
544-76-3	*n*-hexadecane	16	616.49 ± 0.03	616.63 ± 0.04
211-116-8	*n*-nonadecane	19	477.11 ± 0.01	-

Table A.3: Continued

Cas No.	Compound	C#	DCT (20 K/min)	DCT (50 K/min)
629-97-0	*n*-docosane	22	480.97 ± 0.03	490.89 ± 0.01
638-67-5	*n*-tricosane	23	466.66 ± 0.04	484.42 ± 0.03
646-31-1	*n*-tetracosane	24	474.39 ± 0.01	503.46 ± 0.01
629-99-2	*n*-pentacosane	25	485.39 ± 0.04	507.46 ± 0.04
630-01-3	*n*-hexacosane	26	480.60 ± 0.02	512.36 ± 0.04
638-68-6	*n*-triacontane	30	502.38 ± 0.02	514.40 ± 0.06

Table A.4: Recommended AIT values for *n*-alkanes up to carbon number 36 based on the findings of this work. Data type specifies if the value is experimental or predicted. The predicted values from this work were estimated based on all available data including data measured at altitude and correlation with the differences in measured AIT between 1 atm and altitude experiments. Where values of adjacent carbon numbers were measured experimentally, values were predicted via linear interpolation between the experimental values.

CAS No.	Compound	C#	AIT (K)	Reference	Data Type
74-82-8	methane	1	868	[21]	Experimental
74-84-0	ethane	2	788	[12]	Experimental
74-98-6	propane	3	743	[21]	Experimental
106-97-8	*n*-butane	4	645	[18]	Experimental
109-66-0	*n*-pentane	5	531	[10]	Experimental
110-54-3	*n*-hexane	6	500	[17]	Experimental
142-82-5	*n*-heptane	7	486	[17]	Experimental
111-65-9	*n*-octane	8	479	[17]	Experimental
111-84-2	*n*-nonane	9	478	[17]	Experimental
124-18-5	*n*-decane	10	474	[17]	Experimental
1120-21-4	*n*-undecane	11	475	This Work	Predicted
112-40-3	*n*-dodecane	12	476	[10]	Experimental
629-50-5	*n*-tridecane	13	476	This Work	Predicted

Table A.4: Continued

CAS No.	Compound	C#	AIT (K)	Reference	Data Type
629-59-4	*n*-tetradecane	14	475	[12]	Experimental
629-62-9	*n*-pentadecane	15	475	This Work	Predicted
544-76-3	*n*-hexadecane	16	474	This Work	Experimental
629-78-7	*n*-heptadecane	17	476	This Work	Predicted
593-45-3	*n*-octadecane	18	477	This Work	Predicted
629-92-5	*n*-nonadecane	19	478	[21]	Experimental
112-95-8	*n*-eicosane	20	488	This Work	Predicted
629-94-7	*n*-heneicosane	21	493	This Work	Predicted
629-97-0	*n*-docosane	22	498	This Work	Experimental
638-67-5	*n*-tricosane	23	503	This Work	Predicted
646-31-1	*n*-tetracosane	24	508	This Work	Experimental
629-99-2	*n*-pentacosane	25	505	This Work	Experimental
630-01-3	*n*-hexacosane	26	581	This Work	Experimental
593-49-7	*n*-heptacosane	27	583	This Work	Predicted
630-02-4	*n*-octacosane	28	590	This Work	Predicted
630-03-5	*n*-nonacosane	29	595	This Work	Predicted
638-68-6	*n*-triacontane	30	607	This Work	Experimental
630-04-6	*n*-hentriacontane	31	603	This Work	Predicted
544-85-4	*n*-doctriacontane	32	607	This Work	Predicted
630-05-7	*n*-tritriacontane	33	609	This Work	Predicted
14167-59-0	*n*-tetratriacontane	34	611	This Work	Predicted
630-07-9	*n*-pentatriacontane	35	612	This Work	Predicted
630-06-8	*n*-hexatriacontane	36	612	This Work	Predicted

Table A.5: A complete set of AIT values measured in this work which are plotted with recommended literature values in Figure 4.6.

CAS No.	Compound	C#	Measured at Altitude (2013)	Measured at Altitude (2017)	Measured at 1 atm
74-82-8	methane	1			
74-84-0	ethane	2			
74-98-6	propane	3			
106-97-8	*n*-butane	4			
109-66-0	*n*-pentane	5			
110-54-3	*n*-hexane	6	518.15	516.15	
142-82-5	*n*-heptane	7	500.15		493.65
111-65-9	*n*-octane	8			
111-84-2	*n*-nonane	9			
124-18-5	*n*-decane	10	484.15		
1120-21-4	*n*-undecane	11			
112-40-3	*n*-dodecane	12			
629-50-5	*n*-tridecane	13			

Table A.5: Continued

CAS No.	Compound	C#	Measured at Altitude (2013)	Measured at Altitude (2017)	Measured at 1 atm
629-59-4	*n*-tetradecane	14			
629-62-9	*n*-pentadecane	15			
544-76-3	*n*-hexadecane	16	481.15		474.15
629-78-7	*n*-heptadecane	17			
593-45-3	*n*-octadecane	18			
629-92-5	*n*-nonadecane	19			
112-95-8	*n*-eicosane	20	496.15		
629-94-7	*n*-heneicosane	21			
629-97-0	*n*-docosane	22			498.4
638-67-5	*n*-tricosane	23			
646-31-1	*n*-tetracosane	24			507.85
629-99-2	*n*-pentacosane	25	520.15	518.15	505.15
629-99-2	*n*-pentacosane	25			602.15

Table A.5: Continued

CAS No.	Compound	C#	Measured at Altitude (2013)	Measured at Altitude (2017)	Measured at 1 atm
630-01-3	*n*-hexacosane	26	600.15	599.7	586.15
630-01-3	*n*-hexacosane	26			580.9
593-49-7	*n*-heptacosane	27			
630-02-4	*n*-octacosane	28	611.15	601.4	
630-03-5	*n*-nonacosane	29			
638-68-6	*n*-triacontane	30	633.15		606.6
638-68-6	*n*-triacontane	30			610.65
544-85-4	*n*-doctriacontane	32	637.15		
630-06-8	*n*-hexatriacontane	36	649.15		

APPENDIX B. ADDITIONAL EXPERIMENTAL SPECIFICATIONS TO THE ASTM E659 METHOD USED IN THIS WORK

The following sections explain topics that are not specified, or are ambiguous, in ASTM E659. An explanation of the situation is given along with the procedures introduced to clarify the additions. These focus on aspects of ASTM E659 that are not specified or are ambiguous and are all specified in our standard operating procedure.

B.1 Hot Flames

ASTM E659 specifies multiple definitions for an autoignition event, but not all are consistent. The definitions given include:

- *Autoignition is evidenced by the sudden appearance of a flame inside the flask and by a sharp rise in the temperature of the gas mixture.*
- *Autoignition is usually evidenced in these tests by hot flames of various colors, usually yellow, red, or blue, but sometimes by cool flames that appear as faint bluish glows which are visible only in total darkness. Normally, the hot flames produce sharp temperature rises of at least a few hundred degrees or more, whereas the cool flames are accompanied by rises of less than 100°C. Cool flames generally occur at lower flask temperatures than hot flames but may form over an intermediate temperature range, so that the lowest temperature at which any ignition occurs should be recorded. Below these ignition temperatures, nonluminous preflame reactions may occur and are distinguishable by rather weak temperature rises that are barely detectable in some instances.*
- *cool-flame, [noun]-a faint, pale blue luminescence or flame occurring below the autoignition temperature (AIT).*

- *Discussion-Cool-flames occur in rich vapor-air mixtures of most hydrocarbons and oxygenated hydrocarbons. They are the first part of the multistage ignition process.*

Note 3 of ASTM E659 references ASTM D2883 to help define hot-flame reactions [98]:

- *hot-flame reaction, [noun]-a rapid, self-sustaining, luminous, sometimes audible reaction of the sample or its decomposition products with the atmosphere in the combustion chamber.*
- *Discussion-A yellow or blue flame usually accompanies the reaction.*

A few commonalities arise from these definitions:

- The AIT is the lowest temperature at which a "hot-flame" ignition event is observed.
- A "hot-flame" ignition event is defined by the following:
  - A sharp rise in temperature that exceeds 100°C
  - A visible flame that can be red, yellow, or blue
  - A self-sustaining reaction
- A "Cool flame" ignition event is defined by the following
  - A blue flame
  - A temperature rise of less than 100 °C
  - Is below the hot-flame AIT

Given these definitions, we adopted the following criteria to define a hot-flame ignition:

- If any visible flame is observed, it is considered an ignition event
- If the flame has any color other than blue (e.g., red, orange, yellow etc.), it is considered a hot-flame ignition
- A flame color that is **only** blue is considered a cool-flame ignition

The choice to use these criteria is based on the differences between "premixed" and "diffusion" flames. Blue flames occur from kinetically limited reactions. Specifically, the kinetics of the reaction, rather than the rate of mixing (a transport process), are limiting the flame's propagation. For this reason, blue flames are characterized as "premixed flames" and the light emitted is from electronic transitions between quantum states which occur in the blue region of the visible electromagnetic spectrum. In the case of a "diffusion" or transport-limited flame, the kinetics consume fuel and oxygen at a faster rate than the rate of mixing. This allows time for soot particulates to form that emit black body radiation in the red or yellow region of the visible spectrum as oxygen diffuses to the solid surface and combusts. This means a "hot-flame" ignition event, as defined here, designates an ignition event at a sufficiently high temperature that the reaction rates exceed the diffusion rates, and the resulting diffusion flame emits a color other than blue. Moreover, these criteria relating to color were selected to remove ambiguity in identifying an autoignition event because they can be consistently and objectively observed.

B.2 Determining AIT for a Given Sample Size

AIT is defined as the minimum temperature at which an autoignition event occurs given a set of experimental conditions. Determining this value thus requires multiple experiments at different temperatures for a given sample. Once a minimum temperature at which autoignition occurs is found (T_{min}), the sample size is varied and the process repeated. Once at least 3 standard sample sizes have been tested the AIT is reported as the lowest temperature among the T_{min} values among the sample sizes. A bisection method was used for finding the minimum temperature at which autoignition occurs for each sample size. The steps of this method are outlined below.

1. Perform an experiment at a temperature estimated to be near the autoignition temperature and bracket T_{min}.

    - If the initial temperature produced a hot-flame ignition, perform an experiment at 10 K less than the initial temperature. Continue experiments at successively lower temperatures until no ignition occurs.

- If the initial temperature produced a no ignition, perform an experiment at 10 K more than the initial temperature. Continue experiments at successively higher temperatures until a hot-flame ignition occurs.
- If a cold-flame ignition was observed, perform the previous two steps to find a temperature where no ignition was observed and a temperature where a hot-flame ignition was observed.

2. Continue performing experiments to find T_{min} using a bisection method for selecting the temperature of successive experiments until the bracket size $\leq 3.0\ K$.

3. Confirm you have found T_{min} by completing additional experiments to comply with the criteria listed below.

   - Continue experiments at temperatures no more than 3.0 K below the candidate T_{min} until at least 3 experiments in this temperature range do not result in a hot-flame ignition.
   - Change the candidate minimum to lower temperatures if experiments within 3.0 K below the current T_{min} result in hot-flame ignition.
   - Consider cold ignitions as non-ignitions for this process.
   - Finally, there should be 4 non-ignition or cold-ignition experiments within 3.0 K of the lowest hot-ignition temperature (T_{min}).

4. Report T_{min} as the AIT *for that sample size*.

B.3 Sample sizes

The procedure for choosing sample sizes is like that of ASTM E659. The only difference being that if sample sizes do not return sufficiently different results (i.e., they are within 2% on a Celsius scale), then the intermediate sample sizes may be omitted.

The following is an excerpt from our standard operating procedure that specifies our procedure.

The ASTM method specifies five standard sample sizes, depending on the state of the compound, as given below.

- For solids: 50, 70, 100, 150, 200, and 250 milligrams (mg)
- For liquids: 50, 70, 100, 150, 200, and 250 microliters (μL)
- For gases: 50, 70, 100, 150, 200, and 250 milligrams (mg)

Acceptable errors for these sample sizes are +/- 10 mg/μL.

The following steps are followed.

1. Determine the minimum temperature at which ignition occurs for a sample size of 100 mg/uL.
2. Determine the minimum temperature at which ignition occurs for a sample size of 150 mg/uL.
3. Compare the minimum temperatures from the 100 mg/uL and the 150 mg/uL samples.
    - If 100 mg/μL gives a lower AIT, determine the minimum temperature at which ignition occurs using a 50 mg/μL sample.
    - If 150 mg/μL gives a lower AIT, determine the minimum temperature at which ignition occurs using a 250 mg/μL sample.
4. Compare the minima from all three experiments to determine if further tests are needed:
    1. Find the % error between the lowest temperature and the other two values using the following formula $\%Error_i = \frac{|T_{lowest} - T_i|}{T_{lowest}} \cdot 100\%$ where T_{lowest} is the lowest AIT between the three and T_i is the AIT of one of the other two.
    2. Report the lowest temperature among the three samples as the AIT if the two errors are both $\leq 2.0\%$.
    3. Perform further tests as specified below if either or both errors are $> 2.0\%$.
        - If a 50 mg/μL was used in Step 3, determine the minimum temperature at which ignition occurs for a sample size of 70 mg/uL.
        - If a 250 mg/μL was used in Step 3, determine the minimum temperature at which ignition occurs for a sample size of 200 mg/uL.
5. Report the minimum temperature from all the samples as the AIT for the compound.

B.4 Thermocouples

The ASTM E659 Method specifies using a 36-AWG Chromel-Alumel (Type K) thermocouple to be used in measuring the internal temperature of the flask, and 20-AWG gauge or finer Type K thermocouples for measuring the outside of the flask. The apparatus in this work used a 24-AWG Type K thermocouple for the internal temperature of the flask with the outer thermocouples used as specified. A 24-AWG thermocouple responds more slowly than a 36-AWG gauge device, but the difference is unimportant for purposes of this work as ignition was determined visually and not from changes in temperature.

APPENDIX C. AIT DATA SET AND REFERENCES USED TO REGRESS THE SEATON-REDD AND SEATON-REDD2 METHODS

Table C.1: Data Set Used in Regression. Numbered references are included in Table

CAS No.	Name	AIT (K)	Reference	Priority
74-84-0	ethane	788.15	187	5
74-98-6	propane	743.15	116	4
75-28-5	isobutane	733.15	116	4
106-97-8	n-butane	678.15	187	5
106-97-8	n-butane	645.15	42	5
109-66-0	n-pentane	531	161	5
78-78-4	isopentane	693.15	115	4
463-82-1	neopentane	723.15	115	4
110-54-3	n-hexane	500	6	5
110-54-3	n-hexane	513	161	5
110-54-3	n-hexane	507.15	187	5
107-83-5	2-methylpentane	537	6	5
96-14-0	3-methylpentane	551	6	5
75-83-2	2,2-dimethylbutane	678	6	5
79-29-8	2,3-dimethylbutane	669	6	5
142-82-5	n-heptane	486	6	5
142-82-5	n-heptane	496.15	187	5
142-82-5	n-heptane	505.15	42	5
591-76-4	2-methylhexane	553.15	116	4
589-34-4	3-methylhexane	553.15	116	4

Table C.1: Continued

CAS No.	Name	AIT (K)	Reference	Priority
590-35-2	2,2-dimethylpentane	593.15	116	4
565-59-3	2,3-dimethylpentane	603.15	116	4
108-08-7	2,4-dimethylpentane	598.15	116	4
562-49-2	3,3-dimethylpentane	593.15	116	4
464-06-2	2,2,3-trimethylbutane	685	6	5
464-06-2	trimethyl butane	694	161	5
111-65-9	n-octane	479	6	5
592-27-8	2-methylheptane	693.15	35	2
592-27-8	2-methylheptane	691.15	40	2
584-94-1	2,3-dimethylhexane	711.15	40	2
609-26-7	2-methyl-3-ethylpentane	733.15	116	4
564-02-3	2,2,3-trimethylpentane	669	6	5
540-84-1	isooctane	693	161	5
540-84-1	2,2,4-trimethylpentane	691.15	187	5
560-21-4	2,3,3-trimethylpentane	698.15	116	4
111-84-2	n-nonane	478	6	5
111-84-2	n-nonane	484	161	5
111-84-2	n-nonane	479.15	187	5
1067-20-5	3,3-diethylpentane	563.15	187	5
7154-79-2	2,2,3,3-tetramethylpentane	703.15	187	5
1186-53-4	2,2,3,4-tetramethylpentane	703.15	115	4
16747-38-9	2,3,3,4-tetramethylpentane	703.15	115	4
124-18-5	n-decane	474	6	5
124-18-5	n-decane	479	161	5
124-18-5	n-decane	481.15	187	5

Table C.1: Continued

CAS No.	Name	AIT (K)	Reference	Priority
2958-75-0	1-methyl-decalin	537.15	26	2
1678-98-4	iso-butylcyclohexane	547.15	175	1
3178-22-1	tert-butylcyclohexane	613.15	93	1
3178-22-1	tert-butylcyclohexane	615.15	40	2
1120-21-4	n-undecane	513.15	116	4
112-40-3	n-dodecane	476	161	5
112-40-3	n-dodecane	477.15	187	5
629-59-4	n-tetradecane	475.15	187	5
544-76-3	n-cetane	475	161	5
544-76-3	n-hexadecane	474	147	5
544-76-3	n-hexadecane	478.15	187	5
593-45-3	n-octadecane	508.15	116	4
629-92-5	n-nonadecane	478.15	116	4
112-95-8	n-eicosane	503.15	116	4
629-97-0	n-docosane	498	147	5
646-31-1	n-tetracosane	508	147	5
629-99-2	n-pentacosane	505	147	5
630-01-3	n-hexacosane	581	147	5
5911-04-6	3-methylnonane	483.15	116	4
871-83-0	2-methylnonane	483.15	116	4
17301-94-9	4-methylnonane	483.15	116	4
3221-61-2	2-methyloctane	493.15	115	4
2216-33-3	3-methyloctane	493.15	116	4
2216-34-4	4-methyloctane	498.15	116	4
1071-26-7	2,2-dimethylheptane	493.15	116	4

Table C.1: Continued

CAS No.	Name	AIT (K)	Reference	Priority
287-92-3	cyclopentane	634	6	5
96-37-7	methylcyclopentane	531	6	5
1640-89-7	ethylcyclopentane	535.15	187	5
2040-96-2	n-propylcyclopentane	542.15	61	4
3875-51-2	isopropylcyclopentane	556.15	175	1
2040-95-1	n-butylcyclopentane	523.15	57	2
110-82-7	cyclohexane	524	6	5
110-82-7	cyclohexane	519	161	5
110-82-7	cyclohexane	533.15	187	5
108-87-2	methylcyclohexane	512	6	5
108-87-2	methyl cyclohexane	491	161	5
1678-91-7	ethylcyclohexane	511	6	5
1678-91-7	ethylcyclohexane	535.15	187	5
2207-01-4	cis-1,2-dimethylcyclohexane	577.15	51	2
6876-23-9	trans-1,2-dimethylcyclohexane	577.15	51	2
638-04-0	cis-1,3-dimethylcyclohexane	579	51	2
2207-03-6	trans-1,3-dimethylcyclohexane	579	51	2
624-29-3	cis-1,4-dimethylcyclohexane	577	51	2
2207-04-7	trans-1,4-dimethylcyclohexane	577	51	2
1795-26-2	1-trans-3,5-trimethylcyclohexane	587.15	57	2
1678-92-8	n-propylcyclohexane	521.15	40	2
696-29-7	isopropylcyclohexane	556.15	57	2
1678-93-9	n-butylcyclohexane	518.15	116	4
493-01-6	cis-decahydronaphthalene	513.15	116	4
493-02-7	trans-decahydronaphthalene	513.15	116	4
92-51-3	bicyclohexyl	513.15	116	4

Table C.1: Continued

CAS No.	Name	AIT (K)	Reference	Priority
78-01-3	1,1-diethylcyclohexane	513.15	36	2
78-01-3	1,1-diethylcyclohexane	514	68	1
78-01-3	1,1-diethylcyclohexane	515.15	66	1
3891-98-3	2,6,10-trimethyldodecane	470.15	155	1
1072-05-5	2,6-dimethylheptane	493.15	116	4
16747-25-4	2,2,3-trimethylhexane	613.15	116	4
930-90-5	1-methyl-trans-2-ethylcyclopentane	728.15	166	1
1068-87-7	2,4-dimethyl-3-ethylpentane	663.15	116	4
115-07-1	propylene	770	184	4
115-07-1	propylene	728.15	116	4
106-98-9	1-butene	658.15	183	4
106-98-9	1-butene	713.15	116	4
590-18-1	cis-2-butene	598	51	2
590-18-1	cis-2-butene	597.15	50	2
624-64-6	trans-2-butene	598.15	186	2
624-64-6	trans-2-butene	597.15	40	2
115-11-7	isobutene	738.15	187	5
109-67-1	1-pentene	553.15	116	4
646-04-8	trans-2-pentene	543.15	175	1
563-45-1	3-methyl-1-butene	638.15	116	4
513-35-9	2-methyl-2-butene	563.15	116	4
592-41-6	1-hexene	526	6	5
7688-21-3	cis-2-hexene	518	37	1
4050-45-7	trans-2-hexene	528.15	175	1
4050-45-7	trans-2-hexene	518.15	40	2

Table C.1: Continued

CAS No.	Name	AIT (K)	Reference	Priority
763-29-1	2-methyl-1-pentene	573.15	116	4
691-37-2	4-methyl-1-pentene	573.15	116	4
760-21-4	2-ethyl-1-butene	588.15	116	4
563-78-0	2,3-dimethyl-1-butene	633.15	116	4
563-79-1	2,3-dimethyl-2-butene	673.15	116	4
592-76-7	1-heptene	533.15	116	4
14686-13-6	trans-2-heptene	648.15	181	1
594-56-9	2,3,3-trimethyl-1-butene	648.15	116	4
111-66-0	1-octene	503	6	5
591-49-1	1-methylcyclohexene	493.15	116	4
3710-30-3	1,7-octadiene	503.15	116	4
107-39-1	2,4,4-trimethyl-1-pentene	650	6	5
107-40-4	2,4,4-trimethyl-2-pentene	578.15	116	4
872-05-9	1-decene	508.15	116	4
821-95-4	1-undecene	509.95	63	1
112-41-4	1-dodecene	528.15	183	4
112-41-4	1-dodecene	498.15	116	4
1120-36-1	1-tetradecene	508.15	184	4
629-73-2	1-hexadecene	513.15	116	4
112-88-9	1-octadecene	523.15	116	4
142-29-0	cyclopentene	668.15	57	2
110-83-8	cyclohexene	517	6	5
100-40-3	vinylcyclohexene	538.15	116	4
5989-27-5	d-limonene	510	36	2
590-19-2	1,2-butadiene	613.15	116	4

Table C.1: Continued

CAS No.	Name	AIT (K)	Reference	Priority
106-99-0	1,3-butadiene	703.15	31	4
106-99-0	1,3-butadiene	688.15	116	4
78-79-5	isoprene	493.15	184	4
592-42-7	1,5-hexadiene	592.15	119	1
592-42-7	1,5-hexadiene	618.15	175	1
26519-91-5	methylcyclopentadiene	719	180	1
26519-91-5	methylcyclopentadiene	718.15	186	2
592-57-4	1,3-cyclohexadiene	633.15	175	1
20237-34-7	trans-1,3-hexadiene	593.15	175	1
74-86-2	acetylene	578.15	116	4
74-99-7	methylacetylene	613.15	65	2
917-92-0	3,3-dimethyl-1-butyne	663.15	116	4
629-05-0	1-octyne	498.15	116	4
71-43-2	benzene	821	6	5
71-43-2	benzene	832	161	5
71-43-2	benzene	835.15	187	5
108-88-3	toluene	805	6	5
108-88-3	toluene	792	161	5
108-88-3	toluene	809.15	187	5
100-41-4	ethylbenzene	709	6	5
100-41-4	ethylbenzene	705.15	187	5
95-47-6	o-xylene	737.15	187	5
108-38-3	m-xylene	801.15	187	5

Table C.1: Continued

CAS No.	Name	AIT (K)	Reference	Priority
106-42-3	p-xylene	802.15	187	5
103-65-1	n-propylbenzene	723.15	116	4
98-82-8	cumene	697.15	187	5
611-14-3	o-ethyltoluene	713.15	116	4
620-14-4	m-ethyltoluene	753.15	116	4
622-96-8	p-ethyltoluene	748.15	116	4
526-73-8	1,2,3-trimethylbenzene	743.15	116	4
95-63-6	1,2,4-trimethylbenzene	758.15	116	4
108-67-8	mesitylene	778.15	116	4
104-51-8	n-butylbenzene	685.15	187	5
538-93-2	isobutylbenzene	701.15	187	5
135-98-8	sec-butylbenzene	691.15	187	5
98-06-6	tert-butylbenzene	723.15	187	5
99-87-6	p-cymene	709.15	187	5
135-01-3	o-diethylbenzene	653.15	116	4
141-93-5	m-diethylbenzene	723.15	116	4
105-05-5	p-diethylbenzene	703.15	187	5
488-23-3	1,2,3,4-tetramethylbenzene	700.15	40	2
527-53-7	1,2,3,5-tetramethylbenzene	700.15	57	2
700-12-9	pentamethylbenzene	710	36	2
99-62-7	m-diisopropylbenzene	686.15	136	5
100-18-5	p-diisopropylbenzene	686.15	137	5
877-44-1	1,2,4-triethylbenzene	718.15	57	2
92-52-4	biphenyl	839.15	187	5
92-94-4	p-terphenyl	808.15	186	2
92-94-4	p-terphenyl	828.15	41	1

Table C.1: Continued

CAS No.	Name	AIT (K)	Reference	Priority
92-06-8	m-terphenyl	828.15	41	1
84-15-1	o-terphenyl	803.15	41	1
612-00-0	1,1-diphenylethane	713.15	116	4
101-81-5	diphenylmethane	759.15	187	5
103-29-7	1,2-diphenylethane	753.15	116	4
100-42-5	styrene	763.15	116	4
100-80-1	m-methylstyrene	762.15	57	2
577-55-9	o-diisopropylbenzene	722.04	67	1
622-97-9	p-methylstyrene	848.15	62	1
622-97-9	p-methylstyrene	811.15	36	2
98-83-9	alpha-methylstyrene	693.15	116	4
105-06-6	p-divinylbenzene	743	38	1
98-51-1	4-tert-butyltoluene	783.15	146	1
91-20-3	naphthalene	801.15	31	4
91-20-3	naphthalene	813.15	116	4
90-12-0	1-methylnaphthalene	802.15	187	5
1127-76-0	1-ethylnaphthalene	753.15	116	4
119-64-2	1,2,3,4-tetrahydronaphthalene	663.15	116	4
1634-09-9	1-n-butylnaphthalene	633.15	57	2
120-12-7	anthracene	813.15	187	5
281-23-2	adamantane	560.15	35	2
3048-64-4	vinylnorbornene	688.15	116	4
496-11-7	indane	569.15	40	2
7058-01-7	sec-butylcyclohexane	550.15	39	2
80-56-8	alpha-pinene	528.15	116	4
127-91-3	beta-pinene	528.15	116	4

Table C.1: Continued

CAS No.	Name	AIT (K)	Reference	Priority
19089-47-5	2-ethoxy-1-propanol	528.15	116	4
123-38-6	propanal	480.37	183	4
123-38-6	propanal	463.15	116	4
123-72-8	butanal	503.15	183	4
123-72-8	butanal	463.15	116	4
78-84-2	2-methylpropanal	469.26	183	4
78-84-2	2-methylpropanal	438.15	116	4
110-62-3	pentanal	483.15	116	4
111-71-7	heptanal	478.15	116	4
66-25-1	hexanal	493.15	116	4
124-19-6	nonanal	473.15	116	4
123-05-7	2-ethylhexanal	453.15	116	4
107-22-2	glyoxal	557.15	46	1
112-31-2	decanal	468.15	116	4
112-54-9	dodecanal	478.15	116	4
96-17-3	2-methylbutyraldehyde	463.15	116	4
590-86-3	3-methylbutyraldehyde	728.15	187	5
107-02-8	acrolein	488.15	116	4
123-73-9	trans-crotonaldehyde	505	184	4
123-73-9	trans-crotonaldehyde	503.15	116	4
104-87-0	p-tolualdehyde	668.15	89	1
104-87-0	p-tolualdehyde	697.15	128	1
123-63-7	paraldehyde	508.15	116	4
67-64-1	acetone	764	161	5
78-93-3	methyl ethyl ketone	738.15	116	4

Table C.1: Continued

CAS No.	Name	AIT (K)	Reference	Priority
96-22-0	3-pentanone	718.15	116	4
108-10-1	methyl isobutyl ketone	748.15	116	4
123-19-3	4-heptanone	703.15	116	4
107-87-9	2-pentanone	718.15	116	4
563-80-4	methyl isopropyl ketone	748.15	116	4
591-78-6	2-hexanone	697	184	4
591-78-6	2-hexanone	803.15	116	4
110-43-0	2-heptanone	631.15	141	5
110-12-3	5-methyl-2-hexanone	673.15	134	5
141-79-7	mesityl oxide	613.15	116	4
108-83-8	diisobutyl ketone	669.15	40	2
872-50-4	n-methyl-2-pyrrolidone	538.15	116	4
502-56-7	5-nonanone	603.15	116	4
821-55-6	2-nonanone	678.15	116	4
84-65-1	anthraquinone	923.15	116	4
123-54-6	acetylacetone	613	187	5
78-59-1	isophorone	735.37	183	4
78-59-1	isophorone	723.15	116	4
120-92-3	cyclopentanone	718.15	116	4
108-94-1	cyclohexanone	693.15	187	5
111-13-7	2-octanone	693.15	116	4
119-61-9	benzophenone	833.15	116	4
98-86-2	acetophenone	844.15	187	5
96-48-0	gamma-butyrolactone	728.15	116	4
502-44-3	epsilon-caprolactone	611	37	1
106-51-4	quinone	833.15	57	2

Table C.1: Continued

CAS No.	Name	AIT (K)	Reference	Priority
674-82-8	diketene	548.15	116	4
67-56-1	methyl alcohol	701	161	5
67-56-1	methanol	706.25	21	5
64-17-5	ethyl alcohol	664	161	5
64-17-5	ethanol	629.85	20	5
64-17-5	ethanol	641.95	21	5
71-23-8	1-propanol	653.15	21	5
67-63-0	isopropanol	698.15	116	4
71-36-3	1-butanol	587.15	21	5
78-83-1	2-methyl-1-propanol	681.15	31	4
78-83-1	2-methyl-1-propanol	678.15	116	4
78-92-2	2-butanol	679.15	187	5
78-92-2	2-butanol	670.25	21	5
75-65-0	2-methyl-2-propanol	743.15	116	4
71-41-0	1-pentanol	573.15	187	5
6032-29-7	2-pentanol	603.15	116	4
75-85-4	2-methyl-2-butanol	710.15	187	5
137-32-6	2-methyl-1-butanol	613.15	116	4
75-84-3	2,2-dimethyl-1-propanol	693.15	116	4
111-27-3	1-hexanol	558.15	116	4
105-30-6	2-methyl-1-pentanol	583.15	36	2
584-02-1	3-pentanol	633.15	116	4
104-76-7	2-ethyl-1-hexanol	543.15	116	4
123-51-3	3-methyl-1-butanol	620.15	187	5
111-70-6	1-heptanol	543.15	116	4
108-11-2	4-methyl-2-pentanol	608.15	116	4

Table C.1: Continued

CAS No.	Name	AIT (K)	Reference	Priority
111-87-5	1-octanol	543.15	116	4
123-96-6	2-octanol	538.15	116	4
143-08-8	1-nonanol	533.15	116	4
112-30-1	1-decanol	523.15	116	4
112-53-8	1-dodecanol	548.15	183	4
112-53-8	1-dodecanol	523.15	116	4
112-72-1	1-tetradecanol	513.15	116	4
36653-82-4	1-hexadecanol	518.15	116	4
97-95-0	2-ethyl-1-butanol	588.15	116	4
108-93-0	cyclohexanol	573.15	187	5
590-67-0	1-methylcyclohexanol	568.15	186	2
7443-70-1	cis-2-methylcyclohexanol	569.15	187	5
7443-52-9	trans-2-methylcyclohexanol	569.15	187	5
7731-28-4	cis-4-methylcyclohexanol	568.15	187	5
7731-29-5	trans-4-methylcyclohexanol	568.15	187	5
97-99-4	tetrahydrofurfuryl alcohol	553.15	116	4
107-18-6	allyl alcohol	715.927	184	4
107-18-6	allyl alcohol	648.15	116	4
526-75-0	2,3-xylenol	773.15	116	4
105-67-9	2,4-xylenol	753.15	116	4
576-26-1	2,6-xylenol	872	184	4
576-26-1	2,6-xylenol	773.15	116	4
95-65-8	3,4-xylenol	828.15	116	4
108-68-9	3,5-xylenol	828.15	116	4
107-19-7	propargyl alcohol	638.15	116	4

Table C.1: Continued

CAS No.	Name	AIT (K)	Reference	Priority
100-51-6	benzyl alcohol	709.26	183	4
100-51-6	benzyl alcohol	688.15	116	4
108-95-2	phenol	868.15	116	4
95-48-7	o-cresol	828.15	116	4
108-39-4	m-cresol	832	184	4
106-44-5	p-cresol	832	184	4
106-44-5	p-cresol	828.15	116	4
123-31-9	p-hydroquinone	788.15	116	4
80-05-7	bisphenol a	818.15	118	1
107-21-1	ethylene glycol	671	161	5
111-46-6	diethylene glycol	628.15	116	4
112-27-6	triethylene glycol	643.15	116	4
112-60-7	tetraethylene glycol	613.15	116	4
3010-96-6	2,2,4,4-tetramethyl-1,3-cyclobutanediol	575.15	131	4
57-55-6	1,2-propylene glycol	693.15	116	4
504-63-2	1,3-propylene glycol	673.15	116	4
25265-71-8	dipropylene glycol	605.15	82	1
126-30-7	neopentyl glycol	648.15	116	4
115-84-4	2-butyl-2-ethyl-1,3-propanediol	583.15	55	1
115-84-4	2-butyl-2-ethyl-1,3-propanediol	579.15	142	1
2163-42-0	2-methyl-1,3-propanediol	653.15	71	1
584-03-2	1,2-butanediol	663.15	116	4
107-88-0	1,3-butanediol	648.15	116	4
107-41-5	hexylene glycol	682.95	21	5
5343-92-0	1,2-pentanediol	653.15	150	1

Table C.1: Continued

CAS No.	Name	AIT (K)	Reference	Priority
56-81-5	glycerine	662	161	5
1948-33-0	mono-tert-butylhydroquinone	730.15	172	1
144-19-4	2,2,4-trimethyl-1,3-pentanediol	573.15	77	1
144-19-4	2,2,4-trimethyl-1,3-pentanediol	619.15	40	2
513-85-9	2,3-butanediol	673.15	116	4
110-63-4	1,4-butanediol	643.15	116	4
111-29-5	1,5-pentanediol	603.15	116	4
629-11-8	1,6-hexanediol	593.15	116	4
108-46-3	1,3-benzenediol	878.15	116	4
77-99-6	trimethylolpropane	648.15	53	1
79-09-4	propionic acid	713.15	116	4
334-48-5	n-decanoic acid	503.15	116	4
107-92-6	n-butyric acid	725.15	187	5
116-53-0	2-methylbutyric acid	633.15	40	2
109-52-4	n-pentanoic acid	648.15	116	4
112-05-0	n-nonanoic acid	678.15	116	4
79-31-2	isobutyric acid	775	184	4
79-31-2	isobutyric acid	733.15	116	4
503-74-2	isovaleric acid	658.15	116	4
142-62-1	n-hexanoic acid	603.15	116	4
619-82-9	1,4-cyclohexanedicarboxylic acid	689.15	76	1
124-07-2	n-octanoic acid	518.15	116	4
143-07-7	n-dodecanoic acid	503.15	116	4
544-63-8	n-tetradecanoic acid	508.15	116	4
57-10-3	n-hexadecanoic acid	513.15	116	4
503-64-0	cis-crotonic acid	663.15	116	4

Table C.1: Continued

CAS No.	Name	AIT (K)	Reference	Priority
107-93-7	trans-crotonic acid	663.15	116	4
3004-93-1	stearic acid	510.03	103	5
79-10-7	acrylic acid	668.15	116	4
79-41-4	methacrylic acid	658.15	116	4
112-80-1	oleic acid	523.15	116	4
65-85-0	benzoic acid	843.15	116	4
99-94-5	p-toluic acid	843.15	43	1
69-72-7	salicylic acid	818.15	159	1
69-72-7	salicylic acid	813.15	40	2
124-04-9	adipic acid	695.15	187	5
88-99-3	phthalic acid	863.15	116	4
121-91-5	isophthalic acid	843.15	116	4
100-21-0	terephthalic acid	853.15	116	4
79-21-0	peracetic acid	473.15	184	4
108-24-7	acetic anhydride	607	31	4
108-24-7	acetic anhydride	603.15	116	4
123-62-6	propionic anhydride	555.15	140	5
106-31-0	butyric anhydride	582.15	139	5
85-44-9	phthalic anhydride	853.15	116	4
108-31-6	maleic anhydride	653.15	116	4
107-31-3	methyl formate	740	161	5
592-84-7	n-butyl formate	558.15	116	4
592-84-7	n-butyl formate	593.15	116	4
542-55-2	isobutyl formate	593.15	116	4
638-49-3	n-pentyl formate	538.15	116	4
79-20-9	methyl acetate	748.15	116	4

Table C.1: Continued

CAS No.	Name	AIT (K)	Reference	Priority
141-78-6	ethyl acetate	733.15	116	4
109-60-4	n-propyl acetate	703.15	116	4
123-86-4	n-butyl acetate	603.15	116	4
110-19-0	isobutyl acetate	696.15	187	5
123-92-2	isopentyl acetate	643.15	116	4
591-87-7	allyl acetate	648.15	116	4
108-21-4	isopropyl acetate	698.15	116	4
105-46-4	sec-butyl acetate	683.15	116	4
108-05-4	vinyl acetate	658.15	116	4
554-12-1	methyl propionate	728.15	116	4
105-37-3	ethyl propionate	718.15	116	4
106-36-5	n-propyl propionate	703.15	116	4
590-01-2	n-butyl propionate	658.15	116	4
105-66-8	n-propyl n-butyrate	693.15	116	4
105-38-4	vinyl propionate	658.15	116	4
623-42-7	methyl n-butyrate	728.15	116	4
105-54-4	ethyl n-butyrate	713.15	116	4
105-54-4	ethyl n-butyrate	733.15	116	4
644-49-5	n-propyl isobutyrate	708.15	116	4
3319-31-1	trioctyl trimellitate	683.15	112	1
3319-31-1	trioctyl trimellitate	658.15	177	1
96-33-3	methyl acrylate	688.15	116	4
140-88-5	ethyl acrylate	656	184	4
140-88-5	ethyl acrylate	623.15	116	4
141-32-2	n-butyl acrylate	548.15	116	4
108-64-5	ethyl isovalerate	693.15	116	4

Table C.1: Continued

CAS No.	Name	AIT (K)	Reference	Priority
624-24-8	methyl pentanoate	693.15	116	4
80-62-6	methyl methacrylate	703.15	116	4
97-63-2	ethyl methacrylate	683.15	116	4
117-81-7	dioctyl phthalate	643.15	116	4
27554-26-3	diisooctyl phthalate	663.15	116	4
628-63-7	n-pentyl acetate	563.15	116	4
103-09-3	2-ethylhexyl acetate	503.15	116	4
140-11-4	benzyl acetate	733.15	116	4
97-85-8	isobutyl isobutyrate	705.15	39	2
659-70-1	isopentyl isovalerate	583.15	116	4
142-92-7	n-hexyl acetate	528.15	116	4
120-51-4	benzyl benzoate	754.15	187	5
136-60-7	n-butyl benzoate	708.15	116	4
96-49-1	ethylene carbonate	738.15	116	4
112-14-1	n-octyl acetate	493.15	116	4
112-17-4	n-decyl acetate	488.15	116	4
26761-40-0	diisodecyl phthalate	675	184	4
119-36-8	methyl salicylate	723.15	116	4
84-69-5	diisobutyl phthalate	705.15	57	2
120-61-6	dimethyl terephthalate	778.15	116	4
123-95-5	n-butyl stearate	628.15	187	5
109-43-3	dibutyl sebacate	638.15	57	2
109-21-7	n-butyl n-butyrate	623.15	116	4
103-11-7	2-ethylhexyl acrylate	531	184	4

Table C.1: Continued

CAS No.	Name	AIT (K)	Reference	Priority
103-11-7	2-ethylhexyl acrylate	518.15	116	4
111-55-7	ethylene glycol diacetate	755.37	183	4
97-86-9	isobutyl methacrylate	658.15	116	4
97-88-1	n-butyl methacrylate	563.15	116	4
93-58-3	methyl benzoate	783.15	116	4
93-89-0	ethyl benzoate	763.15	116	4
105-58-8	diethyl carbonate	718.15	116	4
94-60-0	dimethyl-1,4-cyclohexanedicarboxylate	661.15	153	5
96-47-9	2-methyltetrahydrofuran	543.15	80	1
115-10-6	dimethyl ether	513.15	116	4
60-29-7	diethyl ether	443.15	116	4
108-20-3	diisopropyl ether	678.15	116	4
142-96-1	di-n-butyl ether	448.15	116	4
1634-04-4	methyl tert-butyl ether	733.15	116	4
540-67-0	methyl ethyl ether	463.15	116	4
112-58-3	di-n-hexyl ether	460.15	187	5
109-93-3	divinyl ether	633.15	116	4
123-91-1	1,4-dioxane	652.15	31	4
123-91-1	1,4-dioxane	648.15	116	4
629-82-3	di-n-octyl ether	478.15	40	2
693-65-2	di-n-pentyl ether	444.15	187	5
994-05-8	methyl tert-pentyl ether	618.15	116	4
637-92-3	tert-butyl ethyl ether	583.15	174	1
109-87-5	methylal	510.15	187	5
105-57-7	acetal	503.15	116	4
122-51-0	triethyl orthoformate	453.15	116	4

Table C.1: Continued

CAS No.	Name	AIT (K)	Reference	Priority
558-30-5	1,2-epoxy-2-methylpropane	712.15	57	2
558-30-5	1,2-epoxy-2-methylpropane	618	78	1
75-21-8	ethylene oxide	713.15	116	4
75-56-9	1,2-propylene oxide	703.15	116	4
109-92-2	ethyl vinyl ether	463.15	116	4
111-43-3	di-n-propyl ether	488.15	37	1
111-34-2	butyl vinyl ether	498.15	116	4
112-49-2	triethylene glycol dimethyl ether	468.15	116	4
110-71-4	1,2-dimethoxyethane	503.15	116	4
111-96-6	diethylene glycol dimethyl ether	463.15	116	4
112-36-7	diethylene glycol diethyl ether	489	165	1
112-36-7	diethylene glycol diethyl ether	478.15	175	1
112-36-7	diethylene glycol diethyl ether	447.15	27	1
112-73-2	diethylene glycol di-n-butyl ether	476	165	1
112-73-2	diethylene glycol di-n-butyl ether	583.15	40	2
100-66-3	anisole	748.15	116	4
101-84-8	diphenyl ether	891.15	187	5
107-25-5	methyl vinyl ether	493.15	116	4
106-88-7	1,2-epoxybutane	788	184	4
106-88-7	1,2-epoxybutane	643.15	116	4
80-15-9	cumene hydroperoxide	422.039	184	4
110-00-9	furan	663.15	116	4
109-99-9	tetrahydrofuran	497.15	31	4
109-99-9	tetrahydrofuran	488.15	116	4
94-36-0	benzoyl peroxide	353	159	1
94-36-0	benzoyl peroxide	376	14	1

Table C.1: Continued

CAS No.	Name	AIT (K)	Reference	Priority
497-26-7	2-methyl-1,3-dioxolane	489.15	18	1
497-26-7	2-methyl-1,3-dioxolane	494.15	18	1
497-26-7	2-methyl-1,3-dioxolane	511.15	18	1
646-06-0	1,3-dioxolane	547.15	105	1
74-87-3	methyl chloride	905.37	183	4
74-87-3	methyl chloride	898.15	116	4
75-00-3	ethyl chloride	725.15	187	5
75-01-4	vinyl chloride	688.15	116	4
75-09-2	dichloromethane	878.15	116	4
75-34-3	1,1-dichloroethane	713.15	15	2
75-34-3	1,1-dichloroethane	731.15	40	2
107-06-2	1,2-dichloroethane	749.15	42	5
79-00-5	1,1,2-trichloroethane	733.15	116	4
78-87-5	1,2-dichloropropane	828.15	116	4
71-55-6	1,1,1-trichloroethane	759.15	42	5
75-29-6	isopropyl chloride	766.25	19	5
96-18-4	1,2,3-trichloropropane	577.15	40	2
513-36-0	isobutyl chloride	711.95	19	5
616-21-7	1,2-dichlorobutane	548.15	116	4
79-01-6	trichloroethylene	683.15	184	4
107-05-1	3-chloropropene	663.15	116	4
87-68-3	hexachloro-1,3-butadiene	883.15	116	4
100-44-7	benzyl chloride	858.15	187	5
108-90-7	monochlorobenzene	911.15	187	5
95-50-1	o-dichlorobenzene	921	184	4
95-50-1	o-dichlorobenzene	913.15	116	4

Table C.1: Continued

CAS No.	Name	AIT (K)	Reference	Priority
95-49-8	o-chlorotoluene	823.15	116	4
106-43-4	p-chlorotoluene	843.15	116	4
95-73-8	2,4-dichlorotoluene	923.15	116	4
156-59-2	cis-1,2-dichloroethylene	733.15	116	4
156-60-5	trans-1,2-dichloroethylene	713.15	116	4
126-99-8	chloroprene	713.15	116	4
540-54-5	propyl chloride	793.15	116	4
109-69-3	n-butyl chloride	523	42	5
109-69-3	n-butyl chloride	517.15	19	5
543-59-9	1-chloropentane	525.15	19	5
75-35-4	1,1-dichloroethylene	803.15	116	4
120-82-1	1,2,4-trichlorobenzene	843.15	116	4
98-87-3	benzyl dichloride	798.15	116	4
75-45-6	chlorodifluoromethane	905	159	1
420-46-2	1,1,1-trifluoroethane	993.15	116	4
75-38-7	1,1-difluoroethylene	653.15	116	4
75-37-6	1,1-difluoroethane	728.15	116	4
74-83-9	bromomethane	810	184	4
74-83-9	bromomethane	808.15	116	4
74-96-4	bromoethane	784.15	65	2
74-96-4	bromoethane	783.15	54	1
79-27-6	1,1,2,2-tetrabromoethane	608.15	116	4
106-94-5	1-bromopropane	763.15	116	4
109-65-9	1-bromobutane	538.15	187	5
106-93-4	1,2-dibromoethane	763.15	116	4
108-86-1	bromobenzene	839.15	187	5

Table C.1: Continued

CAS No.	Name	AIT (K)	Reference	Priority
74-88-4	methyl iodide	628.15	116	4
75-43-4	dichlorofluoromethane	825.15	167	1
74-89-5	methylamine	703.15	116	4
124-40-3	dimethylamine	673.15	116	4
75-50-3	trimethylamine	463.15	116	4
75-04-7	ethylamine	657	180	1
75-04-7	ethylamine	658.15	186	2
594-39-8	2-methyl-2-aminobutane	663.15	116	4
121-44-8	triethylamine	488.15	116	4
142-84-7	di-n-propylamine	533.15	116	4
109-89-7	diethylamine	585	184	4
109-89-7	diethylamine	583.15	116	4
107-10-8	n-propylamine	593.15	116	4
109-73-9	n-butylamine	583.15	116	4
78-81-9	isobutylamine	651.15	187	5
765-30-0	cyclopropylamine	548.15	116	4
110-96-3	diisobutylamine	521.65	121	1
110-96-3	diisobutylamine	523.15	121	1
110-96-3	diisobutylamine	563.15	40	2
75-31-0	isopropylamine	603.15	116	4
105-59-9	methyl diethanolamine	683.15	8	1
141-43-5	monoethanolamine	683.15	116	4
111-42-2	diethanolamine	628.15	116	4
102-71-6	triethanolamine	598.15	116	4
13952-84-6	sec-butylamine	651.15	40	2

Table C.1: Continued

CAS No.	Name	AIT (K)	Reference	Priority
75-64-9	tert-butylamine	648.15	116	4
108-91-8	cyclohexylamine	548.15	116	4
1446-61-3	dehydroabietylamine	494	159	1
95-80-7	2,4-diaminotoluene	638.15	116	4
100-46-9	benzylamine	663.15	116	4
95-53-4	o-toluidine	753.15	116	4
108-44-1	m-toluidine	753.15	116	4
106-49-0	p-toluidine	753.15	116	4
112-24-3	triethylenetetramine	608.15	116	4
107-11-9	allylamine	643.15	116	4
107-15-3	ethylenediamine	658.15	116	4
151-56-4	ethyleneimine	593.15	184	4
108-18-9	diisopropylamine	588.705	184	4
108-18-9	diisopropylamine	558.15	116	4
111-92-2	di-n-butylamine	533.15	116	4
110-89-4	piperidine	593.15	116	4
91-22-5	quinoline	753.15	116	4
140-31-8	n-aminoethyl piperazine	588.15	116	4
78-90-0	1,2-propanediamine	689.15	40	2
91-66-7	n,n-diethylaniline	605.15	114	1
96-54-8	n-methylpyrrole	603.15	116	4
96-54-8	n-methylpyrrole	673.15	116	4
122-39-4	diphenylamine	907.15	187	5
75-52-5	nitromethane	691	184	4
75-52-5	nitromethane	688.15	116	4
79-24-3	nitroethane	688	184	4

Table C.1: Continued

CAS No.	Name	AIT (K)	Reference	Priority
79-24-3	nitroethane	683.15	116	4
108-03-2	1-nitropropane	693.15	116	4
79-46-9	2-nitropropane	701	184	4
79-46-9	2-nitropropane	698.15	116	4
109-78-4	hydracrylonitrile	768	184	4
110-91-8	morpholine	583.15	184	4
110-91-8	morpholine	503.15	116	4
123-75-1	pyrrolidine	618.15	116	4
75-05-8	acetonitrile	797.04	183	4
75-05-8	acetonitrile	798.15	116	4
107-12-0	propionitrile	788.15	116	4
107-13-1	acrylonitrile	754.26	183	4
107-13-1	acrylonitrile	753.15	116	4
126-98-7	methacrylonitrile	738.15	116	4
111-69-3	adiponitrile	823.15	40	2
88-72-2	o-nitrotoluene	678.15	116	4
99-99-0	p-nitrotoluene	663.15	116	4
109-74-0	butyronitrile	773.15	116	4
78-82-0	isobutyronitrile	753.15	116	4
100-47-0	benzonitrile	888.15	116	4
110-86-1	pyridine	755	184	4
110-86-1	pyridine	823.15	116	4
62-53-3	aniline	890.15	187	5
584-84-9	2,4-toluene diisocyanate	893.15	116	4
111-49-9	hexamethyleneimine	528.15	116	4
100-61-8	n-methylaniline	773.15	116	4

Table C.1: Continued

CAS No.	Name	AIT (K)	Reference	Priority
121-69-7	n,n-dimethylaniline	643.15	116	4
109-06-8	2-methylpyridine	808.15	116	4
74-93-1	methyl mercaptan	633.15	116	4
75-08-1	ethyl mercaptan	568.15	116	4
111-88-6	n-octyl mercaptan	513.15	116	4
75-18-3	dimethyl sulfide	488.15	116	4
110-02-1	thiophene	668.15	116	4
110-01-0	tetrahydrothiophene	473.15	116	4
67-68-5	dimethyl sulfoxide	488.15	159	1
126-33-0	sulfolane	801.15	168	1
75-36-5	acetyl chloride	663.15	187	5
79-36-7	dichloroacetyl chloride	858.15	116	4
98-88-4	benzoyl chloride	804.05	19	5
462-06-6	fluorobenzene	903.15	116	4
111-44-4	di(2-chloroethyl)ether	638.15	116	4
3268-49-3	3-(methylmercapto)propanal	528.15	116	4
68-12-2	n,n-dimethylformamide	713.15	116	4
105-60-2	epsilon-caprolactam	648.15	43	1
105-60-2	epsilon-caprolactam	647.15	32	1
105-60-2	epsilon-caprolactam	668.15	33	1
106-89-8	alpha-epichlorohydrin	658.15	116	4
75-86-5	acetone cyanohydrin	813.15	116	4
98-95-3	nitrobenzene	753.15	116	4
107-89-1	acetaldol	521.15	187	5
98-01-1	furfural	666	183	4
98-01-1	furfural	588.15	116	4

Table C.1: Continued

CAS No.	Name	AIT (K)	Reference	Priority
108-65-6	propylene glycol monomethyl ether acetate	627.15	40	2
108-65-6	propylene glycol monomethyl ether acetate	545.65	173	1
1314-80-3	phosphorus pentasulfide	548.15	184	4
4109-96-0	dichlorosilane	317.15	16	5
10025-78-2	trichlorosilane	455.15	16	5
75-15-0	carbon disulfide	375.15	31	4
75-15-0	carbon disulfide	368.15	116	4
999-97-3	hexamethyldisilazane	598.15	116	4
107-46-0	hexamethyldisiloxane	583.15	116	4
541-05-9	hexamethylcyclotrisiloxane	659.15	133	1
141-63-9	dodecamethylpentasiloxane	623.15	69	3
124-70-9	methyl vinyl dichlorosilane	622.15	148	1
75-76-3	tetramethylsilane	603.15	116	4
556-67-2	octamethylcyclotetrasiloxane	673.15	116	4
638-68-6	n-triacontane	607	147	5
106-68-3	3-octanone	631.15	47	5
7146-60-3	2,3-dimethyloctane	498.15	116	4
2051-30-1	2,6-dimethyloctane	493.15	116	4
60-12-8	2-phenylethanol	683.15	116	4
108-82-7	2,6-dimethyl-4-heptanol	563.15	116	4
98-85-1	alpha-methylbenzyl alcohol	753.15	116	4
105-08-8	1,4-cyclohexanedimethanol	589.15	57	2
105-08-8	1,4-cyclohexanedimethanol	579.82	8	1
105-08-8	1,4-cyclohexanedimethanol	603.15	72	1
105-08-8	1,4-cyclohexanedimethanol	580.15	1	1

Table C.1: Continued

CAS No.	Name	AIT (K)	Reference	Priority
123-99-9	azelaic acid	658.75	103	5
75-98-9	neopentanoic acid	723.15	116	4
149-57-5	2-ethyl hexanoic acid	644	36	2
149-57-5	2-ethyl hexanoic acid	593.15	106	1
149-57-5	2-ethyl hexanoic acid	583.15	171	1
111-14-8	n-heptanoic acid	548.15	116	4
505-48-6	cinnamic acid	720.90	103	5
505-48-6	suberic acid	703.15	116	4
88-09-5	2-ethyl butyric acid	658.15	116	4
629-33-4	n-hexyl formate	523.15	116	4
540-88-5	tert-butyl acetate	708.15	116	4
547-63-7	methyl isobutyrate	723.15	116	4
97-62-1	ethyl isobutyrate	713.15	116	4
622-45-7	cyclohexyl acetate	607.15	187	5
108-32-7	propylene carbonate	703.15	116	4
102-76-1	glyceryl triacetate	703.15	116	4
28553-12-0	diisononyl phthalate	623.15	58	5
28553-12-0	diisononyl phthalate	643.15	58	5
28553-12-0	diisononyl phthalate	673.15	58	5
84-66-2	diethyl phthalate	723.15	116	4
84-74-2	di-n-butyl phthalate	673.15	116	4
131-11-3	dimethyl phthalate	828.15	115	4
131-11-3	dimethyl phthalate	753.15	116	4

Table C.1: Continued

CAS No.	Name	AIT (K)	Reference	Priority
106-63-8	isobutyl acrylate	623.15	116	4
111-82-0	methyl laurate	485.58	103	5
141-05-9	diethyl maleate	623.15	40	2
616-38-6	dimethyl carbonate	738.15	116	4
505-22-6	1,3-dioxane	547.15	149	1
462-95-3	ethylal	447.15	116	4
629-14-1	1,2-diethoxyethane	478.15	116	4
1191-99-7	2,3-dihydrofuran	582.15	123	1
78-88-6	2,3-dichloropropene	783.15	116	4
677-21-4	3,3,3-trifluoropropene	808.15	116	4
460-73-1	1,1,1,3,3-pentafluoropropane	685	49	1
98-08-8	benzotrifluoride	893.15	116	4
78-76-2	2-bromobutane	538.15	116	4
593-60-2	vinyl bromide	773.15	116	4
75-68-3	1-chloro-1,1-difluoroethane	905	102	1
75-02-5	vinyl fluoride	658.15	184	4
75-02-5	vinyl fluoride	733.15	116	4
111-26-2	n-hexylamine	543.15	116	4
111-86-4	n-octylamine	523.65	121	1
111-86-4	n-octylamine	525.15	121	1
102-82-9	tri-n-butylamine	463.15	116	4
111-40-0	diethylenetriamine	631	184	4
111-40-0	diethylenetriamine	668.15	116	4
112-57-2	tetraethylenepentamine	573.15	184	4
102-69-2	tripropylamine	453.15	116	4
108-45-2	m-phenylenediamine	833.15	116	4

Table C.1: Continued

CAS No.	Name	AIT (K)	Reference	Priority
1003-03-8	cyclopentylamine	533.15	25	1
111-41-1	n-aminoethyl ethanolamine	641	184	4
111-41-1	n-aminoethyl ethanolamine	638.15	116	4
124-02-7	diallylamine	543.15	121	1
124-02-7	diallylamine	546.15	121	1
110-85-0	piperazine	728.15	184	4
110-85-0	piperazine	593.15	116	4
55-63-0	nitroglycerine	543.15	40	2
88-74-4	o-nitroaniline	794.15	167	1
100-01-6	p-nitroaniline	773.15	116	4
92-67-1	p-aminodiphenyl	908.15	60	1
92-67-1	p-aminodiphenyl	723.15	68	1
579-66-8	2,6-diethylaniline	733.15	116	4
624-83-9	methyl isocyanate	803.15	115	4
108-99-6	3-methylpyridine	773.15	186	2
108-89-4	4-methylpyridine	773.15	43	1
822-06-0	1,6-hexamethylene diisocyanate	673.15	116	4
4098-71-9	isophorone diisocyanate	703.15	116	4
25103-58-6	tert-dodecyl mercaptan	503.15	116	4
25103-58-6	tert-dodecyl mercaptan	487.15	23	1
25360-10-5	tert-nonyl mercaptan	485.15	24	1
76-22-2	camphor	739.15	40	2
98-00-0	furfuryl alcohol	664.261	184	4

Table C.1: Continued

CAS No.	Name	AIT (K)	Reference	Priority
98-00-0	furfuryl alcohol	663.15	116	4
127-19-5	n,n-dimethylacetamide	627.15	167	1
127-19-5	n,n-dimethylacetamide	763.15	40	2
150-76-5	p-methoxyphenol	694.15	57	2
109-86-4	2-methoxyethanol	558.15	116	4
110-80-5	2-ethoxyethanol	508.15	116	4
111-76-2	2-butoxyethanol	513.15	116	4
111-77-3	2-(2-methoxyethoxy)ethanol	488.15	116	4
111-90-0	2-(2-ethoxyethoxy)ethanol	463.15	116	4
929-06-6	2-aminoethoxyethanol	643.15	116	4
21282-97-3	2-acetoacetoxy ethyl methacrylate	602.15	109	1
547-64-8	methyl lactate	658.15	35	2
121-73-3	m-chloronitrobenzene	773.15	116	4
50-78-2	acetylsalicylic acid	773.15	116	4
156-43-4	p-phenetidine	733.15	116	4
77-68-9	2-methyl-, 3-hydroxy-2,2,4-trimethylpentyl propanoate	666.15	124	1
107-07-3	2-chloroethanol	698.15	184	4
4394-85-8	4-formylmorpholine	643.15	43	1
4394-85-8	4-formylmorpholine	618.15	101	1
107-51-7	octamethyltrisiloxane	623.15	69	3
107-51-7	octamethyltrisiloxane	691.15	10	1
631-36-7	tetraethyl silane	606.15	48	3
631-36-7	tetraethyl silane	508.15	10	1
927-49-1	diamyl ketone	538.15	116	4

Table C.1: Continued

CAS No.	Name	AIT (K)	Reference	Priority
78-94-4	3-buten-2-one	764.15	15	2
78-94-4	3-buten-2-one	763.71	40	2
78-94-4	3-buten-2-one	643.15	87	1
96-41-3	cyclopentanol	648.15	99	1
143-28-2	oleyl alcohol	605.93	110	1
88-18-6	o-tert-butylphenol	628.15	5	1
2425-77-6	2-hexyl-1-decanol	513.15	59	1
2425-77-6	2-hexyl-1-decanol	533.15	96	1
5333-42-6	2-octyl-1-dodecanol	530.93	97	1
58670-89-6	2-decyl-1-tetradecanol	578.15	156	1
128-39-2	2,6-di-tert-butylphenol	648.15	11	1
693-23-2	dodecanedioic acid	663.15	108	1
1759-53-1	cyclopropane carboxylic acid	718.65	127	1
2724-58-5	isostearic acid	573.15	157	1
97-72-3	isobutyric anhydride	623.15	138	5
6846-50-0	2,2,4-trimethyl-1,3-pentanediol diisobutyrate	678.15	116	4
6422-86-2	di(2-ethylhexyl) terephthalate	672	83	1
6422-86-2	di(2-ethylhexyl) terephthalate	660.15	154	1
131-17-9	diallyl phthalate	658.15	7	1
112-61-8	methyl stearate	498.15	103	5
111-61-5	ethyl stearate	508.65	103	5
110-38-3	ethyl caprate	493.15	116	4
106-33-2	ethyl laurate	482.65	103	5
13048-33-4	1,6-hexanediol diacrylate	508.15	170	1

Table C.1: Continued

CAS No.	Name	AIT (K)	Reference	Priority
5444-75-7	2-ethylhexyl benzoate	517.15	113	1
5444-75-7	2-ethylhexyl benzoate	671.15	143	1
1962-75-0	dibutyl terephthalate	692.15	129	5
142-16-5	di-(2-ethylhexyl) maleate	583.15	34	5
1119-40-0	dimethyl glutarate	638.15	73	1
142-90-5	n-dodecyl methacrylate	569.15	176	1
553-90-2	dimethyl oxalate	753.15	116	4
623-43-8	methyl-e-crotonate	588.15	116	4
106-70-7	methyl hexanoate	528.15	116	4
103-23-1	di(2-ethylhexyl) adipate	613.15	116	4
108-59-8	dimethylmalonate	713.15	116	4
406-58-6	1,1,1,3,3-pentafluorobutane	863.15	115	4
754-12-1	2,3,3,3-tetrafluoropropene	678.15	164	5
355-37-3	1h-perfluoro-n-hexane	878.15	116	4
102687-65-0	trans-1-chloro-3,3,3-trifluoro-1-propene	653.15	185	1
95-68-1	2,4-dimethylaniline	773.15	116	4
109-55-7	3-(n,n-dimethylamino) propylamine	488.15	116	4
96-29-7	2-butoxime	588.15	2	1
626-67-5	n-methylpiperidine	488.15	116	4
288-32-4	imidazole	753.15	85	1
90-41-5	2-aminodiphenyl	725.15	187	5
110-95-2	n,n,n',n'-tetramethyl-1,3-propanediamine	453.15	158	1
616-47-7	1-methylimidazole	798.15	9	1
616-47-7	1-methylimidazole	761.15	162	1
103-83-3	benzyldimethylamine	683.15	116	4

Table C.1: Continued

CAS No.	Name	AIT (K)	Reference	Priority
98-94-2	n,n-dimethylcyclohexylamine	488.15	116	4
109-76-2	1,3-propanediamine	623.15	116	4
103-69-5	n-ethylaniline	752.15	57	2
92-84-2	phenothiazine	743.15	98	1
107-98-2	propylene glycol monomethyl ether	543.15	116	4
34590-94-8	dipropylene glycol monomethyl ether	543.15	116	4
57018-52-7	propylene glycol 1-tert-butyl ether	645.65	173	1
6881-94-3	diethylene glycol monopropyl ether	477.15	29	1
106-47-8	p-chloroaniline	958.15	116	4
556-52-5	2,3-epoxy-1-propanol	688.15	116	4
112-25-4	2-hexoxyethanol	553.15	57	2
124-17-4	diethylene glycol monobutyl ether acetate	522.15	130	5
3710-84-7	n,n-diethylhydroxylamine	538.15	151	1
1569-02-4	1-ethoxy-2-propanol	528.15	116	4
98-16-8	3-(trifluoromethyl)aniline	873.15	152	1
78-10-4	tetraethoxysilane	503.15	116	4
919-30-2	gamma-aminopropyltriethoxysilane	573.15	74	1
75-54-7	methyl dichlorosilane	503.15	117	1
75-54-7	methyl dichlorosilane	517.15	119	1
75-54-7	methyl dichlorosilane	589.15	40	2
75-94-5	vinyltrichlorosilane	536.15	52	5
1067-53-4	tris(2-methoxyethoxy)vinylsilane	493.15	70	1
2530-87-2	3-chloropropyltrimethoxysilane	493.15	116	4

Table C.1: Continued

CAS No.	Name	AIT (K)	Reference	Priority
10545-99-0	sulfur dichloride	507.04	145	1
2530-83-8	[3-(2,3-epoxyproxy)propyl]trimethoxysilane	673.15	116	4
2550-06-3	3-chloropropyltrichlorosilane	669.15	52	5
675-62-7	(3,3,3-trifluoropropyl)methyldichlorosilane	671.15	132	1
992-94-9	methyl silane	403.15	48	3
1111-74-6	dimethyl silane	503.15	48	3
993-07-7	trimethyl silane	593.15	48	3
1066-35-9	dimethylchlorosilane	548.15	116	4
75-77-4	trimethylchlorosilane	668.15	184	4
75-77-4	trimethylchlorosilane	693.15	116	4
75-78-5	dimethyldichlorosilane	698.15	116	4
541-02-6	decamethylcyclopentasiloxane	653.15	116	4
540-97-6	dodecamethylcyclohexasiloxane	665	120	1
115-21-9	ethyltrichlorosilane	678.15	52	5
13465-77-5	hexachlorosilane	569.15	64	3
2807-30-9	ethylene glycol monopropyl ether	529.15	135	5
112-34-5	2-(2-butoxyethoxy)ethanol	501	184	4
112-34-5	2-(2-butoxyethoxy)ethanol	498.15	116	4
108-42-9	m-chloroaniline	978.15	116	4
102-36-3	3,4-dichlorophenyl isocyanate	923.15	116	4
97-00-7	1-chloro-2,4-dinitrobenzene	705.15	167	1
541-41-3	ethyl chloroformate	773.15	184	4
79-22-1	methyl chloroformate	748.15	116	4
78-40-0	triethyl phosphate	753.15	116	4

Table C.1: Continued

CAS No.	Name	AIT (K)	Reference	Priority
100-64-1	cyclohexanone oxime	285	43	1
2768-02-7	vinyltrimethoxysilane	508.15	116	4
1112-39-6	dimethyldimethoxysilane	625.15	122	1
98-13-5	phenyltrichlorosilane	817.15	52	5
1066-40-6	trimethyl silanol	653.15	116	4
107-52-8	tetradecamethylhexasiloxane	623.15	69	3
141-62-8	decamethyltetrasiloxane	623.15	125	1
78-30-8	tri-o-cresyl phosphate	658.15	116	4
156-87-6	3-amino-1-propanol	648.15	116	4
78-96-6	1-amino-2-propanol	608.15	116	4
96-34-4	methyl chloroacetate	738.15	116	4
102-01-2	acetoacetanilide	725.15	4	1
103-84-4	acetanilide	820.15	187	5
77-78-1	dimethyl sulfate	743.15	43	1
64-67-5	diethyl sulfate	633.15	116	4
133-37-9	tartaric acid	698.15	116	4
97-64-3	ethyl lactate	673.15	116	4
111-15-9	2-ethoxyethyl acetate	653.15	116	4
112-15-2	diethylene glycol ethyl ether acetate	539.15	130	5
141-97-9	ethyl acetoacetate	568.15	184	4
141-97-9	ethyl acetoacetate	623.15	116	4
105-34-0	methyl cyanoacetate	748.15	116	4
100-20-9	terephthaloyl chloride	723.15	90	1
994-30-9	chlorotriethylsilane	553.15	17	1
617-86-7	triethyl silane	569.15	48	3
617-86-7	triethyl silane	523.15	179	1

Table C.1: Continued

CAS No.	Name	AIT (K)	Reference	Priority
102-85-2	tributyl phosphite	613.15	169	1
79-16-3	n-methylacetamide	763.15	116	4
111-48-8	thiodiglycol	571.15	40	2
60-24-2	2-mercaptoethanol	568.15	3	1
100-37-8	diethylethanolamine	593.15	40	2
109-83-1	methylethanolamine	623.15	43	1
108-01-0	dimethylethanolamine	493.15	116	4
110-97-4	diisopropanolamine	563.15	116	4
103-76-4	n-(2-hydroxyethyl)piperazine	553.15	43	1
112-07-2	ethylene glycol monobutyl ether acetate	614	183	4
112-07-2	ethylene glycol monobutyl ether acetate	628.15	116	4
763-69-9	ethyl-3-ethoxypropionate	650.15	30	4
108-22-5	1-methylvinyl acetate	668.15	116	4
1571-08-0	methyl-4-formylbenzoate	700	126	1
1115-20-4	hydroxypivalyl hydroxypivalate	613	12	1
99-75-2	methyl para-toluate	773.15	86	1
122-79-2	phenyl acetate	858.15	116	4
5131-66-8	propylene glycol n-butyl ether	533.15	45	1
29911-28-2	dipropylene glycol n-butyl ether	467	44	1
94-28-0	triethylene glycol bis(2-ethylhexanoate)	658.15	94	1
94-28-0	triethylene glycol bis(2-ethylhexanoate)	618.15	111	1
1694-31-1	t-butyl acetoacetate	608.15	92	1
1694-31-1	t-butyl acetoacetate	663.15	91	1
2038-03-1	4-(2-aminoethyl)morpholine	503.15	81	1
100-74-3	n-ethylmorpholine	458.15	182	1

Table C.1: Continued

CAS No.	Name	AIT (K)	Reference	Priority
375-03-1	heptafluoropropyl methyl ether	688.15	84	1
148462-57-1	1-methoxy-2-propanol propanoate	633.15	104	1
539-88-8	ethyl levulinate	698.15	100	1
126-13-6	sucrose acetate isobutyrate	672.15	144	1
513-86-0	acetoin	588.15	116	4
80-73-9	1,3-dimethyl-2-imidazolidinone	578.15	75	1
342573-75-5	1-ethyl-3-methylimidazolium ethylsulfate	696.25	22	5
126-73-8	tri-n-butyl phosphate	683.15	8	1
126-73-8	tri-n-butyl phosphate	755.15	95	1
126-73-8	tri-n-butyl phosphate	673.15	178	1
124-68-5	2-amino-2-methyl-1-propanol	711.15	79	1
90-04-0	o-anisidine	688.15	88	1
88-89-1	2,4,6-trinitrophenol	573.15	40	2
88-89-1	2,4,6-trinitrophenol	578.15	13	3
88-89-1	2,4,6-trinitrophenol	583.15	13	3
118-71-8	maltol	666.48	107	1
102-09-0	diphenyl carbonate	893.15	28	1
7660-25-5	d-fructose	633.15	56	1
111-75-1	n-butylaminoethanol	538.15	116	4
58-55-9	theophylline	883.15	160	1
110-73-6	ethylaminoethanol	603.15	116	4
104-94-9	p-anisidine	788.15	9	1
90-72-2	2,4,6-tris(dimethylaminomethyl)phenol	655.15	163	1

Table C.2: References to Data Set Used in Regression

Reference Number	Reference
1	1,4-Cyclohexane Dimethanol. In: http://www.ecem.com 8, (2013) pp. 16
2	2-Butanone Oxime. In: http://www.chem007.com/specification_d/chemicals/supplier/cas/2-Butanone%20oxime.asp 5, (2006) pp. 22
3	2-Mercaptoethanol. "Material Safety Data Sheet". BASF Wyandotte Corporation, Parsippany, New Jersey. (1981)
4	Acetoacetanilide. "Data Sheet". Eastman Chemicals, Kingsport TN. (1984)
5	Acros Organics Material Safety Data Sheet 2-tert-Butylphenol. In: http://www.acros.com/DesktopModules/Acros_Search_Results/Acros_Search_Results.aspx 18-6 3, (2009) pp. 12
6	Affens WA, Johnson J, Carhart HW. "Effect of chemical structure on spontaneous ignition of hydrocarbons". J Chem Eng Data 1961;6(4):613–9.
7	Aldrich Advancing Science. Aldrich, Milwaukee, WI. (2005)
8	Aldrich Advancing Science. Aldrich, Milwaukee, WI. (2007)
9	Aldrich Chemistry 2012-2014 Handbook of Fine Chemicals. Sigma-Aldrich. (2012)
10	Anderson, R.; Larson, G.L.; Smith, C., "Silicon Compounds: Register and Review, 5th. Ed.". Huls America, Piscataway, NJ. (1991)
11	Ashok, B.; Nanthagopal, K.; Jeevanantham, A.K.; Bhowmick, P.; Malhotra, D.; Argarwal, P., "An assessment of calophyllum inophyllum biodiesel fuelled diesel engine characteristics using novel antioxidant additives". In: Energy Convers. Manage. 148, (2017) pp. 935-943
12	BASF Safety data sheet for Hydroxypivalyl Hydroxypivalate. BASF Aktiengesellschaft. (2002)

Table C.2: Continued

Reference Number	Reference
13	Belajev, A. F.; Yusephovich, N. A., “Thermal Inflammation and the Boiling Point of the Given Explosive Compound”. In: Dokl. Akad. Nauk SSSR 27, 2 (1940) pp. 133-136
14	Benzoyl Peroxide. “Material Safety Data Sheet”. Fisher Scientific Co., Fairlawn, NJ 07410. (1985)
15	Bond, J., “Sources of Ignition”. Butterworth. (1991)
16	Britton, L.G., “Combustion Hazards of Silane and its Chlorides”. In: Plant/Oper. Prog. 9, 1 (1990) pp. 16
17	Chemical Book entry for chlorotriethylsilane. In: https://www.chemicalbook.com/ 6, (2019) pp. 18 (From the main website, search for CAS RN 994-30-9 then click on “Chemical Properties.”)
18	Chemical Safety Data Sheet for 2-METHYL-1,3-DIOXOLANE. Technical Safety Laboratory, Eastman Kodak Company. 5, (1979) pp. 11
19	Chen, C.; Chen, C.; Han, T., “Autoignition Temperature Data for Isopropyl Chloride, Butyl Chloride, Isobutyl Chloride, Pentyl Chloride, Pentyl Bromide, Chlorocyclohexane, and Benzoyl Chloride”. In: Ind. Eng. Chem. Res. 52, 23 (2013) pp. 7986-7992
20	Chen, C.-C.; Hsieh, Y.-C., “Effect of Experimental Conditions on Measuring Autoignition Temperatures of Liquid Chemicals”. In: Ind. Eng. Chem. Res. 49, 12 (2010) pp. 5925-5932
21	Chen, C.-C.; Liaw, H.-J.; Shu, C.-M.; Hsieh, Y.-C., “Autoignition temperature data for methanol, ethanol, propanol, 2-butanol, 1-butanol, and 2-methyl-2,4-pentanediol”. In: J. Chem. Eng. Data 55, 11 (2010) pp. 5059-5064
22	Chen, Y.-T.; Chen, C.-C.; Su, C.-H.; Liaw, H.-J., “Auto-ignition characteristics of selected ionic liquids”. In: Procedia Eng. 84, (2014) pp. 285-292

Table C.2: Continued

Reference Number	Reference
23	Chevron Phillips Chemical Company Safety Data Sheet for Sulfole 120 Mercaptan (tert-Dodecyl Mercaptan). In: http://www.cpchem.com 9, (2018) pp. 6 (Version 3.11; Revision Date 2017-05-31. Search for "sulfole 120." Then select Sulfole 120 t-Dodecyl Mercaptan. Then select "View" or "Download" under "Safety Data Sheets.")
24	Chevron Phillips Chemical Company Safety Data Sheet for Sulfole 90 Mercaptan (tert-nonyl Mercaptan). In: http://www.cpchem.com 9, (2018) pp. 6 (Version 2.3; Revision Date 2016-05-17. Search via CAS: 25360-10-5. Then select "View" or "Download" under "Safety Data Sheets.")
25	Cyclopentylamine. "Data Sheet". BASF. (January 1990)
26	Data Guides. Safety Management Services, Inc. (1999)
27	Diethylene Glycol Diethyl Ether Information Sheet. In: https://www.cdc.gov/niosh/ 6, (2017) pp. 14
28	Diphenyl Carbonate SIDS Initial Assessment Report for SIAM 19. In: http://www.chem.unep.ch/irptc/sids/oecdsids/102090.pdf 5, (2012) pp. 17
29	DP Solvent. "Material Safety Data Sheet". Eastman Chemical Company, Kingsport, TN 37662. (1994)
30	Eastman Chemicals, "Ethyl 3-Ethoxypropionate". Eastman Chemical Products, Kingsport TN. (1988) (Publication No. M-252B)
31	Electrical Apparatus for Explosive Gas Atmospheres. Part 4. Method of Test for Ignition Temperature. "Publication 79-4A". International Electrotechnical Commission, Geneva. (1970) (Supplement 1)
32	Epsilon-Caprolactam, Material Safety Data Sheet. Aldrich Chemical Co., Inc. (2000)
33	Epsilon-Caprolactam, Material Safety Data Sheet. BASF CORPORATION. (2005)

Table C.2: Continued

Reference Number	Reference
34	European Chemicals Industry, “IUCLID Dataset for di(2-ethylhexyl) maleate”. European Chemicals Industry. 5, (2011) pp. 25 (Website Accessed on May 25 2011.)
35	Fire Hazardous Properties: Flash Points, Flammability Limits, and Autoignition Temperatures. “Item 82030”. Engineering Science Data, London. (1982)
36	Fire Protection Guide on Hazardous Materials, 10th ed. National Fire Protection Assoc., Boston, MA. (1991)
37	Fire Protection Guide on Hazardous Materials, 7th Ed. National Fire Protection Association, Boston, MA. (1978)
38	Fire Protection Guide on Hazardous Materials. National Fire Protection Association, Boston, MA. (1994)
39	Fire Protection Guide to Hazardous Materials. National Fire Protection Association. (1997) (12th ed.)
40	Fire Protection Guide to Hazardous Materials. National Fire Protection Association. (2002) (13th ed., Quincy, Mass)
41	Friz, G.; Kuhlborsch, G.; Nehren, R.; Reiter, F.; Ispra, “Physical Properties of Diphenyl, o-, m-, and p-Terphenyl and Their Mixtures”. In: Atomkernergie 13, (1968) pp. 25
42	Furno, A.L.; Imhof, A.C.; Kuchta, J.M., “Effect of Pressure and Oxidant Concentration on Autoignition Temperatures of Selected Combustibles in Various Oxygen and Nitrogen Tetroxide Atmospheres”. In: J. Chem. Eng. Data 13, 2 (1968) pp. 243
43	Gerhartz, W.; Ullmann, F.; Yamamoto, Y. S., “Ullmann’s Encyclopedia of Industrial Chemistry (5th Ed.)”. VCH Publishers, Deerfield Beach, FL. (1985)

Table C.2: Continued

Reference Number	Reference
44	Global Product Information for Dowanol DPnB (Dipropylene Glycol n-Butyl Ether). The Dow Chemical Company. (2004) (ACCESSED 2-6-2008 AT http://www.dow.com)
45	Global Product Information for Dowanol PnB (Propylene Glycol n-Butyl Ether). The Dow Chemical Company. (2003) (ACCESSED 5-7-2003 AT http://www.dow.com)
46	Glyoxal 40% Solution, Material Safety Data Sheet. Sigma Chemical. (1999)
47	Godde, M.; Brandes, E.; Cammenga, H.K., "Zundtemperaturen homologer Reihen - Teil 2: Untersuchungen zum Einfluss funktioneller Gruppen". In: PTB-Mitt. 108, 6 (1998) pp. 437-441
48	Griffiths, S.T.; Wilson, R.R., "The Spontaneous Ignition of Alkyl Silanes". In: Combust. Flame 2, (1958) pp. 244
49	HFC-245fa Material Safety Data Sheet. Allied Signal. (1999)
50	Hilado, C.J., "Flammability Test Methods Handbook". (1973)
51	Hilado, C.J.; Clark, S.W., "Autoignition Temperatures of Organic Chemicals". In: Chem. Eng. 79, 19 (1972) pp. 75-80
52	Hshieh, F.Y.; Hirsch, D.B.; Williams, J.H., "Short Communication: Autoignition Temperature of Trichlorosilanes". In: Fire Mater. 26, (2002) pp. 289-290
53	In: www.mgc.co.jp 6, (2004)
54	Information on Bromomethane, Bromoethane, 1-Bromopropane, 1-Bromobutane, 1-Bromoheptane, and 1-Bromododecane. In: www.chemnetbase.com/scripts/ccdweb.exe 5, (2005) pp. 10 (The Combined Chemical Dictionary, Online Chemical Database)

Table C.2: Continued

Reference Number	Reference
55	Information Sheet for 2-BUTYL-2-ETHYL-1,3-PROPANEDIOL (BEPG). Kyowa Hakko Chemical Co., Ltd. In: http://www.kyowachemical.co.jp (2008) (Copyright 2008)
56	International Chemical Safety Cards: Fructose. In: http://www.cdc.gov/niosh/ipcsneng/neng1554.html 2, (2013) pp. 7 (Website Accessed on Feb 7 2013.)
57	Item No. 82030. Engineering Science Data. (Oct. 1982)
58	IUCLID Dataset: Diisononyl Phthalate. In: http://esis.jrc.ec.europa.eu/doc/IUCLID/data_sheets/28553120.pdf 6, (2013) pp. 13
59	IUCLID DATASHEET for 2-hexyl-1-decanol. In: https://iuclid6.echa.europa.eu/get-iuclid-data 1, (2014) pp. 14
60	Karvonen, A., "Das Spektrochemische Verhalten di Alkoxylessigsaure, RO.Ch2.Co2H (Funfte Mitteilung uber den Einflus der Position, Resp. Anhaufung der Substituenten in Spektrochemischer Hinsicht.)". In: Chem. Zentralbl. III (1919) pp. 987
61	Kim, Y.S.; Lee, S.K.; Kim, J.H.; Kim, J.S.; No, K.T., "Prediction of Autoignition Temperatures (AITs) for Hydrocarbons and Compounds Containing Heteroatoms by the Quantitative Structure-property Relationship". In: J. Chem. Soc. 2, 12 (2002) pp. 2087-2092
62	Kirk-Othmer, "Encyclopedia of Chemical Technology, 3rd ed.". Interscience, New York. (1978)
63	Kirk-Othmer, "Encyclopedia of Chemical Technology, 4th Ed.". Interscience, New York. (1991)
64	Knyazev, A.I.; Mikeev, V.S., "Issledovanie Vzryvoopasnosti Smesei Geksakhlordisilana S Vozdukhom". In: Vysokochistye Veshchestva 5 (1987) pp. 77-79

Table C.2: Continued

Reference Number	Reference
65	Kuchta, J.M., “Investigation of Fire and Explosion Accidents in the Chemical, Mining, and Fuel-related Industries - A Manual”. “U.S. Bur. Mines Bull. No. 680”. Washington, D.C. (1985)
66	Kuchta, J.M.; Zabetakis, M.G., “Flammability and Autoignition of Hydrocarbon Fuels Under Static and Dynamic Conditions”. “Bur. of Mines Rept. of Inves. RI5992”. (1962)
67	Lewis, R, J., “Sax’s Dangerous Properties of Industrial Materials, 11th edition”. John Wiley & Sons. (2004)
68	Lewis, R.J., “Sax’s Dangerous Properties of Industrial Materials, 8th Ed.”. Van Nostrand, New York. (1992)
69	Lipowitz; J. Ziemelis, M., “Flammability of Poly(Dimethylsiloxanes.) II. Flammability and Five Hazard Properties”. In: J. Fire Flamm. 7, (1976) pp. 504
70	Ludeck, W., “Use, mode of action, and properties of silane adhesive agents for plastics in electrical engineering”. In: Elektrie 28, 4 (1974) pp. 217-219
71	Lyondell Chemical Company, “High Production Volume (HPV) Chemical Challenge Program: Data Review and Test Plan for 2-methyl-1,3-propanediol (MPDiol Glycol) CAS RN 2163-42-0”. Environmental Protection Agency. In: http://www.epa.gov/HPV/pubs/summaries/2mth3pro/c14924tc.htm (2013) (Website Accessed on 10/1/2013. Document dated 12/16/2003 with assigned # 201-14924)
72	Material Safety Data Sheet 1,4-Cyclohexanedimethanol, mixture of cis and trans. In: http://fscimage.fishersci.com 8, (2013) pp. 16
73	Material Safety Data Sheet Dimethyl glutarate. In: www.fishersci.com 6, (2012) pp. 1

Table C.2: Continued

Reference Number	Reference
74	Material safety data sheet for 3-aminopropyltriethoxysilane", 99%". Fisher scientific. (2002) (Accessed at 1-8-2002 at https://fscimage.fishersci.com/msds/85861.htm)
75	Material Safety Data Sheet for 1,3-Dimethyl-2-imidazolidinone, 97%. "http://www.fishersci.com". Acros Organics N.V. 5, (2008)
76	Material Safety Data Sheet for 1,4-cyclohexanedicarboxylic acid, 98% purity. In: http://www.eastman.com/markets/resin_intermediates/producthome.asp?product=7100116 7, (2005) pp. 14 (Publisher: Eastman Chemical Company)
77	Material Safety Data Sheet for 2,2,4-Trimethylpentane-1,3-diol, 98%" ". Acros Organics. (2000) (ACCESSED 4-18-2003 AT http://www.fscimage.fishersci.com/msds/95911.htm)
78	Material Safety Data Sheet for 2,2-Dimethyloxirane for synthesis" Purity >=90% to <=100%". In: www.emdmillipore.com 10, (2016) pp. 19
79	Material Safety Data Sheet for 2-Amino-2-methyl-1-propanol. "http://www.osha.gov/dts/sltc/methods/partial/pv2145/pv2145.html". U.S. Dept. Labor. OSHA. 05, (2009) pp. 08
80	Material Safety Data Sheet for 2-methyltetrahydrofuran. "http://www.polysciences.com/Catalog/Department/Product/98/categoryId__8/productId__ Polyscience Inc. 05, (2009) pp. 08
81	Material Safety Data Sheet for 4-(2-aminoethyl) morpholine. In: www.sigmaaldrich.com 6, (2005) pp. 6
82	Material Safety Data Sheet for Dipropylene Glycol, 99%. In: www.dow.com 3, (2014) pp. 24 (Website Accessed on Mar 24 2014.)
83	Material Safety Data Sheet for Eastman Plasticizer 168. Eastman. (2003) (Accessed on 5/16/2003 at www.eastman.com)

Table C.2: Continued

Reference Number	Reference
84	Material Safety Data Sheet for Heptafluoropropyl Methyl Ether, 99.5 %. In: http://multimedia.mmm.com/mws/mediawebserver.dyn?333333DkeO8TD5KLj7syw66oy 4, (2005) pp. 28 (This information can be accessed by going to www.3M.com, searching the site for "HFE-7000," selecting "3M(TM) Novec(TM) Engineered Fluid HFE-7000," and selecting "Material Safety Data Sheet.")
85	Material Safety Data Sheet for Imidazole. "www.sigma-aldrich.com". Sigma-Aldrich Corporation. 2, (2008) pp. 14
86	Material Safety Data Sheet for Methyl p-Toluate, 99.0% Purity. Fluka Chemical Corp. (2001) (Accessed 12-21-2001 at www.sigmaaldrich.com)
87	Material Safety Data Sheet for Methyl Vinyl Ketone, Stabilized. In: www.fishersci.com 5, (2014) pp. 10 (Acros Organics MSDS# 96190 - Revision #7 Date 7/20/2009)
88	Material Safety Data Sheet for o-Anisidine. "http://ww.fishersci.com". Fisher Safety. 06, (2009) pp. 10
89	Material Safety Data Sheet for p-Tolylaldehyde, >=98% purity. "http://worldaccount.basf.com/wa/PublicMSDS/Search". BASF The Chemical Company. 4, (2009) pp. 23 (Search for p-Tolylaldehyde)
90	Material Safety Data Sheet for Terephthaloyl Chloride, 99+% (Acros Organics N. V.). In: https://fscimage.fishersci.com Feb, (2005) pp. 11
91	Material Safety data Sheet for Tert.-Butyl Acetoacetate, 99% Purity. Acros Organics N.V. (2003) (Printed 6/2/04 from http://www.fishersci.com/)
92	Material Safety Data Sheet for Tert-Butyl Acetoacetate, 98% purity. Sigma-Aldrich. (2004) (Printed 5/28/04 from https://www.sigma-aldrich.com/SAWS.nsf/msdshelp?OpenForm)

Table C.2: Continued

Reference Number	Reference
93	Material Safety Data Sheet for tert-Butylcyclohexane. (7-30-03) http://ull.chemistry.uakron.edu/erd/chemicals/3/2147.html)
94	Material Safety Data Sheet for Triethylene Glycol bis(2-Ethylhexanoate)“ “. Eastman Chemical Company. (2001) (ACCESSED 4-24-03 AT http://www.eastman.com)
95	Material Safety Data Sheet for Tri-n-butyl Phosphate, 99%. “http://www.fishersci.com”. 1, (2008) pp. 31
96	Material Safety Data Sheet Jarcol I-16. In: http://www.jarchem.com/ 4, (2014) pp. 29
97	Material Safety Data Sheet Jarcol I-20. In: http://www.jarchem.com/ 3, (2014) pp. 29
98	Material Safety Data Sheet Phenothiazine, 99%. Fisher Scientific. (2000)
99	Material Safety Data Sheet, Cyclopentanol, 99%. Acros Organics. 5, (2012) pp. 23 (Revision date: 7/20/2009)
100	Material Safety Data Sheet, Ethyl Levulinate, 98%. In: http://search.acros.be/physical 05, (2006) pp. 31
101	Material Safety Data Sheet, n-Formylmorpholine. Fisher Scientific. (1996)
102	Matheson Gas Data Book, unabridged ed. Matheson Company, Inc., East Rutherford, New Jersey. (1974) (4 vols.)
103	Measured by DIPPR staff (between 2019 and 2021) using the apparatus described in ref 63 (Redd 2021)
104	Methotate Specifications. In: http://www.rierdenchemical.com/Specifications/methotate_specifications.htm 5, (2006) pp. 18
105	MSDS for 1,3-Dioxolane. In: www.acros.com 2, (2013) pp. 27 (Revision Date: 6/1/2010)

Table C.2: Continued

Reference Number	Reference
106	MSDS for 2-Ethylhexanoic acid. In: http://www.chemvip.com/ChemVIP%20Active/Products5.nsf/(*All*)/5096555822*E*2*BFD*3 EN-CEL-NA-MSDS-187.rtf?OpenElement 3, (2005) pp. 28
107	MSDS for 3-Hydroxy-2-methyl-4-pyrone, 97+%. In: http://www.fishersci.com/ecomm/servlet/msdsproxy?productName=AC121550050&produ Hydroxy-2-methyl-4- pyrone%2C+99%25%2C+Acros+Organics&catNo=AC12155- 0050&vendorId=VN00032119&storeId=10652 5, (2012) pp. 8
108	MSDS for Adipic Acid, Azelaic Acid, Sebacic Acid, Dodecanedioic Acid. In: www.chemdat.info 6, (2006) pp. 24
109	MSDS for Eastman AAEM. In: www.eastman.com 5, (2004) pp. 21
110	MSDS for Oleyl Alcohol, >98%. In: http://datasheets.scbt.com/sc-215628.pdf 7, (2012) pp. 25
111	MSDS for triethylene glycol bis(2-ethylhexanoate). Celanese. 1, (2007) pp. 26
112	MSDS of Tris(2-ethylhexyl) trimellitate. In: www.sigma-aldrich.com 5, (2004) pp. May 7, 200 (Issue: May 7)
113	MSDS Velate 368. “http://www.eastman.com”. Genovique Specialties. (2008) (Accessed 2/3/2011)
114	N,N-Diethylaniline. “Material Safety Data Sheet”. DuPont, Wilmington, DE. (October 1985)
115	Nabert, K.; Schon, G., “Sicherheitstechnische Kennzahlen brennbarer Gase und Dämpfe”. Deutscher Eichverlag GmbH. Braunschweig. (1978)
116	Nabert, K.; Schön, G.; Redeker, T., “Sicherheitstechnische Kenngrößen brennbarer Gase und Dämpfe”. Deutscher Eichverlag. (2004)
117	Private Communication (1989)
118	Private Communication (1989)

Table C.2: Continued

Reference Number	Reference
119	Private Communication (1992)
120	Private Communication (1993)
121	Private Communication (1994)
122	Private Communication (1995)
123	Private Communication (2002)
124	Private Communication (2004)
125	Private Communication (2005)
126	Private Communication (2005)
127	Private Communication (2005)
128	Private Communication (2009)
129	Private Communication (2011)
130	Private Communication (2011)
131	Private Communication (2011)
132	Private Communication (2011)
133	Private Communication (2011)
134	Private Communication (2012)
135	Private Communication (2013)
136	Private Communication (2015)
137	Private Communication (2015)
138	Private Communication (2018)
139	Private Communication (2018)
140	Private Communication (2018)
141	Private Communication (2020)
142	Product Data Sheet for BEPD. In: https://www.perstorp.com 12, (2019) pp. 9 (Issue: 5; Approved: 01 Jul 2013)
143	Product Data Sheet Velate 368 Coalescent. “http://www.eastman.com/”. Eastman Chemical Company. (2010) (Accessed 2/3/2011)

Table C.2: Continued

Reference Number	Reference
144	Product Information for Eastman SAIB. In: www.eastman.com 04, (2006) pp. 11
145	Properties of Flammable Liquids, Gases, and Solids. In: Ind. Eng. Chem. 32, (1940) pp. 880-884 (The Associated Factory Mutual Fire Insurance Companies, Boston, Mass.)
146	p-tert-Butyltoluene. In: http://www.ilo.org/dyn/icsc/showcard.display?p_card_id=1068 6, (2017) pp. 2 (International Chemical Safety Cards)
147	Redd (M. E.), Joseph C. Bloxham, Neil F. Giles, Thomas A. Knotts, W. Vincent Wilding, "A study of unexpected autoignition temperature trends for pure n-alkanes", Fuel, Volume 06, 2021, 121710, ISSN 0016-2361,https://doi.org/10.1016/j.fuel.2021.121710.
148	Reuther, H., "Zundtemperaturen von Siliziumorganischen Verbindungen". In: Chem. Tech. 22, (1970) pp. 171
149	Riddick, J.A.; Bunger, W.B.; Sakano, T.K., "Organic Solvents: Physical Properties and Methods of Purification, 4th ed.". Wiley Interscience, New York. (1986)
150	Safety Data Sheet 1,2 Pentanediol. In: http://basf.com 1, (2018) pp. 18 (Revision Date: 2016/12/04; Version: 3.0)
151	Safety Data Sheet DEHA anhydrous. In: eastman.com 06, (2019) pp. 17 (Click on "Products", search for DEHA and click on "SDS" for anhydrous product; Revision Date: 10/10/2018; Date of last issue: 10/30/2017; Date of first issue: 09/06/2016)
152	Safety Data Sheet for 3-(Trifluoromethyl)aniline. In: www.thermofisher.com 3, (2020) pp. 11 (Product No.: A15910; Revision Number 2; Revision Date 14-Feb-2020)

Table C.2: Continued

Reference Number	Reference
153	Safety Data Sheet for Eastman (TM) DMCD. In: www.eastman.com 6, (2014) pp. 26 (Revision Date 02/01/2013 Version 2.0)
154	Safety Data Sheet for Eastman 168(TM) non-phthalate plasticizer, >98%. In: www.eastman.com 5, (2017) pp. 12 (Product Number EAN 975786, Revision Date 1/15/2016)
155	Safety Data Sheet for Farnesane. In: https://amyris.com 9, (2015) pp. 10 (Revision date: 29 October 2012, Version: DRAFT)
156	Safety Data Sheet for Jarcol I-24. In: https://www.jarchem.com/ 5, (2019) pp. 21 (Date Revised: 4/24/2019)
157	Safety Data Sheet. Isostearic Acid. In: www.mpbio.com/ 5, (2016) pp. 18 (Product number 02102104. Search for 30399-84-9.)
158	Saftey Data Sheet for N,N,N',N'-Tetramethyl-1,3-propanediamine. In: http://www.fishersci.com 4, (2016) pp. 29 (Revision Date: 10Feb2015; Revision #: 1)
159	Sax, N.I., "Dangerous Properties of Industrial Materials, 5th ed.". VanNostrand Reinhold Company, New York. (1979)
160	SDS for Theophylline. In: http://www.sigmaaldrich.com/safety-center.html 5, (2016) pp. 11
161	Setchkin, N. P., Self-ignition Temperatures of Combustible Liquids, Journal of Research of the National Bureau of Standards, 1954, 53, 49-66
162	Sigma-Aldrich Safety Data Sheet for 1-Methylimidazole. In: https://www.sigmaaldrich.com 5, (2017) pp. 23 (Search by product number "M50834." Version 4.10. Revision Date 7/22/2015.)

Table C.2: Continued

Reference Number	Reference
163	Sigma-Aldrich Safety Data Sheet for 2,4,6-Tris(dimethylaminomethyl)phenol. In: https://www.sigmaaldrich.com 5, (2018) pp. 8 (Search by CAS "90-72-2." Select "SDS." Product Number: T58203. Version 4.6. Revision Date 10/15/2014.)
164	Spatz, M.; Minor, B., "HFO-1234yf Low GWP Refrigerant Update". "http://www2.dupont.com/Refrigerants/en_US/assets/downloads/SmartAutoAC/MAC_Pur Honeywell. 5, (2010) pp. 17
165	Specialty Chem. Products, "Glycol Diethers". Specialty Chem. Corporation Marinette WI. (1988)
166	SPEX CertiPrep Safety Data Sheet for trans-1-ethyl-2-methylcyclopentane. In: https://www.spexcertiprep.com 3, (2016) pp. 3 (Search by CAS "930-90-5." Select "trans-1-Ethyl-2-Methylcyclopentane." Select "Safety Data Sheet.")
167	Steere, N.V., "Handbook of Laboratory Safety, 2nd Ed.". CRC Press Inc., Boca Raton, FL. (1971)
168	Stewart, O.; Minnear, L., "Sulfolane Technical Assistance and Evaluation Report". Oasis Environmental. In: dec.alaska.gov/spar/csp/sites/north-pole-refinery/docs/SulfolaneReportFinal.pdf (2010) (Prepared for: Alaska Department of Environmental Conservation)
169	Strem Safety Data Sheet for Tri-n-butylphosphite. In: https://www.strem.com 2, (2018) pp. 5 (Search CAS# 102-85-2)
170	Technical Data Sheet for 1,6-Hexandiol Diacrylate. "http://www.osha.gov/dts/sltc/methods/partial/pv2133/pv2133.httml". US Department of Labor. Occupational Safety & Health Administration. 05, (2009) pp. 08

Table C.2: Continued

Reference Number	Reference
171	Technical Data Sheet for 2-Ethyl Hexanoic Acid, 99.5%. BASF Corporation. In: http://www.basf.com/usa/intermediates 10, (2005)
172	TERT-BUTYLHYDROQUINONE, >=98.0%. “Material Safety Data Sheet”. Sigma-Aldrich. In: http://www.sigma-aldrich.com 5, 3 (2007)
173	Test Report from Hazards Research Corporation (Rockaway, NJ) to ARCO Chemical Company.
174	Test Report from Safety Consulting Engineers, Inc. (Schaumburg, IL) to ARCO Chemical Company.
175	Tetteh, J.; Metcalfe, E.; Howells, S. L., “Optimisation of Radial Basis and Backpropagation Neural Networks for Modelling Auto-Ignition Temperature by Quantitative-Structure Property Relationships”. In: Chemom. Intell. Lab. Syst. 32, (1996) pp. 177-191
176	ThermoFisher Scientific Safety Data Sheet for Lauryl Methacrylate. In: https://www.fishersci.com 1, (2018) pp. 24 (Search by CAS “142-90-5.” Select “Lauryl methacrylate, 97%, stabilized, ACROS OrganicsTM.” Select “SDS.” Creation Date 01-May-2012. Revision Date 26-May-2017. Revision Number 2.)
177	Tri Iso Octyl Trimellitate. In: www.deltrex.com 5, (2004) pp. May 7, 200 (Issue: May 7)
178	Tributyl Phosphate Information Sheet. In: http://www.microkat.gr/msdspd90-99/Tributyl%20phosphate.htm 9, (2015) pp. 8
179	Triethylsilane, 98%, Safety Data Sheet SIT8330.0. In: https://www.gelest.com 7, (2019) pp. 1 (Search for CAS RN 617-86-7. Date of Issue: 1/9/2015, Version: 1.0)
180	Tryon, G.H., “Fire Protection Handbook, 12th ed.”. National Fire Protection Association, Boston, Massachusetts. (1962)

Table C.2: Continued

Reference Number	Reference
181	Vincoli, J. W., “Risk Management for Hazardous Chemicals Vol. II”. CRC Lewis Publishers, Boca Raton, FL. (1997)
182	Vincoli, J.W., “Risk Management for Hazardous Chemicals”. Lewis Publishers, New York. (1997)
183	Weiss, G., “(book:) Hazardous Chemicals Data Book”. “Hazardous Chemicals Data Book: Second Edition”. Noyes Data Corp. Park Ridge, NJ. (1986)
184	Weiss, G., “Hazardous Chemicals Data Book”. Noyes Data Corporation, Park Ridge, New Jersey. (1980)
185	Workplace Environment Exposure Level - trans-1-chloro-3,3,3-trifluoropropene (1233zd(E)) 2013. Oars Weel. (2015) (Copyright 2013; Website Accessed 5/11/2015)
186	Zabetakis, M.G., “Flammability Characteristics of Combustible Gases and Vapors”. “Bulletin No. 627”. U.S. Bureau of Mines. (1965)
187	Zabetakis, M.G.; Furno, A.L.; Jones, G.W., “Minimum Spontaneous Ignition Temperatures of Combustibles in Air”. In: Ind. Eng. Chem. 46, 10 (1954) pp. 2173-2178

APPENDIX D. PARAMETER SETS AND STATISTICAL RESULTS FOR THE SEATON-REDD AND SEATON-REDD2 METHODS

Table D.1: Groups and Parameter Values from Seaton's Implementation The notation includes the following conventions. C/B is an aromatic carbon, C/d is a double-bonded carbon, CO is a carbonyl group, and C/p is an aromatic carbon with membership in two rings like carbons 9 and 10 in naphthalene. The last four groups do not contribute to molecular structure and act as corrections to existing groups.

Group	A	p	E	C_O
C-(C)/4	119.585	0.312362	2011.67	2
C-(C)/3(H)	66.5058	0.0672858	406.329	2.5
C-(C)/2(C/B)(H)	219.703	0.00822159	34.0775	2.5
C-(C)/2(C/d)(H)	104.53	0.0205878	52.1273	2.5
C-(C)/2(CO)(H)	-120.729	0.0563816	1869.07	2.5
C-(C)/2(H)/2	329.521	0.00994568	254.653	3
C-(C)/2(H)(N)	1017.85	0.00941814	838.78	2.5
C-(C)/2(H)(O)	-73.9528	0.169975	1071.17	2.5
C-(C)(C/B)(H)/2	7346.55	0.00703003	2638.53	3
C-(C)(C/d)(H)/2	811.181	0.680719	2996.78	3
C-(C)(CO)(H)/2	-129.007	0.121179	2406.74	3
C-(C)(CO)(H)(O)	-1834.18	0.0158643	1463.02	2.5
C-(C)(H)/3	216.19	0.0104783	458.563	3.5
C-(C)(H)/2(CL)	405.05	0.0498032	2615.16	2.5
C-(C)(H)/2(N)	8144.37	0.0283757	2989.09	3
C-(C)(H)/2(O)	-24.544	0.246877	431.367	3
C-(C/B)(H)/3	4538.06	0.00477119	2304.65	3.5
C-(C/d)(H)/3	3.17939	0.0272239	29.0713	3.5

Table D.1: Continued

Group	A	p	E	C_O
C-(CO)(H)/3	-132.579	0.359843	2730.32	3.5
C-(H)/3(N)	4303.02	0.014888	2256.88	3.5
C-(H)/3(O)	-360.232	0.013422	7.68462	3.5
C/B-(C)	122.151	0.0202309	672.45	2
C/B-(C/B)	47.1377	0.0912324	905.845	2
C/B-(CO)	65.0188	0.245543	2107.68	2
C/B-(H)	98.7229	0.0109487	0.458586	2.5
C/B-(O)	3578.79	0.000958487	2108.21	2
C/d-(C)/2	285.905	0.0227391	323.767	2
C/d-(C)(H)	5420.8	0.0164575	2177.96	2.5
C/d-(CO)(H)	481.894	0.160459	2853.49	2.5
C/d-(H)/2	1693.45	0.0398333	3000	3
C/d-(H)(O)	299.7	0.409423	1613.73	2.5
CO-(C)/2	3837.32	0.0599739	2998.83	1
CO-(C)(H)	6711.53	0.126881	2637.01	1.5
CO-(C)(O)	1749.7	0.133042	2993.14	1
CO-(C/B)(O)	865.853	0.0134551	1573.58	1
CO-(C/d)(O)	386.496	0.389658	2853.02	1
CO-(H)(O)	185.345	0.202548	2076.37	1.5
C/p-(C/B)/2(C/p)	238.417	0.011072	819.019	2
N-(C)/3	346.171	0.0167043	237.42	0
N-(C)/2(H)	3071.5	0.0350284	2942.74	0.5
N-(C)(H)/2	-2188.13	0.00726061	2383.82	1
N/B,Pyridine-Type N	131.844	0.0103325	1039.79	0
O-(C)/2	8398.26	0.141836	2386.15	-1
O-(C)(C/d)	164.909	0.999023	2292.48	-1
O-(C)(CO)	1189.52	0.148071	2857.63	-1

Table D.1: Continued

Group	A	p	E	C_O
O-(C)(H)	3517.57	0.104911	2973.42	-0.5
O-(C/B)(H)	124.355	0.0106752	1262.81	-0.5
O-(CO)(H)	-3.82764	0.526859	1.7391	-0.5
Cyclopentane Ring	-231.17	0.0921327	1158.6	0
Cyclohexane Ring	-22.4987	0.0960342	39.2632	0
Cyclohexene Ring	84.9321	0.0199416	1355.54	0
Cis Interaction at non-aromatic double bond	439.873	0.0152494	1170.47	0

Table D.2: Special Cases in Seaton's Implementation

Special Case	A	p	E	C_O
One instance of C-(C)/2(H)/2	9991.94	0.00649755	2639.51	3
Two instances of C-(C)/2(H)/2	428.816	0.00935343	422.789	3
One instance of C-(C)(H)/3	753.975	0.0153971	1419.54	3.5
Two instances of C-(C)(H)/3	347.576	0.0129353	837.952	3.5
One instance of C-(C)/3(H)	33.7808	0.151135	476.016	2.5
C-(C)(C/d)(H)/2 if $N_{groups} = 4$	9991.94	0.00649755	2639.51	3

Table D.3: Functional Groups with corresponding indices, SMARTS formulas, oxygen-atom contributions, and group molecular weights used in the Seaton-Redd and Seaton Redd2 methods (Spaces are added to longer SMARTS formulas to allow for line breaks.)

				Group	
Index	Group	SMARTS Formula	C_O	MW	Sum
0	CH3-(C)	`[$([CH3](-[#6]))]`	3.5	15.03	1336
1	CH3-(O)	`[$([CH3](-[#8]))]`	3.5	15.03	79
2	CH3-(N)	`[$([CH3](-[#7]))]`	3.5	15.03	50
3	CH3-(Other)	`[$([CH3](-[Si,P,S,F,Cl,Br,I]))]`	3.5	15.03	141

Table D.3: Continued

Index	Group	SMARTS Formula	C_O	Group MW	Sum
4	CH2-(C,C)	[$([!R;CX4H2](-[#6])(-[#6]))]	3.0	14.03	1658
5	CH2-(C,O)	[$([!R;CX4H2](-[#6])(-[#8]))]	3.0	14.03	434
6	CH2-(C,N)	[$([!R;CX4H2](-[#6])(-[#7]))]	3.0	14.03	120
7	CH2-(C,Other)	[$([!R;CX4H2](-[#6])(-[Si,P,S,F,Cl,Br]))]	3.0	14.03	58
8	CH2-(O,O)	[$([!R;CX4H2](-[#8])(-[#8]))]	3.0	14.03	2
9	CH2-(Other,Other)	[$([!R;CX4H2](-[Si,P,S,F,Cl,Br])(-[Si,P,S,F,Cl,Br]))]	3.0	14.03	1
10	CH	[!R;CX4H]	2.5	13.02	261
11	C	[!R;CX4H0]	2.0	12.01	88
12	rCH2-(C,C)	[$([R;CX4H2](-[#6])(-[#6]))]	3.0	14.03	392
13	rCH2-(C,O)	[$([R;CX4H2](-[#6])(-[#8]))]	3.0	14.03	53
14	rCH2-(C,N)	[$([R;CX4H2](-[#6])(-[#7]))]	3.0	14.03	44
15	rCH2-(C,Other)	[$([R;CX4H2](-[#6])(-[Si,P,S,F,Cl,Br]))]	3.0	14.03	4
16	rCH2-(O,O)	[$([R;CX4H2](-[#8])(-[#8]))]	3.0	14.03	2
17	rCH	[!R0;CX4H]	2.5	13.02	117
18	rC	[!R0;CX4H0]	2.0	12.01	20
19	=CH2	[$([CH2](=[*;!O]))]	3.0	14.03	112
20	=CH-(C)	[$([$([CH](=[*;!O]))](-[#6]))]	2.5	13.02	145
21	=CH-(O)	[$([$([CH](=[*;!O]))](-[#8]))]	2.5	13.02	8
22	=CH-(Other)	[$([$([CH](=[*;!O]))](-[Si,P,S,F,Cl,Br]))]	2.5	13.02	14
23	=C	[$([CH0](=[*;!O]));!$([C](=[N])(=[O]))]	2.0	12.01	48
24	#CH	[$([CH](#[*]))]	2.5	13.02	6
25	#C	[$([CH0](#[*]))]	2.0	12.01	18
26	cH	[cH]	2.5	13.02	1000

Table D.3: Continued

Index	Group	SMARTS Formula	C_O	Group MW	Sum
27	c-(C)	[$([cH0;R1](-[#6]))]	2.0	12.01	249
28	c-(O)	[$([cH0;R1](-[#8]))]	2.0	12.01	44
29	c-(N)	[$([cH0;R1](-[#7]))]	2.0	12.01	49
30	c-(Other)	[$([cH0;R1](-[Si,P,S,F,Cl,Br]))]	2.0	12.01	21
31	c=(c)	[c;R2]	2.0	12.01	34
32	O=CH	[$([CH]=[O])]	1.5	29.02	36
33	O=C-(C,C)	[$([$([#6H0]=[O])](~[#6])(~[#6]))]	1.0	28.01	44
34	O=C-(C,O)	[$([$([#6H0]=[O])](~[#6])(~;!=[#8]))]	1.0	28.01	243
35	O=C-(C,N)	[$([$([#6H0]=[O])](~[#6])(~[#7]))]	1.0	28.01	10
36	O=C-(C,Other)	[$([$([#6H0]=[O])](~[#6])(~[Si,P,S,F,Cl,Br]))]	1.0	28.01	5
37	O=C-(O,O)	[$([$([#6H0]=[O])](~;!=[#8])(~;!=[#8]))]	1.0	28.01	5
38	O=C-(O,Other)	[$([$([#6H0]=[O])](~;!=[#8])(~[Si,P,S,F,Cl,Br]))]	1.0	28.01	2
39	O=C-(N,N)	[$([$([#6H0]=[O])](~[#7])(~[#7]))]	1.0	28.01	2
40	OH	[OH;!$([O]=[*])]	-0.5	17.01	272
41	O-(C,C)	[$([#8H0;!$([O]=[*]);!$([O-]-[N+])](~[#6])(~[#6]))]	-1.0	16.00	350
42	O-(C,O)	[$([#8H0;!$([O]=[*]);!$([O-]-[N+])](~[#6])(~[#8]))]	-1.0	16.00	6
43	O-(C,N)	[$([#8H0;!$([O]=[*]);!$([O-]-[N+])](~[#6])(~[#7]))]	-1.0	16.00	3
44	O-(C,Other)	[$([#8H0;!$([O]=[*]);!$([O-]-[N+])](~[#6])(~[Si,P,S,F,Cl,Br]))]	-1.0	16.00	44

Table D.3: Continued

Index	Group	SMARTS Formula	C_O	Group MW	Sum
45	O-(Other,Other)	[$([#8H0;!$([O]=[*]);!$([O-]-[N+])](~[Si,P,S,F,Cl,Br])(~[Si,P,S,F,Cl,Br]))]	- 1.0	16.00	35
46	=O	[$([O]=[*;!#6;!#7]),O-;!$([O]-[N+](=[O]))]	- 1.0	16.00	15
47	NH2	[NH2;!$([N+](=[O])-[O]);!$([N]-[N])]	1.0	16.02	65
48	NH	[#7H;!$([N+](=[O])-[O]);!$([N]-[N])]	0.5	15.01	51
49	N	[NH0;D3;!$([N+](=[O])-[O]);!$([N]-[N])]	0.0	14.01	32
50	=N	[$([N]=[*]);!$([N+](=[O])-[O]);!$([N]=[C]=[O])]	0.0	14.01	2
51	n	[nH0]	0.0	14.01	18
52	#N	[$([N]#[*])]	0.0	14.01	14
53	NO2	[$([N+](=[O])-[O])]	- 2.0	46.01	27
54	OCN	[$([N](=[C]=[O]))]	1.0	42.02	8
55	SH	[#16H;!$([S]-[S])]	2.5	33.08	7
56	S	[#16H0;!$([S]-[S])]	2.0	32.07	26
57	P	[P]	10.0	30.97	10
58	F	[F]	0.0	19.00	64
59	Cl-(C)	[$([Cl](-[#6]))]	0.0	35.50	92
60	Cl-(Other)	[$([Cl](-[Si,P,S,F,Cl,Br]))]	0.0	35.50	41
61	Br	[Br]	0.0	79.90	15
62	SiH3	[SiH3]	3.5	31.12	1
63	SiH2	[SiH2]	3.0	30.11	2
64	SiH	[SiH]	2.5	29.10	8
65	Si	[SiH0]	2.0	28.09	66

Table D.3: Continued

Index	Group	SMARTS Formula	C_O	Group MW	Sum
66	I	[I]	0.0	126.90	1

The groups given here follow these notation conventions:

- The first-order part of the group is given first including all atoms that contribute to the group's molecular weight.
- The second-order parts to the group, if applicable, are given in a comma-separated list in parentheses after the first-order part and connected with a dash to indicate a single bond. For example, "CH2-(C,N)" represents a methylene group that is attached to a carbon atom and a nitrogen atom such as in ethylamine (CAS No. 75-04-7).
- A lower-case "r" is prepended to an atomic symbol to indicate membership in an aliphatic ring.
- An equals sign ("=") indicates a double bond.
- An octothorpe ("#") indicates a triple bond
- A lower-case chemical symbol (e.g. "c") indicates membership in aromatic rings
- "O=C" represents a carbonyl group
- "Other" in the second-order part indicates connection to any element in the data set that is not carbon, hydrogen, oxygen or nitrogen (i.e., fluorine, chlorine, bromine, iodine, silicon, phosphorus, and sulfur).

Table D.4: Model parameters regressed without a testing set that correspond to the Seaton-Redd method and the indices in Table D.3

Index	A	p	E
0	17426.17886	0.004201346	2537.206383
1	-19998.24968	2.64E-05	442.4629402
2	6474.462321	0.466088959	4832.238838
3	19999.92996	0.999992658	10122.07251
4	461.211662	0.016536307	643.335464
5	19747.90326	0.348220514	5971.241588
6	4068.140244	0.012165772	1756.870476
7	19961.41118	0.230576289	6948.921162
8	19747.90326	0.348220514	5971.241588
9	19961.41118	0.230576289	6948.921162
10	19990.8488	0.046916884	4074.220878
11	17440.20071	0.472877985	6637.022924
12	12930.65467	0.000621293	836.9377542
13	-7.514510711	0.987337183	204.6803023
14	19960.43731	0.002359727	2212.487422
15	19960.43731	0.002359727	2212.487422
16	-7.514510711	0.987337183	204.6803023
17	3648.364349	0.196195662	3622.293122
18	12274.70891	0.000127162	8.014666237
19	8289.349566	0.830096027	5773.679574
20	19621.97609	0.000679887	1176.714455
21	342.6604988	0.975127981	2754.424608
22	19095.4097	0.700081679	5823.783107
23	19926.11382	0.640163865	5597.119994
24	210.8878302	0.991319278	156.1693123
25	-174.8080307	0.973864935	42.7898967

Table D.4: Continued

Index	A	p	E
26	19981.5649	0.070833594	6060.455672
27	19975.9574	0.149801724	5653.534028
28	-500.0115314	0.642629361	4141.073611
29	19787.49098	0.002969105	2244.078942
30	-66.59897448	0.945392141	3455.020751
31	1951.278346	0.246745543	3877.888625
32	9402.884217	0.155359843	4003.810908
33	-19999.9286	0.000164747	0.000770869
34	-19795.93178	0.000206947	1.242861082
35	-3.893524339	0.874961664	160.5215984
36	-3.893524339	0.874961664	160.5215984
37	-19997.96656	0.002891237	1265.806438
38	-3.893524339	0.874961664	160.5215984
39	-3.893524339	0.874961664	160.5215984
40	19889.43548	0.502392388	6951.256998
41	19930.57217	0.003359453	1718.16578
42	19921.96101	0.062975354	1923.886405
43	-19895.60577	0.996758949	18.61350291
44	19879.853	0.000336872	2130.502054
45	-62.09269011	0.157538297	0.002356374
46	-1964.84124	0.121430252	2097.828693
47	-19999.9442	6.30E-05	1.08103338
48	19963.92127	0.993365744	8563.928957
49	9950.545032	0.085599827	3179.735051
50	19319.92717	0.00294474	1152.101145
51	19996.17537	0.999950541	7430.154688
52	680.9798926	0.994618999	1139.802843

Table D.4: Continued

Index	A	p	E
53	-3.102526614	0.877619063	294.26773
54	-19834.51784	0.000649634	676.9161973
55	19999.17521	0.999982721	4446.474039
56	19951.58361	0.119126223	3263.254572
57	19999.98625	1	5286.938118
58	-748.687348	0.286080871	3248.683887
59	-19983.15066	6.89E-06	3.464088896
60	-19885.09729	0.067720093	3528.478326
61	19999.87942	0.431841319	7359.063655
62	19997.07099	0.171475384	3405.902482
63	19997.07099	0.171475384	3405.902482
64	19997.07099	0.171475384	3405.902482
65	19997.07099	0.171475384	3405.902482
66	15971.12863	0.972999277	5631.987637

Table D.5: Model parameters regressed with an 80-20 training-testing split that correspond to the Seaton-Redd method and the indices in Table D.3

Index	A	p	E
0	19798.31297	0.014345961	3505.355572
1	-8368.539292	0.000618118	1164.529502
2	13618.51507	0.331599018	4983.465794
3	630.0214589	0.334910216	4365.851862
4	515.2177127	0.017384533	694.4966132
5	19570.249	0.255949936	5751.614601
6	19799.40059	0.02340341	3033.158659
7	19987.38682	0.238025859	7455.435352

Table D.5: Continued

Index	A	p	E
8	19570.249	0.255949936	5751.614601
9	19987.38682	0.238025859	7455.435352
10	15904.70727	0.044316962	3806.013544
11	2232.54304	0.339709297	4420.284466
12	19999.807	0.003870793	2173.796894
13	-61.55963237	1	1265.18602
14	19990.93295	0.022733725	3704.818205
15	19990.93295	0.022733725	3704.818205
16	-61.55963237	1	1265.18602
17	1781.8961	0.470374434	3318.114389
18	1037.863698	0.804145208	3529.817295
19	19933.44331	0.998725597	6628.271818
20	4175.026776	0.103657941	3287.424485
21	316.9042434	1	2490.306333
22	19997.70321	0.755753002	5861.211886
23	19994.45137	0.675594042	5565.476895
24	19979.24812	0.998350703	1830.8467
25	-19943.55177	0.047972569	0.042145599
26	19991.78524	0.066303612	6251.432934
27	19975.88053	0.090415322	5330.158766
28	-321.7234491	0.999999997	3870.176764
29	19987.8368	0.003173584	2144.621723
30	-310.0972307	0.999998548	5043.927355
31	17562.25144	0.311178708	5844.887996
32	4572.578063	0.366092074	3920.511396
33	-19996.07249	0.000219307	0.3861156
34	-19999.98264	0.000246527	0.040839094

Table D.5: Continued

Index	A	p	E
35	-19999.8125	0.000175015	0.001768398
36	-19999.8125	0.000175015	0.001768398
37	-19964.28728	0.000630802	0.0005156
38	-19999.8125	0.000175015	0.001768398
39	-19999.8125	0.000175015	0.001768398
40	19668.16181	0.268442115	6372.093158
41	4040.489933	0.032662822	2034.106271
42	19994.12894	0.096811718	2064.726921
43	-19103.46332	0.266361016	5612.569019
44	18948.63738	0.593562923	4676.549307
45	-8143.238298	0.033416463	2153.999881
46	-18845.69748	0.009668166	1955.205815
47	-19973.10332	0.000134483	215.9057376
48	-109.0175081	0.304876737	4837.741983
49	1488.504427	0.320076388	2769.386503
50	19999.99993	0.98840206	3569.071
51	19999.99406	0.999973271	7472.207417
52	19681.72996	0.052899159	69.24872984
53	-21.24277811	0.561935799	1357.269013
54	-19845.70289	0.000896688	644.0207832
55	19998.71135	0.991019219	4263.894646
56	12337.88945	0.064564646	2674.638809
57	19997.83101	0.999687904	6706.906101
58	-941.008749	0.190596204	3118.847488
59	19999.96358	0.999990002	13046.91684
60	-11183.53315	0.011260054	2344.065073
61	19902.7624	0.320886449	7635.385226

Table D.5: Continued

Index	A	p	E
62	19830.02774	0.021549116	2278.676762
63	19830.02774	0.021549116	2278.676762
64	19830.02774	0.021549116	2278.676762
65	19830.02774	0.021549116	2278.676762
66	19523.38605	0.20245412	4838.840312

Table D.6: Model parameters regressed without a testing set that correspond to the Seaton-Redd2 method and the indices in Table D.3

Index	A	p	E	d
0	12413.98	0.038865	4006.151	1.448129
1	-7840.62	0.166274	3964.311	3816.241
2	18150.44	0.654211	6632.609	1.638013
3	19997.67	0.980925	9527.6	3.613118
4	19868.2	0.017504	788.8135	0.029425
5	7879.299	0.067536	5440.739	9.55695
6	19999.67	0.299333	5996.577	102.072
7	15776.48	0.063108	6397.101	10.40795
8	7879.299	0.067536	5440.739	9.55695
9	15776.48	0.063108	6397.101	10.40795
10	2234.599	0.082342	3977.343	5.569628
11	-13135.5	0.398586	2811.333	0.007631
12	19625.18	0.000186	1657.077	17.8124
13	-2458.81	0.999124	27.57515	0.001234
14	19926.94	0.50802	69.77079	3.52E-05
15	19926.94	0.50802	69.77079	3.52E-05
16	-2458.81	0.999124	27.57515	0.001234

Table D.6: Continued

Index	A	p	E	d
17	10663.13	0.350546	6139.148	31.73291
18	17115.55	0.044701	1.774775	9.32E+08
19	15177.26	0.013695	4509.048	2392.774
20	16187.49	0.433152	1680.662	0.006833
21	19877.96	0.979171	11.86867	0.000156
22	19474.72	0.597735	4304.441	1674.799
23	15992.6	0.706608	6412.638	7.228658
24	7315.056	0.149684	2776.686	854.5203
25	-19673.2	0.676689	2.040653	1739229
26	15950.2	0.057284	7789.188	46.8376
27	17611.76	0.170439	8474.75	85.4819
28	-20000	0.852581	6.96E-13	5087114
29	8398.977	0.12831	504.3922	0.003481
30	18848.83	0.249505	2101.993	0.002528
31	19436.97	0.977592	4245.486	2852.406
32	4892.203	0.557194	3619.875	0.352591
33	-19983.7	0.999574	52.53753	0.00024
34	-19985.3	3.55E-05	43.65165	18.99098
35	-16864.1	0.993832	1.443416	5584408
36	-16864.1	0.993832	1.443416	5584408
37	-19431.4	0.000701	1034.808	68.16238
38	-16864.1	0.993832	1.443416	5584408
39	-16864.1	0.993832	1.443416	5584408
40	19896.61	0.290716	6874.884	6.418428
41	4463.948	0.032885	3414.164	19.15163
42	18152.21	0.009734	1990.046	41.22982
43	-1921.41	0.15469	7166.062	1.274614

Table D.6: Continued

Index	A	p	E	d
44	-12009.2	0.825408	13.74303	0.000742
45	16937.25	0.218268	1752.29	298518.4
46	-19924.6	2.78E-05	10.17549	88.51232
47	19999.37	0.0604	2215.566	229130.6
48	19726.61	0.000854	10.29338	0.162843
49	7468.925	0.022651	2144.335	1.324299
50	19661.49	0.999997	0.758003	4168406
51	19021.18	0.999986	8078.596	24.37753
52	-19999.3	0.016964	0.00617	880371.1
53	19999.71	0.003159	4934.913	33.46925
54	-19993.3	0.00619	7.53078	38238.28
55	19021.11	0.955672	4289.314	1504.531
56	13073.25	0.072048	1414.639	0.059999
57	19997.49	0.122096	4874.43	2498.74
58	-19996.7	0.284574	1830.857	0.00218
59	-13051.7	0.872518	3198.116	108780.4
60	-19793.5	0.002341	112.5835	3917.756
61	19810.85	0.634647	8812.438	2.602776
62	11282.55	0.635476	3248.766	0.405652
63	11282.55	0.635476	3248.766	0.405652
64	11282.55	0.635476	3248.766	0.405652
65	11282.55	0.635476	3248.766	0.405652
66	19741.22	0.990376	6361.223	5.758281

Table D.7: Model parameters regressed with an 80-20 training-testing split that correspond to the Seaton-Redd2 method and the indices in Table D.3

Index	A	p	E	d
0	3775.719	0.206712	5231.779	102.4755
1	-1712.2	0.306995	3955.115	1022.797
2	12560.69	0.382774	6201.211	9.219352
3	-19684	0.236488	357.7131	1034918
4	20000	0.000635	1842.886	5.722682
5	-19937.6	0.999986	19.50345	6.66E-05
6	19998.24	0.318757	5467.622	248.0369
7	19645.71	0.032559	6699.289	84.42737
8	-19937.6	0.999986	19.50345	6.66E-05
9	19645.71	0.032559	6699.289	84.42737
10	4013.617	0.246597	5498.093	21.28306
11	-19999.7	0.000505	31.54028	0.170557
12	8695.082	0.016691	3860.141	76.0263
13	-20000	0.999962	0.018342	1856188
14	18530.41	0.455847	6346.141	4.815467
15	18530.41	0.455847	6346.141	4.815467
16	-20000	0.999962	0.018342	1856188
17	20000	0.998391	3.64E-05	4.52E-05
18	17371.41	0.995867	91.60631	18282887
19	19973.25	0.537916	8270.018	12.99105
20	15036.05	0.273253	110.6731	0.000853
21	18653.27	8.00E-05	517.8352	18.15832
22	19551.77	0.512349	5750.988	199.9302
23	19767.57	0.901606	5717.801	575.4745
24	17753.18	0.268598	4752.296	87.7362
25	-19986.3	9.28E-05	0.058717	232.5518

Table D.7: Continued

Index	A	p	E	d
26	19943.88	0.044141	7580.627	168.8427
27	-19875.4	0.42122	7.549808	6447233
28	-9932.3	0.536153	675.0027	307713.9
29	19999.93	0.00089	0.017109	0.020154
30	-15079.4	0.519965	1236.51	243871.3
31	-19562.1	0.022033	64.97479	0.000739
32	17519.67	0.614726	3823.104	0.174001
33	-20000	1	17.65849	5874474
34	-19953.2	6.72E-05	57.97367	12.96312
35	-19590.8	0.999882	19.40181	0.000109
36	-19590.8	0.999882	19.40181	0.000109
37	-19858.9	0.000135	1.014646	17.99194
38	-19590.8	0.999882	19.40181	0.000109
39	-19590.8	0.999882	19.40181	0.000109
40	18003.42	0.321161	6208.453	10.59525
41	1072.948	0.057266	2544.6	21.57971
42	19169.62	0.022744	2206.547	44.90624
43	-6367.45	0.856309	6271.165	1.05559
44	-19873.6	0.930972	14.43712	0.002311
45	18413.03	0.236833	2836.149	32549.26
46	-19828.4	0.695123	234.2018	1280613
47	19658.36	0.086826	6486.606	162.8466
48	19993.01	0.002326	457.2375	0.045045
49	19341.87	0.000341	0.027743	4921.117
50	19999	0.996333	0.062093	3350405
51	18926.58	0.999552	8399.066	4.966299
52	19964.73	0.970111	9556.526	3.412378

Table D.7: Continued

Index	A	p	E	d
53	19989.74	0.015844	4654.645	13.2758
54	-19999.9	7.33E-05	1.465514	13.46688
55	16463.4	0.131372	3484.335	475.9444
56	19727.94	0.159621	1954.9	0.052316
57	19983.23	0.271326	5071.172	513.153
58	19999.67	0.999472	9440.419	169.7523
59	19453.5	0.347929	7737.966	44.7968
60	-19911.5	0.001293	171.5867	1451.15
61	19999.99	0.347715	7124.649	25.90274
62	15310.4	0.551682	4060.077	2.055923
63	15310.4	0.551682	4060.077	2.055923
64	15310.4	0.551682	4060.077	2.055923
65	15310.4	0.551682	4060.077	2.055923
66	19164.79	0.260148	5452.386	9.274048

Table D.8: Statistical Performance Metrics for all of the Parameter Sets

	AAD	$ARD(\%)$	$Bias$	$max(D)$	R^2
Seaton-Redd					
No Testing Set	47.14	7.64	0.49	281.87	0.71
80-20 Training Set	47.6	7.69	0.27	251.54	0.71
80-20 Testing Set	51.2	8.31	3.84	229.74	0.68
Seaton-Redd2					
No Testing Set	44.05	7.18	0.70	190.35	0.75
80-20 Training Set	44.66	7.20	0.09	223.69	0.74
80-20 Testing Set	49.25	7.74	-5.09	233.46	0.69

APPENDIX E. TABLES OF AIT VALUES REFERENCED IN CHAPTER 5

Table E.1: Recommended AIT Values presented in this work, grouped and sorted by chemical family. Carbon number (C#) refers to the carbon number used to plot the various AIT values in their respective figures. Under "Data Type", "Exp" and "Pred" refer to experimental and predicted values respectively. A single asterisk ("*") indicates that the value was measured as part of this work per ASTM E659 but at an ambient pressure of ˜0.85 atm. A double asterisk ("**") indicates that the AIT value was inferred from flash points, AIT family trends, and nearest members of the family.

CAS No.	Compound Name	Chemical Family	C#	AIT (K)	Data Type	Reference
74-82-8	methane	n-alkanes	1	868	Exp	[21]
74-84-0	ethane	n-alkanes	2	788	Exp	[12]
74-98-6	propane	n-alkanes	3	743	Exp	[21]
106-97-8	n-butane	n-alkanes	4	645	Exp	[18]
109-66-0	n-pentane	n-alkanes	5	531	Exp	[10]
110-54-3	n-hexane	n-alkanes	6	500	Exp	[17]
142-82-5	n-heptane	n-alkanes	7	486	Exp	[17]
111-65-9	n-octane	n-alkanes	8	479	Exp	[17]

Table E.1: Continued

CAS No.	Compound Name	Chemical Family	C#	AIT (K)	Data Type	Reference
111-84-2	n-nonane	n-alkanes	9	478	Exp	[17]
124-18-5	n-decane	n-alkanes	10	474	Exp	[17]
1120-21-4	n-undecane	n-alkanes	11	472	Exp	[75]
112-40-3	n-dodecane	n-alkanes	12	473	Exp	[75]
629-50-5	n-tridecane	n-alkanes	13	473	Pred	This Work
629-59-4	n-tetradecane	n-alkanes	14	473	Exp	[21]
629-62-9	n-pentadecane	n-alkanes	15	473	Pred	This Work
544-76-3	n-hexadecane	n-alkanes	16	474	Exp	This Work
629-78-7	n-heptadecane	n-alkanes	17	475	Pred	This Work
593-45-3	n-octadecane	n-alkanes	18	477	Pred	This Work
629-92-5	n-nonadecane	n-alkanes	19	478	Exp	[21]
112-95-8	n-eicosane	n-alkanes	20	480	Pred	This Work
629-94-7	n-heneicosane	n-alkanes	21	482	Pred	This Work

Table E.1: Continued

CAS No.	Compound Name	Chemical Family	C#	AIT (K)	Data Type	Reference
629-97-0	n-docosane	n-alkanes	22	485	Pred	This Work
638-67-5	n-tricosane	n-alkanes	23	493	Pred	This Work
646-31-1	n-tetracosane	n-alkanes	24	499	Pred	This Work
629-99-2	n-pentacosane	n-alkanes	25	505	Exp	This Work
74-85-1	ethylene	1-alkenes	2	698	Exp	[21]
115-07-1	propylene	1-alkenes	3	728	Exp	[21]
106-98-9	1-butene	1-alkenes	4	620	Exp	[72]
109-67-1	1-pentene	1-alkenes	5	553	Exp	[21]
592-41-6	1-hexene	1-alkenes	6	526	Exp	[17]
592-76-7	1-heptene	1-alkenes	7	514	Pred	This Work **
111-66-0	1-octene	1-alkenes	8	503	Exp	[17]
124-11-8	1-nonene	1-alkenes	9	503	Pred	This Work **
872-05-9	1-decene	1-alkenes	10	505	Exp	[72]

Table E.1: Continued

CAS No.	Compound Name	Chemical Family	C#	AIT (K)	Data Type	Reference
821-95-4	1-undecene	1-alkenes	11	503	Pred	This Work **
112-41-4	1-dodecene	1-alkenes	12	498	Exp	[21]
2437-56-1	1-tridecene	1-alkenes	13	502	Pred	Seaton-Redd2 Chapter 6
1120-36-1	1-tetradecene	1-alkenes	14	500	Exp	[72]
13360-61-7	1-pentadecene	1-alkenes	15	499	Pred	Seaton-Redd2 Chapter 6
629-73-2	1-hexadecene	1-alkenes	16	513	Exp	[21]
6765-39-5	1-heptadecene	1-alkenes	17	518	Pred	This Work **
112-88-9	1-octadecene	1-alkenes	18	523	Exp	[21]
74-86-2	acetylene	1-alkynes	2	578	Exp	[21]
74-99-7	methylacetylene	1-alkynes	3	613	Exp	[63]
107-00-6	ethylacetylene	1-alkynes	4	560	Pred	This Work **
627-19-0	1-pentyne	1-alkynes	5	530	Pred	This Work **
693-02-7	1-hexyne	1-alkynes	6	515	Pred	This Work **

Table E.1: Continued

CAS No.	Compound Name	Chemical Family	C#	AIT (K)	Data Type	Reference
628-71-7	1-heptyne	1-alkynes	7	505	Pred	This Work **
629-05-0	1-octyne	1-alkynes	8	498	Exp	[21]
3452-09-3	1-nonyne	1-alkynes	9	498	Pred	This Work **
764-93-2	1-decyne	1-alkynes	10	499	Exp	This Work
75-19-4	cyclopropane	cycloalkanes	3	768	Exp	[21]
287-23-0	cyclobutane	cycloalkanes	4	700	Pred	This Work **
287-92-3	cyclopentane	cycloalkanes	5	593	Exp	[81]
110-82-7	cyclohexane	cycloalkanes	6	519	Exp	[10]
291-64-5	cycloheptane	cycloalkanes	7	510	Exp	This Work
292-64-8	cyclooctane	cycloalkanes	8	517	Exp	This Work
293-96-9	cyclodecane	cycloalkanes	10	490	Pred	AITMP™ 95C Chapter 6
71-43-2	benzene	n-alkylbenzenes	0	821	Exp	[17]
108-88-3	toluene	n-alkylbenzenes	1	792	Exp	[10]

Table E.1: Continued

CAS No.	Compound Name	Chemical Family	C#	AIT (K)	Data Type	Reference
100-41-4	ethylbenzene	n-alkylbenzenes	2	705	Exp	[12]
103-65-1	n-propylbenzene	n-alkylbenzenes	3	723	Exp	[81]
104-51-8	n-butylbenzene	n-alkylbenzenes	4	683	Exp	[21]
538-68-1	n-pentylbenzene	n-alkylbenzenes	5	550	Pred	This Work **
1077-16-3	n-hexylbenzene	n-alkylbenzenes	6	520	Pred	This Work **
1078-71-3	n-heptylbenzene	n-alkylbenzenes	7	505	Pred	This Work **
2189-60-8	n-octylbenzene	n-alkylbenzenes	8	495	Pred	This Work **
1081-77-2	n-nonylbenzene	n-alkylbenzenes	9	491	Pred	This Work **
104-72-3	n-decylbenzene	n-alkylbenzenes	10	491	Pred	This Work **
6742-54-7	n-undecylbenzene	n-alkylbenzenes	11	491	Exp	This Work
123-01-3	n-dodecylbenzene	n-alkylbenzenes	12	491	Pred	This Work **
123-02-4	n-tridecylbenzene	n-alkylbenzenes	13	491	Pred	This Work **
1459-10-5	n-tetradecylbenzene	n-alkylbenzenes	14	491	Pred	This Work **

Table E.1: Continued

CAS No.	Compound Name	Chemical Family	C#	AIT (K)	Data Type	Reference
2131-18-2	n-pentadecylbenzene	n-alkylbenzenes	15	492	Pred	This Work **
1459-09-2	n-hexadecylbenzene	n-alkylbenzenes	16	493	Pred	This Work **
14752-75-1	n-heptadecylbenzene	n-alkylbenzenes	17	495	Pred	This Work **
4445-07-2	n-octadecylbenzene	n-alkylbenzenes	18	500	Pred	This Work **
74-89-5	methylamine	n-primary amines	1	703	Exp	[21]
75-04-7	ethylamine	n-primary amines	2	658	Exp	[14]
107-10-8	n-propylamine	n-primary amines	3	593	Exp	[21]
109-73-9	n-butylamine	n-primary amines	4	583	Exp	[21]
110-58-7	n-pentylamine	n-primary amines	5	553	Pred	Seaton-Redd2 Chapter 6
111-26-2	n-hexylamine	n-primary amines	6	543	Exp	[21]
111-68-2	n-heptylamine	n-primary amines	7	528	Pred	Seaton-Redd2 Chapter 6
111-86-4	n-octylamine	n-primary amines	8	524	Exp	Cited in: Appendix C
112-20-9	n-nonylamine	n-primary amines	9	514	Pred	Seaton-Redd2 Chapter 6

Table E.1: Continued

CAS No.	Compound Name	Chemical Family	C#	AIT (K)	Data Type	Reference
2016-57-1	n-decylamine	n-primary amines	10	509	Pred	Seaton-Redd2 Chapter 6
7307-55-3	undecylamine	n-primary amines	11	505	Pred	Seaton-Redd2 Chapter 6
124-22-1	n-dodecylamine	n-primary amines	12	502	Pred	Seaton-Redd2 Chapter 6
2016-42-4	n-tetradecylamine	n-primary amines	14	498	Pred	Seaton-Redd2 Chapter 6
67-56-1	methanol	1-alcohols	1	701	Exp	[10]
64-17-5	ethanol	1-alcohols	2	630	Exp	[99]
71-23-8	1-propanol	1-alcohols	3	653	Exp	[100]
71-36-3	1-butanol	1-alcohols	4	587	Exp	[100]
71-41-0	1-pentanol	1-alcohols	5	568	Exp	[21]
111-27-3	1-hexanol	1-alcohols	6	558	Exp	[21]
111-70-6	1-heptanol	1-alcohols	7	543	Exp	[21]
111-87-5	1-octanol	1-alcohols	8	543	Exp	[21]
143-08-8	1-nonanol	1-alcohols	9	533	Exp	[21]

Table E.1: Continued

CAS No.	Compound Name	Chemical Family	C#	AIT (K)	Data Type	Reference
112-30-1	1-decanol	1-alcohols	10	523	Exp	[21]
112-42-5	1-undecanol	1-alcohols	11	523	Pred	Seaton-Redd2 Chapter 6
112-53-8	1-dodecanol	1-alcohols	12	523	Exp	[21]
112-70-9	1-tridecanol	1-alcohols	13	516	Pred	Seaton-Redd2 Chapter 6
112-72-1	1-tetradecanol	1-alcohols	14	513	Exp	[21]
629-76-5	1-pentadecanol	1-alcohols	15	512	Pred	This Work **
36653-82-4	1-hexadecanol	1-alcohols	16	511	Exp	This Work *
1454-85-9	1-heptadecanol	1-alcohols	17	513	Pred	This Work **
112-92-5	1-octadecanol	1-alcohols	18	515	Pred	This Work **
1454-84-8	1-nonadecanol	1-alcohols	19	518	Pred	This Work **
629-96-9	1-eicosanol	1-alcohols	20	520	Pred	This Work **
15594-90-8	1-heneicosanol	1-alcohols	21	522	Pred	This Work **
661-19-8	1-docosanol	1-alcohols	22	524	Exp	This Work *

Table E.1: Continued

CAS No.	Compound Name	Chemical Family	C#	AIT (K)	Data Type	Reference
107-21-1	ethylene glycol	glycols	2	671	Exp	[10]
504-63-2	1,3-propylene glycol	glycols	3	673	Exp	[21]
110-63-4	1,4-butanediol	glycols	4	643	Exp	[21]
111-29-5	1,5-pentanediol	glycols	5	603	Exp	[21]
629-11-8	1,6-hexanediol	glycols	6	593	Exp	[21]
540-67-0	methyl ethyl ether	methyl ethers	3	463	Exp	[21]
115-10-6	dimethyl ether	symmetric ethers	2	513	Exp	[21]
60-29-7	diethyl ether	symmetric ethers	4	443	Exp	[21]
111-43-3	di-n-propyl ether	symmetric ethers	6	452	Exp	[75]
142-96-1	di-n-butyl ether	symmetric ethers	8	448	Exp	[21]
693-65-2	di-n-pentyl ether	symmetric ethers	10	444	Exp	[12]
112-58-3	di-n-hexyl ether	symmetric ethers	12	460	Exp	[12]
629-64-1	di-n-heptyl ether	symmetric ethers	14	470	Pred	This Work **

Table E.1: Continued

CAS No.	Compound Name	Chemical Family	C#	AIT (K)	Data Type	Reference
629-82-3	di-n-octyl ether	symmetric ethers	16	480	Exp	[75]
50-00-0	formaldehyde	n-alkanals	1	693	Exp	[21]
75-07-0	acetaldehyde	n-alkanals	2	413	Exp	[21]
123-38-6	propanal	n-alkanals	3	467	Exp	[75]
123-72-8	butanal	n-alkanals	4	478	Exp	[75]
110-62-3	pentanal	n-alkanals	5	479	Exp	[75]
66-25-1	hexanal	n-alkanals	6	472	Exp	[75]
111-71-7	heptanal	n-alkanals	7	470	Exp	Cited in: Appendix C
124-13-0	octanal	n-alkanals	8	466	Pred	AITMP™ 95C Chapter 6
124-19-6	nonanal	n-alkanals	9	469	Exp	Cited in: Appendix C
112-31-2	decanal	n-alkanals	10	468	Exp	[21]
112-44-7	undecanal	n-alkanals	11	462	Pred	AITMP™ 95C Chapter 6
112-54-9	dodecanal	n-alkanals	12	461	Pred	AITMP™ 95C Chapter 6

Table E.1: Continued

CAS No.	Compound Name	Chemical Family	C#	AIT (K)	Data Type	Reference
10486-19-8	tridecanal	n-alkanals	13	462	Pred	AITMP™ 95C Chapter 6
78-84-2	2-methylpropanal	branched alkanals	3.00	438	Exp	[21]
96-17-3	2-methylbutyraldehyde	branched alkanals	3.67	463	Exp	[21]
123-05-7	2-ethylhexanal	branched alkanals	5.67	453	Exp	[21]
67-64-1	acetone	2-alkanones	1	764	Exp	[10]
78-93-3	methyl ethyl ketone	2-alkanones	2	749	Exp	[75]
107-87-9	2-pentanone	2-alkanones	2	720	Exp	[75]
591-78-6	2-hexanone	2-alkanones	3	693	Exp	[75]
110-43-0	2-heptanone	2-alkanones	4	580	Exp	[72]
111-13-7	2-octanone	2-alkanones	5	572	Exp	[72]
821-55-6	2-nonanone	2-alkanones	6	504	Exp	This Work
96-22-0	3-pentanone	3-alkanones	2	728	Exp	[75]
589-38-8	3-hexanone	3-alkanones	3	707	Pred	This Work **

Table E.1: Continued

CAS No.	Compound Name	Chemical Family	C#	AIT (K)	Data Type	Reference
106-35-4	3-heptanone	3-alkanones	4	686	Exp	[72]
106-68-3	3-octanone	3-alkanones	5	631	Exp	[72]
925-78-0	3-nonanone	3-alkanones	6	609	Exp	[72]
123-19-3	4-heptanone	4-alkanones	3	693	Exp	[72]
589-63-9	4-octanone	4-alkanones	4	620	Pred	Cited in: Appendix C
502-56-7	5-nonanone	4-alkanones	4	603	Exp	[21]
4485-09-0	4-nonanone	4-alkanones	5	579	Pred	Cited in: Appendix C
927-49-1	diamyl ketone	5-alkanones	5	540	Exp	[75]
64-18-6	formic acid	n-carboxylic acids	1	793	Exp	[21]
64-19-7	acetic acid	n-carboxylic acids	2	761	Exp	[10]
79-09-4	propionic acid	n-carboxylic acids	3	713	Exp	[21]
107-92-6	n-butyric acid	n-carboxylic acids	4	698	Exp	[101]
109-52-4	n-pentanoic acid	n-carboxylic acids	5	648	Exp	[21]

Table E.1: Continued

CAS No.	Compound Name	Chemical Family	C#	AIT (K)	Data Type	Reference
142-62-1	n-hexanoic acid	n-carboxylic acids	6	603	Exp	[21]
111-14-8	n-heptanoic acid	n-carboxylic acids	7	528	Exp	[81]
124-07-2	n-octanoic acid	n-carboxylic acids	8	518	Exp	[21]
112-05-0	n-nonanoic acid	n-carboxylic acids	9	518	Exp	Cited in: Appendix C
334-48-5	n-decanoic acid	n-carboxylic acids	10	503	Exp	[21]
112-37-8	n-undecanoic acid	n-carboxylic acids	11	503	Pred	This Work **
143-07-7	n-dodecanoic acid	n-carboxylic acids	12	503	Exp	[21]
638-53-9	n-tridecanoic acid	n-carboxylic acids	13	505	Pred	This Work **
544-63-8	n-tetradecanoic acid	n-carboxylic acids	14	508	Exp	[21]
1002-84-2	n-pentadecanoic acid	n-carboxylic acids	15	510	Pred	This Work **
57-10-3	n-hexadecanoic acid	n-carboxylic acids	16	513	Exp	[21]
506-12-7	n-heptadecanoic acid	n-carboxylic acids	17	510	Pred	This Work **
57-11-4	n-octadecanoic acid	n-carboxylic acids	18	510	Exp	This Work

Table E.1: Continued

CAS No.	Compound Name	Chemical Family	C#	AIT (K)	Data Type	Reference
646-30-0	n-nonadecanoic acid	n-carboxylic acids	19	510	Pred	This Work **
506-30-9	n-eicosanic acid	n-carboxylic acids	20	510	Pred	This Work **
144-62-7	oxalic acid	dicarboxylic acids	2	799	Pred	Seaton-Redd2 Chapter 6
141-82-2	malonic acid	dicarboxylic acids	3	754	Pred	Seaton-Redd2 Chapter 6
110-15-6	succinic acid	dicarboxylic acids	4	733	Pred	This Work **
110-94-1	glutaric acid	dicarboxylic acids	5	713	Pred	This Work **
124-04-9	adipic acid	dicarboxylic acids	6	693	Exp	[21]
111-16-0	pimelic acid	dicarboxylic acids	7	686	Pred	Seaton-Redd2 Chapter 6
505-48-6	suberic acid	dicarboxylic acids	8	673	Pred	Seaton-Redd2 Chapter 6
123-99-9	azelaic acid	dicarboxylic acids	9	659	Exp	This Work
111-20-6	sebacic acid	dicarboxylic acids	10	650	Pred	Seaton-Redd2 Chapter 6
693-23-2	dodecanedioic acid	dicarboxylic acids	12	631	Pred	Seaton-Redd2 Chapter 6
821-38-5	tetradecanedioic acid	dicarboxylic acids	14	615	Pred	Seaton-Redd2 Chapter 6

Table E.1: Continued

CAS No.	Compound Name	Chemical Family	C#	AIT (K)	Data Type	Reference
107-31-3	methyl formate	methyl esters	1	723	Exp	[21]
79-20-9	methyl acetate	methyl esters	2	748	Exp	[21]
554-12-1	methyl propionate	methyl esters	3	728	Exp	[21]
623-42-7	methyl butyrate	methyl esters	4	728	Exp	[21]
624-24-8	methyl valerate	methyl esters	5	693	Exp	[21]
106-70-7	methyl caproate	methyl esters	6	528	Exp	[21]
106-73-0	methyl enanthate	methyl esters	7	509	Pred	This Work **
111-11-5	methyl caprylate	methyl esters	8	490	Pred	This Work **
1731-84-6	methyl pelargonate	methyl esters	9	488	Pred	This Work **
110-42-9	methyl caprate	methyl esters	10	486	Pred	This Work **
111-81-9	methyl undecylate	methyl esters	11	486	Pred	This Work **
111-82-0	methyl laurate	methyl esters	12	486	Exp	This Work
1731-88-0	methyl n-tridecanoate	methyl esters	13	486	Pred	This Work **

Table E.1: Continued

CAS No.	Compound Name	Chemical Family	C#	AIT (K)	Data Type	Reference
124-10-7	methyl myristate	methyl esters	14	486	Pred	This Work **
7132-64-1	methyl n-pentadecanoate	methyl esters	15	489	Pred	This Work **
112-39-0	methyl palmitate	methyl esters	16	492	Pred	This Work **
1731-92-6	methyl margarate	methyl esters	17	495	Pred	This Work **
112-61-8	methyl stearate	methyl esters	18	498	Exp	This Work
109-94-4	ethyl formate	ethyl esters	1	668	Pred	This Work **
141-78-6	ethyl acetate	ethyl esters	2	744	Exp	[75]
105-37-3	ethyl propionate	ethyl esters	3	729	Exp	[75]
105-54-4	ethyl butyrate	ethyl esters	4	713	Exp	[75]
539-82-2	ethyl valerate	ethyl esters	5	690	Pred	This Work **
123-66-0	ethyl caproate	ethyl esters	6	520	Pred	This Work **
106-30-9	ethyl enanthate	ethyl esters	7	500	Pred	This Work **
106-32-1	ethyl caprylate	ethyl esters	8	486	Pred	This Work **

Table E.1: Continued

CAS No.	Compound Name	Chemical Family	C#	AIT (K)	Data Type	Reference
123-29-5	ethyl pelargonate	ethyl esters	9	486	Pred	This Work **
110-38-3	ethyl caprate	ethyl esters	10	486	Pred	This Work **
627-90-7	ethyl undecylate	ethyl esters	11	484	Pred	This Work **
106-33-2	ethyl laurate	ethyl esters	12	483	Exp	This Work
28267-29-0	ethyl n-tridecanoate	ethyl esters	13	486	Pred	This Work **
124-06-1	ethyl myristate	ethyl esters	14	489	Pred	This Work **
41114-00-5	ethyl n-pentadecanoate	ethyl esters	15	492	Pred	This Work **
628-97-7	ethyl palmitate	ethyl esters	16	495	Pred	This Work **
14010-23-2	ethyl margarate	ethyl esters	17	502	Pred	This Work **
111-61-5	ethyl stearate	ethyl esters	18	509	Exp	This Work
123-95-5	n-butyl stearate	n-butyl esters	18	513	Exp	[21]
57-13-6	urea	polyfunctional	1	>800	Exp	This Work
140-10-3	*trans*-cinnamic acid	polyfunctional	9	721	Exp	This Work

Table E.2: Additional AIT measurements per ASTM E659 at altitude (ambient pressure = ˜ 0.85 atm) for 1-alcohols as part of this work and a previous work This Work

CAS No.	name	C#	AIT (K)
36653-82-4	1-hexadecanol	16	511
661-19-8	1-docosanol	22	524

Table E.3: Predicted AIT values from the *n*-alkylbenzene chemical family that constitute the recommended family trend previous to this work (See Figure 5.6). All values were Pred using the Seaton-Redd2 method Chapter 6.

CAS No.	Compound Name	Straight Carbon Chain Length	AIT (K)
1078-71-3	*n*-heptylbenzene	7	634
2189-60-8	*n*-octylbenzene	8	628
1081-77-2	*n*-nonylbenzene	9	624
104-72-3	*n*-decylbenzene	10	621
123-01-3	*n*-dodecylbenzene	12	618
123-02-4	*n*-tridecylbenzene	13	617
1459-10-5	*n*-tetradecylbenzene	14	617
2131-18-2	*n*-pentadecylbenzene	15	618
1459-09-2	*n*-hexadecylbenzene	16	619
14752-75-1	*n*-heptadecylbenzene	17	619
4445-07-2	*n*-octadecylbenzene	18	621

Table E.4: AIT values for methyl esters that were not recommended but plotted in Figure 5.14. "C#" corresponds to the carbon number used to plot these values in the same figure. Under "Data Type", "Exp" and "Pred" refer to experimental and predicted values respectively. "NS" indicates that the source did not specify whether the value was experimental or predicted.

CAS No.	Compound Name	C#	AIT (K)	Data Type	Ref
107-31-3	methyl formate	1	722	NS	[58]
107-31-3	methyl formate	1	722	NS	[68]
107-31-3	methyl formate	1	723	Exp	[29]
107-31-3	methyl formate	1	729	Exp	[102]
107-31-3	methyl formate	1	771	Exp	[19]
79-20-9	methyl acetate	2	727	NS	[68]
79-20-9	methyl acetate	2	727	NS	[68]
79-20-9	methyl acetate	2	748	Exp	[29]
79-20-9	methyl acetate	2	748	Exp	[29]
79-20-9	methyl acetate	2	775	Exp	[102]
79-20-9	methyl acetate	2	775	NS	[58]
554-12-1	methyl propionate	3	728	NS	[29]
554-12-1	methyl propionate	3	742	Exp	[102]
623-42-7	methyl *n*-butyrate	4	728	NS	[29]
624-24-8	methyl pentanoate	5	656	Exp	[103]

Table E.4: Continued

CAS No.	Compound Name	C#	AIT (K)	Data Type	Ref
624-24-8	methyl pentanoate	5	670	Exp	[104]
106-70-7	methyl hexanoate	6	625	Exp	[104]
107-31-3	methyl formate	1	738	Exp	[63]
79-20-9	methyl acetate	2	775	Exp	[63]
79-20-9	methyl acetate	2	775	Exp	[63]
554-12-1	methyl propionate	3	742	Exp	[63]
79-20-9	methyl acetate	2	748	Exp	[21]
107-31-3	methyl formate	1	723	Exp	[81]
79-20-9	methyl acetate	2	748	Exp	[81]
624-24-8	methyl pentanoate	5	693	Exp	[81]
106-70-7	methyl hexanoate	6	528	Exp	[81]
107-31-3	methyl formate	1	740	Exp	[10]
107-31-3	methyl formate	1	738	Exp	[14]
106-70-7	methyl hexanoate	6	687	Pred	AITMP™ 95C Chapter 6
111-11-5	methyl caprylate	8	654	Pred	AITMP™ 95C Chapter 6

Table E.4: Continued

CAS No.	Compound Name	C#	AIT (K)	Data Type	Ref
110-42-9	methyl decanoate	10	630	Pred	AITMP™ 95C Chapter 6
111-82-0	methyl dodecanoate	12	610	Pred	AITMP™ 95C Chapter 6
124-10-7	methyl myristate	14	597	Pred	AITMP™ 95C Chapter 6
124-10-7	methyl myristate	14	597	Pred	AITMP™ 95C Chapter 6
112-39-0	methyl palmitate	16	588	Pred	AITMP™ 95C Chapter 6
1731-92-6	methyl heptadecanoate	17	585	Pred	AITMP™ 95C Chapter 6
112-61-8	methyl stearate	18	582	Pred	AITMP™ 95C Chapter 6
107-31-3	methyl formate	1	517	Pred	Seaton-Redd2 Chapter 6
79-20-9	methyl acetate	2	724	Pred	Seaton-Redd2 Chapter 6
79-20-9	methyl acetate	2	724	Pred	Seaton-Redd2 Chapter 6
554-12-1	methyl propionate	3	662	Pred	Seaton-Redd2 Chapter 6
623-42-7	methyl *n*-butyrate	4	629	Pred	Seaton-Redd2 Chapter 6
624-24-8	methyl pentanoate	5	607	Pred	Seaton-Redd2 Chapter 6
106-70-7	methyl hexanoate	6	593	Pred	Seaton-Redd2 Chapter 6

Table E.4: Continued

CAS No.	Compound Name	C#	AIT (K)	Data Type	Ref
111-11-5	methyl caprylate	8	573	Pred	Seaton-Redd2 Chapter 6
110-42-9	methyl decanoate	10	560	Pred	Seaton-Redd2 Chapter 6
111-82-0	methyl dodecanoate	12	552	Pred	Seaton-Redd2 Chapter 6
124-10-7	methyl myristate	14	545	Pred	Seaton-Redd2 Chapter 6
124-10-7	methyl myristate	14	545	Pred	Seaton-Redd2 Chapter 6
7132-64-1	methyl pentadecanoate	15	543	Pred	Seaton-Redd2 Chapter 6
112-39-0	methyl palmitate	16	541	Pred	Seaton-Redd2 Chapter 6
1731-92-6	methyl heptadecanoate	17	539	Pred	Seaton-Redd2 Chapter 6
112-61-8	methyl stearate	18	537	Pred	Seaton-Redd2 Chapter 6

Table E.5: AIT values for ethyl esters that were not recommended but plotted in Figure 5.14. "C#" corresponds to the carbon number used to plot these values in the same figure. Under "Data Type", "Exp" and "Pred" refer to experimental and predicted values respectively. "NS" indicates that the source did not specify whether the value was experimental or predicted.

CAS No.	Compound Name	C#	AIT (K)	Data Type	Reference
109-94-4	ethyl formate	1	557	Pred	Seaton-Redd2 Chapter 6
109-94-4	ethyl formate	1	708	NS	[29]
109-94-4	ethyl formate	1	713	Exp	[21]
109-94-4	ethyl formate	1	719	Exp	[75]
109-94-4	ethyl formate	1	728	Exp	[102]
109-94-4	ethyl formate	1	728	Exp	[14]
109-94-4	ethyl formate	1	728	Exp	[63]
141-78-6	ethyl acetate	2	698	NS	[29]
141-78-6	ethyl acetate	2	699	NS	[68]
141-78-6	ethyl acetate	2	700	Exp	[102]
141-78-6	ethyl acetate	2	700	Exp	[63]
141-78-6	ethyl acetate	2	701	Pred	Seaton-Redd2 Chapter 6

Table E.5: Continued

CAS No.	Compound Name	C#	AIT (K)	Data Type	Reference
141-78-6	ethyl acetate	2	733	Exp	[21]
141-78-6	ethyl acetate	2	759	NS	[58]
105-37-3	ethyl propionate	3	656	Pred	Seaton-Redd2 Chapter 6
105-37-3	ethyl propionate	3	713	Exp	[14]
105-37-3	ethyl propionate	3	713	Exp	[63]
105-37-3	ethyl propionate	3	713	NS	[68]
105-37-3	ethyl propionate	3	718	Exp	[21]
105-37-3	ethyl propionate	3	718	NS	[29]
105-37-3	ethyl propionate	3	750	Exp	[102]
105-54-4	ethyl *n*-butyrate	4	627	Pred	Seaton-Redd2 Chapter 6
105-54-4	ethyl *n*-butyrate	4	713	Exp	[29]
105-54-4	ethyl *n*-butyrate	4	713	Exp	[21]
105-54-4	ethyl *n*-butyrate	4	733	Exp	[21]

Table E.5: Continued

CAS No.	Compound Name	C#	AIT (K)	Data Type	Reference
105-54-4	ethyl *n*-butyrate	4	733	Exp	[81]
105-54-4	ethyl *n*-butyrate	4	736	Exp	[102]
105-54-4	ethyl *n*-butyrate	4	736	Exp	[60]
106-32-1	ethyl caprylate	8	572	Pred	Seaton-Redd2 Chapter 6
106-32-1	ethyl caprylate	8	600	Exp	[75]
106-32-1	ethyl caprylate	8	623	Pred	AITMP™ 95C Chapter 6
110-38-3	ethyl caprate	10	493	Exp	[81]
110-38-3	ethyl caprate	10	493	Exp	[21]
110-38-3	ethyl caprate	10	558	Pred	Seaton-Redd2 Chapter 6
110-38-3	ethyl caprate	10	583	Exp	[75]
106-33-2	ethyl laurate	12	493	Exp	[81]
106-33-2	ethyl laurate	12	548	Pred	Seaton-Redd2 Chapter 6
106-33-2	ethyl laurate	12	582	Pred	AITMP™ 95C Chapter 6

Table E.5: Continued

CAS No.	Compound Name	C#	AIT (K)	Data Type	Reference
106-33-2	ethyl laurate	12	584	Exp	[75]
124-06-1	ethyl myristate	14	540	Pred	Seaton-Redd2 Chapter 6
124-06-1	ethyl myristate	14	570	Pred	AITMP™ 95C Chapter 6
124-06-1	ethyl myristate	14	590	Exp	[75]
628-97-7	ethyl palmitate	16	534	Pred	Seaton-Redd2 Chapter 6
628-97-7	ethyl palmitate	16	563	Pred	AITMP™ 95C Chapter 6
628-97-7	ethyl palmitate	16	612	Exp	[75]
111-61-5	ethyl stearate	18	529	Pred	Seaton-Redd2 Chapter 6
111-61-5	ethyl stearate	18	559	Pred	AITMP™ 95C Chapter 6

Table E.6: AIT values for *n*-butyl esters that were not recommended but plotted in Figure 5.14. "C#" corresponds to the carbon number used to plot these values in the same figure. Under "Data Type", "Exp" and "Pred" refer to experimental and predicted values respectively.

CAS No.	Compound Name	C#	AIT (K)	Data Type	Reference
123-95-5	*n*-butyl stearate	18	525	Pred	Seaton-Redd2 Chapter 6

Table E.6: Continued

CAS No.	Compound Name	C#	AIT (K)	Data Type	Reference
123-95-5	*n*-butyl stearate	18	628	Exp	[12]